Robert C. Reid

A kinematic and kinetic study of alpine skiing technique in slalom

DISSERTATION FROM THE NORWEGIAN SCHOOL OF SPORT SCIENCES • 2010

ISBN nr 978-82-502-0440-9

TO ANE AND MINA,

WHO GIVE MY LIFE MEANING,

WITH LOVE.

ACKNOWLEDGEMENTS

The success of any project of this magnitude is often the direct result of the efforts, investment and selfless collaboration of a large team of individuals. Nowhere is this more the case than on this project where numerous individuals have made invaluable contributions.

First, and foremost, I would like to thank my wonderful wife, and partner in life, Ane, and our beautiful daughter, Mina, for your patience, understanding, and unconditional support through what has been a most challenging process. This project would never have reached completion without you. I look forward to moving into a new phase of life together.

A wise person I know once wrote that completing a PhD, and being given the opportunity to immerse oneself in the study of a topic of personal interest, is an unequalled privilege. I could not agree more and I would like to express my sincere gratitude to the Norwegian School of Sport Sciences, the Norwegian Ski Federation, and Olympiatoppen for providing the financial means and political support that have allowed me to pursue the study of a topic about which I am passionate.

A core team of individuals have truly made this project what it is today. I would like to thank Gerald Smith, my head advisor, for your tireless patience in taking on the challenge of advising a beginner in the realm of biomechanics; for your fantastic, inquisitive nature and creative, inspiring ideas; for endless hours of reading and patiently editing manuscript drafts; and for your friendship, support, and inspiration in the final, challenging hours of preparing this dissertation. To Per Haugen, my co-advisor, I can not even begin to express in words how deeply appreciative I am of your contributions, not only to this project, but to all aspects of my development as a student, researcher, coach, and person. From the initial planning, to endless theodolite

measurements in −20° C temperatures at two o'clock in the morning, to feedback and encouragement during the final writing process, your input during all phases of this project has extended far, far beyond what anyone could ever ask. I would also like to express my gratitude to Ronald Kipp who, in providing important input during the planning of the project, assisting during data collections, sharing his thoughts about technique, and providing valuable feedback on manuscripts, was an essential member of my advising team. I only hope that in some small way this dissertation reflects the quality of work for which Gerald, Per, and Ron stand.

In addition to my advisors, I have been fortunate enough to have an outstanding group of Masters students on the team. Thank you Tron Moger, Håvard Tjørhom, Matthias Gilgien, Marjaana Lappi, Inger Svandal, Øyvind Tøftegaard, and Angelo Brack. Your enthusiasm, relentless energy, and creative initiative have inpired me to reach for new heights. I have learned greatly from working with you.

I would particularly like to thank the coaches and athletes who have participated in this project. Your contributions to this dissertation as well as my studies have been invaluable. Although the interviews conducted during the initial phase of this project are not included in this report, they are represented in that they define the enitire foundation upon which this dissertation is built. My hope in writing this report is that it will, perhaps in some small way, assist you to gain new insight into the mechanics of skiing technique.

A number of individuals have made important contributions over the course of this project. First, I would like to thank Atle Skaardal for seeing the potential behind such a project and inspiring me to take on the challenge. I would also like to thank Marius Arnesen, Martin Andersen, Jørund Li, and the coaches, staff, and athletes of the Norwegian Ski Teams for both their support and sharing of their creative thoughts and ideas with me. I would like to thank Trond Eiken for volunteering his time to train us in theodolite measurement and allowing us to use his equipment during data

collections. Thank you also to Rolle Johansson, Peter Lederer, Atle Skaardal, Jan Tischauser, Nicolas Lemyre, Svein Mundal and the Hafjell World Cup Organizing Committee for their support during the Hafjell data collection; to Knut Einar Haug and Ål Ski Center for their support during the Ål data collection; and to Andy Taylor, Varingskollen Ski Center, and Hakadal Alpin for their support during this investigation's main data collection. I would also like to thank Matej Supej, Hermann Schwameder, Erich Müller, Josef Kröll, and the many colleagues and friends who have provided constructive feedback during this project. Thank you also to Matthew Brodie, for generously sharing his pixel counting algorithm, and to Federico Gori of Microgate S.r.l., for providing timing equipment.

In completing a PhD project, access to previous literature is of paramount importance. I would therefore like to direct a special thank you to the library services staff at the Norwegian School of Sport Sciences for their assistance in finding difficult to locate materials and for providing an outstanding library where you really do feel that the world is at your fingers. Additionally, I would like to thank the staff of the school's printing office for advice regarding the manuscript's layout and assistance in the final printing of this dissertation. Thank you also to Cindy Slater at the United States Olympic Committee library services.

Finally, I would like to thank my parents, Henry and Patsy, for introducing me to the joys of skiing and providing me the opportunity to chase my dreams. Along the same lines, I would like to take this opportunity to thank Thomas Bloch, Jimmy Galligan, Russ Speirn, Ben Chidlaw, Ray Discius, Mary Gunesch, Bill Gunesch, Stever Sarich, Jeff Pickering and Jeff Kai—my coaches—for standing on the hill with me, through both good weather and bad, and teaching me the sport of alpine ski racing. Your enthusiasm for the sport, and dedication to developing young athletes, still inspires me to this day.

Robert Reid
Oslo, January 1st, 2010

-10^{o} C 0300 hrs April 11th, 2006

There is no “i” in the word team.

ABSTRACT

Despite a large body of lay and professional literature covering numerous aspects of alpine skiing technique, only a limited number of published scientific investigations have examined the relationship between skier technical and tactical characteristics and racing performance. As a consequence, our scientific understanding of how the underlying mechanics of alpine ski racing technique relate to performance is surprisingly weak. The purpose of this research project was therefore to identify, describe, and study aspects of alpine ski racing technique which play an important role in determining skier performance. Since this is the first project of its kind for our research group, an additional purpose was to establish the theoretical and methodological foundation for a line of future research on this topic.

Initially, a conceptual model of turning technique was developed to provide the theoretical framework for defining research questions. This model was built on the basis of a literature review and 17 in-depth interviews with highly-experienced coaches from 6 nations. Research questions were then defined on the basis of this model for a quantitative, motion analysis study of turning technique, the purpose of which was to quantitatively describe the various components of the aforementioned model and to explore their interrelationships with the ultimate aim of further developing our understanding of how turning mechanics relate to racing performance.

Towards this end, a 3-dimensional, video-based photogrammetric method utilizing multiple panning cameras was implemented to capture the performances of six highly-skilled athletes during slalom race simulations on courses with 10 and 13 m linear gate distances. The resulting data were then used to examine kinematic, kinetic, and energetic questions related to ski motion, skier technique, and performance. A comparison between courses was made in the hope that understanding how skiers adapted to the differing circumstances would shed further light on the relationship

between turning mechanics and performance. This dissertation describes in detail the methods and results of this investigation.

In terms of ski motion, the results of this investigation provide observational evidence in support of current theoretical models of ski snow interaction mechanics and may provide insight into both ski design and injury prevention issues. Many of the differences observed between courses in terms of ski motion, skier kinematics and skier kinetics seem to be reminiscent of differences between carving and skidding mechanics, which is perhaps not surprising considering that there was a greater degree of carving on the 13 m course.

Perhaps a finding of particular significance was the difference in turn cycle structure observed between courses. While the skiers' trajectories were symmetrically distributed about the gate on the 10 m course, there was a prolonged Initiation Phase on the 13 m course, resulting in an asymmetrical trajectory about the gate. This difference in turn structure and trajectory shape may to a large degree be the result of the different gate distances and the skis' physical properties. Further work to understand why this difference occurred may help to improve our understanding of how ski characteristics influence turn mechanics.

In terms of kinetics, maximal snow reaction forces were high, reaching over 3000 N and 3.5 times bodyweight on both courses. There was a clear difference in the timing of the snow reaction force relative to the turn cycle between courses. On the 10 m course, large reaction forces were generated at about 50 % of the turn cycle, or approximately gate passage. In contrast, peak forces were delayed on the 13 m course, occurring just after gate passage, or about 65 % of the turn cycle. In addition, there was a greater degree of unloading in the vertical component of the snow reaction force during the Initiation Phase on the 13 m course. The air drag force was larger on the 13 m course due to increased skier speeds.

Mechanical energy dissipation, introduced by Supej, Kugovnic, and Nemec (2005a), was calculated based on skier center of mass motion. A cyclical pattern of energy dissipation was observed on both courses with high dissipations occurring during the turn and low dissipations during the transition between turns. Negative dissipations—situations where skier kinetic energy increased by more than what can be attributed to changes in skier potential energy—were observed at the transition between turns on the 10 m course and early in the turn cycle on the 13 m course. This may provide evidence of skiers increasing their kinetic energy through muscular work, although in this study these increases were small, representing less than 3 % of skier kinetic energy gains.

To help understand what factors acted to slow the skier, the negative work of each of the external forces acting on the skier was calculated. About 20 % of skier total mechanical energy loss in the investigated situation was due to air drag. The remaining majority of mechanical energy losses were attributed to a drag component of the snow reaction force. However, this study does provide evidence suggesting that the energy cost of gate clearance in slalom may play a significant role and needs to be accounted for in future work.

In terms of racing performance, both skier vertical and fore/aft actions correlated well with elapsed time through the investigated sequence. The relatively strong correlation observed between skier fore/aft position and mechanical energy loss further indicates that this is a parameter whose role in skiing mechanics and performance should be investigated further.

In summary, this project has provided a conceptual model of turning technique in alpine ski racing that is based on both scientific and practitioner knowledge and that can be used to guide future research efforts. The results of this investigation are limited in that generalization from a single situation, and a single group of athletes, to other circumstances needs to be considered very carefully, particularly in light of the

infinitely variable conditions possible in alpine ski racing. Moreover, the observational design of this study does not provide evidence of cause and effect relationships. In light of these limitations, perhaps the most important scientific contribution of this study lies in the identification of turning technique parameters which need to be better understood to further develop our knowledge of how the mechanics of turning technique relates to performance. Perhaps of particular importance in future work will be the development of our understanding of how skier actions influence the ski snow interaction and, ultimately, ski and skier motion.

TABLE OF CONTENTS

LIST OF TABLES

LIST OF FIGURES

ABBREVIATIONS AND SYMBOLS

GENERAL ABBREVIATIONS

DLT	Direct Linear Transformation
FIS	International Ski Federation
GPS	Global positioning system.
ISO	International Organization for Standardization
RMSE	Root mean square error.

WRITING CONVENTIONS

$\vec{A}$	Vector.
$\left\|\vec{A}\right\|$	Vector norm.
$\hat{A}$	Unit vector.
A	Scalar.
$\dot{\vec{A}}, \dot{\hat{A}}$	First derivative.
$\dot{A}$	Norm of the first derivative.
$\ddot{\vec{A}}, \ddot{\hat{A}}$	Second derivative.
$\ddot{A}$	Norm of the second derivative.
$\left\|\vec{A} - \vec{B}\right\|$	Euclidian distance.
$\vec{A}(t)$	Vector as a function of time, t.
$\vec{A}(i)$	Vector as a function of analysis time point, i.
A(t)	Scalar as a function of time, t.

A(i)	Scalar as a function of analysis time point, i.
$\vec{A}$(E)	Vector as a function of position along the ski longitudinal axis E.
A(E)	Scalar as a function of position along the ski longitudinal axis E.
$\vec{A}$(E, F)	Vector as a function of position on the ski sole E,F.
A(E, F)	Scalar as a function of position on the ski sole E,F.

COORDINATE SYSTEMS

X Y Z, $\hat{\boldsymbol{X}}\,\hat{\boldsymbol{Y}}\,\hat{\boldsymbol{Z}}$	Theodolite coordinate system, object-space coordinate system.
X′ Y′ Z′, $\hat{\boldsymbol{X}}'\,\hat{\boldsymbol{Y}}'\,\hat{\boldsymbol{Z}}'$	Course coordinate system.
E F G, $\hat{\boldsymbol{E}}\,\hat{\boldsymbol{F}}\,\hat{\boldsymbol{G}}$	Ski coordinate system.
E′ F′ G′, $\hat{\boldsymbol{E}}'\,\hat{\boldsymbol{F}}'\,\hat{\boldsymbol{G}}'$	Ski velocity coordinate system.
$e_E f_E g_E$, $\hat{\boldsymbol{e}}_E\,\hat{\boldsymbol{f}}_E\,\hat{\boldsymbol{g}}_E$	Local ski coordinate system at a point E along the ski's longitudinal axis.
$e'_E f'_E g'_E$, $\hat{\boldsymbol{e}}'_E\,\hat{\boldsymbol{f}}'_E\,\hat{\boldsymbol{g}}'_E$	Local ski velocity coordinate system at a point E along the ski's longitudinal axis.
Q R S, $\hat{\boldsymbol{Q}}\,\hat{\boldsymbol{R}}\,\hat{\boldsymbol{S}}$	Accelerated, local coordinate system used in various parameter calculations.
A B C, $\hat{\boldsymbol{A}}\,\hat{\boldsymbol{B}}\,\hat{\boldsymbol{C}}$	Accelerated, local coordinate system used in various parameter calculations.
U V, $\hat{\boldsymbol{U}}\,\hat{\boldsymbol{V}}$	Comparator-space coordinate system.

GENERAL VARIABLES

t	Time.
i	Time point index.
$\vec{\boldsymbol{P}}_X$	Position vector for point X.
$\dot{\vec{\boldsymbol{P}}}_X$	First time derivative of $\vec{\boldsymbol{P}}_X$ in an inertial reference frame. Velocity vector for point X.
$\dot{P}_X$	Norm of vector $\dot{\vec{\boldsymbol{P}}}_X$. Speed of point X.
$\ddot{\vec{\boldsymbol{P}}}_X$	Second time derivative of $\vec{\boldsymbol{P}}_X$ in an inertial reference frame. Acceleration vector for point X.
$\ddot{P}_X$	Norm of vector $\ddot{\vec{\boldsymbol{P}}}_X$. Acceleration magnitude of point X.
$\hat{\boldsymbol{N}}$	Normal vector to the least squares plane of the snow surface.
$\hat{\boldsymbol{n}}_{x,y}$	Local normal vector to the snow surface at grid point [x,y].
$\hat{\boldsymbol{g}}_{x,y}$	Local gradient vector parallel to the snow surface at grid point [x,y].
g	Gravitational acceleration.
m	Mass.
v	Velocity.
v_X	Velocity in the X′-dimension.
a	Acceleration
a_X	Acceleration in the X′-dimension.
I	Moment of inertia.
ω	Angular velocity.
L	Angular momentum.

T	Rotational kinetic energy.
$L_1 \ldots L_{11}$	DLT camera calibration constants
$\delta U, \delta V$	DLT optimization error in the comparator-space coordinate sytem U- and V-dimensions.
$\bar{\xi}$	Mean DLT optimization error. May be reported in either comparator-space or object-space units.

SKIER AND EQUIPMENT LANDMARKS

HEAD	Head, helmet and goggles center of mass.
R_SJC, L_SJC	Right and left shoulder joint center.
R_EJC, L_EJC	Right and left elbow joint center.
R_WJC, L_WJC	Right and left wrist joint center.
R_HCOM, L_HCOM	Right and left hand, glove, and pole grip center of mass.
R_POLE, L_POLE	Right and left pole tip.
R_HJC, L_HJC	Right and left hip joint center.
R_KJC, L_KJC	Right and left knee joint center.
R_AJC, L_AJC	Right and left ankle joint center.
R_TIP, L_TIP	Right and left ski tip.
R_TAIL, L_TAIL	Right and left ski tail.
R_MID, L_MID	Right and left ski mid point.
MIDS	Mid point between shoulder joint centers.
MIDH	Mid point between hip joint centers.

EXTERNAL FORCES ACTING ON THE SKIER

$\vec{F}_G$	Gravitational force vector.
P_G	Gravitational force power acting on the skier center of mass.
W_G	Gravitational force work on the skier center of mass.
$\vec{F}_R$	Snow reaction force vector.
$\vec{F}_{VERT}$	Component of the reaction force acting normal to the local snow surface.
$\overline{F}_{VERT}^{INIT}$	Mean magnitude over the Initiation Phase of the vertical component of the snow reaction force.
P_R	Snow reaction force power acting on the skier center of mass.
$\overline{P}_R$	Mean turn cycle reaction force power.
W_R	Work of the snow reaction force on the skier center of mass.
$\vec{F}_D$	Air drag force vector.
P_D	Air drag force power acting on the skier center of mass.
$\overline{P}_D$	Mean turn cycle air drag force power.
W_D	Work of the air drag force on the skier center of mass.
ρ	Air density.
A	Skier frontal area.
C_D	Air drag coefficient.

SKI GEOMETRICAL CHARACTERISTICS

C	Ski contact length.

T	Ski taper.
W_S	Ski shovel width.
W_W	Ski waist or nominal width.
W_T	Ski tail width.
SC	Ski side camber.
R_{SC}	Ski sidecut radius.

SKI-SNOW INTERACTION MECHANICS

$\vec{\boldsymbol{M}}(E)$	Ski midline position vector at point E along the ski's longitudinal axis.
$\vec{\boldsymbol{S}}(E)$	Ski edge position vector at point E along the ski's longitudinal axis.
$\vec{\boldsymbol{F}}_P$	Penetration component of the snow reaction force.
$\vec{\boldsymbol{F}}_C$	Cutting component of the snow reaction force.
$\vec{\boldsymbol{F}}_F$	Friction component of the snow reaction force.
$\vec{\boldsymbol{F}}_H$	Horizontal component of $\vec{\boldsymbol{F}}_C$.
$\vec{\boldsymbol{F}}_T$	Transverse component of $\vec{\boldsymbol{F}}_C$.
$\vec{\boldsymbol{F}}_P(E)$	Local penetration component of the snow reaction force acting at point E along the ski's longitudinal axis.
$\vec{\boldsymbol{F}}_C(E)$	Local cutting component of the snow reaction force acting at point E along the ski's longitudinal axis.
$\vec{\boldsymbol{F}}_F(E)$	Local friction component of the snow reaction force acting at point E along the ski's longitudinal axis.

$\vec{\boldsymbol{M}}_{R}(E)$	Local reaction force moment acting at point E along the ski's longitudinal axis.
$p_{R}(E,F)$	Local ski snow contact pressure at position E,F on the ski base.
θ	Whole ski edge angle.
θ_{E}	Local ski edge angle at position E along the ski's longitudinal axis.
φ	Whole ski attack angle.
φ_{E}	Local ski attack angle at position E along the ski's longitudinal axis.
$\overline{\varphi}^{INIT}$	Mean Initiation Phase outside ski attack angle.
ψ	Ski tilt angle.
β	Angle between the ski's longitudinal axis ($\hat{\boldsymbol{E}}$) and the slope horizontal.
λ	Center of mass attack angle.
γ	Platform angle.
D_{P}	Ski penetration depth.
D'_{P}	Ski penetration distance.
RSPD	Running surface pressure distribution

SKI AND SKIER TRAJECTORY CHARACTERISTICS

R_{COM}	Center of mass turn radius.
R_{SKI}	Outside ski turn radius.
R_{L_MID}	Left ski middle point turn radius.
R_{R_MID}	Right ski middle point turn radius.

PT	Performance time.
L_{XYZ}	Total 3-D center of mass trajectory length from the first to the third switch.
L_Y	Center of mass trajectory length in the Y′- dimension.
L_Z	Center of mass trajectory length in the Z′- dimension.

SKIER FORE/AFT ACTION CHARACTERISTICS

Q_{COM}	Center of mass position in the Q-dimension of the outside ankle joint center QRS coordinate system.
$\bar{Q}_{COM}$	Mean turn cycle center of mass position in the Q-dimension of the outside ankle joint center QRS coordinate system.
Q_{ROM}	Turn cycle center of mass range of motion in the Q-dimension of the outside ankle joint center QRS coordinate system.

SKIER VERTICAL ACTION CHARACTERISTICS

Z'_{COM}	Center of mass position in the Z′-dimension.
$\bar{Z}'_{AMP}$	Mean peak-to-peak amplitude of the center of mass motion in the Z′- dimension.
D_{AJC}	Euclidian distance between the center of mass and the outside ankle joint center.

SKIER LATERAL ACTION CHARACTERISTICS

A	Total skier angulation.

ς	Center of mass inclination angle.
κ	Hip angulation angle.
η	Knee angulation angle.

SKIER MECHANICAL ENERGY CHARACTERISTICS

E_{MECH}	Skier mechanical energy.
E_{KIN}	Skier kinetic energy.
E_{POT}	Skier potential energy.
E_{DISS}	Mechanical energy dissipation.
$\overline{E}_{DISS}$	Mean turn cycle mechanical energy dissipation.
T	Rotational kinetic energy.

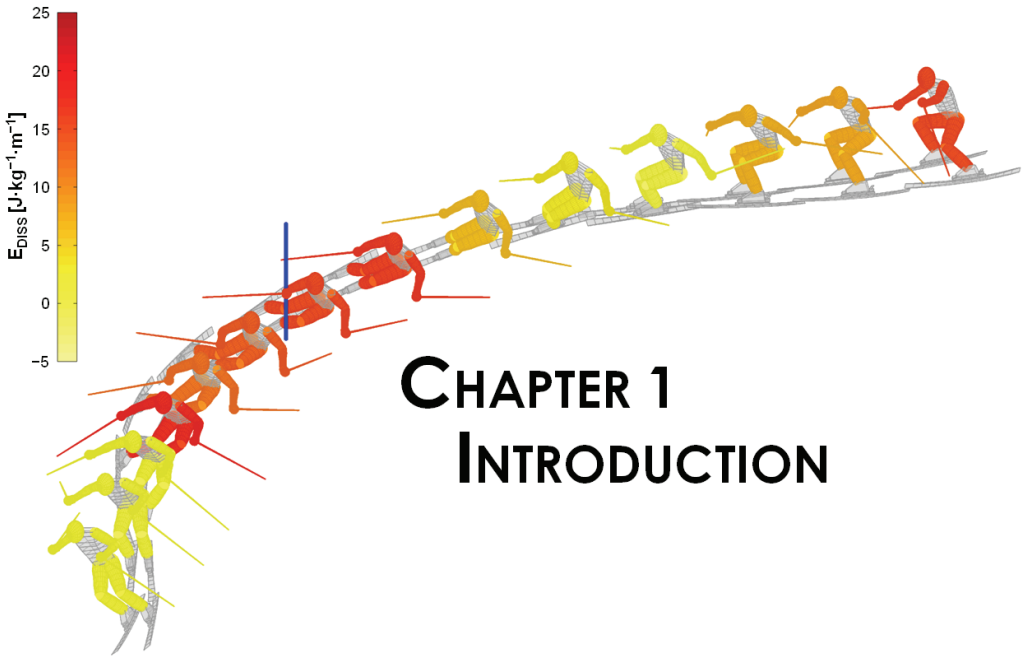

CHAPTER 1
INTRODUCTION

CHAPTER 1. INTRODUCTION

1.1 BACKGROUND

In the sport of alpine ski racing, time differences between top racers are often remarkably small. In fact, it is not uncommon for races lasting over two minutes to be won by mere hundredths of a second. Perhaps what makes such close margins so extraordinary is that ski racing is a sport in which a relatively large number and variety of factors have an impact on performance. For instance, to be competitive at the highest level requires a high degree of physical conditioning, strong psychological and sociological skills, and equipment that is not only on the cutting edge of development, but also individually fine-tuned for competition conditions.

Technique is undoubtedly an important performance factor, as can readily be ascertained by the attention it receives from coaches and athletes and from the sheer number of publications addressing the topic. The majority of this literature might be best classified as "expert opinion" and can be found in both lay magazines as well as in professional coaching journals and textbooks (e.g., Bear, 1976; Howe, 2001; Joubert, 1978/1980; LeMaster, 1999; Lind & Sanders, 2004; Major & Larsson, 1979/1979; Witherell, 1972; Witherell & Evrard, 1993).

Of the research literature, injury mechanisms and equipment development to reduce injury risk are topics which have received considerable attention, and rightfully so considering the alarming injury rates and the severity of these injuries (Klous, 2007). In addition, numerous biomechanical and physiological investigations of skiing technique have focused on describing the physical demands of the sport and have made significant contributions towards conditioning efforts (e.g., Burtscher, Raschner, Zallinger, Schwameder, & Müller, 2001; Frick, Schmidtbleicher, Raschner, & Müller, 1997; Hintermeister et al., 1995; Karlsson, Eriksson, Forsberg, Kallberg, & Tesch, 1978; Raschner, Müller, & Schwameder, 1997; Tesch, 1995).

Of the studies more directly focused on technique mechanics, many have described general skier kinematic and kinetic characteristics under various conditions (e.g., Pozzo, Canclini, Casasola, et al., 2005; Pozzo, Canclini, Cotelli, & Baroni, 2001, 2004, 2005; Raschner et al., 1999; Scott, 2004; Supej, Kugovnik, & Nemec, 2005b; Yoneyama, Scott, & Kagawa, 2006). Some investigations have compared various types of turning techniques (e.g., Kugovnik, Supej, & Nemec, 2004, 2005; Müller, 1994; Supej, Kugovnik, & Nemec, 2004). In particular, contrasting the techniques used by skiers while performing on equipment of varying characteristics has been an important research topic for understanding the role of equipment in skiing mechanics (e.g., Müller, Schiefermüller, Kröll, Raschner, & Schwameder, 2005; Müller & Schwameder, 2003; Niessen, Müller, Schwameder, Wimmer, & Riepler, 1998; Nigg, Schwameder, Stefanyshyn, & Tscharner, 2001; Raschner et al., 2001; Schiefermüller, Lindinger, & Müller, 2005; Schwameder, Nigg, Tscharner, & Stefanyshyn, 2001; Yoneyama, Kagawa, Okamoto, & Sawada, 2001). Other studies have taken the approach of comparing the technical and tactical approaches of skiers of various skill levels (e.g., Förg-Rob & Nachbauer, 1988; Müller et al., 1998; Nachbauer, 1987a, 1987b; Supej, 2008; Supej, Kugovnik, & Nemec, 2005c). Taken all together, these investigations have provided valuable information for understanding skiing mechanics and developing ski instruction and coaching manuals.

Despite this rather large body of research, only a limited number of studies have attempted to examine the relationship between skier technical and tactical characteristics and racing performance, at least in the published literature. As a consequence, our understanding of how the underlying mechanics of alpine ski racing technique relate to performance is surprisingly weak.

1.2 DISSERTATION OBJECTIVES

The purpose of this dissertation was therefore to identify, describe, and compare aspects of alpine ski racing technique which play an important role in determining skier performance. Due to its relative importance, this project focused on turning technique in particular.

It is hoped that the results of this project will contribute towards raising practitioner awareness and understanding of the underlying mechanics of turning technique as they relate to skier performance. Not only is the body of literature regarding skiing technique immense, much of it is not quality-controlled. Moreover, coaches are almost continually bombarded with new ideas or thoughts about technique for which there may or may not be a sound justification. The coach must make his own judgements as to the validity of the information. In this regard, it is hoped that this project will help coaches to base their own technique philosophies on the solid foundation of physics and that in so doing they will be better able to evaluate what they hear and read about skiing technique and to coach their athletes more effectively.

In addition, this dissertation was aimed at establishing the foundation for a long-term line of on-going research in alpine skiing technique at the Norwegian School of Sport Sciences in Oslo, Norway. As a consequence, particular attention has been given to the development of a theoretical basis to guide research efforts, as will be described shortly. As this was the first study of its kind for our research group, great effort was

also taken to understand, validate, and implement the motion analysis methods required for the kinematic studies. Seen in this light, this dissertation itself is only a small brick in the foundation of what is hoped to be a long-term research program.

Finally, and on a more personal note, skiing technique is a topic that I have always found challenging, both as an athlete and as a coach. This dissertation reflects a personal journey with an aim to better understand the fundamentals of skiing technique and how they relate to performance.

1.3 DISSERTATION PLAN

The four-year term of this research project, running from the Fall of 2004 to the Fall of 2008, was divided into three main phases. Each of these phases is described briefly here.

PHASE 1: IMMERSION

The purpose of the first phase was to establish a theoretically- and practically-sound model of turning technique to guide research efforts and from which to define research questions of interest to both researchers and practitioners. Three approaches were used to accomplish this task. First, in-depth, unstructured interviews (Kvale, 1996) with eighteen expert coaches from six different countries were completed between the Spring of 2004 and the Fall of 2005. At the same time, systematic observations were made of the Norwegian national ski teams during both training and competition over a two-year period. This included on-hill filming and study of skiers as well as observation of post-training video analysis sessions and the related communication between athletes and coaches. The goal of this work was to establish a broad, practitioner-based understanding of technique. Finally, a review of the research and coaching literature regarding skiing technique was conducted. On the basis of the interviews, observation, and literature review done in this phase of the project, a

theoretical model of turning technique was developed, the purpose of which was to (1) identify key components of turning technique and some of their important inter-relationships and (2) provide the basis from which to define research questions as well as interpret the meaning of results.

PHASE 2: QUANTITATIVE ANALYSIS

In the second phase, specific research questions related to the aforementioned model were defined and investigated through a 3-dimensional kinematic and kinetic study of a group of highly-skilled skiers in a slalom race simulation. This phase included the development, implementation and validation of the associated motion analysis methods and the execution of a series of data collections, the results of which form the core of this dissertation as well as that of four Masters theses (Gilgien, 2008; Laapi, 2009; Moger, 2007; Tjørhom, 2007).

PHASE 3: REPORTING

The final phase of this project was reserved for analyzing results and writing of the dissertation. Of particular importance in this process has been frequent and regular contact with selected, highly experienced coaches to discuss the practical significance of the results. This communication with practitioners has been a vital part of understanding the practical implications of the findings from the quantitative studies. In terms of reporting, it is hoped that this dissertation can serve as the basis for the further development of coach's education materials.

1.4 ORGANIZATION OF THE DISSERTATION

This report presents and explores the results of an investigation into skier kinematic, kinetic, and energetic characteristics undertaken during the second phase of this project. Chapter 2 introduces the model of turning technique that was developed in the

Immersion Phase as a basis for defining the research objectives for the current investigation. Chapter 3 reviews the mechanics of turning in alpine skiing and is divided into three main sections. The mechanics of the interaction between ski and snow are examined in the first part as the basis for exploring the mechanics of skier actions in the second part. Finally, in the third part, a review of the research literature regarding skier actions in turning is presented. In Chapter 4, the theoretical background of the methods used in this study is reviewed and some of their potential limitations are identified. A thorough description of the implemented methods is given in Chapter 5 while Chapter 6 presents the results of the analyses, focusing on the description of general, group trends. In Chapter 7, the results are discussed against the background of the previous literature. Specific examples are brought forth from the data to help give the reader insight into the diversity of individual technical approaches that were observed. In addition, limitations of the various measures are identified and discussed. Based on the results and limitations of this study, suggestions are also made for future investigations. Finally, Chapter 8 concludes by addressing the original research objectives and summarizing the investigation's main findings.

Appendices with supplemental information and individual result summaries are presented in a second volume. The purpose of presenting these individual results is to allow the reader to examine and appreciate the diversity of individual approaches. The reader is repeatedly referred to these Appendices throughout the results and discussion chapters.

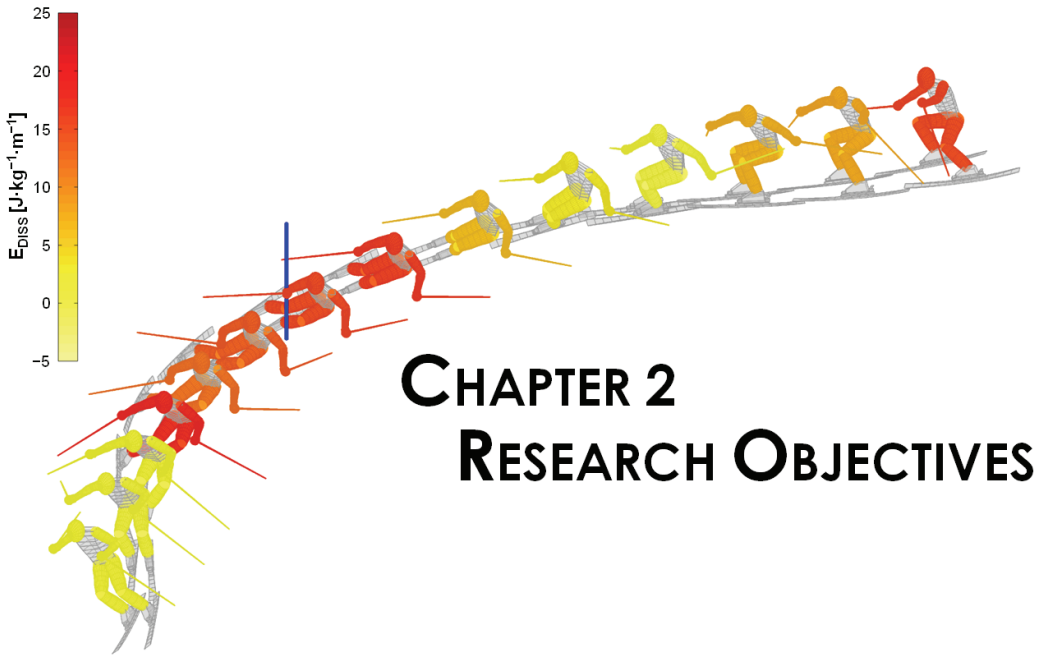

CHAPTER 2
RESEARCH OBJECTIVES

CHAPTER 2. RESEARCH OBJECTIVES

The purpose of this chapter is to familiarize the reader with the research objectives of the video-based motion analysis investigation of skier techniques undertaken in the second phase of this project. On the basis of the interviews, observation, and literature review conducted in the Immersion Phase, a theoretical model of turning technique was constructed to guide the more analytical work in the second phase. This model is briefly introduced in the first part of this chapter to help the reader understand the approach taken in defining the research objectives. A thorough description of the different model components is given during the review of literature in Chapter 3, the Mechanics of Turning, and more precise, mathematical definitions of the various parameters are presented in the methods chapter, Chapter 5. The description of the model is then followed by a presentation of the main research objectives and questions for this project.

2.1 A MODEL OF TURNING TECHNIQUE

The purpose of the conceptual model of turning technique developed in the Immersion Phase (Figure 2.1) is two-fold. First, the model provides a theoretical framework to guide research efforts in the study of turning technique, not only on this project but also in future work. In this regard, the model both defines key technique parameters and identifies what are thought to be some of their more important interrelationships.

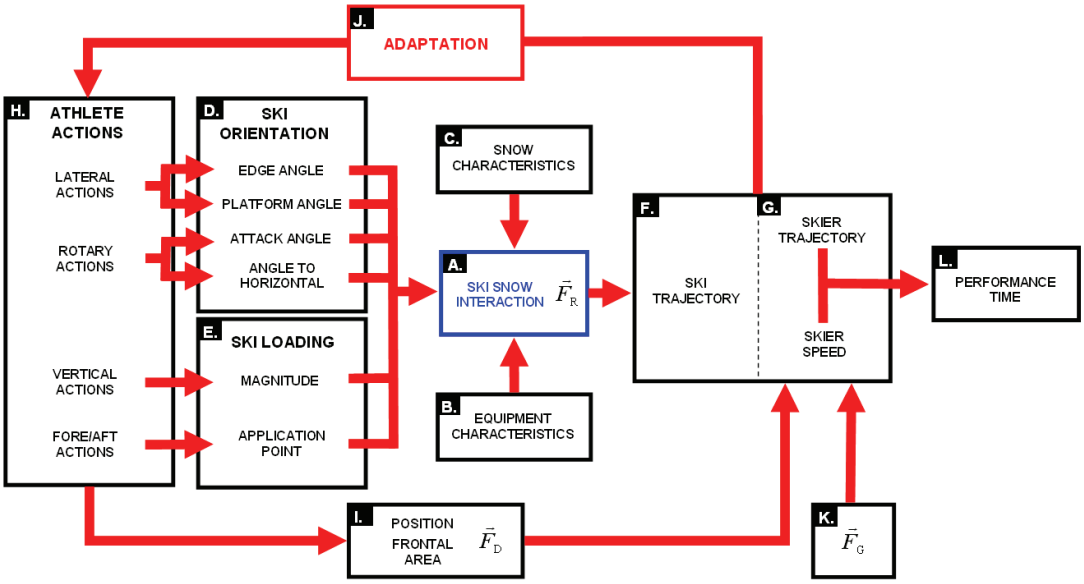

FIGURE 2.1. The conceptual model of turning technique in alpine ski racing developed during the Immersion Phase of this project. The interaction between ski and snow (Box A) forms the core of the model. It is this interaction that determines the ski's trajectory across the snow surface (Box F), providing the platform for the skier to guide her trajectory (Box G). The skier regulates the interaction between ski and snow by controlling the ski's orientation and loading characteristics (Boxes D & E) through their actions (Box H).

The second purpose of this model is to serve as the basis for the organization of this particular dissertation's research objectives, results, and discussion. The main components of the model include (a) the external forces acting on the skier; (b) the ski and skier trajectories; (c) the ski's orientation and loading; and (d) the skier's actions. Each of these components will be briefly introduced here.

THE EXTERNAL FORCES (Figure 2.1, Boxes A, I, and K)

The three external forces acting on the skier when turning are shown in Figure 2.2. The gravitational force, $\vec{F}_G$, is the force of attraction between the mass of the skier and that of the Earth and is the primary source of skier mechanical energy. The air drag force, $\vec{F}_D$, is a non-conservative force arising as a result of the skier's motion through the surrounding air molecules. The magnitude and orientation of the air drag force is determined by numerous factors, but the ones under the athlete's control while skiing include his body position and frontal area that is exposed to the wind. Finally, the snow reaction force, $\vec{F}_R$, arises as a result of the snow's resistance to compaction and shear under the applied load from the skier.

Much of the thinking behind this model is influenced by LeMaster's (1999) approach to understanding turning technique where a fundamental concept is the idea that the skier controls her trajectory and speed through regulating the ski's interaction with the snow and, thereby, controlling the size and orientation of the snow reaction force. The term ski-snow interaction will be used throughout this document to refer to this interaction and its associated mechanics. The placement of the ski-snow interaction and the snow reaction force at the center of the model in Box A is meant to reflect its importance in turning technique.

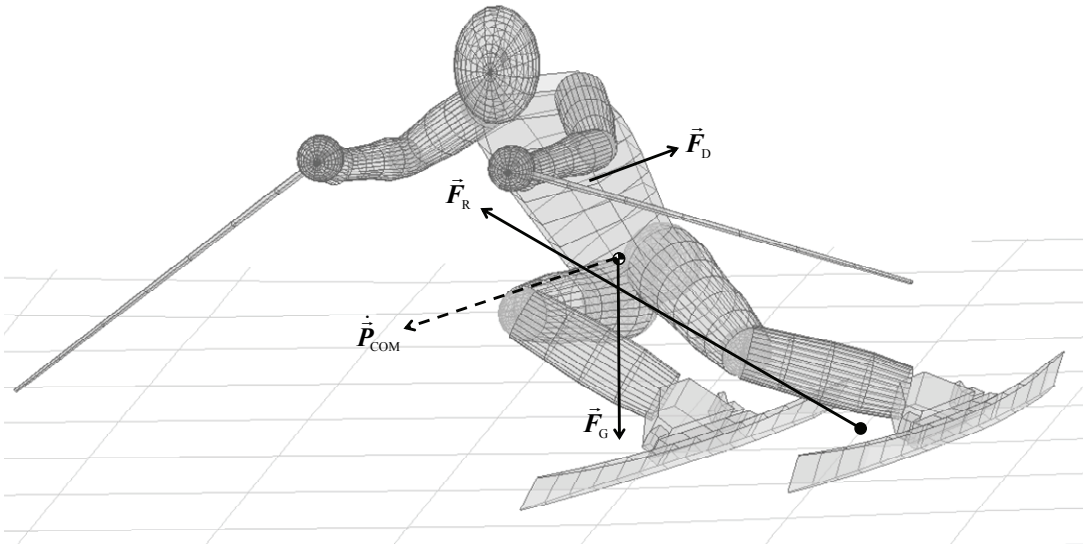

FIGURE 2.2. The external forces acting on a skier during turning. $\vec{F}_R$, $\vec{F}_D$, and $\vec{F}_G$ are the snow reaction force, air drag force, and gravitational force, respectively. $\dot{\vec{P}}_{COM}$ is the center of mass velocity vector. Note that $\vec{F}_R$ is indicated here as acting at a point midway between skis. In reality, $\vec{F}_R$ is the sum of reaction forces acting through both skis. The true point of force application will thus be dependent upon the force distribution between skis.

SKI AND SKIER TRAJECTORIES (Figure 2.1, Boxes F and G)

The snow reaction force and the gravitational force act together to determine the ski's trajectory on the snow surface (Box F). The turning ski then provides the platform that the skier can use to change her trajectory and speed (Box G). A dashed line is placed at the intersection between ski and skier trajectories to indicate that at some points during the turn, the skier and skis function as a single unit and large snow reaction forces act to turn both skis and skier together. In other portions of the turn, however, the skis and skier are loosely coupled and travel to a certain degree independently. As a result, any reaction force from the snow acts to change the ski's trajectory but has less influence on the skier. At these time points, the skier's trajectory is primarily under the influence of the air drag and gravitational forces.

SKI ORIENTATION (Figure 2.1, Box F)

Ski orientation refers to the placement and orientation of the ski relative to both the snow surface and the skier. Parameters of ski orientation collectively play an important role in determining the nature of the ski-snow interaction and the effect that it will have on both the ski's and the skier's motion. The ski edge angle (θ), defined as the angle between the ski base and the local plane of the snow surface (Lieu, 1982; Lieu & Mote, 1985), is important in determining the ski's turning behavior. Closely related to the ski's edge angle is the angle of the applied force vector to the ski's base. Referred to as the "platform angle" (LeMaster, 2009, p. 19)[1], this angle plays an important role in determining whether the engaged ski edge will hold laterally on the snow surface.

The ski attack angle (φ) is defined as the angle between the ski's direction of motion and its longitudinal axis (Lieu, 1982; Lieu & Mote, 1985) and characterizes the skidding

[1] The "platform angle" was earlier referred to as the "critical edge angle" (LeMaster, 1999, p. 20).

component of the ski's motion over the snow surface. A related parameter is the center of mass attack angle (λ) which is the angle between the center of mass velocity vector and the ski's longitudinal axis (Müller et al., 1998). The center of mass attack angle is important in determining not only the magnitude of the snow reaction force, but also the relative degree to which the reaction force turns and slows the skier's motion.

Due to the low friction between ski and snow, the snow reaction force acts approximately perpendicular to the ski's base along its longitudinal axis (Brown, 2009; Hirano & Tada, 1996). Thus, the angle between the ski's longitudinal axis and the slope horizontal (β) characterizes the orientation of the snow reaction force relative to the gravitational force, which, in turn, is important in determining the size of the snow reaction force necessary to achieve a certain turn radius.

SKI LOADING (Figure 2.1, Box G)

The magnitude of ski loading refers to the size of the total snow reaction force. The force application point refers to the point along the ski's longitudinal axis where the skier applied force acts, which is thought to be an important factor affecting the ski's turning behavior.

SKIER ACTIONS (Figure 2.1, Box H)

The skier's actions are directed towards both controlling the ski's orientation (Box F) and regulating its loading characteristics (Box G). Skier lateral actions refer to those whose purposes include regulating the ski edge angle, aligning the body segments to resist external forces and inclining the center of mass into the turn to balance against those forces. Skier rotary actions comprise those taken by the skier to regulate the rotary motion of the skis. In some instances, this may include upper body actions such as pole planting. Skier vertical actions refer to those taken by the skier to regulate the degree of loading between ski and snow. And finally, skier fore/aft actions are defined

as those actions taken to regulate the distribution of pressure along the ski snow interface.

ADAPTATION (Figure 2.1, Box I)

Turning technique in alpine skiing involves a continual process of adaptation to the surrounding environment. The skier senses the nature of the ski-snow interaction and adapts her movements to guide her trajectory in the desired direction and to regulate her speed.

PERFORMANCE TIME (Figure 2.1, Box J)

Skier performance is presented as resulting from a balance between skier trajectory characteristics and speed. The balance point in this interaction is expected to be both complicated and dependent upon the external conditions as well as individual factors and preferences.

MODEL LIMITATIONS

As with any model, this one is also an over-simplification of what in reality is a much more complicated process. For instance, from a holistic, practitioner point of view, it is often difficult to separate out skier's actions into the lateral, vertical, fore/aft, and rotary categories given here. Actions will typically involve aspects of all categories and influence both ski orientation and loading characteristics at the same time. For instance, Joubert's definition of "avalement" (Joubert, 1978/1980, p. 301) is a technique that involves skier vertical actions (a rapid flexion of the hips and lower back), fore/aft actions (a forward displacement of the feet), and rotary actions that combine synergistically so that the whole is indeed greater than the sum of the parts. Despite this weakness, the model does achieve its purpose in helping to organize a complex reality into a format that can be studied.

2.2 RESEARCH OBJECTIVES AND QUESTIONS

Based on the Immersion Phase of this project, and the model of turning technique developed in this phase, a motion analysis investigation was designed to examine the performances of a group of highly-skilled skiers during slalom race simulations. The general aim of this investigation was to describe and explore the various components of the aforementioned model for this select group of athletes. Towards this end, skier performances were captured on two different courses—set with 10 and 13 m linear distances—in the hope of gaining deeper insight into skiing technique by comparing how this group of skiers adapted to the two conditions. These course settings in particular were chosen as they span the gate distances skiers normally encounter in competition. Research questions were aimed at comparing skier kinematic and kinetic characteristics for the two courses and at clarifying some of the interactions between selected kinematic and kinetic characteristics.

KINEMATIC OBJECTIVE AND QUESTION

Describe ski and skier kinematic characteristics concerning trajectory, speed, ski orientation, and skier actions.

How do ski and skier trajectories interact?

Are ski and skier kinematic characteristics different for slalom turns on courses with 10 and 13 m linear gate distances?

KINETIC OBJECTIVES AND QUESTIONS

Describe the timing and magnitude with which the snow reaction force and air drag force act on the skier during slalom turns on courses with 10 and 13 m linear gate distances.

Are snow reaction force and air drag force characteristics different for slalom turns on courses with 10 and 13 m linear gate distances?

Describe the patterns of mechanical energy dissipation during slalom turns on courses with 10 and 13 m linear gate distances.

Are mechanical energy dissipation patterns during a turn cycle different for 10 and 13 m courses?

What are the relative contributions of the snow reaction force and air drag force work to the total mechanical energy dissipated by the skier?

INTERACTION OF PERFORMANCE AND MECHANICAL CHARACTERISTICS QUESTIONS

Are ski and skier kinematic characteristics related to mechanical energy dissipation during slalom turns on courses with 10 and 13 m linear gate distances?

Are ski and skier kinematic characteristics related to performance time on slalom courses with 10 and 13 m linear gate distances?

Is mechanical energy dissipation related to performance time on courses with 10 and 13 m linear gate distances?

In the following chapter, a review of the skiing technique literature is given, exploring each of the main components of the aforementioned technique model and giving the reader an overview of the background literature regarding this project's research objectives.

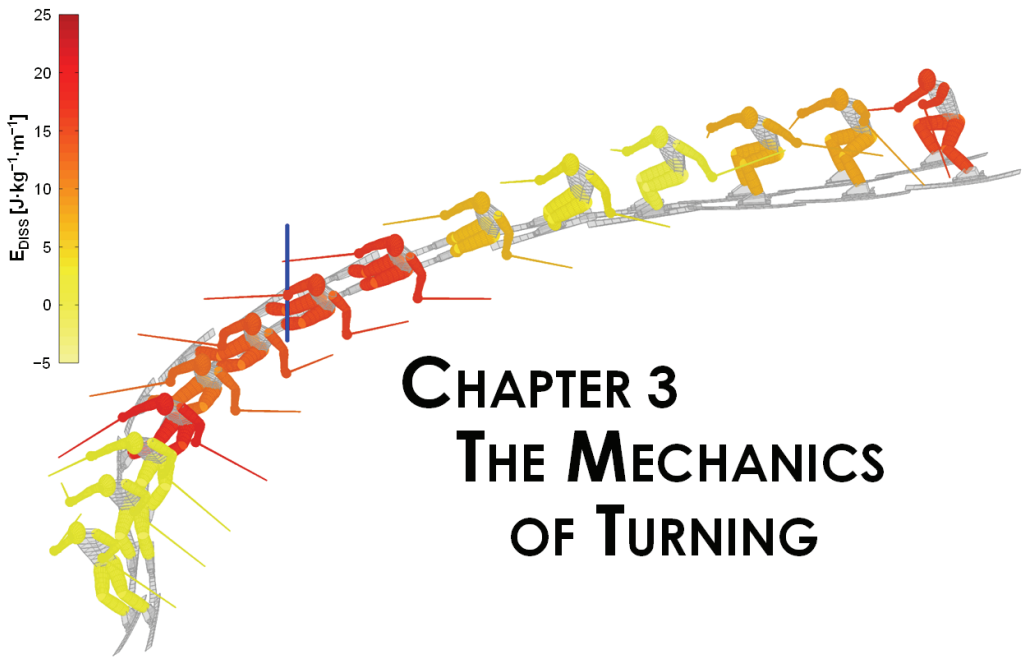

CHAPTER 3
THE MECHANICS OF TURNING

CHAPTER 3. THE MECHANICS OF TURNING

"Years ago I read an article about a successful race car driver that changed the way I thought about skiing. The driver said that everything he did behind the wheel was motivated and judged by the effect on the four patches of contact his tires made with the pavement. Since then, I have come to think that every element of ski technique should be evaluated in terms of how it affects our interaction with the snow. We turn or slow down because the snow pushes on us and our skis in a particular way, and so we manipulate our skis and align our bodies in a particular way to extract and balance against the force from the snow."(LeMaster, 1999, p. 3)

3.1 INTRODUCTION

When I first read the above quote, I had already been working as an alpine coach for a number of years. I can remember that at the time, we (coaches) often talked about coaching athletes based on the intended effect in skiing, as opposed to the skier's movements alone. This was certainly not a revolutionary or even new concept in technique training. In the motor learning literature, a person's "movements" are often differentiated from their "actions." Whereas an action is defined as a motor task that has a specific goal or purpose to achieve, movements are the specific limb motions that a person uses to accomplish this task (Magill, 2007). This is an important distinction that has implications for coaching practice. How athletes move to achieve the same "action goal" (Magill, 2007, p. 5) is likely to be both highly individual as well as situation-specific.

In retrospect, I must admit that at the time I did not understand the true meaning of coaching based on the "action goal" of the skier's movements, at least as it related to skiing technique. In fact, I am not even sure if I understood what the action goals were. It was not until I read LeMaster's (1999) text that I really began to understand turning technique as a complex interaction between the skier, the equipment, and the snow. In fact, I have now begun to understand this interaction—and the athlete's ability to regulate it—as the very key to skiing fast. It is the ski's interaction with the snow that provides the platform from which the skier controls both her direction of motion and speed. The placement of the ski-snow interaction at the center of the turning technique model developed in the Immersion Phase of this project (Figure 2.1, p. 10) is meant to reflect this importance. Seen in this way, the role of skier actions in turning is to manipulate the skis' orientation and loading so as to regulate the magnitude and direction of the reaction force arising from the resulting interaction with the snow surface.

The aim of this chapter is to review the current theoretical and scientific knowledge regarding the various components of the aforementioned model. To this end, this chapter is organized into three main sections. The mechanics of the interaction between ski and snow are described in the first part, including a review of the corresponding research literature. Although this dissertation is ultimately a study of skier actions, this section is of central importance as it defines the intended effects of a skier's actions and thereby gives us insight into why skiers perform the actions they do. This is followed in the second section by a presentation of the actions skiers use to regulate the ski-snow interaction, based to a large extent on key practitioner textbooks on skiing technique. The main focus in this part is to understand the mechanics of how skier actions create the intended effects at the ski-snow interaction. Finally, the available research literature regarding turning technique mechanics is reviewed in the third section.

3.2 THE MECHANICS OF THE SKI-SNOW INTERACTION

Grasping the mechanics of how the ski interacts with the snow surface lays the foundation for understanding the purpose of an athlete's actions. The intention of the following section is therefore to give the reader a solid understanding of the ski-snow interaction mechanics as a basis for studying how athletes manipulate this interaction through their technique. In terms of the model, our focus will be directed towards the central portion that is highlighted in Figure 3.1 and which, to a certain extent, can be regarded as representing the specific goals or effects athletes strive to achieve through their actions. In particular, we will examine how the ski's characteristics, orientation, and loading affect the interaction of the ski with the snow surface and, consequently, the ski's turning behavior and trajectory.

When describing the ski's motion along the snow surface, two processes are generally recognized, namely, carving and skidding. During carving, the ski shovel digs into the snow surface, creating a groove in which the rest of the ski follows (Federolf, 2005; Lieu & Mote, 1985). By definition, a point along the ski's edge that is carving is said to follow in the track cut by proceeding ski segments with minimal or no lateral displacement (Brown & Outwater, 1989; Brown, 2009; Lieu, 1982; Lieu & Mote, 1985; Renshaw & Mote, 1989). In contrast, a ski that is sliding sideways across the snow surface as it moves forward is said to be skidding (LeMaster, 1999). A point on the ski's edge that is skidding does not follow in the path of proceeding points but rather shears through new snow as it moves across the snow surface (Brown & Outwater, 1989; Brown, 2009; Lieu, 1982; Lieu & Mote, 1985).

In practitioner terms, an entire ski is often described as either skidding or carving. However, such a classification is an oversimplification as both carving and skidding can occur at the same time along different segments of a ski's length. "Complete skidding" and "complete carving" thus lie at the two extremes of a continuum. When

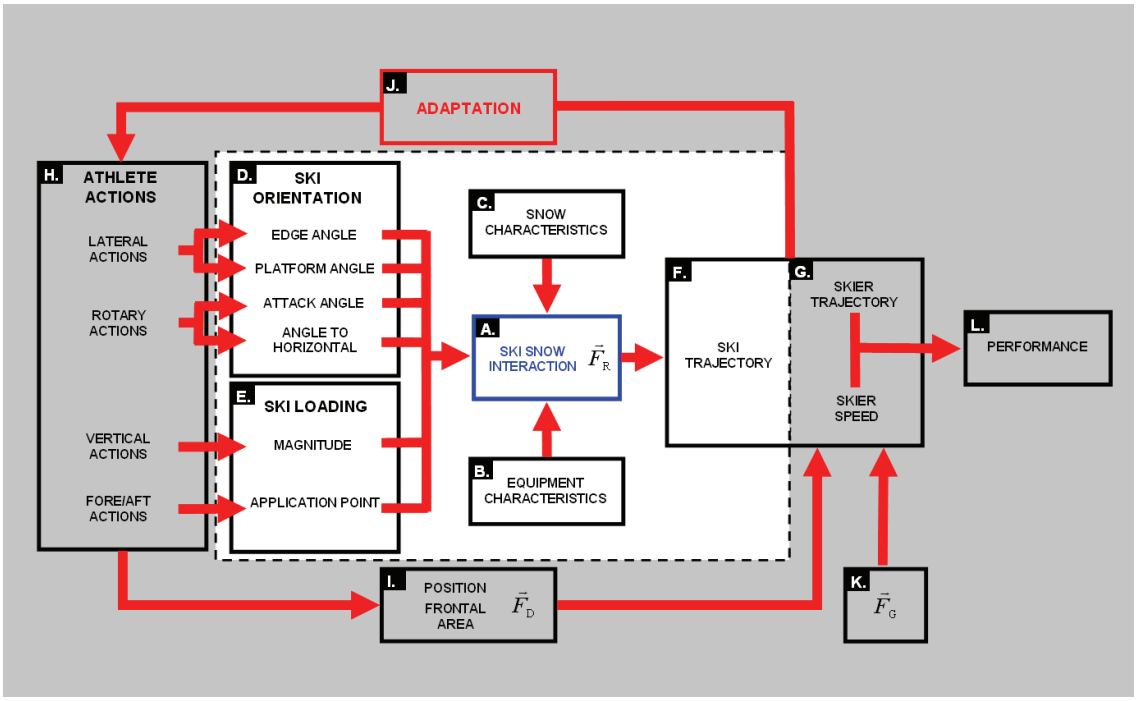

FIGURE 3.1. The conceptual model of turning technique in alpine ski racing developed during the Immersion Phase of this project with emphasis placed on the core factors influencing the mechanics of the ski-snow interaction.

each point along the entire ski's length is cutting new snow, the entire ski is said to be skidding (Brown & Outwater, 1989; Lieu & Mote, 1985). On the other hand, "complete carving," where every point along the ski's length follows in the track of proceeding points, probably never occurs in practice for reasons which will be described shortly.

The following presentation of ski-snow interaction mechanics is divided into four main parts. In the first, ski characteristics are defined which are important for understanding the interaction between ski and snow (Figure 3.1, Box B). In the following two parts, the mechanics of the two extremes of the skidding/carving continuum are presented. Particular attention is directed towards understanding how the ski's orientation and loading characteristics (Figure 3.1, Boxes D and E, respectively) influence the ski-snow interaction (Box A) and, ultimately, the ski's trajectory (Box F). In the final part, the mechanics of the transition from skidding to carving are described, a topic which has not received a lot of attention in the research literature but which is of practical importance.

SKI CHARACTERISTICS

Skis have both geometrical and physical properties which influence their behavior and are thus important to consider when studying the ski-snow interaction. Some of the more central geometrical and physical ski characteristics are defined here.

SKI GEOMETRICAL PROPERTIES

First, a ski's length is measured in several ways depending on the intended use. One common measure is the so-called chord length, defined as the straight line distance from the tip to the tail (Howe, 2001; Lind & Sanders, 2004). This is not a very functional measure of ski length, however. A more important measure in terms of how the ski will perform on snow is the contact—or running surface—length (C) (Howe, 2001; International Organization for Standardization [ISO], 2003; Lind & Sanders, 2004)

which represents the length of the ski running surface that will be in contact with the snow when pressed flat against a planar surface.

The ski's width changes continually along its length giving it a smooth, curved edge profile referred to as the ski's sidecut (Howe, 2001; ISO, 2003). Three widths of particular importance in studying how the ski will perform on snow are (1) the maximum width at the shovel (W_S); (2) the minimum width at the waist (W_W), also referred to as the nominal width; and (3) the maximum width at the tail (W_T).

Ski's are typically constructed with slightly wider shovels than tails, a characteristic referred to as the ski's taper (Lind & Sanders, 2004). Taper (T) can be calculated knowing the shovel and tail widths according to the formula (ISO, 2003):

$$T = \frac{W_S - W_T}{2} \qquad [3.1]$$

The ski's sidecamber (SC) is the distance between the ski at the narrowest part (waist) and a straight line between the tail and the shovel (Federolf, 2005; Hirano & Tada, 1996; Kaps, Mössner, Nachbauer, & Stenberg, 2001; Lind & Sanders, 2004). The sidecamber can be determined knowing the tail, shovel, and waist widths according to Howe (2001):

$$SC = \frac{\left(W_T + W_S - 2W_W\right)}{4} \qquad [3.2]$$

The sidecut radius (R_{SC}) refers to the radius of a circle that intersects the side of the ski at the shovel, waist, and tail points while the ski is laying flat on a planar surface (Kaps et al., 2001; Lind & Sanders, 2004). Equation [3.3] can be used to estimate R_{SC} (Howe, 2001):

$$R_{SC} = \frac{C^2}{8SC} \quad [3.3]$$

where C is the contact length and SC is the sidecamber as calculated in Equation [3.2]. R_{SC} should be seen as an approximation however, as the sidecut profile probably is not a true circle (Howe, 2001; Lind & Sanders, 2004). Further, it is important to recognize that R_{SC} in itself does not correspond to an actual turn radius, although it does influence the degree to which the ski will deform when edged and loaded which, in turn, is an important factor in determining turn radius (Federolf, 2005; LeMaster, 1999).

SKI MECHANICAL PROPERTIES

Flexural stiffness refers to the ski's resistance to longitudinal deformation. Primarily a function of the ski's width, thickness, and the materials used in its construction (Federolf, 2005; Howe, 2001; Lind & Sanders, 2004), the ski's flexural stiffness varies along its length. In addition, the ski is pre-stressed during construction as its layers are glued together causing the unloaded ski to take on a bent shape that is referred to as camber (Federolf, 2005; Howe, 2001; Lind & Sanders, 2004). Together with the flexural stiffness distribution, the ski's camber affects the distribution of pressure under the ski's running surface when it is loaded (Federolf, 2005; Howe, 2001; Lind & Sanders, 2004). For example, given two skis with equal bending stiffness characteristics but differing amounts of camber, the ski with greater camber will distribute a greater portion of the load to the ski's extremities and thus demonstrate a flatter running surface pressure distribution when loaded.

Torsional stiffness refers to the ski's ability to resist torsional deformation about its longitudinal axis (Howe, 2001; Lind & Sanders, 2004) and plays an important role in determining how aggressively the ski tip and tail interact with the snow when the ski is edged (LeMaster, 1999). Flexural stiffness, camber, and torsional stiffness all have to be balanced to give the ski its desired performance characteristics (Lind & Sanders, 2004).

In the following sections, we will examine how the ski's geometrical and physical properties play an important role in determining the ski's behavior on snow.

CARVING SKI MECHANICS

There is a great deal of research literature that has focused on developing numerical simulations of the carving and skidding processes. Understanding how investigators have approached the problem of modeling these processes is helpful to understanding the nature of the ski's interaction with the snow, so a review of this literature is included in this discussion. Prior to presenting the actual mechanics, it is important to define reference systems for describing the ski's orientation and motion.

SKI REFERENCE SYSTEMS

To describe a ski's motion and orientation in space, Lieu (1982) introduced a system of two accelerated coordinate systems attached to the center point of a moving ski (Figure 3.2). The Ski Coordinate System EFG defines the orientation of the ski within an inertial reference frame, XYZ. $\hat{\boldsymbol{E}}$ is oriented parallel to the undeformed ski's longitudinal axis, while $\hat{\boldsymbol{F}}$ and $\hat{\boldsymbol{G}}$ are directed lateral and normal to the ski sole surface, respectively.

The E′F′G′ coordinate system, also originating at the ski center point, defines both the direction of ski motion as well as the orientation of the local snow surface. $\hat{\boldsymbol{E}}'$ is parallel to the projection of the ski center velocity vector onto the local plane of the snow surface, $\hat{\boldsymbol{G}}'$ is normal to the local snow surface, and $\hat{\boldsymbol{F}}'$ is both normal to the projected trajectory and lies in the plane of the local snow surface.

The three angles θ, φ, and ψ specify the ski's orientation relative to the snow surface and its direction of motion. θ is the "edge angle" between the plane of the local snow surface and the running surface of the ski. The ski's "skew angle" (φ) is the angle between the ski's longitudinal axis and the center point's velocity vector in the plane of

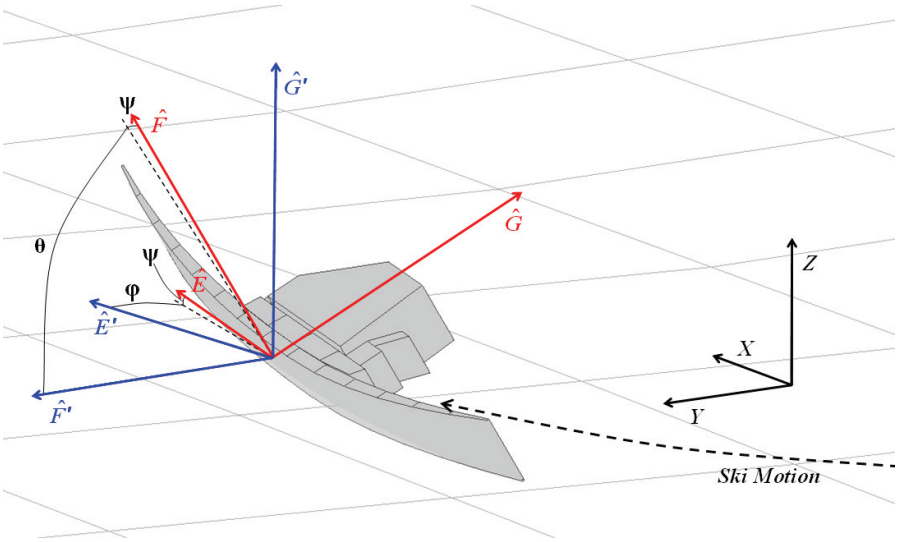

FIGURE 3.2. The Ski Coordinate System (EFG) and the Ski Velocity Coordinate System (E′F′G′) as adapted from Lieu (1982). See text for details.

the snow surface and will here be referred to as the ski's angle of attack. While φ represents the whole ski angle of attack, the local angle of attack at each position along the ski's length varies according to the ski's geometrical properties, its deformed shape under edging and loading, and its rotational and translational motion relative to the snow surface (Hirano, 2006; Hirano & Tada, 1996; LeMaster, 1999; Tada & Hirano, 2002). There are typically larger local attack angles on the ski forebody than on the ski afterbody, a fact that plays an important role in the ski's turning behavior. Finally, the ski's "tilt angle", ψ, is the angle between the ski's longitudinal axis and the local plane of the snow surface.

While the three aforementioned angles characterize the ski's orientation relative to the snow surface, two other angles are defined in the literature to describe the ski's orientation relative to the skier. In addition to the ski's own angle of attack (φ), the skier's momentum also has an angle of attack on the ski's longitudinal axis, referred to in this dissertation as the center of mass attack angle, λ. Originally described as the "downhill ski to movement direction angle" by Müller et al. (1998, p. 547), and also as the "steering angle" by LeMaster (1999, p. 22), this angle is important in determining the magnitude of the snow reaction force and the degree to which it acts to either turn or slow the skier.

In addition, LeMaster (2009) defines the platform angle (γ) as the angle between the sidewall of the groove that the ski cuts into the snow and the applied force vector from the skier. The platform angle is an important factor in determining whether a carving ski will hold or skid.

Chapter 3

THE FORCES OF CARVING

The external forces acting on a carving ski at a position E along its longitudinal axis include the gravitational force $\vec{F}_G(E)$, the applied force from the skier $\vec{F}_A(E)$, and the reaction force from the snow surface $\vec{F}_R(E)$ (Figure 3.3 A)[2,3]. When a ski is turned on edge and loaded onto the snow surface, the applied force from the skier is transmitted from the boot-binding-plate system and distributed along the ski's length according to the ski's geometrical and physical properties. To balance the local applied force, a local snow reaction force $\vec{F}_R(E)$ arises from a combination of (a) the snow's resistance to compaction, (b) the snow's resistance to cutting, (c) the snow's resistance to acceleration (inertia), and (d) friction between the ski base and the snow surface.

The component of $\vec{F}_R(E)$ due to snow penetration ($\vec{F}_P(E)$) acts normal to the snow surface and arises primarily as a result of snow resistance to compaction (Brown, 2009) (Figure 3.3 B). Based on experimental measurement of ski penetration forces, $\vec{F}_P(E)$ has been shown to increase linearly with increasing penetration depth ($D_P(E)$) for low ski edge angles (Federolf, 2005; Federolf et al., 2006; Federolf et al., 2004). At edge angles above 30° to 45° however, Federolf found that the process of snow penetration is characterized by periods of compaction interspersed with random snow fracturing processes that result in temporary unloading. The random nature of these fractures makes their incorporation into mathematical models of $\vec{F}_P(E)$ challenging. As a result, $\vec{F}_P(E)$ is typically modeled as a linear function of penetration depth in numerical simulations, even though it is known that this is somewhat of an oversimplification.

---

[2] An air drag force also acts on the ski, but in studying turning mechanics this force is normally considered to be small and negligible.

[3] Note that while the total snow reaction force acting on the skier is distributed between the two skis, the following discussion will be limited to the component of the total snow reaction force acting on only one of the skis.

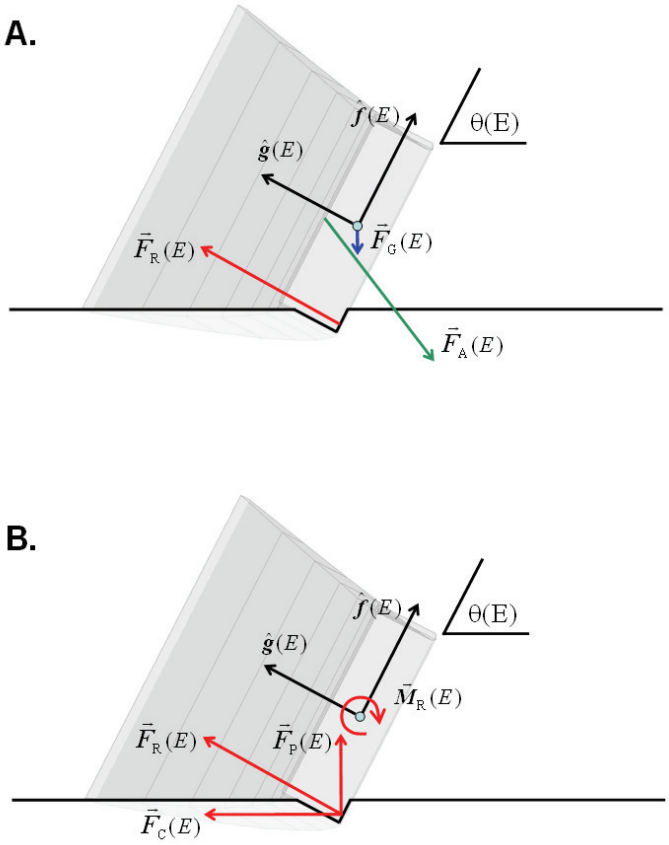

FIGURE 3.3. Definition of the forces acting on a carving ski cross-section. (A) Free body diagram of a carving ski cross-section at point E along the ski's longitudinal axis. θ(E) is the local ski edge angle. $\vec{F}_A(E)$, $\vec{F}_R(E)$, $\vec{F}_G(E)$ are the skier applied force, snow reaction force, and gravitational force acting at point E, respectively. (B) Free body diagram indicating the decomposition of the snow reaction force into penetration $\vec{F}_P(E)$ and cutting $\vec{F}_C(E)$ components. $\vec{M}_R(E)$ is the reaction force moment.

An important factor determining $\vec{F}_P(E)$ during carving is the plastic nature of snow and ice surfaces which can readily be observed by the fact that deformations remain in the snow surface after a penetrating object has been removed. For a carving ski, this means that points on the ski afterbody that travel in the indent created by the prior passage of more heavily loaded portions of the ski will be relatively unloaded in penetration and that $\vec{F}_R(E)$ at these points will be determined primarily by the snow's resistance to shear. Kaps et al. (2001) and Mössner et al. (2005) have proposed a hypoplastic force-penetration relationship to account for this characteristic of snow which seems to have gained acceptance in the research community and is now included in many numerical simulations of the carving ski-snow interaction (Casolo & Lorenzi, 2001; Federolf, 2005; Heinrich, Kaps, Mössner, Schretter, & Nachbauer, 2009; Heinrich, Mössner, Kaps, Schretter, & Nachbauer, 2005; Mössner et al., 2006; Mössner, Heinrich, Kaps, Schretter, & Nachbauer, 2009).

The cutting component of the snow reaction force ($\vec{F}_C(E)$) acts parallel to the snow surface and arises from the snow's resistance to shear (Brown, 2009; Lieu, 1982; Lieu & Mote, 1985; Renshaw & Mote, 1989). It is this component of the snow reaction force that causes the acceleration of the turning ski and skier. $\vec{F}_C(E)$ acts normal to the cutting ski edge and its magnitude is a function of a number of factors including snow surface shear strength, the penetration depth, the edge angle, the length of ski engaging the snow, and the transverse friction between ski and snow (Brown, 2009; Lieu, 1982; Lieu & Mote, 1985; Mössner et al., 2009; Renshaw & Mote, 1989).

Kinetic friction is also a component of the snow reaction force, with friction forces ($\vec{F}_F(E)$) acting tangent to the point E's trajectory and opposite the direction of motion as the ski slides forward through the snow (Mössner et al., 2009). The magnitude of the friction force ($F_F(E)$) is typically modeled as a function of the penetration force, using the equation for Coulomb friction (Heinrich et al., 2009; Heinrich et al., 2005; Heinrich,

Mössner, Kaps, Schretter, & Nachbauer, 2006; Lind & Sanders, 2004; Mössner et al., 2009).

THE RUNNING SURFACE PRESSURE DISTRIBUTION

The pressure between ski and snow varies along both the length and width of the ski-snow contact area as a function of (a) the ski's properties including camber and flexural and torsional stiffness distributions; (b) differences in the local ski edge angle, attack angle, and penetration depth; and (c) the application point of the applied force from the skier. This distribution of pressure, referred to here as the running surface pressure distribution (RSPD), is an important factor determining a ski's turning behavior. The RSPD determines the magnitude and direction of the resultant reaction force and moments acting on the ski that cause it to turn and rotate as it slides forward across the snow, in effect turning itself (Federolf, 2005). This behavior characteristic of skis has been referred to in the practitioner literature as the ski's "directional effect" (Joubert, 1978/1980, p. 258) and the ski's "self-steering effect" (LeMaster, 1999, p. 23). As will be described shortly, much of a skier's actions in turning are focused on regulating the ski's self-steering effect.

Knowing the RSPD, the reaction force acting on the ski can be calculated. As previously described, it is thought that pressure increases linearly across the width of the ski-snow contact area as a function of penetration depth (Figure 3.4 A). The snow reaction force acting at position E along the ski's length can thus be determined by integrating the pressure distributed across the width of the ski snow contact area at that point:

$$\vec{\boldsymbol{F}}_{\mathrm{R}}(\mathrm{E}) = \int \mathrm{p}_{\mathrm{R}}(\mathrm{E},\mathrm{F})\, \hat{\boldsymbol{g}}_{\mathrm{E}}\, \mathrm{dF} \qquad [3.4]$$

where $\mathrm{p}_{\mathrm{R}}(\mathrm{E},\mathrm{F})$ and $\hat{\boldsymbol{g}}_{\mathrm{E}}$ are the ski-snow contact pressure and the local normal vector to the ski base at position (E,F), respectively.

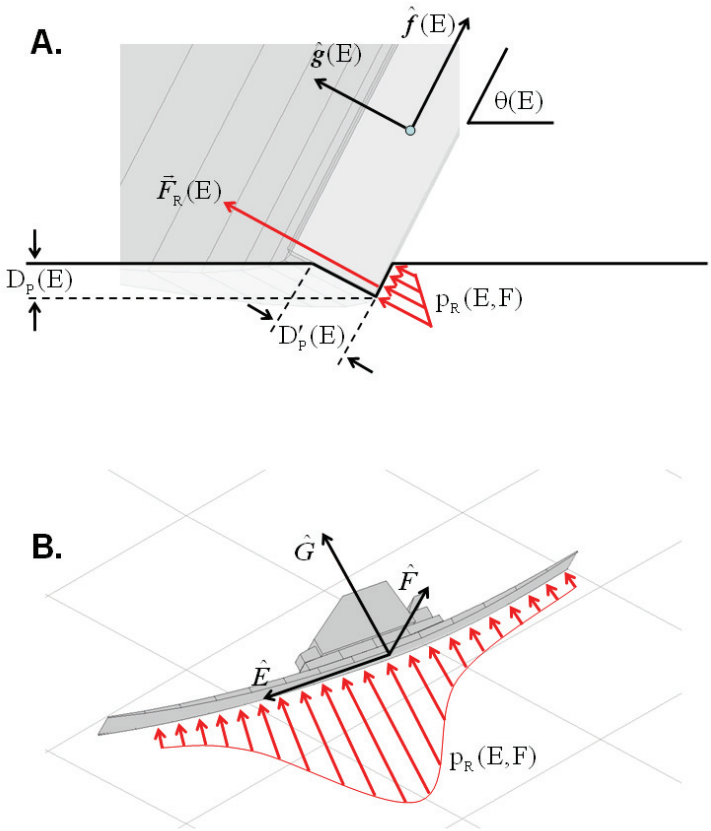

FIGURE 3.4. (A) The distribution of ski-snow contact pressure across the width of the contact area. D_P(E) and D'_P(E) are the penetration depth and penetration distance at point E, respectively. (B) The running surface pressure distribution.

Along the ski's length, pressure under the forebody generally increases progressively from the ski tip, reaching maximal values in the region beneath the boot and binding (Figure 3.4 B) (Scott, Yoneyama, Kagawa, & Osada, 2007). Moving further aft, pressure is then gradually reduced. The snow reaction force for the entire ski can be determined by calculating the double integral of the ski-snow pressure vector field over the entire contact area C:

$$\vec{\boldsymbol{F}}_{\mathrm{R}} = \iint_{\mathrm{C}} \mathrm{p}_{\mathrm{R}}(\mathrm{E},\mathrm{F})\, \hat{\boldsymbol{g}}_{\mathrm{E}}\, \mathrm{dA} \qquad [3.5]$$

where again, $\mathrm{p}_{\mathrm{R}}(\mathrm{E},\mathrm{F})$ and $\hat{\boldsymbol{g}}_{\mathrm{E}}$ are the ski-snow contact pressure and the local normal vector to the ski base at position (E,F), respectively.

Despite its importance in determining the ski's turning behavior, relatively few studies have been conducted where the RSPD has been measured during skiing, likely due to the methodological challenges associated with such measurements. As early as 1970, Piziali (1970) reported on some of the first pressure distribution measurements using skis instrumented with a series of between 8 and 9 semi-conductor pressure transducers mounted along the ski's length, near the edge. It was not before almost 40 years later that a group from Australia and Japan (Kagawa, Yoneyama, Tatsuno, Scott, & Osada, 2009; Scott et al., 2007; Tatsuno, Yoneyama, Kagawa, Scott, & Osada, 2009) followed up Piziali's initial work with a series of studies measuring the RSPD during carved turns. Consistent among these measurements are pressure distributions exhibiting maximal pressures at the boot and a skewed distribution towards the ski forebody during carved turns (Figure 3.5). It is also interesting to note that Tatsuno et al. observed a progressive shift aft of the RSPD over the course of carving turns.

In contrast to direct measurement studies, a large number of numerical simulations of the RSPD have been reported in the literature. These studies have been important in

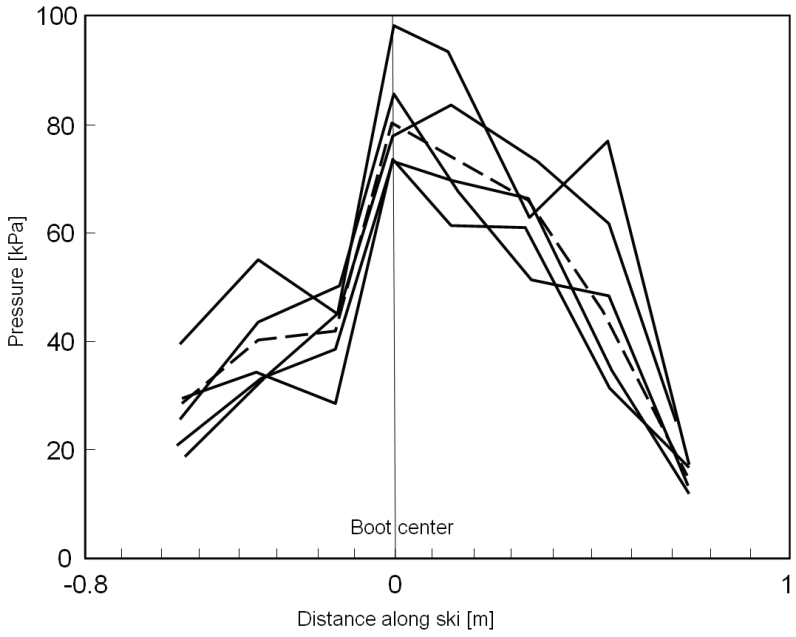

FIGURE 3.5. Experimental measurements of the running surface pressure distribution of a carving ski (adapted from Scott et al., 2007).

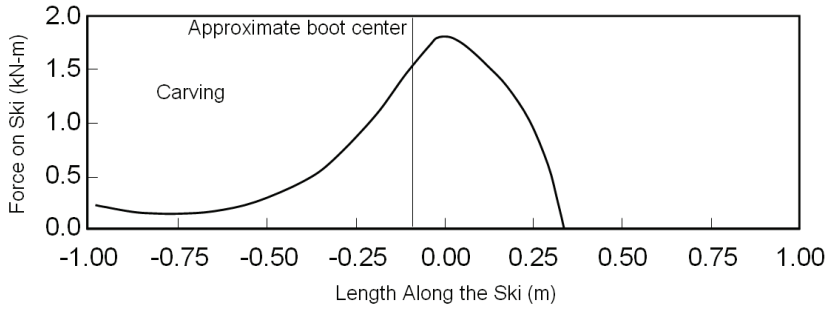

FIGURE 3.6. Numerical simulation of the running surface pressure distribution for a carving ski (adapted from Renshaw and Mote, 1989).

identifying and understanding some of the key factors that influence the RSPD. Lieu (1982), Lieu and Mote (1985), and Renshaw and Mote (1989) predicted pressure distributions for both carved and skidded turns, basing their models on metal cutting theory and force measurements taken during orthogonal ice cutting. For carved turns, they predicted a non-symmetric pressure distribution that was, on the one hand, shifted aft along the ski's longitudinal axis, and on the other hand, skewed forward (Figure 3.6), correlating well with the experimental measurements of the RSPD taken during carved turns (Kagawa et al., 2009; Piziali, 1970; Scott et al., 2007; Tatsuno et al., 2009).

Beginning in 2000, several research groups published the results of numerical simulations examining the influence of ski mechanical and geometrical properties on the RSPD during primarily carved turns. Casolo and Lorenzi (2001) implemented a deformable, elastic snow surface to study the behavior of different types of skis. Kaps et al. (2001) pointed out the importance of taking into account the plastic nature of the snow surface in simulations of the penetration force of carved turns and modeled the RSPD for skis loaded onto a plastic snow surface under static conditions. Heinrich et al. (2005, 2006) and Mössner et al. (2009) implemented a numerical simulation of Bruck, Lugner, and Schretter's (2003) skiing sledge to analyze the influence of a ski's flexural stiffness distribution on its RSPD and turning performance. Federolf (2005) and Federolf et al. (2004) used extensive field measurements to characterize the forces involved during snow surface penetration and to develop a finite element simulation of a carving ski.

These numerical simulation studies have shown the importance of ski flexural and torsional stiffness properties in determining the RSPD as the ski is loaded onto the snow surface. Common to many of these studies are predictions of pressure distributions that are slightly skewed aft (Figure 3.7 A & B), in contrast to the results of Lieu, Renshaw and Mote (Lieu, 1982; Lieu & Mote, 1985; Renshaw & Mote, 1989) and

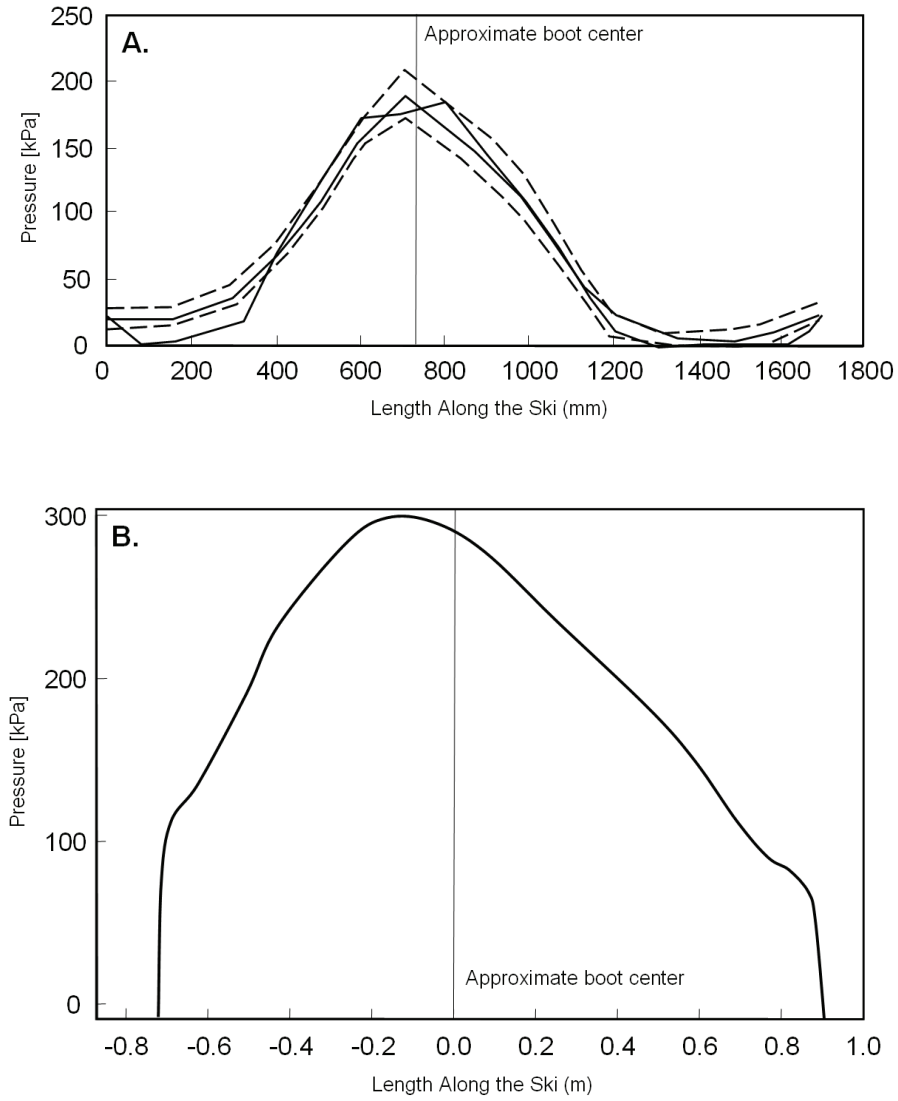

FIGURE 3.7. Example numerical simulations of the running surface pressure distribution for carving skis. Note the difference in distributions observed here and those presented in Figures 3.5 and 3.6. (A) Adapted from Casolo and Lorenzi (2001). (B) Adapted from Kaps et al. (2001).

the experimental studies (Kagawa et al., 2009; Piziali, 1970; Scott et al., 2007; Tatsuno et al., 2009). The reason for this difference is unclear but is perhaps related to limitations in modeling the mechanics of a forward moving ski as it establishes a groove in the snow surface.

GROOVE FORMATION AND THE FUNCTION OF THE SKI FOREBODY

An important aspect of the ski-snow interaction in carving is the formation of the groove in which the ski will carve. As the forebody of an edged and loaded ski passes over a point on the snow surface, the first points along the edge to contact the snow are not heavily loaded and are often associated with a portion of the ski that is relatively soft in torsion and flexion. Accordingly, this portion of the ski may not penetrate the snow, but rather skid across the surface, vibrating in both flexion and torsion. With each passing point of the ski, stiffer portions of the ski forebody meet the new snow and begin to develop enough pressure to finally push the ski into the snow surface. From this point on, the ski continues to push deeper into the snow with each subsequent passing point (Federolf, 2005; Heinrich et al., 2009; Tatsuno et al., 2009). The increasing pressure progressively compresses the snow in the groove sidewall and increases the depth of penetration, both of which improve the groove's resistance to shear in preparation for the high forces which will occur as the boot passes (Mössner et al., 2006; Tatsuno et al., 2009). From the point of maximal pressure, the remainder of the ski is relatively unloaded in penetration and rides in the groove generated by the passage of the forebody.

Seen in this way, the ski forebody does not ever carve—in a very strict sense of the word—since points along the forebody edge will always trace their own trajectory, cutting new snow in the process, as has been predicted in both the research literature (Casolo & Lorenzi, 2001; Lieu, 1982; Lieu & Mote, 1985; Sahashi & Ichino, 1998) and practitioner textbooks (Joubert, 1978/1980). The task of the ski forebody is to dig and

pack a groove of sufficient strength to withstand the forces necessary to turn the skier by the time the middle of the ski passes.

This understanding of ski forebody function raises an important implication for ski design. As the ski's forebody passes over a point in the snow, the groove progressively becomes deeper and the surrounding snow more compact, increasing the groove's resistance to shear. However, too sharp of an increase in the ski flexural and torsional stiffness distributions relative to the groove's developing shear strength will result in skidding (Casolo & Lorenzi, 2001). Thus, as Heinrich et al. (2005) suggest, an important factor to avoid skidding may be an optimization of the match between ski characteristics and the snow surface conditions.

There is some indirect evidence suggesting that this may be the case. Nachbauer, Rainer, Schindelwig, and Kaps (2004) reported on a field study where experienced skiers evaluated the performances of skis with varying stiffness distributions and found that skis with different stiffness characteristics performed better on different slopes. The snow surface conditions were not reported, but if the slopes somehow differed in terrain or snow conditions (which is not unlikely), then these results might reflect how the different stiffness distributions affected the RSPD and ultimately the mechanics of groove formation in each condition. In another example, Lüthi, Federolf, Fauve, and Rhyner (2006) found that plates and bindings act to distribute a greater portion of the running surface pressure towards the ski extremities. They have further suggested that in certain conditions this can be advantageous in that it will decrease the peak pressures in loading that the snow must be able to sustain, thereby reducing the risk of snow failure and skidding. They also point out, however, that the opposite might be true on very hard snow conditions, where a very high pressure may be required to penetrate into the snow surface.

THE CARVING SKI'S TRAJECTORY

Understanding which factors influence the ski's self-steering effect—and how—has been a topic of interest for researchers in skiing mechanics. Early attempts to model the turning radius of a carving ski were based on the geometrical properties of the ski and the resulting shape of the deformed ski edge on the snow surface alone. As a result of its sidecut profile, a ski that is turned onto edge and loaded will bend until the entire edge comes into contact with the snow surface[4]. If pressed onto a planar snow surface, the bent ski's edge will assume approximately the form of a circular arc. Assuming that the snow surface is perfectly rigid and planar, then the instantaneous turn radius of the ski (R_{SKI}) is expected to be a function of the ski's geometrical properties and edge angle alone and can be approximated using the following equation taken from Howe (2001):

$$R_{SKI} = R_{SC} \cos\theta \qquad [3.6]$$

where R_{SC} is the sidecut radius and θ is the edge angle. As Equation [3.6] suggests, one way of decreasing the turn radius is to increase the edge angle. As the ski is turned more onto its edge, it will need to bend more to come in contact with the snow surface resulting in greater ski deformation and a decreased turn radius, a phenomenon that has been demonstrated in a number of studies (e.g., Heinrich et al., 2006). Similarly, it has also been shown that increasing a ski's SC also amplifies the bending deformation of the ski for a given edge angle, thus resulting in a decreased turn radius (e.g., Hirano & Tada, 1996). Despite these results, Equation [3.6] is an oversimplification in a couple of important ways.

[4] It is assumed that the loading force is large enough to bend the ski to meet the snow surface, a requirement that is normally readily fulfilled during turning (Howe, 2001).

First, although the snow surface may be extremely hard in certain situations, it is never perfectly rigid in reality. As previously described, the ski will penetrate into the snow surface to a depth dependent upon the loading force, the snow's resistance to penetration, and the edging angle (Brown & Outwater, 1989; Federolf, 2005; Lieu & Mote, 1985; Tada & Hirano, 2002). This increases the flexural deformation of the ski and thereby reduces R_{SKI} to a value lower than that estimated by Equation [3.6] (Howe, 2001; Kaps et al., 2001). Howe thus proposed a modification to Equation [3.6] to account for non-rigid snow surfaces:

$$R_{SKI} = \frac{C^2}{8\,[(SC / \cos\theta) + D'_p \sin\theta]} \qquad [3.7]$$

where C is the contact length, SC is the sidecut, θ is the edge angle, and D'_p is the penetration distance.[5]

A second limitation of both Equations [3.6] and [3.7] is that they are based on the assumption that the entire length of the ski edge is in contact with the snow and is carving (i.e., that all points along the ski's edge follow in the track of proceeding points). However, it is unlikely that this is ever the case. In reality, certain portions of the ski's edge will always transition between carving and skidding modes depending on the balance between the local running surface pressure, the local edge angle and the local snow's shear strength.

The ski's torsional stiffness distribution plays an important role in this regard as the torsionally soft ski shovel and tail will twist under the moments generated during their interaction with the snow. If the resulting torsional deformations are large enough to

[5] Note that this is the penetration distance as measured normal to the ski sole, and not the penetration depth as measured normal to the snow surface.

reduce the ski's local edge angle below a certain threshold, that portion of the ski will disengage from the snow and begin to skid. LeMaster (1999) explained that this reduces the engaged, carving section of the ski to the middle portion that has less sidecut, in effect decreasing the ski's self-steering effect. This phenomenon may be important in that it allows the skier to carve at much higher turn radii than what Equation [3.6] predicts for low edge angles, as one might require during turn completion. It might also help explain why Wimmer (2001) found only modest correlations (0.39 – 0.57) between ski turn radius, as derived from reconstructed ski trajectories during a motion analysis study of elite skiers, and that calculated using Equation [3.6]. Wimmer reported particularly large differences between reconstructed and predicted turn radii around turn transitions where the actual ski turn radius approached large values and the calculated turn radius approached a limit of R_{SC}.

Even in situations where the rest of the ski edge is carving, it is thought that a certain portion of the ski forebody will always be in a skid modus as the shovel forms the groove in the snow surface in which the rest of the ski follows (Casolo & Lorenzi, 2001; Lieu, 1982; Lieu & Mote, 1985). There is some experimental evidence providing support for this argument.

Several researchers have recently reported observations where carving skis did not follow exactly in the circle defined by the shape of the deflected edge on the snow surface, as both Equations [3.6] and [3.7] assume. Kagawa et al. (2009), Tatsuno et al. (2009) and Yoneyama, Scott, Kagawa, and Osada (2008) experimentally measured ski deformations in carved turns using instrumented skis. Although they did not measure the ski's trajectory during the data collection, they estimated that the actual ski trajectory turn radius was approximately twice that of the radius defined by the deformed ski edge. This they related to the mechanics of groove formation during carving and the idea that the ski forebody does not carve as it ploughs through the snow, establishing the groove.

Based on the results of a finite element simulation of a carving ski, Federolf (2005) reported that the radius the ski actually carved corresponded more to the shape of the ski afterbody than the whole ski, since the ski forebody was bent too much relative to the actual turn radius. This seems to agree well with the work done by Yoneyama, Kagawa, Tatsuno and colleagues (Kagawa et al, 2009; Tatsuno et al., 2009; Yoneyama et al., 2008). As a consequence, Federolf further suggested that instead of using the deformed shape of the entire ski edge to estimate the carving ski's turn radius, that three points along the ski's afterbody should be used. These points consisted of the edge position at the ski boot, a position 5 cm in front of the ski's tail, and a point in the middle between these two points.

Mössner et al. (2009) also found Equations [3.6] and [3.7] to perform poorly in a numerical simulation of carved turns, the cause of which they attributed to skidding portions of the ski. They thus suggested that the ski's trajectory can not be determined by the geometry of the deformed ski edge alone, but rather in combination with the nature of the forces and moments generated at the ski-snow interaction. In other words, to precisely determine the carving ski's turn radius, one needs to measure or calculate the resultant force and moments acting on the ski based on the RSPD. Seen in this way, the geometry of the deformed ski is still important in that it determines the local attack angles along the ski-snow contact area which, in turn, are important in determining the RSPD and ultimately the ski's self-steering effect (LeMaster, 1999).

SKIDDING SKI MECHANICS

THE FORCES OF SKIDDING

Models of skidding ski mechanics are based to a large extent on parallels drawn from metal cutting theory where the ski is seen as a tool that cuts, fractures, and displaces the upper layer of the snow surface as it moves forward, similar to a metal cutting tool on a workpiece (Brown, 2007, 2009; Federolf, 2005; Hirano & Tada, 1996; Lieu, 1982;

Lieu & Mote, 1985; Renshaw & Mote, 1989; Tada & Hirano, 1998, 2002). Similar to carving, local snow reaction forces are generally decomposed into components acting normal to the snow surface, parallel to the snow surface, and kinetic friction (Figure 3.8) (Federolf, 2005; Heinrich et al., 2009; Heinrich et al., 2005; Hirano & Tada, 1996; Lieu, 1982; Lieu & Mote, 1985; Mössner et al., 2006). Both the penetration $\vec{F}_{\mathrm{P}}$ and friction $\vec{F}_{\mathrm{F}}$ components are modeled in a similar manner to that in carving. Also similar to carving, the component of the snow reaction force acting parallel to the snow surface in skidding is referred to as the cutting force $\vec{F}_{\mathrm{C}}$ and it is again this component of the reaction force that provides the necessary acceleration to turn both the skis and skier (Lieu, 1982). However, there are some subtle differences between carving and skidding in terms of the cutting component of the reaction force.

First, the applied force from the skier at a position on the ski that is carving does not exceed the snow's capacity to resist shear and the cutting component of the reaction force is thus generated primarily by the snow's shear strength. In skidding however, the snow's capacity to resist shear is exceeded and the ski cuts through a layer of the snow surface, ejecting loose snow out of its path. The cutting force component thus arises not only from the snow's resistance to shear, but also the sheared snow's resistance to acceleration, or inertia. As the ski overcomes the snow's resistance strength, the ski will accelerate laterally until equilibrium is established between the applied force and the reaction force arising from both the snow's shear strength and inertia (Mössner et al., 2009). To describe this phenomena in numerical simulations, Hirano and Tada (Hirano & Tada, 1996; Tada & Hirano, 1998, 2002) have proposed using models based on metal cutting theory when either the ski is moving slowly, or the snow is very hard, both situations where the snow's resistance to cutting are expected to predominate. However, when the snow is soft, or the ski is moving at a high velocity, they have proposed a so-called "water jet analogy" to emphasize the importance of the forces necessary to accelerate the cut snow.

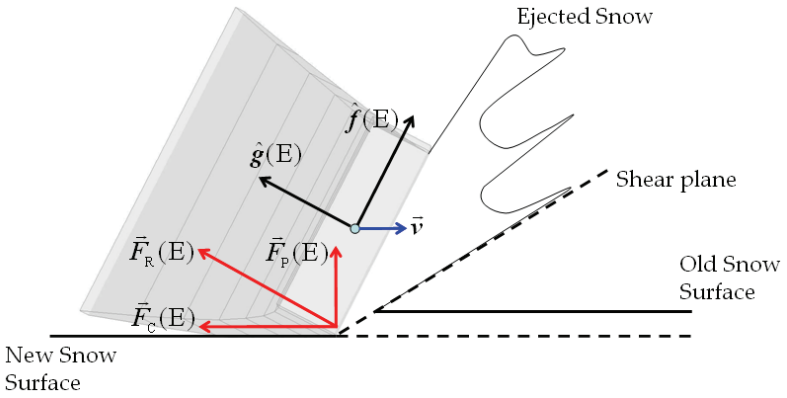

FIGURE 3.8. Free body diagram of a skidding ski cross-section at point E along the ski's longitudinal axis. The decomposition of the snow reaction force into penetration $\vec{F}_P(E)$ and cutting $\vec{F}_C(E)$ components is shown. $\vec{v}$ indicates the ski's velocity vector.

A second important difference between carving and skidding is that while all of the cutting force is used to turn the ski in carving, only the component of the cutting force acting normal to the ski's velocity vector—referred to as the transverse force $\vec{F}_T$ —acts to change it's direction of motion in skidding (Brown, 2009; Hirano & Tada, 1996; Tada & Hirano, 1998, 2002) (Figure 3.9). The remaining horizontal component, $\vec{F}_H$, acts to slow the ski down. Thus, different components of the cutting force are used for either turning or braking the ski's motion, depending upon the size of the ski's angle of attack (φ).

To turn the skier during skidding, the ski edge must penetrate the snow surface to a depth sufficient enough to generate the required shear forces (Hirano & Tada, 1996). In this regard, Brown (2009) has classified types of skidding according to the degree to which snow reaction forces are generated. "Chip formation" occurs when the skidding ski penetrates the snow surface deeply enough to scrape off a layer of snow, generating large forces in the process. "Drifting," on the other hand, describes skidding where the ski does not penetrate into the snow to any appreciable extent and instead slides sideways across the snow surface, generating little or no forces.

THE SKIDDING SKI'S TRAJECTORY

Similar to carving, the shape of the deformed ski edge is indirectly important in determining the ski's turn radius in skidding. The ski's shape on the snow surface influences the gradient of local attack angles acting along the ski-snow contact area. This, in turn, impacts the RSPD and thus ultimately also the reaction force and moments acting to turn the ski as it moves forward across the snow surface. In contrast to carving, however, only the component of the reaction force acting perpendicular to the ski's velocity turns it. Thus, knowing the cutting component of the snow reaction force, a skidding ski's turn radius can be calculated according to Equation [3.8] (Brown, 2009):

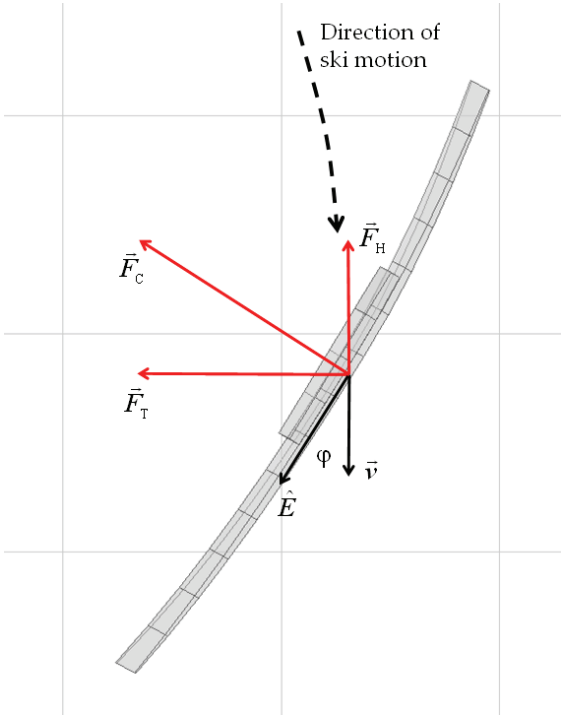

FIGURE 3.9. Free body diagram of a skidding ski from an overhead view showing the decomposition of the cutting force ($\vec{F}_C$) into transverse ($\vec{F}_T$) and horizontal ($\vec{F}_H$) components. $\hat{E}$ is the ski longitudinal axis, $\vec{v}$ is the ski velocity vector, and φ is the whole ski angle of attack.

$$R_{SKI} = \frac{mv^2}{F_C \cos\varphi} \qquad [3.8]$$

where m is the mass, v is the ski's velocity, F_C is the magnitude of the cutting force, and φ is the angle of attack. According to this equation, both increasing the cutting force and reducing the angle of attack will act to reduce the ski turn radius.

THE TRANSITION FROM CARVING TO SKIDDING

Pure carving and skidding, as described in the previous two sections, define the two extremes of a continuum. In reality, much of skiing is likely to transition back and forth between these two modes of ski motion. For instance, a typical transition might be where a skier initiates the turn with skidding and gradually shifts to carving over the course of the turn. While the mechanics of this transition have not been studied rigorously, there are a couple of studies which have looked at this process and have reported findings worthy of note.

Lieu (1982) and Lieu and Mote (1985) modeled the motion of skis through constant radius, constant speed turns and studied the effect of decreasing the ski angle of attack on ski motion. They found that at attack angles of approximately 11° and greater, all points along the ski's length were in a skid mode. The upper panel of Figure 3.10, adapted from Lieu and Mote, shows a skidding ski where each point along the ski's edge traces its own trajectory, cutting new snow in the process. As the angle of attack was lowered to below 9°, Lieu and Mote found that carving initiated at the tail of the ski, although the actual transition occurred at slightly different attack angles depending on the ski's mechanical properties. This is shown in Figure 3.10 B where it can be seen that points along the ski's tail have begun to follow in the track established by proceeding points. Further decreases in attack angle were associated with increased

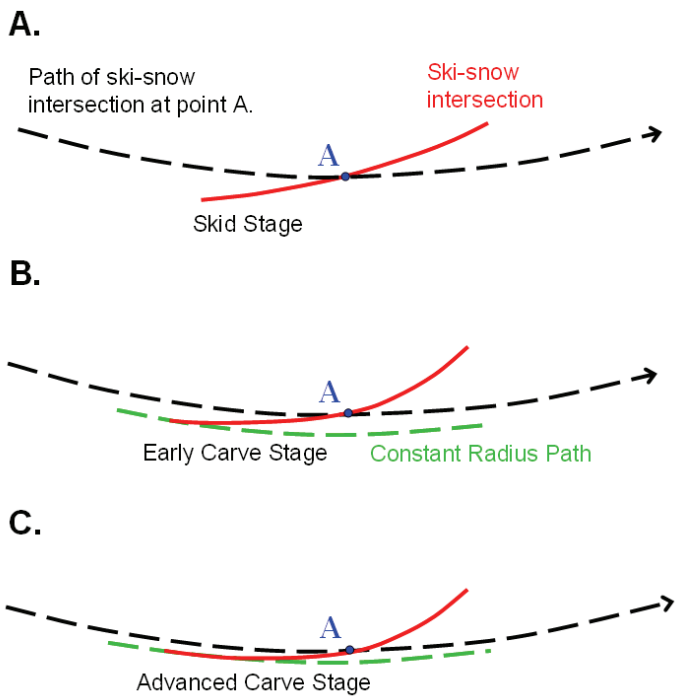

FIGURE 3.10. Lieu and Mote's predictions of edge point trajectories for carving and skidding skis (adapted from Lieu & Mote, 1985). Note that for the skidding ski, all edge points trace their own trajectory. Also, note that even in the most advanced carving stage, ski forebody points still trace their own trajectories.

portions of the ski afterbody transitioning to carving. However, even in advanced carving stages, Lieu and Mote found that carving was limited to the ski's afterbody.

Both Lieu and Mote (1985) and Renshaw and Mote (1989) further examined changes to the running surface pressure distribution (RSPD) during the transition from skidding to carving. During skidding, their models predicted a symmetrical RSPD centered about either the ski center (Lieu, 1982) or a point along the ski forebody (Renshaw & Mote, 1989) (Figure 3.11 A). With the initation of carving along the ski afterbody, the pressure distribution is shifted aft along the ski and skewed towards the ski forebody (Figure 3.11 B and C). This may help explain the results of Tatsuno et al. (2009) who measured the RSPD during carved turns and observed a pattern where the RSPD shifted aft over the course of the turn. If the skier had some small degree of skidding during the first portion of the turn and then transitioned to more carving through the turn, one might expect to see this shift aft in the RSPD according to Lieu, Renshaw, and Mote's measurements (Lieu, 1982; Lieu & Mote., 1985; Renshaw & Mote, 1989).

3.3 THE MECHANICS OF SKIER ACTIONS

It has been suggested that the external forces, ski physical and geometrical properties, and the mechanics of the ski-snow interaction are alone enough to turn the skier with minimal input on the skier's part (Joubert, 1978/1980). To prove this point, Glitsch (2001) completed a series of experiments using a completely passive physical model of a skier consisting of two skis, two legs, and an interconnecting bar. As the model slid down a carpeted incline, the external forces between the skis and carpet surface were able to push the model through a series of alternating turns.

In spite of these observations, skiing completely at the mercy of external forces is probably not very enjoyable and is likely not to be fast in terms of performance. Fortunately, the athlete is able to manage, to a certain extent, these forces so as to turn

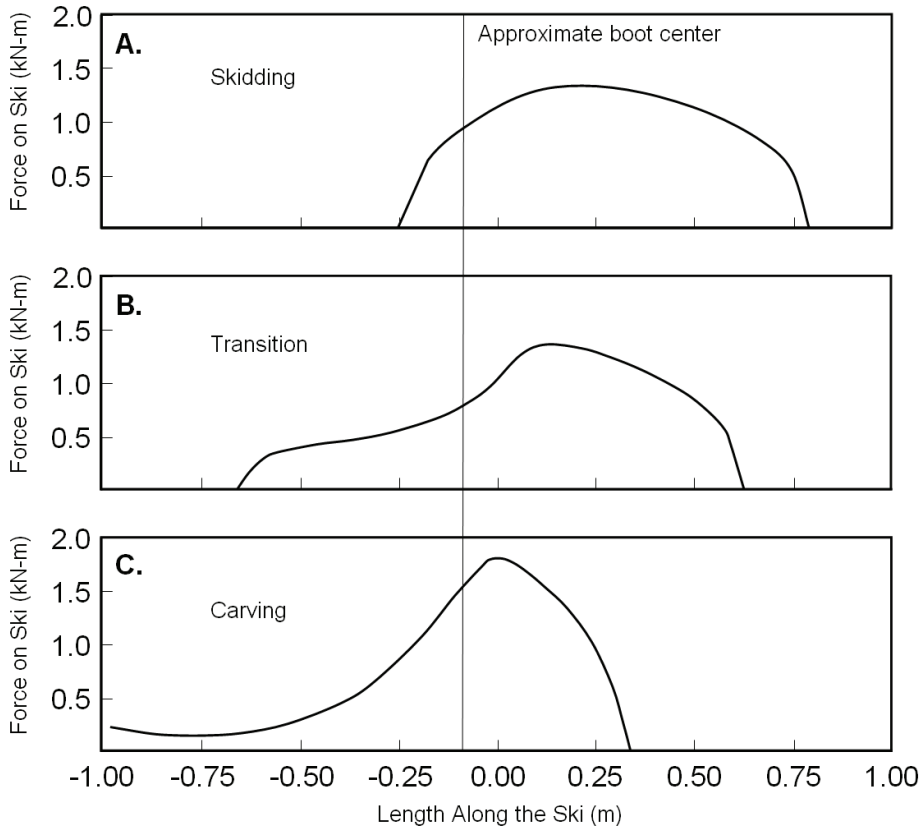

FIGURE 3.11. Predictions of the force distribution along the ski running surface based on a numerical simulation of skidding and carving skis (adapted from Renshaw & Mote, 1989).

where intended while simultaneously controlling speed as needed. This is the essence of turning technique in alpine skiing. The athlete controls the ski's self-steering effect and trajectory, as well as the impact that the ski has on his trajectory and speed, through manipulating the path, orientation, and loading of the skis (LeMaster, 1999; Lind & Sanders, 2004).

In the following sections of this chapter, our focus will shift from the details of the ski-snow interaction, and the central portion of the model, to the actions skiers can take to regulate this interaction (Figure 3.12). Particular attention will be placed on understanding how the skier's actions affect the ski's orientation and loading, thereby influencing the nature of the ski-snow interaction, the resulting reaction force, and the ski's self-steering effect. Whenever possible, the focus of the following discussion is on skier actions as opposed to body movements since, as described earlier, the actual movements used to accomplish actions will not only be highly individual but also situation-specific. Much of the following discussion is based on key practitioner textbooks on skiing technique including the works of Joubert (1978/1980), Major and Larsson (1979/1979), Witherell (1972), Witherell and Evrard (1993), LeMaster (1999; 2009), and Bear (1976), as well as the more technical works of Howe (2001) and Lind and Sanders (2004). Obviously, this selection represents only a small fraction of the available literature in skiing technique. In this regard, a particular limitation of the following discussion is the absence of the German-language literature, owing to the author's somewhat limited language skills.

In the first section, the external forces acting on the skier are re-visited and certain aspects about the nature of these forces that are important to consider in turning technique are presented (Figure 3.12, Boxes A, I, and K). This is followed by an examination of skier lateral, rotary, vertical and fore/aft actions (Figure 3.12, Box H). Particular attention is paid to describing the goals of these actions as described in the literature. In addition, some examples are given to illustrate techniques skiers

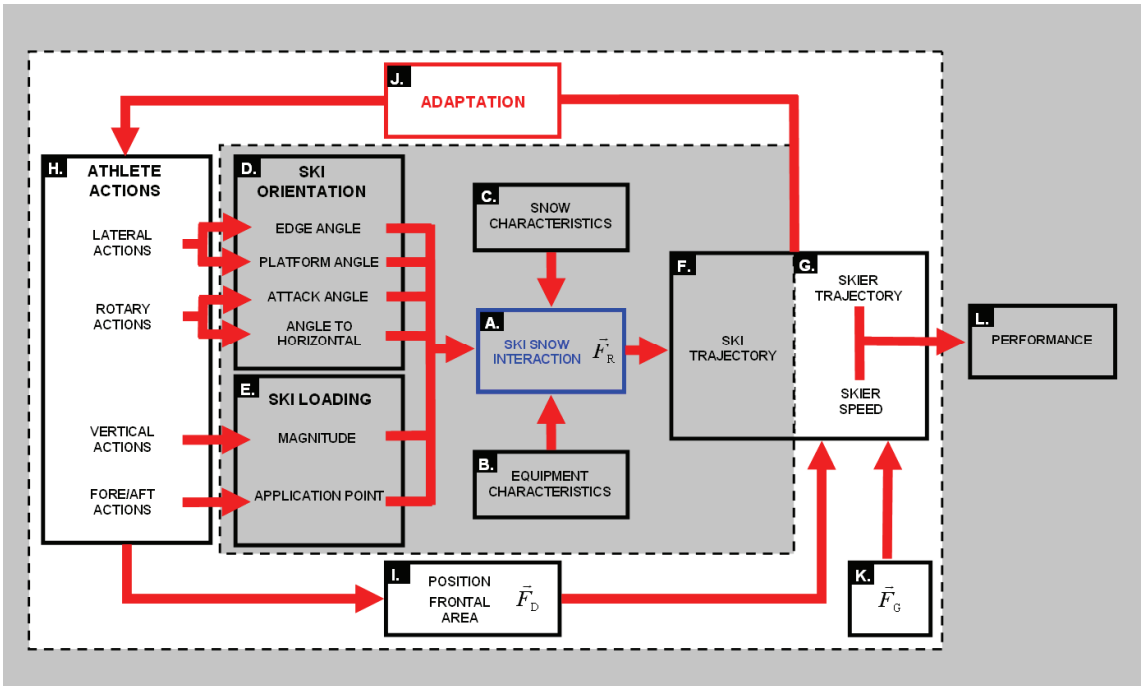

FIGURE 3.12. The conceptual model of turning technique in alpine ski racing developed during the Immersion Phase of this project with emphasis placed on skier actions and trajectory.

sometimes use to achieve these action goals. In the following discussion, the term "ski" is often used without specifying whether it is the inside or outside ski. Unless otherwise indicated, "ski" is used to refer to the outside ski.

THE EXTERNAL FORCES ACTING ON THE SKIER

Although the three external forces acting on the skier ($\vec{F}_G$, $\vec{F}_D$, and $\vec{F}_R$) have been previously introduced in this dissertation (Figure 2.2, p. 13), two aspects of their role in skier technique are important to consider and will therefore be described briefly before moving on to look at specific skier actions. First, Figure 3.13 shows the external forces acting on a skier who is travelling straight down the slope from a side view. From this perspective, it is important to note that the gravitational force acts to accelerate the skier not only down the slope, but also—and just as importantly—towards the snow surface. So, in terms of turning technique, the gravitational force plays an important dual-role. On the one hand, it is the primary force acting to increase the skier's speed which is, naturally enough, very important in terms of racing performance. On the other hand, the gravitational force also accelerates the skier towards the snow, thereby providing much of the force necessary to drive the ski into the snow surface, an essential aspect of the ski-snow interaction that allows the skier to use the snow reaction force to either turn or slow down.

The second important factor to consider is that the relative orientation of the gravitational and snow reaction forces changes over the course of the turn cycle. Figure 3.14 shows these forces acting on a skier from an overhead perspective as she negotiates a turn. In the upper portion of the turn, the gravitational and snow reaction forces act in the same general direction and a component of the gravitational force will help to accelerate the skier in the direction of the new turn. Conversely, in the lower portion of the turn, the gravitational and snow reaction forces act to an extent against each other. For the skier to turn in this portion of the turn cycle, she will be required to

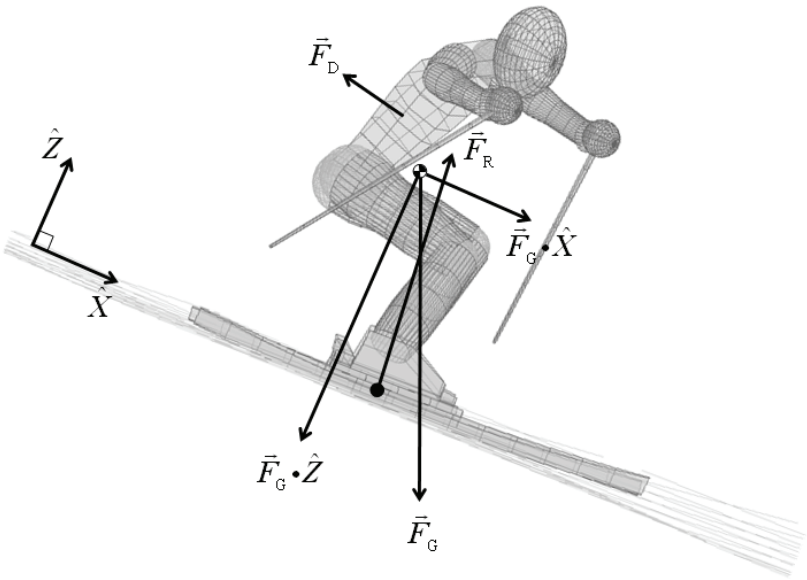

FIGURE 3.13. Free body diagram of a skier travelling straight down the slope fall line showing the decomposition of the gravitational force into components acting parallel to and normal to the snow surface.

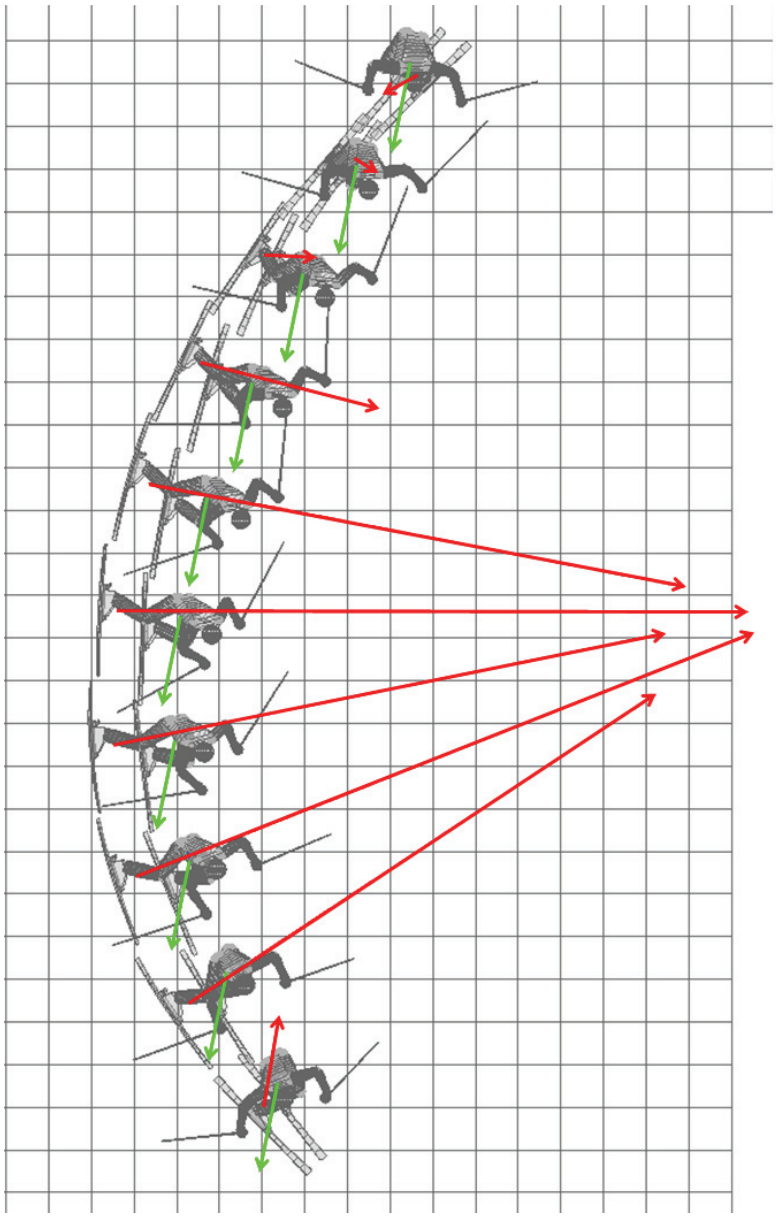

FIGURE 3.14. Free body diagram of a skier from an overhead view showing the changing orientation between the snow reaction force vector (red) and the gravitational force vector (green) over the course of a turn.

generate a snow reaction force of sufficient magnitude so as to exceed the component of gravity resisting turning so that the resultant force accelerates her in the desired direction. As will be seen, this is an important consideration in the timing of the turn.

SKIER ACTIONS

The next sections will present skier actions and try to relate them to specific action goals in terms of controlling the ski's orientation and loading characteristics. Towards this end, it is useful to introduce a reference system defining planes of skier movement. The system described here is based on that introduced by Joubert (1978/1980) in which the origin is placed at the skier's center of mass, and an axis is defined as running along the line from the point of force application on the snow surface to the skier's center of mass. The skier sagittal plane—referred to by Joubert as the "fore/aft" plane (p. 270)—is that defined by this axis and the center of mass velocity vector. Similarly, the skier frontal plane (referred to as the "lateral" plane by Joubert) is that defined by the skier's axis and the normal vector to the sagittal plane. Finally, the horizontal plane is defined as orthogonal to the sagittal and frontal planes.

In the presented model, skier actions are categorized as lateral, rotary, vertical, or fore/aft based on both the action's goal(s) as well as the primary plane of skier movement associated with the action. This categorization scheme is by no means new. In fact, numerous authors have categorized skier actions in a similar manner, although the actual terminology used may vary somewhat. In the following sections, the goals of lateral, rotary, vertical and fore/aft actions are described and some examples of skier actions to achieve these goals are presented.

LATERAL ACTIONS

DEFINITION: Skier lateral actions are defined as those actions occurring primarily in the skier's frontal plane and whose goals include (a) inclining the center of mass into the turn to balance the external forces; (b) regulating the ski edge angle to control the ski's self-steering effect; and (c) aligning the body segments to efficiently and safely resist the external forces.

Skier Lateral Action Goals

The literature describes several important purposes of skier lateral actions. First, inclining the center of mass to the inside of the turn in order to balance against the snow reaction force during the turn is an important effect of lateral actions (Howe, 2001; Joubert, 1978/1980; LeMaster, 1999; Lind & Sanders, 2004; Witherell, 1972). The degree of inclination required for the reaction force line of action to pass through the skier's center of mass is dependent upon the reaction force's orientation and magnitude, which in turn is a function of the skier's turn radius, mass, velocity and the orientation of the gravitational force vector ($\vec{F}_G$) relative to the skier's axis of rotation.

Figure 3.15 shows the gravitational and snow reaction forces acting on the skier in the frontal plane early in the turn (A) and late in the turn (B). The RS reference system in Figure 3.15 is defined so that $\hat{R}$ is directed parallel to the snow surface and perpendicular to the center of mass velocity vector while $\hat{S}$ is normal to the snow surface. Knowing the penetration and cutting components of the snow reaction force ($\vec{F}_P$ and $\vec{F}_C$, respectively) the inclination angle (ς) required for the center of mass to balance the reaction force can be calculated according to Equation [3.9] which is based on the work of Howe (2001):

$$\varsigma = \tan^{-1}\left(\frac{F_C}{F_P}\right) = \tan^{-1}\left(\frac{ma_{\hat{R}} - F_G \cdot \hat{R}}{ma_{\hat{S}} - F_G \cdot \hat{S}}\right) \qquad [3.9]$$

where m is the skier's mass and $a_{\hat{R}}$ and $a_{\hat{S}}$ are the resultant center of mass accelerations in the $\hat{\boldsymbol{R}}$ and $\hat{\boldsymbol{S}}$ dimensions, respectively. Prior to crossing the fall line (Figure 3.15 A), $\vec{\boldsymbol{F}}_{\mathrm{G}}$ has a centripetal component that acts with $\vec{\boldsymbol{F}}_{\mathrm{R}}$ to turn the skier, reducing the inclination angle necessary to balance the reaction force for a given speed and turn radius. In contrast, after turning out of the fall line, $\vec{\boldsymbol{F}}_{\mathrm{G}}$ has a component directed away from the turn center (Figure 3.15 B), increasing the inclination angle necessary for a given speed and turn radius.

Second, skiers use lateral actions to modify the ski's edge angle and thereby regulate the ski's self-steering effect (Howe, 2001; Joubert, 1978/1980; LeMaster, 1999; Lind & Sanders, 2004; Witherell, 1972). As described previously, increasing the edge angle increases the ski's deformation, thereby increasing the ski's self-steering effect. Conversely, reducing the edge angle has the opposite effect.

Third, skier lateral actions are important for creating sufficient conditions for the ski to hold when carving. Controlling the force distribution between the inside and outside ski is important in this regard. On hard snow surfaces, the skier may be required to balance on one ski to concentrate the available force to as small an area as possible and thereby generate enough pressure to penetrate the ski into the snow surface (LeMaster, 1999). Conversely, the skier may try to spread the force between both skis to avoid excessive snow penetration on soft conditions. Another important goal of lateral actions in terms of ski holding is to increase the ski edge angle, and thus reduce the platform angle, to reach a level sufficient for the ski to hold (LeMaster, 1999).

Finally, skiers use lateral actions to align body segments so that they are able to resist the external forces as efficiently and safely as possible (LeMaster, 2009). This goal may at times conflict with the need to edge the ski. As will be described shortly, skiers are sometimes required to change their ski edge angle without interfering with the center of mass inclination. This can be done but requires angling between different body

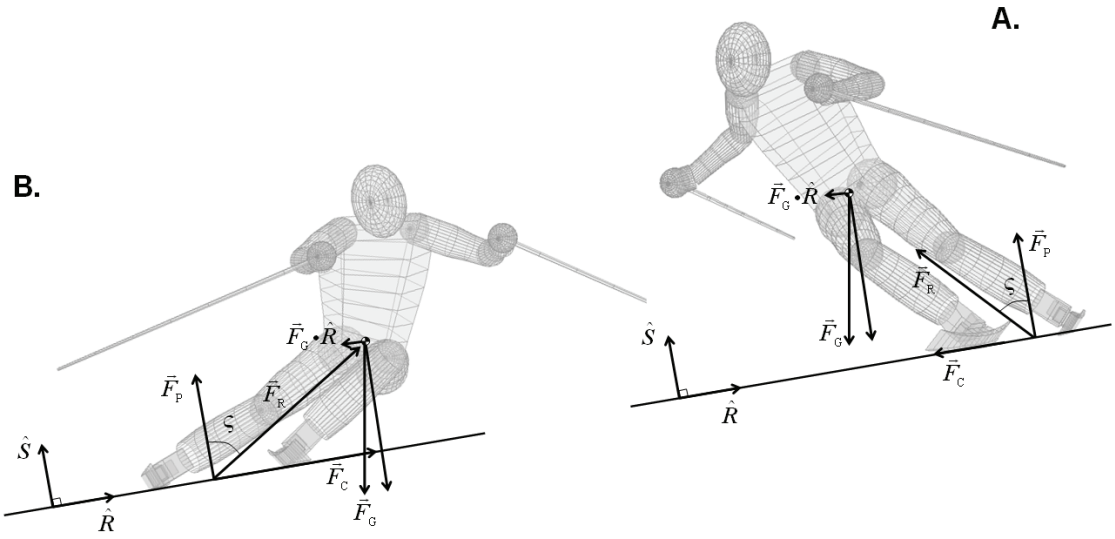

FIGURE 3.15. Free body diagram of the skier in the upper (A) and the lower portions of the turn (B). $\hat{\boldsymbol{R}}$ lies in the plane of the snow surface and is oriented perpendicular to the center of mass velocity vector. $\hat{\boldsymbol{S}}$ is oriented normal to the snow surface.

segments which can put the skier in positions that are both inefficient and hazardous when external forces are high.

Examples of Skier Lateral Actions

Common examples of skier lateral actions given in the literature include (a) ski and skier trajectory divergence; (b) stance width and stepping; (c) hip angulation; and (d) knee angulation. Perhaps the primary action affecting center of mass inclination into the turn is the "divergence" (Witherell & Evrard, 1993, p. 120) of skier and ski trajectories through the transition between turns (Joubert, 1978/1980; LeMaster, 1999; Major & Larsson, 1979/1979; Witherell, 1972). Bear (1976) refers to this concept as "anticipation," presumably to convey the idea that the divergence of trajectories requires the skier to momentarily fall into the turn in anticipation of the forthcoming snow reaction force, in a manner similar to the mechanics of walking. LeMaster (2009) suggests that the ability to fall from turn-to-turn precisely—not too much, nor too little—is a skill that distinguishes highly-skilled skiers.

An important aspect of divergence is the requirement that skier and ski trajectories cross each other during the turn transition. One way to ensure that this happens is to complete the turn with the skis and center of mass on intersecting trajectories (Takahashi & Yoneyama, 2001, 2002). This can be accomplished, for example, by turning the skis slightly more than the center of mass through the completion phase of the turn (Morawski, 1973). For instance, Joubert (1978/1980) describes a "pre-turn" technique where the skier sharply turns the skis up and to the outside of the following turn during the transition between turns. In another example, LeMaster (1999) describes how skiers can flex their legs during turn completion, in effect disengaging themselves from their skis and the snow reaction force. At the same time, the skis remain loaded onto the snow surface enough to deform so that the self-steering effect continues to turn the skis, and the skier and skis eventually come onto intersecting trajectories. Both LeMaster and Joubert also describe actions that the athlete can use to

slow down or even momentarily stop the skis so that the center of mass overtakes them and crosses over to the inside of the new turn.

Major and Larsson (1979/1979) point out that using a wide stance can facilitate the establishment of an initial inclination angle. With a wide stance through the transition between turns, the center of mass is already inclined to the inside of the new turn relative to the new outside ski as the skier switches over to turn in the new direction. In a similar manner, stepping the new ski to the outside can be used to establish inclination (Bear, 1976; LeMaster, 1999; Major and Larsson, 1979/1979).

The inclination of the center of mass into the turn, to a large degree the result of ski and skier trajectory divergence, is the main factor determining the ski edge angle (Witherell, 1972) and therefore plays an important role in determining the resulting ski turn radius. Skiers can, however, make some adjustments to the edge angle independently of center of mass inclination through angulation techniques (Lind & Sanders, 2004). Hip angulation refers to angling in the body that "brings the head of the outside femur closer to the center of the turn without moving the center of mass laterally" (LeMaster, 1999, p. 108), in effect increasing the ski's edge angle from that given by center of mass inclination. A similar effect can be achieved through knee angulation which refers to "angling in the lower limb that brings the knee closer to the body mid-line without disturbing the center of mass laterally" (LeMaster, 1999, p. 105). Witherell and Evrard (1993) suggest that since the knee is closest to the snow, this type of angulation requires the least movement of body mass and will therefore have the least effect on balance. At the same time, however, Joubert (1978/1980) warns that knee angulation can place the lower limb in a structurally unstable position to resist forces as well as expose knee ligaments to increased strain. Finally, although ankle movement is small, it does play an important role in fine tuning of the edge angle.

Inclination through divergence of the ski and skier trajectories, hip angulation, and knee angulation are all used in various combinations to achieve the aforementioned

goals, depending on the situation and the individual. In fact, Bear (1976) suggests that there are considerable individual differences in how the best skiers use these actions in combination to ultimately achieve the same effect.

ROTARY ACTIONS

DEFINITION: Skier rotary actions are defined as those actions directed towards controlling the rotary motion of the skis and occurring predominantly in the skier's horizontal plane.

Rotary Action Goals

Rotating the skis can have several important purposes in turning technique. As Müller (1994) points out, ski rotation can be particularly important at turn initiation. The radius a ski can carve through a turn is limited, depending upon a number of factors including the snow conditions, the ski's geometrical and physical characteristics, and the skier's technical and physical capabilities. If the forthcoming turn requires a shorter radius than that possible given the above-mentioned factors, the skier can rotate the skis during turn initiation to an angle from which it is possible to carve the remainder of the turn (Major and Larsson, 1979/1979).

A second reason for an initial rotation of the skis can be to establish an initial angle of attack between the direction of the skier's momentum and the ski's longitudinal axis, referred to by LeMaster as the "initial steering angle" (LeMaster, 1999, p. 87). While divergence of ski and skier trajectories is necessary for the two to cross sides during the transition, and for the skier to be in an inclined position to balance against the snow reaction force, convergence of the trajectories is necessary to achieve the large reaction forces necessary to turn the skier (LeMaster, 1999). In a carved turn, this is accomplished by edging and pressing the ski onto the snow surface enough to deform the ski and initiate its self-steering effect so that it turns itself to an angle with the skier's momentum. However, in situations where the skier must generate reaction

forces quickly, he may be required to rotate his skis to an angle with his direction of travel. A small initial steering angle results in a progressive build-up of reaction force, as in carving. Conversely, a large initial steering angle initiates a rapid build-up of reaction force.

Another goal of rotary actions can be to control speed. By controlling the size of the angle between his momentum and the ski's longitudinal axis, a skier can regulate the degree to which the snow reaction force turns his trajectory or brakes his speed. In certain situations, skiers may use relatively large attack angles during turn initiation so that the braking component of the reaction force dominates. This may allow the skier to slow down without interfering with the timing of the following turn (LeMaster, 2008).

A final goal of rotary actions is to regulate the ski's self-steering effect during the turn, an action Joubert refers to as "piloting" (Joubert, 1978/1980, p. 303) and others have referred to as "steering" (Witherell, 1972). Witherell and Evrard (1993) point out that when the skier is inclined into the turn and the ski is engaged in the snow, skier rotary actions cause changes in the ski's tilt angle rather than the ski's angle of attack. They therefore distinguish between rotary actions, which are typically directed at changing the ski's angle of attack, and steering movements which are directed towards changing the ski's tilt angle when the ski is edged and engaged in the snow surface. It is thought that rotary actions that press the ski forebody into the snow act to increase the ski's self-steering effect and, conversely, actions that lift the ski's forebody from the snow act to reduce the effect.

Examples of Skier Rotary Actions

There are, generally-speaking, three forms of skier rotary actions described in the literature: Upper body rotation, counter-rotation, and thigh rotation. First, upper body rotation can be used to transfer angular momentum generated in the upper body to the skis (Bear, 1976; Joubert, 1978/1980; LeMaster, 1999). This action requires the skier to

accelerate an upper body segment in the direction of desired rotation. To achieve this, the skis must be engaged with the snow to give the skier the necessary platform from which to initiate the motion. Once the segment is accelerated, the skier can both release the skis from the snow surface and contract his muscles to block the upper body rotation and transfer the angular momentum to the skis. This is a difficult action to use in short turns as it requires the entire body to acquire angular momentum (LeMaster, 1999).

A second form of rotary action used to transfer angular momentum to the skis is referred to as counter-rotation (Bear, 1976; LeMaster, 1999; Major & Larsson, 1979/1979) or "vissage" (Joubert, 1978/1980, p. 297). When the skis are disengaged from the snow, the upper body can be rotated in one direction causing the skis to rotate in the opposite direction. The magnitude of the rotational effect on the skis will depend upon the relative moments of inertia between the upper and lower body. Through actions that stabilize the upper body, the skier is able to impart a greater moment to the lower body. For instance, one way skiers can accomplish this is by holding the arms and poles wide during rotation, effectively increasing the upper body's moment of inertia. A pole plant that produces a torque on the upper body can further increase upper body stability (Joubert, 1978/1980). These types of actions are important in short turns on steep terrain where a large torque on the lower body is required to quickly rotate the skis (LeMaster, 1999).

Counter-rotation is the basis for a type of skier action referred to in the literature as anticipation, or wind-up and release (Joubert, 1978/1980; LeMaster, 1999; Major & Larsson, 1979/1979). In the first phase of the wind-up and release, the upper body is twisted to face downhill as the skis continue to turn underneath the body. The resulting torsion built up in the skier's body stores mechanical energy in the stretched muscles, ligaments and tendons. In the second, release phase, the skis are disengaged from the snow allowing the stretched muscles to rotate the skis back into alignment

with the upper body. To stabilize the upper body and maximize ski rotation, it is important in the release phase that rotation of the upper body is blocked, usually with a pole plant and a wide positioning of the arms to increase the upper body's moment of inertia (Major & Larsson, 1979/1979). This technique is very effective for short radius turns that require large initial steering angles (LeMaster, 1999).

Finally, thigh rotation about the hip joint can be used to rotate the skis. The importance of thigh rotation probably lies in the fact that it can be used without having to generate rotations in other body parts, thus allowing the skier to rotate the ski while independently performing other actions. For instance, thigh rotation allows the skier to adjust the steering angle of both skis independently of each other. Thigh rotation is probably also important for fine-tuning the rotary effects generated using upper body rotation and counter-rotation actions.

VERTICAL ACTIONS

DEFINTION: Skier vertical actions are those actions that take place largely in the skier's sagittal plane and whose goals include (a)regulating the magnitude of the snow reaction force; (b) aligning body segments to efficiently and safely resist the external forces during the turn and (c) increasing skier speed.

Skier Vertical Action Goals

An important purpose of skier vertical actions is to regulate and adjust the magnitude of the snow reaction force to control the degree and timing of the snow's influence on the skier's trajectory (LeMaster, 1999). In this connection, unweighting is defined as a reduction in the snow reaction force, while weighting refers to an increase in the snow reaction force (LeMaster, 1999; Müller, 1994).

Due to the nature of the ski's trajectory and the relative alignment of the snow reaction and gravitational force vectors through the turn (Figure 3.14), a skier without vertical motion will tend to unweight in the first portion of the turn and weight in the latter

part of the turn (LeMaster, 1999). This is often an undesirable pattern of loading as it increases the chances that the forces between ski and snow in the latter portion of the turn will exceed the snow's shear strength, resulting in skidding and significant dissipation of skier kinetic energy (Bear, 1976). An important aspect of skier vertical actions is therefore typically directed towards generating larger snow reaction forces early in the turn and reducing reaction forces in the latter portion of the turn.

Towards this end, skier vertical actions are often used to limit the degree of unweighting during the transition between turns, and to re-establish a reaction force as early as possible after the transition, since the tendency to unweight during the transition can be severe (Joubert, 1978/1980; Major & Larsson, 1979/1979). This does not mean that unweighting is undesirable. To the contrary, unweighting can be very important such as when the skis must be disengaged from the snow to allow certain rotary actions to take effect (LeMaster, 1999; Müller, 1994). Rather, the point is that the skier, through his vertical actions, controls the magnitude, duration and timing of the unweighting.

The skier is also able to increase the reaction force through her vertical actions. On hard snow surfaces, the component of the gravitational force acting normal to the snow surface may not be great enough for the skis to penetrate into the snow surface. If such is the case, the skier can increase the penetration force by actively pushing and accelerating her mass away from the ski and snow surface. Using vertical actions, skiers may also be able to modify the centripetal component of the reaction force so that a greater portion of turning is accomplished prior to, and less turning after, crossing the fall line.

In addition to regulating the magnitude of the reaction force, LeMaster (1999) also suggests that skier vertical actions are important for aligning body segments so that the skier can either efficiently resist the external forces during the turn or solve other actions more effectively. For instance, while a tall stance allows the skier to efficiently

resist the external forces in the turn, a somewhat shorter stance places the skier in a more powerful position to execute rotary actions during the transition between turns.

Finally, it has been suggested that a skier can use vertical actions to increase his speed during turning (Brodie, Walmsley, & Page, 2008; Brown, 2009; Hoff, 1997; Lind & Sanders, 2004; Louie & Mote, 1982; Mote & Louie, 1983; Takahashi & Yoneyama, 2001, 2002) although the extent of this contribution to performance is a topic of debate (Supej, 2003).

Examples of Skier Vertical Actions

In terms of reducing the snow reaction force and unweighting, two types of action are identified in the literature. Up-unweighting refers to an action where an initial extension by the skier increases the snow reaction force and accelerates the center of mass away from the point of force application and the snow surface. This is followed by a period of reduced reaction force as the center of mass is accelerated by gravity back towards the snow (Bear, 1976; Joubert, 1978/1980; LeMaster, 1999; Major & Larsson, 1979/1979; Müller, 1994).

Down-unweighting, on the other hand, refers to a reduction in snow reaction force through an immediate acceleration of the center of mass towards the snow surface, without a preceding upwards acceleration (Bear, 1976; LeMaster, 1999; Major & Larsson, 1979/1979; Müller, 1994). Some authors differentiate between passive and active down-unweighting (LeMaster, 1999; Major & Larsson, 1979/1979), referred to by Joubert as "active and passive flexion avalement" (1978/1980, p. 293). Passive down-unweighting is where the skier simply relaxes his muscles and allows either the gravitational force to accelerate his center of mass towards the snow surface, or the snow reaction force to accelerate his feet towards his center of mass (or a combination of both) thus resulting in unweighting. An example of this type of action is when the skier absorbs a bump in the terrain by relaxing his lower body muscles to allow the

snow to push his feet and knees upwards. Conversely, in active down-unweighting, the skier actively flexes at the hip and torso pulling the upper body down towards the skis and retracting the legs up and under the body.

Both up- and down-unweighting are thought to have advantages and disadvantages depending upon the situation. One advantage of up-unweighting is that the skier can more precisely manipulate both the magnitude and duration of the unweighting phase by controlling the magnitude of the initial upwards acceleration (LeMaster, 1999). In contrast, the duration of down-unweighting is limited as the skier will after a short time need to halt his downwards acceleration. On the other hand, down-unweighting allows the skier to effectively unweight instantly while up-unweighting requires an initial upwards acceleration (LeMaster, 1999). Major and Larsson (1979/1979) and LeMaster also suggest that the somewhat more extended body positions achieved during up-unweighting are conducive for both giving the muscles a chance to relax as well as improving blood flow. One disadvantage of up-unweighting is that once the skier is unweighted, only gravity can return him to the snow surface. This means that the skier is temporarily at the mercy of the gravitational force and will not be able to generate ground reaction forces until landing from the unweighting phase. In contrast, the skier is typically in a position to reestablish ground reaction forces instantly by simply resisting their downwards acceleration in down-unweighting.

Two mechanisms have been proposed of how skiers may, through their muscular work, increase their speed when turning. The first type of action, described by Takahashi & Yoneyama (2001; 2002), consists of a skating-type motion in the first half of the turn where a component of the reaction force acts to accelerate the skier down the hill. To accomplish this, the skier and skis must have divergent trajectories (Brodie et al., 2008) which they normally do in the first portion of the turn. Although there will be some vertical component, this action could have just as easily been classified as a lateral action, depending on the skier's inclination at the time of the skating motion.

The second type of action used to increase speed is referred to as pumping and was originally described by Louie and Mote (1982) and Mote and Louie (1983) and later again by Lind and Sanders (2004). In essence, this action consists of pumping up and down at certain points in the turn cycle. Louie and Mote's original work used a numerical simulation of a skier gliding straight down the fall line through undulating terrain to examine the effect of different pumping strategies. Their work predicted that skiers can increase their velocity over that which the gravitational acceleration provides when descending over undulating terrain by vertical pumping actions combined with fore/aft rocking. In particular, Louie and Mote's simulation predicted that up-pumping and rocking back when the normal component of the reaction force is greatest increases the skier's velocity. Conversely, down-pumping and back-rocking results in a decrease in velocity although, depending on when the down-pump occurs, the decrease can be minimized. Louie and Mote concluded that the best strategy to maximize velocity is to up-pump and rock back at times when the normal reaction force would be greatest without pumping, and to down-pump and rock forward at times when the normal force without pumping would be least.

Louie and Mote's work was done when straight running through rolling terrain. So, it is not immediately clear how the mechanics of pumping in this straight running model might translate to turning mechanics. To explain how a skier's muscular work during an up-pump when turning can be transformed into increased speed, Lind and Sanders (2004) used a model of a skier sliding along frictionless rails through a sequence of turns. In this simplified model, the skier's rotational kinetic energy (T) at any point along her trajectory is given by the equation:

$$T = \frac{I\omega^2}{2} \qquad [3.10]$$

where I is the skier's moment of inertia about the axis of rotation and ω is her angular velocity (Ohanian & Markert, 2007). Considering that the skier's angular momentum (L) is equal to $I\omega$, and by multiplying the right-hand side of Equation [3.10] by I/I, the following equation relating the skier's rotational kinetic energy, angular momentum, and moment of inertia can be obtained (Lind & Sanders, 2004):

$$T = \frac{L^2}{2I} \qquad [3.11]$$

If the skier, at some point during the turn, uses her muscles to extend and move her center of mass towards the center of the turn, her moment of inertia I will decrease. Since, by definition in this simplified model, no external torque acts on the skier to change her angular momentum, this decrease in moment of inertia will result in an increase in her rotational kinetic energy following Equation [3.11]. The magnitude of this increase will be equal to the mechanical work the skier's muscles do against the inertial, centrifugal force (Louie & Mote, 1982; Mote & Louie, 1983) and can thus be given by:

$$\Delta T = \frac{mv^2}{r} d \qquad [3.12]$$

where m is the skier's mass, v is her tangential velocity, r is her turn radius, and d is the distance the skier pushes her center of mass towards the axis of rotation (Lind & Sanders, 2004). If the up-pump action is carried out when the forces during the turn are high, even a relatively small displacement of the center of mass can result in a substantial increase in kinetic energy.

Although Lind and Sanders (2004) explained the mechanics of the up-pump portion of pumping, they did not examine the down-pump or fore/aft rocking components of Louie and Mote's predictions (Louie & Mote, 1982; Mote & Louie, 1983). If one were to

translate Louie and Mote's findings to turning situations, and take into account Lind and Sanders explanation of the up-pump mechanics, this would suggest that the pumping strategy that best maximizes skier velocity will be one where the skier (1) up-pumps and rocks back when the centripetal component of the snow reaction force is greatest and the skier is inclined towards the center of rotation and (2) down-pumps and rocks forward when the centripetal component of the snow reaction force is least.

There is some debate, however, as to what extent pumping mechanics are applicable in reality. For instance, Supej (2003) argues that any benefit one might gain from pumping will be small and normally outweighed by increases in friction and wind drag forces. Similarly, Brodie et al. (2008) acknowledge that there is a possibility to increase speed during the turn, but suggest that pumping may have other, detrimental side effects, such as increased ski slippage, loss of balance, or poor timing. They therefore speculate that, after a skier has come up to speed on the course, performance may be a question more of how not to lose too much energy during the turn, rather than how to gain energy at a certain part of the turn.

FORE / AFT ACTIONS

DEFINITION: Skier fore/aft actions are defined as those actions occurring predominantly in the skier's sagittal plane and whose action goals include (a) regulating the ski's self-steering effect; (b) balancing against the external forces in the sagittal plane; (c) maintaining perpendicularity with the snow surface in the sagittal plane; and (d) regulating speed.

Skier Fore/Aft Action Goals

Skier fore/aft actions have received substantial attention in the literature and numerous goals for this type of action have been proposed. First, and perhaps most importantly, it is thought that the application point of the skier applied force relative to the ski's midpoint along the longitudinal axis is an important factor determining the ski's running surface pressure distribution and the resulting shape of the deformed ski

when it is edged and engaged in the snow during a turn (LeMaster, 1999; Lind & Sanders, 2004; Major & Larsson, 1979/1979). Consequently, it is thought that the skier can control the ski's self-steering effect by regulating her fore/aft position relative to the ski. For instance, by moving her position forward, a skier can shift the pressure distribution forward on the ski, resulting in increased forebody deformation and a greater self-steering effect (LeMaster, 1999), referred to as oversteering by Major and Larsson. Conversely, the skier can reduce the ski's self-steering effect by moving her center of mass position aft, thus placing less pressure on the ski forebody (LeMaster, 1999), referred to as understeering by Major and Larsson. Witherell (1972) suggests that a mid center of mass position with a mid-pressure is ideal for turns of a constant radius.

Based on this reasoning, it is thought that skiers should begin the turn with more forward pressure to increase the ski's self-steering effect and induce the ski to turn (LeMaster, 1999; Witherell, 1972). Then, as the turn is completed, the skier should move the pressure distribution aft along the ski to reduce ski forebody deformation and thereby stop the ski from turning. However, both Joubert (1978/1980) and LeMaster (1999) also point out that skier fore/aft actions are just as often used to maintain a certain running surface pressure distribution—and ski self-steering effect—as they are to change it. This suggests that both the goals of maintaining and changing the ski's self-steering effect require skier fore/aft actions, depending on the situation.

In addition to influencing the ski's self-steering effect, the shape of the running surface distribution is thought to affect the ski's stability. Joubert (1978/1980) suggests that skiers are thus able to modify the ski's stability through their fore/aft actions. In particular, more forward positions are thought to result in a running surface pressure distribution in which the ski is relatively easy to pivot. As the center of mass is moved aft, the self-steering affect is reduced and, at the same time, a more stable configuration is achieved for better holding (Joubert, 1978/1980).

It has also been suggested that the skier's fore/aft positioning affects the ski's behavior in absorbing irregularities on the snow surface. When the skier is positioned aft, pressure on the forebody is reduced and the shovel is thus free to flex and twist, absorbing irregularities in the snow (Major & Larsson, 1979/1979). Conversely, when the skier is forward, the forebody is more aggressively pressed into the snow surface and will thus not absorb as well.

Another important goal of skier fore/aft actions is to balance the moments about the center of mass generated by the snow reaction and wind drag forces. In this regard, skier vertical and fore/aft actions must work together to balance the fore/aft moments about the center of mass. Along these lines, Joubert (1978/1980) writes that it is important for skiers to be able to execute vertical actions without creating fore/aft imbalances. He further suggests that this is done by maintaining a fore/aft position that is perpendicular to the snow surface in the sagittal plane so that skier vertical actions may take place along an axis that is normal to the snow. In the first half of the turn, the skier turns into the fall line and the hill in effect gets steeper, requiring the skier to move forward in order to maintain a position perpendicular to the snow in the sagittal plane. Conversely, in the second half of the turn, the skier essentially turns onto a flatter slope and must move back to maintain perpendicularity.

Finally, both Major and Larsson (1979/1979) and Joubert (1978/1980) have suggested that aft positions are associated with improved gliding performance. It is thought that part of the reason for this is that a more aft position is often associated with more relaxed muscles around the ankle and foot, which reduces friction and enhances ski gliding (Joubert, 1978/1980). When the skier is turning, moving aft may reduce the friction produced under the ski's forebody which is thought to have larger attack angles.

Examples of Skier Fore/Aft Actions

A number of skier fore/aft actions are used to accomplish the aforementioned goals. Primary skier movements include flexion and extension in the sagittal plane at the hip, knee, and ankle joints (Joubert, 1978/1980). Due to the low friction between ski and snow, skier fore/aft actions often involve rotations about the skier's center of mass in which the upper body and feet move in opposite directions (LeMaster, 1999; Major & Larsson, 1979/1979; Witherell & Evrard, 1993), referred to as "fore/aft banking" by Joubert (1978/1980, p. 271).

The fact that the skier and skis take different trajectories through the transition between turns can also be utilized by skiers to control their fore/aft positioning (LeMaster, 1999). Since the center of mass takes a shorter trajectory through the transition between turns, the skier can in effect catch up with her skis. A skier may also use actions that slow her skis down, but not her center of mass, to assist in catching up.

Finally, LeMaster (1999) points out that skier fore/aft position is related to the skier's angle of attack onto the ski. Increasing the angle of attack through the turn initiation in effect moves the center of mass position forward on the ski.

3.4 RESEARCH ON SKIER ACTIONS

Earlier in this chapter, the mechanics of the ski snow interaction were reviewed and an overview of the skier action mechanics was presented. The purpose of this section is to give the reader an overview of the research literature related to skier actions. In the first portion, different approaches investigators have used to describe the turn cycle structure are presented. This is followed by a review of the research literature organized according to skier lateral, rotary, vertical, and fore/aft actions. Finally, investigations concerning skier mechanical energy behavior and trajectory characteristics are presented.

As previously mentioned, this review is limited primarily to the English language literature due to the author's limited language skills. The reader should be aware that there is a significant body of literature in other languages, particularly German and Japanese. Fortunately, many of these international groups have also published some studies in English where their ideas are accessible to an English reading audience.

TURN CYCLE STRUCTURE

When describing turning mechanics, it is important to define the turn's temporal characteristics. Numerous approaches to defining the turn cycle structure have been used, although clear definitions are not always given in the literature which makes interpreting research results difficult. Three representative approaches to structuring the turn are summarized here.

First, Nachbauer (1987a, 1987b) structured the turn cycle into phases based on measurements of the snow reaction force. Two main phases were identified—the Turn Preparation Phase and the Turn Phase—on the basis of specific characteristics identified in the force-time data. Nachbauer defined action goals in the Turn Preparation Phase to include (a) making preparations for the creation of snow reaction forces in the next turn; (b) transfer of load to the new outer ski; (c) unweighting; and (d) changing of edges. He further divided the Turn Preparation Phase into the Load Change Phase, where the skier begins to transfer load to what will become the new outer ski, and the Unweighting Phase, where the skier reduces the snow reaction force to allow edge change and rotary actions. During the Turn Phase, the skier inclines into the turn, edges the skis and creates the snow reaction forces that change the momentum vector's direction. Nachbauer also further divided the Turn Phase into an Edging Phase and an Exit Phase.

Müller et al. (1998) used a similar system to Nachbauer (1987a, 1987b), dividing the turn into Initiation and Steering Phases. According to Müller et al., the skier unweights,

changes edges, turns the skis in the new turn's direction, and controls his speed in the Initiation Phase. Then, during the Steering Phase, the skier turns his momentum, steering the turn through regulating the ski's edge angle. Müller et al. further divided the turn phase into two parts based on passage of the fall line. This approach makes sense from a mechanics perspective as prior to passage of the fall line, the snow reaction and gravitational forces work together to turn the skier, while after passage of the fall line the snow reaction force must work against the gravitational force to turn the skier.

LeMaster (1999) defines three turn cycle phases. During the Initiation Phase, the skier (a) inclines to the inside of the turn in anticipation of the up-coming snow reaction force; (b) changes edges and establishes an initial steering angle relative to the new outside ski; and (c) aligns his body segments so that they can effectively resist the snow reaction force. In the Control Phase, the skier generates the reaction force that turns his momentum. And in the Completion Phase, the skier acts to reduce the snow reaction force by reducing inclination, reducing the ski's edge angle and shifting balance aft along the ski's longitudinal axis. LeMaster suggests that advanced skiers smoothly transition from the Completion to the Initiation Phases so that one might consider the two as a single phase, particularly in short radius turns.

SKIER ACTIONS

SKIER LATERAL ACTIONS

Although relatively few studies in the skiing research literature describe skier lateral actions, certain characteristics including center of mass inclination angle and ski edge angle have been investigated and described. In an early simulation study of skiing technique, Morawski (1973) attempted to explain ski turn mechanics in terms of an inverted pendulum model of the skier. He concluded that the main factor controlling the intensity of the turn is the inclination of the center of mass into the turn and that to

achieve this inclination, the skis and skier are required to follow separate trajectories, corresponding well with the concept of divergence in the practitioner literature (Joubert, 1978/1980; LeMaster, 1999; Major & Larsson, 1979/1979; Witherell, 1972). Morawski went on to suggest that modern techniques will largely differ in how the initial inclination of the center of mass is achieved.

A couple of studies have reported skier inclination angles. In 1997, Raschner et al. (1997) reported the results of a kinematic study of an Austrian national team member and a group of developing athletes in slalom. They found that the maximum center of mass inclination was approximately 40 degrees and occurred at about gate passage. In 2004, Miura and Miura (2004) reported on a 3-dimensional motion analysis of junior skiers in a giant slalom race. Similar to Raschner et al., they found peak center of mass inclination angles just after gate passage. In addition, they reported that the better ranked skiers demonstrated a single peak in center of mass inclination which they suggested was the result of better timing of the inward lean.

Müller et al. (1998) identified the importance of skier lateral actions in the initiation phase in particular. In a 3-dimensional motion analysis study, they compared the techniques of a group of experienced ski instructors with those of a group of intermediate skiers while executing a selection of different turn types and found that the more experienced skiers were able to attain significantly greater edging angles during turn initiation which they attributed to better edging ability.

Some investigators have examined differences in skier lateral actions when using carving equipment and conventional equipment. Raschner et al. (2001) compared kinematic and kinetic characteristics of a former world cup racer when performing a giant slalom type turn using carving skis (R_{SC} = 14 m) and conventional giant slalom skis (R_{SC} = 32 m). They reported maximum edge angles of between 65 and 70 degrees, with about 10 degrees greater edge angles in the carving technique. Yoneyama et al. (2001) used goniometers to measure hip and knee angles on an experienced ski

instructor making long and short parallel turns on both carving (R_{SC} = 18 m, length = 185 cm) and conventional skis (characteristics not given). They found that the skier used greater body inclination to edge the ski when on carving equipment and greater angulation to edge the ski when on the conventional equipment. In 2005, Supej, Kugovnik and Nemec (2005b) described the results of a series of investigations quantifying the kinematics of elite skiers. In carving slalom turns, they found that skiers often initiate the turn using knee angulation, but that thereafter, hip angulation plays the main role in determining the ski edge angle, similar to LeMaster's (1999) observations.

SKIER ROTARY ACTIONS

In 1994, Müller (1994) reported an extensive investigation describing the kinetics, kinematics, and muscle activities of a group of 21 certified ski instructors while performing a variety of turn types. They found that the main differences in the investigated turning techniques occurred primarily in the initiation phase of the turn. They further reported that one of the more important factors in the initiation phase appeared to be the rotation of the skis in the direction of the fall line, the initial momentum for which was generated in most cases through internal forces. Skiers were observed using elements of both upper-body rotation and counter-rotation, similar to the actions described in the practitioner literature (Bear, 1976; Joubert, 1978/1980; LeMaster, 1999; Major & Larsson, 1979/1979).

In their comparison of carving and conventional turns made by an expert skier, Yoneyama et al. (2001) found that the skier used a rather gradual thigh rotation in short turns using the carving equipment, while he used rapid thigh rotation when initiating turns on conventional skis. It may be that the increased rotary motion observed when the skier used conventional equipment corresponded with the need to actively rotate

the skis to a larger initial steering angle to compensate for the ski's reduced self-steering effect (LeMaster, 1999).

In a single-camera, 2-dimensional study, Knünz, Nachbauer, Mössner, and Schindelwig (2000) measured the ski motion of elite skiers in giant slalom turns and found that even these highly skilled skiers used skidding to a certain extent. They suggested that skidding in the initiation phase when the skier is unweighted might be a technique used by top racers, but that during the steering phase of the turn it should result in increased friction. This corresponds well with Brown's (2009) differentiation between "drifting" and "chip formation" and that skidding will only develop significant forces when the ski penetrates deeply enough in to the snow surface.

SKIER VERTICAL ACTIONS

Kinetic, kinematic and numerical simulation methods have been used by investigators to understand skier vertical action mechanics. As described previously, one of the main functions of skier vertical actions is to regulate the magnitude of the snow reaction force. Field measurements of ground reaction forces during skiing are therefore not only important for understanding the magnitudes of the forces which skiers must sustain, but also for understanding both the function and timing of skier vertical actions.

Nachbauer (1987a, 1987b) and Förg-Rob and Nachbauer (1988) described the ground reaction forces of 34 elite and developing skiers in slalom and giant slalom using dynamometers mounted between the ski and boot. They reported higher ground reaction forces in slalom turns with mean and maximum ground reaction forces reaching as high as 1550 N and 2717 N, respectively. Also of interest, they reported that the fastest skier had the lowest duration of unweighting (0.17 s versus 0.26 s for the group mean) which allowed him to begin generating ground reaction forces earlier than the group mean despite skiing a tighter trajectory.

In his 1994 study of ski instructors, Müller (1994) measured forces acting normal to the ski using strain gauge sensors mounted between the ski and boot. He observed skiers using elements of both down- and up-unweighting in the various turning techniques that were analyzed. During the initiation phase, skiers were typically unweighted to facilitate changing of the edges and rotation of the skis in the direction of the fall line while during the steering phase of the turn skiers were loaded with an average of 140% body weight. On steep, icy slopes, loads approached 175 % of body weight as skiers turned out of the fall line and into the traverse. In turns with down-unweighting on even slopes, they observed knee angles decreasing from 125^{o} to 98^{o} during which time the force on the downhill leg decreased rapidly. Müller also measured nearly continuous neuromuscular activity in the knee extensors during down-unweighting, leading them to suggest that down-unweighting can lead to local fatigue in the knee and hip joint extensors.

Plantar pressure measurements have also been used to quantify the ground reaction force. Lafontaine, Lamontagne, Dupuis and Diallo (1998) measured the plantar pressures of six experienced ski instructors and reported an average maximum force of 1481 N for short radius turns. Laapi (2009) recorded the plantar pressures of 9 highly-skilled skiers during slalom race simulations on two different course settings, one with a 10 m linear distance between gates and the other with a 13 m linear distance—similar to the set-up used in this study. She observed mean peak reaction forces over the 498 analyzed turns of between 2.62 and 2.72 times bodyweight with no significant difference between courses. However, the timing of the turn apex, defined as the 10 % interval of the turn cycle with the highest impulse, was significantly later in the turn cycle on the 13 m course (58 and 61 % of the turn cycle for left and right turns on the 10 m course versus 63 and 67 % of the turn cycle for left and right turns on the 13 m course).

Yoneyama, Kagawa, and Funahashi (2002) built a programmable skiing robot instrumented with load cells to measure the ground reaction force. The robot was programmed to execute both lateral and rotary actions, but not vertical actions. Despite testing three different patterns of rotary and lateral actions, the first half of the turn was characterized by relatively low reaction forces while the latter half had relatively high forces. This finding is significant as it seems to suggest that in the absence of skier vertical actions, the timing of the ground reaction force will be late in the turn cycle. It would be very interesting to see if, through the addition of vertical actions to the robot's movement program, they are able to control the timing of the reaction force through the turn.

While kinetic data have been used to measure the effect of skier vertical actions, researchers have used kinematics to describe the timing and extent of vertical actions. Reporting on the same data set as Raschner et al. (1997), Frick et al. (1997) described the vertical actions of an elite skier and 6 developing athletes in terms of leg and hip extension angles in slalom. They reported that until gate contact, concentric knee extension of the outside leg was prevalent and, conversely, that knee flexion was used after gate passage. Hip angle was described as relatively constant until gate passage and then quickly reduced after this.

One kinematic parameter of particular interest has been the amplitude of center of mass motion orthogonal to the snow surface. In a comparison of a world cup skier's technique when using carving and conventional skis, similar center of mass vertical movement amplitudes between the two techniques were reported; but a more rapid rise in center of mass position in the conventional technique at the transition between turns was observed (Müller et al., 2004; Müller & Schwameder, 2003; Raschner et al., 2001; Schiefermüller et al., 2005). They suggested that this greater acceleration is required in the conventional technique to generate enough unweighting from the snow surface for rotary actions. Brierley and Bartlett (1991) compared the vertical center of

mass motions orthogonal to the snow surface of an experienced and novice skier. They reported that the experienced skier raised his COM more than the novice, presumably with a greater reduction of ski-snow pressure, although this was not measured in this study.

Two groups have examined skier vertical actions during competition. In describing the results from analyses taken during world cup competitions, Supej, Kugovnic, and Nemec (2005b) reported movement amplitudes as high as 45 cm in elite male slalom skiers. He went on to propose that vertical movement amplitudes orthogonal to the snow surface are primarily dependent upon the degree of center of mass inclination required to balance the external forces during the turn. Pozzo and colleagues (Pozzo, Canclini, Casasola, et al., 2005; Pozzo, Canclini, Cotelli & Baroni, 2001) investigated skier kinematics during world cup giant slalom and slalom competitions and reported center of mass vertical displacements of 50 ± 30 cm and 30 cm for giant slalom and slalom, respectively.

Based on the results of a series of investigations looking at the vertical actions of elite slalom skiers, Supej and colleagues (Supej, Kugovnik, & Nemec, 2005b; Supej et al., 2004) and Kugovnik et al. (2004, 2005) differentiated between single- and double-motion techniques based on changes in the distance between the center of mass and the outside ankle joint center (D_{AJC}). As its name implies, the single-motion technique is associated with a single cycle of increasing D_{AJC} from the start of the turn to the middle, and then decreasing D_{AJC} from the middle of the turn to the end, a motion similar to that described by Frick et al. (1997) in their study of slalom skiers. In contrast, the double-motion technique involves two cycles of increasing D_{AJC} over the course of the turn. They hypothesized that the single-motion technique is more conducive to performance due to better contact with the snow surface, lower maximal ground reaction forces, and the skier being in a more extended position conducive to resisting forces in the turn.

In a numerical simulation, Supej et al. (2004) compared the single- and double-motion techniques through four slalom turns with a 13 m linear distance between gates and a 2.5 m offset on a 20° slope. Based on the center of mass motion using each technique, they derived the ground reaction forces and found both higher minimum forces (less unweighting) and lower maximum forces for the single-motion technique. To test the effects of single- and double-motion techniques on performance in the field, Kugovnik et al. (2004, 2005) timed four high-level skiers on 3 different courses (different gate distances and slopes) alternating between the single- and double-motion techniques. They found that between 74 and 86% of the trials on each course were faster using the single-motion technique.

As previously presented, it has been suggested that skiers can contribute to their speed through their muscular work in vertical pumping (Lind & Sanders, 2004; Louie & Mote, 1982; Mote & Louie, 1983) (see p. 70). To investigate this possibility, Kagawa and Yoneyama (2001) created a simplified 2-dimensional numerical model of a skier on a mono-ski and examined the effect of center of mass motions on skiing velocity. This model neglected the effects of ski friction and wind drag forces, so that only the gravitational force and the lateral component of the reaction force were modelled. They compared a passive model with an active one where the skier pushed on the snow towards the inside of the turn. They found that the active case was faster, even though center of mass position differences were small, and reported that the skier's acceleration in the fall-line direction was proportional to the acceleration of the skier's center of mass from the ski's center during pumping. This corresponds well with the work of Louie and Mote who found that the increase in skier kinetic energy was proportional to the center of mass acceleration during the up-pump portion of pumping.

The elimination of ski-snow friction in this study—as well as in the work of Lind and Sanders (2004)—is a limitation because, as Supej (2003) points out, pushing on the

snow in this manner is likely to increase the friction component of the snow reaction force. And if increases in friction are greater than the benefit, such a technique could be counter-productive. Where the balance lies is likely to be dependent upon, among other things, snow and terrain conditions.

In an unpublished study, Hoff (1997) examined the effect of skier vertical actions on performance time when skiing straight down a series of rolls, a situation similar to that modelled in the original Louie and Mote study (Louie & Mote, 1982; Mote & Louie, 1983). Skiers were asked to change the timing of their vertical actions according to three conditions: (1) pushing on the flats, (2) pushing on the steeps, and (3) skiing as fast as they can. The found a 5 to 10 % improvement in performance time over 8 seconds when skiers pushed on the steep portions of the rolls, confirming Louie and Mote's findings. But similar to the limitation of the Louie and Mote study, it is difficult to generalize these findings to turning.

One investigation has made measurements that may give an indication that the skier is in fact able to increase his speed through the muscular work of vertical pumping. Brodie, Walmsley, and Page (2008, 2009) used their recently developed GPS-based motion capture system to describe the kinematics and kinetics of a skilled skier completing a 10-gate giant slalom course. They observed positive ground reaction force power occurring around the apex of some turns, indicating that the ground reaction force had acted to accelerate the skier. At the same time, however, they were skeptical as to the general applicability of such a pumping technique due to the potential negative consequences of pumping motions, such as increased air drag or loss of balance.

SKIER FORE/AFT ACTIONS

Characteristics of skier fore/aft actions have also received a good deal of attention from investigators. A number of approaches have been taken including kinematic studies to

describe skier center of mass fore/aft motion relative to the skis and kinetic measurements to describe the fore/aft action of the center of pressure. In addition, some investigators have measured ski deformation and running surface pressure distributions in an attempt to understand the role of skier fore/aft positioning.

In terms of kinematic studies, Brierley and Bartlett (1991) compared the techniques of an experienced and a novice skier and reported that the experienced skier had a greater range of fore/aft motion (28 cm vs. 20 cm for the experienced and novice skiers, respectively). In Raschner and colleagues' comparison of a highly skilled skier's carving and conventional techniques in giant slalom type turns (Müller et al., 2005; Müller & Schwameder, 2003; Raschner et al., 2001; Schiefermüller et al., 2005), they observed a forward center of mass motion during turn initiation in both techniques. However, the skier had a greater aft movement in the carving technique which was accompanied by increased tibialis anterior EMG activity. They also reported maximal backward leaning angles of 25 and 8 degrees for the carving and conventional techniques, respectively.

In terms of kinetic studies, Yamagish, Fuji, Kato, Tsukawaki, and Ozawa (2003) made plantar pressure measurements on two experienced racers while making carved turns on both conventional and carving equipment. They found that the center of pressure moved aft over the course of the turn, with an increase in heel pressure, particularly on the outside foot. They also observed that the center of pressure trace was further back when skiing on the carving skis, corroborating the findings from the Raschner and co-workers study (Müller et al., 2004, 2005; Müller & Schwameder, 2003; Raschner et al., 2001; Schiefermüller et al., 2005).

Lafontaine et al. (1998) reported on plantar pressure measurements made with ski instructors performing a variety of turn types. They described the center of pressure as moving on a somewhat linear trajectory from the front, medial part of the foot back towards the medial side of the arch over the course of a turn. In longer radius, giant

slalom type turns, the center of pressure moved all the way back to the heel, suggesting a greater range of skier fore/aft action when compared to shorter turns.

Schwameder et al. (2001) measured ground reaction forces of a former world cup racer, two junior racers, and a recreational skier skiing on a rhythmical giant slalom course using skis instrumented with strain gauge cylinders. They observed a cyclical pattern associated with the turn cycle where the moment about the transverse axis was positive during the first part of the turn, indicating that skiers were forward. This was followed by a gradually decreasing moment through the middle of the turn, reaching negative values. This pattern of skier fore/aft action was also reflected in the force application point measurements. Interestingly, they found that the skilled athlete changed his fore/aft positioning so as to maintain a constant relative position between body and skis with changing binding positions.

In a related study, Nigg et al. (2001) also used instrumented skis to measure the ground reaction forces acting on 11 recreational skiers in free skiing and 5 regional ski team members in giant slalom. They also reported a similar cyclical pattern of force application point movement along the ski's longitudinal dimension.

Gufler (2001) used skis instrumented with force plates to measure forces and moments acting at the boot sole for two skilled skiers performing a progression of turn types typically used in Austrian ski schools. Her results also showed a cyclical trend in the force moment about the transverse axis, corresponding to skier fore/aft actions. This trend was particularly evident in short radius turns where the moment ranged between −150 and +150 Nm. Furthermore, Gufler's results indicated that the more a turn involved carving, the further aft the load between skier and ski was shifted, correlating well with the findings of Yamagish et al. (2003) and Raschner and colleagues (Müller et al., 2004, 2005; Müller & Schwameder, 2003; Raschner et al., 2001; Schiefermüller et al., 2005).

Federolf (2005) used force sensor plates mounted between the binding and ski to measure the moments transferred from a skier to the binding during carved, giant slalom type turns. He observed that the largest moments occurred about the plate's transverse axis, again presumably due to the skier's fore/aft positioning. Federolf reported that the observed moment ranged between about –200 and +200 Nm, corresponding to an approximate range of center of mass movement of ± 23 cm. Similar to Schwameder et al. (2001) and Nigg et al. (2001) he also described a cyclical pattern where positive moments were recorded during turn initiation, indicating that the skier shifted his weight forward. Then, as the skier shifted his weight back over the course of the turn, a negative moment was generated.

Scott (2004) used skis instrumented with load cells to measure the ground reaction force acting on a former world cup racer performing both long and short turns. His results seemed to show a rather mid-balanced force distribution in the long turns—despite the athlete expressing that his intention was to move forward at turn initiation and back during the turn. In contrast, there was clear evidence of a changing fore/aft loading pattern in the short turns. The mid-balanced force distribution in the long turn seems to contrast with the findings of those described earlier (Federolf, 2005; Lafontaine et al., 1998; Nigg et al., 2001; Schwameder et al., 2001; Yamagish et al., 2003).

Also using skis instrumented with load cells, Yoneyama et al. (2006) measured the ground reaction forces acting on an expert skier making very long turns on a moderately steep, 20 degree slope. Similar to Scott (2004), they also described a rather static fore/aft pressure distribution where the center of pressure was located mostly near the heel. They did, however, report that heel pressure increased over the course of the turn's steering phase and that the center of pressure moved briefly forward during the transition between turns.

In his kinetic and kinematic study of ski instructors, Müller (1994) reported a nice example showing how skier vertical, fore/aft, and rotary actions are inter-related. He

observed that in down-unweighting on smooth slopes, skier fore/aft positioning shifted back as the knees flexed and moved up in front of the body. As a result, as much as 80 % of the load on the uphill, new outside ski was placed on the rear portion. Müller suggested that this produced a pronounced torque about the skier's longitudinal axis that facilitated rotation of the skis towards the fall line in preparation for the subsequent turn.

Several investigators have started to examine the relationship between (a) skier fore/aft positioning, (b) the RSPD and ski deformation, and (c) the resulting ski turn radius. Tatsuno et al. (2009) measured both ski deflection and ski-snow contact pressures over the length of the ski to describe the RSPD during long, carved turns by a skilled skier on packed snow. They found that the RSPD did in fact correspond to ski deflections on the forebody of the ski. Increased forebody pressures corresponded to increased forebody deflections, and conversely, decreased forebody pressures occurred at the same time as decreased forebody deflection. Tatsuno et al. also observed a general trend of pressure increases on the ski forebody during the first part of the turn followed by a shift aft over the course of the turn.

DeCecco and Angrilli (1999) developed a method for measuring the RSPD of skis loaded under static, laboratory conditions that allowed for adjustments of both the edge angle and the fore/aft positioning of the load application point. They found that more aft load application points resulted in wider RSPD and increased stability, similar to Joubert's (1978/1980) predictions. They went on to suggest that during turn initiation, the skis are flat and the skier moves into a forward position that narrows the ski's RSPD, increasing its manoeuvrability and thereby facilitating rotary actions. Then, as the skier edges the ski and moves aft over the course of the turn, the RSPD broadens increasing the ski's stability. The pressure distributions from Renshaw and Mote's (1989) numerical simulation seem to support this notion that as the ski transitions to carving, a broader RSPD is attained (Figure 3.11).

Fauve, Auer, Lüthi, Rhyner, and Meier (2009) measured ski deformations in both flexion and torsion during skiing using a series of 8 strain gauges mounted along the length of the ski. To examine the influence of skier fore/aft positioning on ski deformation, an expert skier skied two runs on a 10 gate giant slalom with a forward position and two runs with an aft position. They reported 40 % greater bending deformation for the middle part of the ski when the skier was in the forward leaning position.

Margane, Trzecinski, Babiel, & Neumaier (1998) used video-based motion analysis to capture the trajectories of a passive physical model of a skier—similar to that described by Glitsch (2001)—skiing on an actual slope. As the model permitted changes in the skier's fore/aft positioning, they were able to study the effect of skier fore/aft position on the model's turn radius. They reported decreasing turn radii with increasing forward inclination of the model from 0^{o} to 15^{o}. Taken together, the results of Tatsuno et al. (2009), DeCecco and Angrilli (1999), Fauve et al. (2009), and Margane et al. (1998) seem to suggest that skiers are in fact able to regulate the RSPD and ski deformation, and thereby the ski's turning behavior, through their fore/aft positioning.

Not many studies have looked at aspects of skier fore/aft actions and performance. A notable exception is the study by Federolf et al. (2008) who tested the effects of skier fore/aft positioning on running time when straight gliding in a tucked position. They did not observe a significant difference in performance time based on fore/aft position as expected (Joubert, 1978/1980). This test was done on straight run gliding, however, and it would very be interesting to see the results of similar tests done in gliding turns where the ski is edged and the fore/aft positioning is expected to affect ski forebody deformation.

Chapter 3

SKIER MECHANCAL ENERGY

One method that may help us to better understand how technique relates to performance is the estimation of mechanical energy dissipation (E_{DISS}) as proposed by Supej (2008) and Supej, Kugovnik, and Nemec (2005a). This method involves calculating a skier's total mechanical energy (E_{MECH}) at each instant in time, knowing the center of mass altitude (potential energy, E_{POT}) and velocity (kinetic energy, E_{KIN}). According to the principle of conservation of mechanical energy, any change in the skier's E_{MECH} represents either a loss of energy to the surroundings due to the work of non-conservative forces such as ski-snow friction, or the gain of energy due to the skier's muscular work. Calculated as the change in skier E_{MECH} per change in meter altitude, E_{DISS} represents a gauge of how a skier manages the potential energy that is available to him.

Supej and his colleagues have described skier mechanical energy characteristics in several studies. In 2005, they reported the energy behaviour of a group of competitors during a slalom world cup competition from 2003 (Supej, Kugovnik, & Nemec, 2005a). They observed a cyclic pattern of energy dissipation over the turn cycle with low dissipations at turn transition and high dissipations at the gate. They also observed negative energy dissipations, situations where the skier has presumably added energy to the system through muscular work[6].

In another study, based on the collective results from three investigations made during world cup slalom races giving a total of 45 analyzed runs, Supej, Kugovnik, and Nemec (2005c) compared ground reaction forces, ski turn radius, and center of mass turn radius with E_{DISS}. Although there was a relatively large variability in E_{DISS} for a given

[6] In the calculation of energy dissipation, Supej (2008) reversed the sign so that numbers would be more understandable for coaches and athletes. I have switched the sign back so that it matches our data. In this dissertation, positive dissipations refer to energy losses and negative dissipations refer to energy gains.

force, the highest dissipations did occur at the same time as the highest forces. They therefore concluded that it is desirable to reduce the presence of the highest forces in most cases.

In 2008, Supej (2008) reported energy dissipation calculations for 16 competitors in a world cup giant slalom from 2003. Once again, he observed that E_{DISS} had cyclic pattern related to the turn cycle with high dissipations at about gate passage, and minimum dissipations at turn transitions. The measured energy dissipations ranged from 31.55 to –6.63 $J \cdot kg^{-1} \cdot m^{-1}$. Supej suggests that the high energy dissipations during the turn were a result of large ground reaction forces acting on the skier. He further suggests that the negative dissipations were situations where the athlete had contributed to his mechanical energy through muscular work and reports that negative dissipations were not uncommon at turn transitions.

In some ways a similar measure to Supej's E_{DISS}, Renshaw and Mote (1989) quantified the thrust force necessary to maintain a constant radius, constant speed turn in a numerical simulation of a rigid skier on a single ski performing a turn on a level plane. The magnitude of the thrust force was understood as a measure of turn efficiency where turns requiring a larger thrust force to maintain momentum were considered less efficient. Using this model, they tested the effect of skier fore/aft position and ski attack angle on turn efficiency. Figure 3.16 shows the thrust force required to maintain the model's speed and turn radius graphed against the fore/aft position of the center of pressure along the ski's longitudinal axis. Renshaw and Mote found that increased thrust was required to maintain momentum as the center of pressure was adjusted forward along the ski and that, furthermore, this effect was exacerbated as ski attack angle was increased.

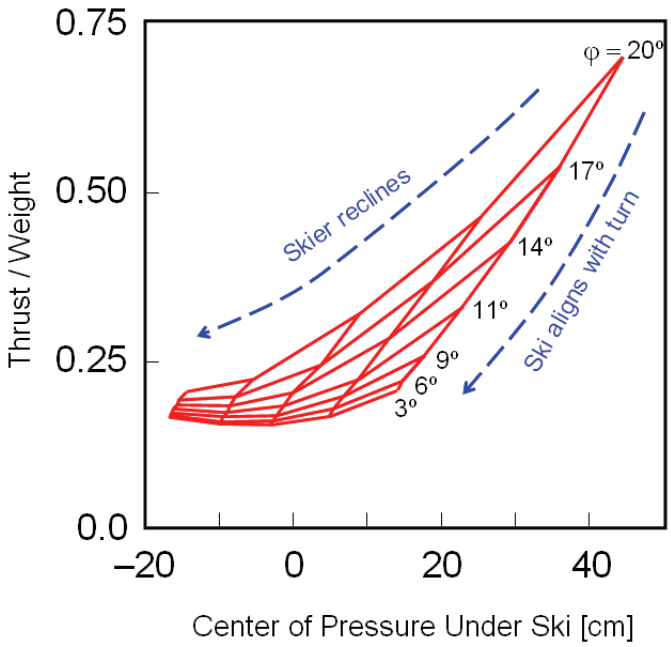

FIGURE 3.16. Numerical simulation results showing the thrust force necessary to maintain momentum through a constant speed, constant radius turn as a function of the center of pressure fore/aft position and ski attack angle, φ (Adapted from Renshaw and Mote, 1989).

SKIER TRAJECTORY LENGTH

Several investigators have examined the relationship between trajectory characteristics and performance time. Nachbauer (1987a, 1987b) and Förg-Rob and Nachbauer (1988) studied the ski trajectory lengths of 34 elite and developing racers in slalom and giant slalom using a 2-dimensional photogrammetric method to quantify ski position. They found that skiers with shorter trajectories had higher mean velocities and better times. In slalom, the fastest skier's line was 27 cm shorter, and his average speed substantially higher, than the mean line over the analyzed turn. Highest ski speeds were reached shortly after turning into the fall line and the slowest speeds were observed at the transition between turns. The fastest skier's skis also traversed the slope at a steeper angle than the group mean (45.8^{o} versus 48.9^{o} for the fastest skier and the group mean, respectively).

To determine if faster competitors skied closer to the gate in slalom, Goodwin (1990a; 1990b) quantified the trajectories of the outside ski boot toe through a portion of a single turn for a selection of competitors during the men's special slalom event at the 1989 World Championships. He found that the lines closest to the gate were not the fastest—as indicated by boot toe velocity—and suggested that there may be an optimal distance from the gate to maximize speed, which in this particular case appeared to be about 40 cm from the gate for the outside boot toe.

Based on an analysis of the mechanical energy dissipation of 16 racers over the course of one turn during a men's world cup giant slalom in 2003, Supej (2008) concluded that the most direct line, with the shortest turning radius was not necessarily the most effective strategy in this situation. In contrast, Miura and Miura (2004) conducted a 3-dimensional kinematic analysis of 11 junior skiers competing in a giant slalom race and found that the better ranked skiers had straighter center of mass trajectories than the lower ranked skiers.

Seifriz and Mester (2001) attempted to create a computer simulation of skier trajectories using genetic algorithms to predict the optimal trajectory. Their work provides a nice example of a situation where a higher velocity at the cost of a longer distance did not pay off in terms of performance time.

To determine if faster skiers choose shorter lines, Žvan and Lešnik (2007) and Lešnik and Žvan (2007) quantified the mean ankle joint position distance to the gate and to the main axis of the course for 18 competitors during a world cup slalom event in 2004. Similar to Goodwin (1990a, 1990b), they found that the ankle joint position of the fastest skiers were not the closest to the gate. They did find that the total trajectory length for the two analyzed turns did negatively correlate with skiing velocity ($r = -.55$, $p = .02$, $n = 18$) and therefore concluded that the shorter, more direct trajectory did increase the likelihood of reaching higher speeds. However, the rather modest correlation suggests that trajectory length was not the only factor influencing skier speed.

It is likely that snow conditions play a role in determining which trajectory will be advantageous in terms of performance. Supej, Nemec, and Kugovnik (2005) investigated the effect of changing course conditions on the trajectory lengths and center of mass speeds of five Slovenian national team members during slalom training. They found decreasing center of mass speeds and increasing trajectory lengths over the course of the training session that they attributed to deteriorating snow conditions.

3.5 SUMMARY

In summary, this chapter has reviewed the theoretical foundation for the conceptual model of turning technique presented in Figure 2.1 and the research questions chosen for this investigation. This review began with an examination of the mechanics of the ski-snow interaction which forms the core of the model. Focus then shifted to a study

of skier actions, to a large degree based on key practitioner textbooks. Emphasis in this discussion was placed on understanding the role of skier actions in regulating the interaction between ski and snow. Finally, key research in skiing technique was summarized with the intention of giving the interested reader a thorough overview of the scientific work on turning technique mechanics that has been reported thus far. Chapter 4 will now describe the theoretical basis for this investigation's methods, including limitations and challenges one can expect to encounter when implementing these methods in the alpine environment.

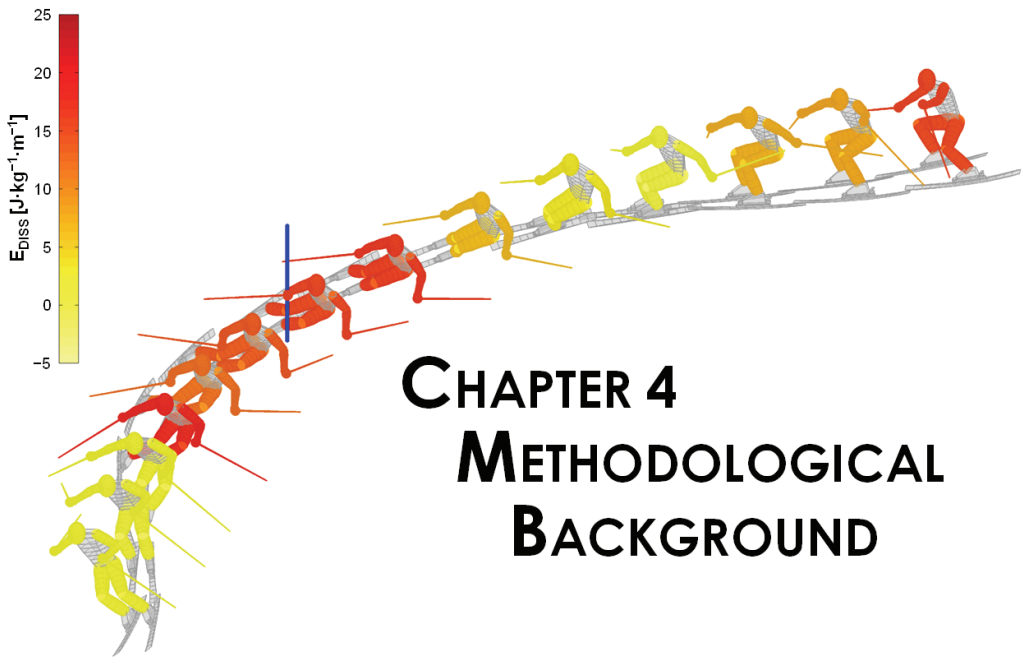

CHAPTER 4
METHODOLOGICAL BACKGROUND

CHAPTER 4. METHODOLOGICAL BACKGROUND

4.1 INTRODUCTION

The purpose of this chapter is to give the reader an overview of the theoretical background of the motion analysis methods implemented in this study, including the camera calibration, camera synchronization and target point reconstruction algorithms. First, the theoretical underpinnings of the Direct Linear Transformation (DLT) method and some of its primary sources of error are presented. Particular attention is given to understanding how traditional fixed-camera techniques have been adapted to allow for subject-tracking cameras. In the second part, camera synchronization methods that have been implemented in the study of human motion are described. Pourcelot, Audigie, Degueurce, Geiger, and Denoix's (2000) software genlock technique is described in detail as this was the method selected for use in this study. Third, a historical review of the video-based motion analysis techniques used in alpine skiing research is presented, including a review of their reported accuracies. And, finally, certain limitations of motion analysis methods in alpine skiing research are explored.

4.2 THE DIRECT LINEAR TRANSFORMATION METHOD

Photogrammetry refers to the science and technology of using image measurement to generate reliable information regarding the geometric properties, position, and orientation of physical objects (Luhmann, Robson, Kyle, & Harley, 2006). Initial photogrammetric techniques were developed as early as the middle of the 19th century and some of the first applications of photogrammetry to describe the motion of human beings were implemented by the end of the 1800's (Winter, 2005). More recently, technological developments in computer hardware, software, and digitial photography have resulted in the widespread use of photogrammetry in numerous fields.

As late as the 1960's, photogrammetric methods required the use of metric cameras with precisely known and calibrated internal geometries to obtain sufficiently accurate information (Luhmann et al., 2006). However in 1971, Abdel-Aziz and Karara (1971) proposed a method that does not require prior knowledge of the internal and external orientation parameters of the camera, thus allowing images from less-expensive, non-metric cameras to be analyzed with a relatively high accuracy. This technique, known as the "Direct Linear Transformation" (Abdel-Aziz & Karara, 1971, p. 1) has made the use of photogrammetric methods possible on a much more widespread basis.

THEORETICAL BASIS OF THE DLT

The first photogrammetric methods required the knowledge of the transformation parameters between four independent reference systems (Luhmann et al., 2006). First, a two-dimensional image-space coordinate system was defined within the image plane in the camera. For digital cameras, this coordinate system is defined by the sensor array. In addition, a three-dimensional coordinate system was defined within the physical construction of the camera with its origin at the projection center. A two-dimensional comparator coordinate system defined coordinates of the projected image that was used to digitize image points. Finally, a three-dimensional object-space or

real-world coordinate system defined the physical space containing the object to be measured.

The main advantage of metric cameras is that the physical relationship between the image-, comparator-, and camera coordinate systems are known with a high degree of precision. This is accomplished through the use of reference points (so-called fiducial marks) that, when projected onto the image during exposure, allow the accurate determination of the transformation parameters between these three reference systems.

The challenge in using non-metric cameras for photogrammetric purposes is that these relationships are not known *a priori* and, moreover, can be expected to change over time (Luhmann et al., 2006). In the DLT however, this problem is circumvented by determining the transformation parameters between the comparator- and object-space coordinate systems directly. The parameters for this transformation are determined experimentally at the time of data collection using a set of so-called control points distributed throughout the object-space and within the camera field of view. When both the comparator- and object-space coordinates of a sufficient number of control points are known, the transformation parameters between these two reference systems can be approximated. At the heart of the DLT method are two linear equations relating a point's 2-d comparator-space coordinates (U,V) with it's 3-d object-space coordinates (X,Y,Z) (Abdel-Aziz & Karara, 1971):

$$U = \frac{L_1X + L_2Y + L_3Z + L_4}{L_9X + L_{10}Y + L_{11}Z + 1} \qquad [4.1]$$

$$V = \frac{L_5X + L_6Y + L_7Z + L_8}{L_9X + L_{10}Y + L_{11}Z + 1} \qquad [4.2]$$

where L_1... L_{11} are referred to as the 11 DLT camera constants. Equations [4.1] and [4.2] can be solved for L_1... L_{11} and rearranged into the matrix form A.x = b to give Equations [4.3] for a set of n control points:

$$\begin{bmatrix} X_1 & Y_1 & Z_1 & 1 & 0 & 0 & 0 & 0 & -1U_1X_1 & -1U_1Y_1 & -1U_1Z_1 \\ 0 & 0 & 0 & 0 & X_1 & Y_1 & Z_1 & 1 & -1V_1X_1 & -1V_1Y_1 & -1V_1Z_1 \\ X_2 & Y_2 & Z_2 & 1 & 0 & 0 & 0 & 0 & -1U_2X_2 & -1U_2Y_2 & -1U_2Z_2 \\ 0 & 0 & 0 & 0 & X_2 & Y_2 & Z_2 & 1 & -1V_2X_2 & -1V_2Y_2 & -1V_2Z_2 \\ \vdots & \vdots & \vdots & \vdots & \vdots & \vdots & \vdots & \vdots & \vdots & \vdots & \vdots \\ X_n & Y_n & Z_n & 1 & 0 & 0 & 0 & 0 & -1U_nX_n & -1U_nY_n & -1U_nZ_n \\ 0 & 0 & 0 & 0 & X_n & Y_n & Z_n & 1 & -1V_nX_n & -1V_nY_n & -1V_nZ_n \end{bmatrix} \begin{bmatrix} L_1 \\ L_2 \\ L_3 \\ L_4 \\ \vdots \\ L_{10} \\ L_{11} \end{bmatrix} = \begin{bmatrix} U_1 \\ V_1 \\ U_2 \\ V_2 \\ \vdots \\ U_n \\ V_n \end{bmatrix} \quad [4.3]$$

where the subscript refers to the control point number. With six or more control points, Equations [4.3] become an over-determined set of 2n linear equations and the 11 unknown camera constants can then be determined using a least-squares technique. Once the constants of a camera are known, Equations [4.1] and [4.2] can again be rearranged, this time solving for the unknown object-space coordinates (X,Y,Z) of a target point to give Equations [4.4]:

$$\begin{bmatrix} (L_1 - L_9U) & (L_2 - L_{10}U) & (L_3 - L_{11}U) \\ (L_5 - L_9V) & (L_6 - L_{10}V) & (L_7 - L_{11}V) \end{bmatrix} \begin{bmatrix} X \\ Y \\ Z \end{bmatrix} = \begin{bmatrix} (U - L_4) \\ (V - L_8) \end{bmatrix} \quad [4.4]$$

When a target point of unknown object-space coordinates is digitized on calibrated images taken by multiple, synchronized cameras, Equations [4.4] for each camera can be combined giving Equations [4.5]:

$$\begin{bmatrix} \left(L_1^1 - L_9^1 U^1\right) & \left(L_2^1 - L_{10}^1 U^1\right) & \left(L_3^1 - L_{11}^1 U^1\right) \\ \left(L_5^1 - L_9^1 V^1\right) & \left(L_6^1 - L_{10}^1 V^1\right) & \left(L_7^1 - L_{11}^1 V^1\right) \\ \left(L_1^2 - L_9^2 U^2\right) & \left(L_2^2 - L_{10}^2 U^2\right) & \left(L_3^2 - L_{11}^2 U^2\right) \\ \left(L_5^2 - L_9^2 V^2\right) & \left(L_6^2 - L_{10}^2 V^2\right) & \left(L_7^2 - L_{11}^2 V^2\right) \\ \vdots & \vdots & \vdots \\ \left(L_5^m - L_9^m V^m\right) & \left(L_5^m - L_9^m V^m\right) & \left(L_5^m - L_9^m V^m\right) \\ \left(L_5^m - L_9^m V^m\right) & \left(L_5^m - L_9^m V^m\right) & \left(L_5^m - L_9^m V^m\right) \end{bmatrix} \begin{bmatrix} X \\ Y \\ Z \end{bmatrix} = \begin{bmatrix} \left(U^1 - L_4^1\right) \\ \left(V^1 - L_8^1\right) \\ \left(U^2 - L_4^2\right) \\ \left(V^2 - L_8^2\right) \\ \vdots \\ \left(U^m - L_4^m\right) \\ \left(V^m - L_8^m\right) \end{bmatrix} \qquad [4.5]$$

for m cameras, where the superscripts refer to camera number. With two equations per camera, a minimum of two cameras will give an over-determined system of 2m equations allowing the object-space coordinates (X,Y,Z) of the target point to be approximated using a least squares technique. Using this method, and a minimum of two calibrated and synchronized video cameras, one can track the position of multiple points in 3-dimensional space over time.

PANNING CAMERA METHODS

In the standard approach, the set of control points are set up in the object-space, recorded for calibration purposes, and then removed prior to the subject's execution of the motion to be analyzed. During data reduction, the calibration frames are digitized and the transformation parameters are approximated as previously described. Assuming that the cameras remained fixed during the entire data collection, these parameters can be used to accurately reconstruct the subject's motion.

Using fixed cameras in this way, however, limits the use of video-based motion analysis to just a few meters or a portion of the movement of interest in field studies of many sporting actions. This is due to the relatively large movement volumes typical in sport and the necessity to have a sufficiently large image of the athlete for accurate digitization (Mössner, Kaps, & Nachbauer, 1996; Nachbauer et al., 1996). This challenge has stimulated the development of numerous methods that allow cameras to track

subjects as they move through the object space, thereby allowing sizeable movement volumes to be covered while maintaining a sufficiently large image of the subject for digitizing purposes. In general, these solutions can be classified as one of three types.

The first type of approach, and perhaps the simplest to implement, essentially consists of individually calibrating every frame from each camera according to standard calibration procedures (Baroni et al., 1998; de Haan & den Brinker, 1988). This "repeated calibration" approach (Baroni et al., 1998) in effect frees cameras to pan, tilt, and zoom without restrictions. There are two drawbacks to this technique, however. First, control points must remain in the object-space during filming which may interfere with the athlete's performance and may not be allowed in certain situations, such as competitions. Second, the repeated calibrations require a very large volume of manual digitization labour.

In the second type of approach, calibration parameters are initially determined for certain positions along the expected motions of each camera (Scheirman, Porter, Leigh, & Musick, 1998; Stivers et al., 1993). These initial measurements are then used to define the calibration parameters as functions of camera displacement. Then, during filming, camera displacement is measured using instrumented tripods and later used in conjunction with the calibration equations to determine the transformation parameters for each image. This method avoids both the problems of having to leave control points in the object-space and the large digitization work volume associated with the repeated calibration approach. The disadvantage of this approach is the requirement for specialized tripods and strict control of camera motion to rotation about one or two axes.

The third approach is similar to the second in that equations of calibration parameters as functions of camera displacement are generated. However, instead of measuring camera motion directly with instrumented tripods, this method uses control information from the digitized images to determine the camera's displacement (Drenk,

1994; Yeadon, 1989; Yu, Koh, & Hay, 1993). In a way, this approach is a compromise between the first two methods in that the volume of manual digitization work associated with the repeated calibration approach is substantially reduced and the instrumented tripods of the second approach are not required. The limitations in this method are that some control points are required in the object space to allow determination of the camera displacement. In addition, camera positions must be known and camera motion must be restricted to rotation about one or two axes.

SOURCES OF ERROR

There is a relatively large body of scientific literature examining error sources in video-based human motion analysis methods. In this section, an overview of the main sources of error identified in this literature is presented. The DLT method can be generally divided into two processes: (1) Approximation of the 11 transformation parameters—referred to as camera calibration—and (2) reconstruction of a target point's object-space coordinates. Each of these processes is associated with different sources of error.

CAMERA CALIBRATION ERROR

For calibration accuracy, the measurement, number, placement, and design of control points play a particularly important role. To calculate the transformation parameters, the control point object-space coordinates must be measured. In field studies, this is often accomplished using a theodolite and standard surveying techniques. Both systematic and random error in these measurements result in a deterioration of the calibration accuracy (Abdel-Aziz & Karara, 1971; Chen, Armstrong, & Raftopoulos, 1994).

Although only six control points are required to determine the camera constants, it is well established that calibration accuracy improves with increasing numbers of control

points (Abdel-Aziz & Karara, 1971; Challis & Kerwin, 1992; Chen et al., 1994; de Haan & den Brinker, 1988; Gazzani, 1993b; Hatze, 1988; Hinrichs & McLean, 1995; Wood & Marshall, 1986). The random error associated with both the measurement and digitization of any single control point has less influence on the overall calibration accuracy when a large number of control points are used (Walton, 1981). At the same time, a point of diminishing returns can be reached where the random component of the calibration error becomes minimized with increasing numbers of control points. At that point, the systematic error associated with system set-up, lens distortion, and image deformation will dominate the calibration error (Chen et al., 1994) and the further inclusion of greater numbers of control points is not likely to improve accuracy significantly. Thus, general recommendations are for the use of between 12 and 20 control points (Chen et al., 1994; de Haan & den Brinker, 1988; Gazzani, 1993b; Hinrichs & McLean, 1995; Shapiro, 1978), although some research has shown continued improvements with as many as 30 (Abdel-Aziz & Karara, 1971) and even 60 control points (Hinrichs & McLean, 1995).

In addition to total number, the placement and distribution of control points in the movement volume is important for calibration accuracy. In particular, the reconstruction of target points that fall outside of the calibrated volume is associated with large errors (Angulo & Dapena, 1992; Bate, 1993; Brewin & Kerwin, 2005; Challis & Kerwin, 1992; Chen et al., 1994; Gazzani, 1993a; Hatze, 1988; Hinrichs & McLean, 1995; Levy & Smith, 1995; Walton, 1981; Wood & Marshall, 1986; Yu et al., 1993). It is therefore important that the control points completely enclose the expected movement volume (Challis & Kerwin, 1992; Chen et al., 1994; Shapiro, 1978).

Human operating error in identifying and digitizing the control point center is another source of calibration error (Abdel-Aziz & Karara, 1971; de Haan & den Brinker, 1988; Van Gheluwe, 1978; Walton, 1981; Wood, 1982). This is in part affected by the quality and resolution of the images being digitized (Angulo & Dapena, 1992; Kennedy,

Wright, & Smith, 1989; Yeadon, 1989; Yu et al., 1993). Correct camera adjustment of shutter speed, aperture, and focus are particularly important in this regard (de Haan & den Brinker, 1988).

Certain aspects of control point design may also be important in terms of digitization accuracy. For instance, the size of the marker can have an impact on manual digitization accuracy (de Haan & den Brinker, 1988). While markers that are too small may be difficult to visualize due to the limited resolution of video, it may be difficult to identify the centroid of markers that are too big. The digitization method may also influence digitizing error. Bahamonde & Stevens (2006) compared accuracy between digitizing all points, frame-by-frame, versus digitizing all frames, point-by-point. They found an improved accuracy when operators digitized one point at a time so that they could track the same point throughout the trial.

Inadequacies of the calibration algorithm in the mathematical modeling of film and lens characteristics, including distortion, also result in calibration error (Abdel-Aziz & Karara, 1971; Chiari, Croce, Leardini, & Cappozzo, 2005). Several modifications to the standard, 11 parameter DLT have been proposed to correct for these distortions (Gazzani, 1993a, 1993b; Hatze, 1988; Marzan & Karara, 1975), however mostly limited improvements in accuracy have been seen using these algorithms, particularly when extrapolation outside of the calibration volume is avoided (Challis & Kerwin, 1992; Gazzani, 1993a, 1993b; Walton, 1981; Wood & Marshall, 1986). This is perhaps due to the relatively high quality of camera lenses that are now available in many semi-professional digital video cameras that are often used in motion analysis applications.

RECONSTRUCTION ERROR

Target point reconstruction error is to a large degree determined by the accuracy of the transformation parameters determined during camera calibration such that all of the aforementioned sources of calibration error are also sources of reconstruction error.

There are, however, a number of factors which directly influence reconstruction accuracy, including digitization error, the number of cameras used in the reconstruction, camera placement and camera synchronization.

In cases where target points are manually digitized, perhaps the largest error in object-space reconstruction is associated with the precision of the individual doing the digitizing (Walton, 1981; Wood, 1982). This can be particularly challenging when digitizing ill-defined points on the human body as one's perception of the location of a point can change as body segments rotate. Digitization errors also occur when target points are automatically tracked and digitized, particularly when target markers are partially or entirely occluded from camera view (Chiari et al., 2005; de Leva, 2008).

Although a minimum of two cameras is required in the DLT to reconstruct a target point, improved accuracy is expected with increased numbers of cameras. The reason for this can be understood if one considers that in an idealized reconstruction, the camera rays intersect at precisely the target marker centroid (Chiari et al., 2005). In this case, only two cameras are needed for a perfect reconstruction and adding cameras will not improve accuracy. In reality however, various sources of error cause the camera rays to deviate from the true marker position so that they do not intersect. The reconstructed position is thus calculated as the quasi-intersection point between rays in a least squares sense. Increasing the number of cameras then can be expected to improve accuracy (Chiari et al., 2005) and this has been demonstrated with three cameras (Levy & Smith, 1995). Further increases in the number of cameras have lead to limited improvements in accuracy. However, more than 3 or 4 cameras may still be required when tracking complicated objects, such as the human body, to ensure that each point is viewed by a minimum of 2 to 3 cameras throughout the range of motion.

The angle between camera optical axes has also been shown to be important for reconstruction accuracy. General recommendations are that the distance:base ratio

should be at least 2:1 or 3:1 (Bate, 1993; Chen et al., 1994; de Haan & den Brinker, 1988; Shapiro, 1978; Wood & Marshall, 1986).

Finally, an important assumption of the DLT method in object-space reconstruction is that exposures from multiple cameras are precisely synchronized in time. While this requirement is not necessary for stationary objects, it is very important for objects in motion as even a small error in synchronization can be expected to result in a substantial deterioration in the reconstruction accuracy of a rapidly moving target point. Owing to its importance in reconstruction accuracy, camera synchronization methods will be discussed in greater detail in the following section.

4.3 CAMERA SYNCHRONIZATION

Camera synchronization methods have developed in parallel in numerous fields. This discussion will be limited to the development of synchronization methods in biomechanics and human motion analysis. The purpose of this section is to give the reader an overview of the various techniques that have been used in human motion analysis. Pourcelot and coworkers' (2000) software genlock algorithm is described in detail as this is the method implemented in this study.

SYNCHRONIZATION TECHNIQUES

Ideally, synchronization is achieved using cameras with generator lock (genlock) capabilities in which one camera controls the others so that exposures are taken at precisely the same time. However, the expense of such cameras has stimulated the development of techniques to synchronize cameras lacking such capability.

The simplest method involves synchronizing cameras to the nearest whole field (0.02 sec for PAL video) by identifying the field in each camera that corresponds to a distinct event. However, this method is not discrete enough to accurately quantify rapid

athletic movements. An improvement upon this method has been achieved by placing a specialized timer within the cameras' fields of view so that the time of each field on each camera can be determined, and the data from slave cameras interpolated to time-match data from the master camera (Blievernicht, 1967; Walton, 1970). A similar solution involves placing devices pulsating at known frequencies on the athlete (Cappozzo, Leo, & Macellari, 1983; Mann et al., 1983). These methods however are limited in that they require either the placement of devices near the movement volume, or on the athlete, both of which may interfere with the athlete's performance and may not be permitted in some situations such as competition.

In studies of high jumpers, Dapena (1978) and Dapena and Chung (1988) solved this problem by identifying fields in each camera associated with a series of distinct events —in this case the landings and take-offs of the run-up strides—and then creating a linear regression equation to mathematically quantify the frame correspondence between cameras. Yeadon (1989) was the first to suggest using the reconstructed displacement data of a subject to determine the timing offset between cameras in a study of ski jumpers. This method was limited however by the requirement that certain aspects of the subject's trajectory be known in advance.

In 1993, Barros and Brenzikofer (1993) proposed a more flexible synchronization method based on determining mathematically the straight line light rays between a reconstructed point and each camera's projection center. In an ideal, synchronized reconstruction, these rays will intersect at the reconstructed point's object-space position. However, these rays normally do not intersect due to error associated with, among other things, camera synchronization. The Barros and Brenzikofer method synchronizes cameras by determining the frame offset corresponding to the minimization of the shortest segment distance between these camera rays. Both Yeadon and King (1999) and Pourcelot et al. (2000) have further elaborated algorithms that are

based on this concept, which is generally referred to as the "software genlock" (Kwon, Yoon, & Sung, 2004, p. 64) within the human motion analysis community.

THE ACCURACY OF SOFTWARE GENLOCK TECHNIQUES

Only a small number of studies have reported on the accuracy of software genlock techniques. Barros and Brenzikofer (1993) evaluated the accuracy of their software genlock algorithm by capturing the motion of a falling ball and estimating its acceleration due to gravity, which they determined to be 9.87 $m \cdot s^{-2}$. Yeadon and King (1999) reported average and maximum synchronization errors of 0.5 and 3.6 ms, respectively, when comparing predicted phase shifts from their genlock algorithm with actual shifts measured using genlocked cameras. Pourcelot et al. (2000) reported the consistency of their phase shift calculations for multiple pairs of cameras and reported maximal inconsistencies of less than 5% of the time interval between two frames. At a film rate of 50 Hz, this corresponds to maximal inconsistencies of less than 1 ms. Kwon et al. (2004) compared actual camera time offsets determined experimentally with those calculated using a software genlock technique and reported a mean synchronization error of approximately 0.13 ms when three target points were used to determine the offset. They also reported a trend of improved synchronization accuracy when the number of target points used in the phase shift determination was increased from one to three.

POURCELOT'S SOFTWARE GENLOCK

This section describes Pourcelot and coworkers' (2000) software genlock algorithm in detail as this was the method selected for use in this study. Pourcelot's algorithm involves varying the phase shift between two cameras to determine that which minimizes the optimization error terms in the two DLT equations:

$$U + \delta U = \frac{L_1X + L_2Y + L_3Z + L_4}{L_9X + L_{10}Y + L_{11}Z + 1} \quad [4.6]$$

$$V + \delta V = \frac{L_5X + L_6Y + L_7Z + L_8}{L_9X + L_{10}Y + L_{11}Z + 1} \quad [4.7]$$

where δU and δV are the optimization error terms in comparator-space coordinates (Pourcelot et al., 2000). Knowing the digitized comparator-space coordinates (U,V) for a point, as well as the reconstructed object-space coordinates (X,Y,Z), one can calculate the optimization error terms for both cameras and both comparator-space dimensions by rearranging Equations [4.6] and [4.7]. The mean DLT optimization error ($\overline{\xi}$) over a series of n time points for a single target point can then be calculated using Equation [4.8]:

$$\overline{\xi} = \frac{\sum_{j=1}^{j=2}\sum_{i=1}^{n}\sqrt{\delta U_{ji}^{\ 2} + \delta V_{ji}^{\ 2}}}{2n} \quad [4.8]$$

where j is the camera number; i is the time point; n is the total number of time points; and δU_{ji} and δV_{ji} are the comparator-space optimization errors for camera j and time point i (Pourcelot et al., 2000). By systematically adjusting the shift between cameras and interpolating slave camera data to match the master camera accordingly, the phase shift minimizing the mean DLT optimization error ($\overline{\xi}$) can be identified. Assuming that all other sources of error are independent of camera synchronization and thus remain constant, the minimum mean DLT optimization error should correspond to the phase shift between cameras.

4.4 VIDEO-BASED MOTION ANALYSIS TECHNIQUES IN ALPINE SKIING

Film- and video-based motion analysis has been a popular method to study skiing technique. The purpose of this section is to describe some of the previous implementations of motion analysis methods in alpine skiing research, discussing potential limitations and problems associated with each method. In addition, the reported accuracies of studies using panning cameras are reviewed. Finally, some potential limitations in field studies of alpine skiing in general are summarized.

HISTORICAL DEVELOPMENT

In a summary of Japanese skiing research, Watanabe (1981) described several investigations using video-based techniques to capture skier kinematics and kinetics starting as early as 1970. It was not before the late 1980's, however, that the first quantitative motion analysis studies of skiing in the English language literature were published. Nachbauer and Förg-Rob (Förg-Rob & Nachbauer, 1988; Nachbauer, 1987a, 1987b) reported on a 2-dimensional study using a single high-speed 16 mm camera filming at 50 Hz to track the position of the binding toe piece on the plane of the snow surface. Similarly, Glenn and Larsson (1987) also conducted a 2-dimensional analysis quantifying ski motion through a single giant slalom turn using multiple photographs taken at 7 Hz. Two-dimensional studies such as these are still sometimes used when the primary interest is in studying ski trajectory characteristics (Ferrario, Sforza, Michielon, Dugnani, & Mauro, 1997; Knünz et al., 2000; Sahashi & Ichino, 1995, 1998; Wimmer, 2001).

These 2-dimensional studies of ski motion are limited to some extent by the fact that the actual shape of the slope and the trajectory of the skis are probably 3-dimensional even when the slope appears to be relatively planar. One notable solution to this problem was implemented by Schiestl and colleagues (Schiestl, 2005; Schiestl, Kaps,

Mössner, & Nachbauer, 2005, 2006) who captured and modeled the position of the snow surface in a 3-dimensional object-space and then tracked ski trajectories on this snow surface using a single-camera approach. The assumption behind this method is that the skis remain on the snow surface which is known to not hold at certain times. However, this may still be an interesting approach for use in studying ski trajectories and motion in situations where a 3-dimensional approach may be difficult to implement, such as in competitions.

The first reported 3-dimensional studies were conducted in the early 1990's. Goodwin (1990a, 1990b) reported on a study conducted during the men's slalom event at the 1989 World Championships in which skier kinematics during the middle portion of a single turn were captured by two 100 Hz synchronized cameras placed near the competition course. Brierley and Bartlett (1991) used two fixed, genlocked video cameras filming at 50 Hz to quantify the vertical dynamics of experienced and novice skiers in three dimensions through a calibrated volume of approximately 6.72 m x 3.03 m x 2.00 m. Similarly, Schaff and Hauser (1993) tested the then newly developed Peak Performance Video Analysis System (Peak Performance Technologies, Inc., Denver, USA) based on S-VHS video. Although these studies represented a significant step forward in terms of methodology, they were limited due to the small size of the movement volume that could be covered by the fixed cameras. This is particularly restrictive in alpine skiing field research as movements occur over relatively large volumes. For instance, to analyze two complete turns in slalom would require a calibrated volume of approximately 30 m long x 10 m wide x 2 m high, about twice the size of the calibrated space in the Brierley and Bartlett study.

Several approaches to this problem have since been implemented in the alpine skiing research. Starting in the mid-1990's, a group of researchers based in Austria (Mössner, Kaps, & Nachbauer, 1995; Mössner et al., 1996; Nachbauer et al., 1996) and another group in Italy (Pozzo, Canclini, Casasola et al., 2005; Pozzo, Canclini, Cotelli et al., 2005;

Pozzo, Canclini, Cotelli, & Baroni, 2001) began using methods similar to the repeated calibration approach described earlier (see p. 104) to study skiers in both experimental and competitive environments using freely moving cameras. This approach, however, requires maintaining a large number of control points in the object-space during data collection and is associated with a large digitization work volume.

These limitations have prompted researchers to shift towards methods that reduce both the number of control points required in the object-space as well as the post-processing digitization volume. A popular method has been the technique developed by Drenk (1994) that is essentially based on the concept of determining the DLT transformation parameters as functions of camera pan and tilt angles (see p. 104). In this approach, camera orientation angles are determined post-recording using the digitized comparator-space coordinates of a limited number of control points that are retained in the object-space during data collection. To accomplish this, specialized camera tripods are required that precisely control both the camera position and rotation axes. This method, referred to here as the Passpoint method, has been used in a number of 3-dimensional studies tracking the entire ski-skier system (Federolf, 2005; Frick et al., 1997; Klous, 2007; Klous & Schwameder, 2003; Lindinger, 2006; Lüthi et al., 2005; Müller et al., 1998; Raschner et al., 1997; Raschner et al., 1999; Raschner et al., 2001; Schiefermüller et al., 2005; Vodičková, Lufinka, & Zůbek, 2005).

Other solutions to the need for a large object-space volume have also been implemented in skiing research. Of particular note are the studies by Supej and colleagues (Lešnik & Žvan, 2003, 2007; Supej, 2008; Supej, Kugovnic, & Nemec, 2005a, 2005c; Supej, Kugovnik, & Nemec, 2003; Supej, Nemec, & Kugovnic, 2005; Žvan & Lešnik, 2007) that have solved the problem of covering a large movement space by using an increased number of fixed cameras (4 to 6) to cover a series of overlapping calibration volumes.

Despite the fact that body landmarks are reconstructed in 3 dimensions, these methods are limited in that they do not allow a full 3-dimensional kinematic description of body segment translational and rotational motion. To the author's knowledge, only one full 3-dimensional motion analysis study in the field has been attempted in the skiing research. Klous (2007) captured the outside leg motion of a skier executing carved and skidded, giant slalom-sized turns using a 5 panning camera set-up. The skier wore a specially designed suit with multiple markers sewn onto the thigh and shank segments to allow full characterization of the thigh and shank segment kinematics.

Recently, methods that combine measurements from satellite-based positioning systems with inertial measurement have been developed to quantify skier kinematics and kinetics (Brodie, Walmsley, & Page, 2007, 2008, 2009; Huber, Waibel, & Spitzenpfeil, 2009; Supej, 2009). Once techniques such as these are fully implemented and validated, they will greatly increase the potential for motion analysis studies in alpine skiing.

ACCURACY

Varying methods have been used to analyze the measurement error in video-based motion analysis studies in alpine skiing. This, combined with the fact that descriptions of how error estimates are made are often lacking, makes comparisons between studies difficult. Important exceptions to this are the dissertations by Federolf (2005), Klous (2007) and Lindinger[7] (2006) where rather detailed analyses of measurement error are described.

Federolf's (2005) analysis is rather unique in that he reports on the discrepancies between two independently operating motion analysis systems that captured the

[7] Lindinger (2006) actually reports on a cross country skiing study. However, the method used and some of the challenges in field implementation are similar to that in alpine skiing.

motion of a skier through two long turns at an indoor skiing hall. One of the systems consisted of two fixed, high speed cameras while the other used three panning analogue cameras. The average absolute difference between the two systems in position reconstruction was 18, 8 and 6 cm in the global coordinate system x-, y-, and z-dimensions, respectively. Discrepancies in center of mass position were lower at 12, 6, and 3 cm in the x-, y-, and z-dimensions. Federolf also compared measurements of ski orientation angles and found average discrepancies of 5.0° and 2.6° for the ski edge angle and the ski angle to the horizontal, respectively. As will be seen shortly, these error estimates are rather large compared to other reports and may reflect limitations of the two (fixed) camera set-up to reconstruct trajectories over a very large movement volume.

Both Klous (2007) and Lindinger (2006) used somewhat similar approaches to evaluate their measurement error. Klous used five panning cameras to track an alpine skier through one giant slalom turn. In Lindinger's study, two panning cameras were used to track cross country skiers over approximately a 70 meter long track. Both Klous and Lindinger conducted several different forms for error analysis including estimations of measurement system validity, reliability, and objectivity.

To assess measurement validity, both Klous (2007) and Lindinger (2006) reported the error in the reconstructed positions of well-defined reference points which were not used in camera calibration, referred to in this report as *non*-control point error[8]. Average *non*-control point reconstruction errors in the x-, y- and z- dimensions were 12, 9, and 13 mm and 10, 9, and 5 mm in the Klous and Lindinger studies, respectively. They reported maximum *non*-control point errors of 32 and 33 mm.

[8] Actually, Klous (2007) and Lindinger (2006) did not specifically state whether or not the points used to determine measurement accuracy were also used to determine the calibration parameters. My assumption is that the points were not used in calibration directly, but may have been used to measure camera displacement as a part of the Passpoint method.

Errors in the lengths of reconstructed segments were also used to assess validity in both studies. Klous (2007) compared reconstructed ski pole lengths to measured lengths and found a maximum error of 33 mm and a root mean squared error of 26 mm. Lindinger (2006) compared reconstructed thigh, shank, upper arm, and lower arm segment lengths to actual measurements and reported average differences ranging from –10.7 to 8.8 mm. These are average differences, however, and while this does indicate the size and direction of any systematic shift in the reconstructed data, it may not reflect the magnitude of errors in the individual reconstructions.

To describe measurement reliability, Klous (2007) reported standard deviations of 1 to 8 mm in the reconstructed positions of a set of *non*-control points that were digitized 10 times. Similarly, Lindinger reported the standard deviations in inter-segment angle calculations based on multiple digitizing. Standard deviations in the hip-, knee- and elbow- angles ranged from 1.0^{o} to 1.7^{o} and standard deviations in the ski edge and orientation angles ranged from 0.6^{o} to 1.4^{o}.

Since each reconstruction is independently digitized and calculated, standard deviations in segment length measurements were also presented as measures of reliability. Towards this end, Klous (2007) reported a standard deviation of 9 mm for ski pole length reconstructions while Lindinger reported standard deviations ranging from 1.2 to 8.1 mm for thigh, shank, upper arm, lower arm, and foot segment length reconstructions.

To assess measurement objectivity, *non*-control points were digitized by four independent operators in the Klous (2007) study. Maximum inter-operator differences were 12, 9, and 3 mm in the x-, y-, and z- dimensions, respectively.

In summary, error in these field studies seems to be slightly higher than what might be attainable under laboratory conditions. Based on these results, maximum errors in position reconstruction of at least up to 30 mm should be expected using these methods

in the field. Considering the very large size of the movement volume and the extreme challenges associated with implementing such methods in the field, this level of accuracy is impressive. Nevertheless, the size of these errors does limit the use of such methods. In the next section, some of these limitations will be examined.

LIMITATIONS OF VIDEO-BASED MOTION ANALYSIS IN SKIING RESEARCH

Relative to other methods of capturing skier kinematics and kinetics, the primary advantage of video-based motion analysis is that it can be used to measure skiing performances with minimal interference to the athlete—even to the extent that it has been used in competitive situations (e.g., Pozzo, Canclini, Casasola et al., 2005; Pozzo, Canclini, Cotelli et al., 2005; Pozzo, Canclini, Cotelli et al., 2001; Pozzo, Canclini, Cotelli, Martinelli, & Rockmann, 2001; Schiestl, 2005; Supej, 2008; Supej, Kugovnik, & Nemec, 2005c). There are certain limitations in the use of video-based motion analysis to study skiing technique, however, and some of these will be examined here.

First, it is generally agreed upon that calculations of accelerations, forces, and moments based on kinematic data in skiing should be interpreted with caution due to the sizeable error (Lüthi et al., 2005; Supej, Kugovnik, & Nemec, 2005b). Analyses where reconstructed position data are twice differentiated to obtain accelerations and forces should be limited to describing the overall time course and absolute magnitude of these forces (Lüthi et al., 2005).

Another limitation of video-based motion analysis techniques is the rather limited movement space that can be covered. Even with panning cameras, analyses will be limited to a maximum of several turns in slalom, and even fewer in the other disciplines. As Brodie and colleagues (2007, 2008, 2009) point out, performance on any chosen sequence of turns on a course will be intimately interrelated with the skier's performances on both the previous and the subsequent sections of the course.

Consequently, understanding how parameters measured on a short sequence of turns relate to overall skier performance is problematic.

Furthermore, the substantial resources that such investigations require in terms of time and man-power severely limit the total number of athletes, situations, and turns that can be analyzed. Given the highly variable nature of the sport—not only in terms of external conditions but also in terms of athlete technical styles—this is certainly one of the main challenges faced by scientific efforts to the study of skiing today. As a very good example, the one data collection used in this dissertation has taken over three years to analyze (albeit that a substantial amount of this time was used for method development, implementation and validation since it was the first study of its kind at our institution).

The development of GPS and inertial measurement systems (Brodie et al., 2007, 2008, 2009; Huber et al., 2009; Supej, 2009) has the potential to significantly advance scientific understanding of skiing technique. Not only will such methods allow the measurement of skiers over the entire course, making performance analyses possible, the more rapid turn-around of information will allow for a greater number of athletes to be studied in a greater number of situations.

A limitation of field methods in general in alpine skiing is that an enormous number of factors can affect an individual performance, many over which the investigator has no control (e.g., weather and snow condition changes during the investigation). Perhaps the most difficult challenge in studying alpine skiing is the fact that turning technique involves a continual process of athlete adaptation to the surrounding conditions, which, in turn, are infinitely variable. This complicates the study of turning technique as how skiers solve one turn may not necessarily generalize to any other situations. Moreover, technique is highly individual and it is unlikely that there is any one "optimal" technique that would work best for all skiers. This can be readily observed by the large diversity of technical styles in today's top skiers. These facts to a large

degree limit studies of skiing technique to observational designs. Artificially imposing technical or tactical performance constraints on an individual athlete in an experimental design may require an athlete to ski in a way that is sub-optimal for her (and her equipment set-up) in that particular situation.

4.5 SUMMARY

This chapter has reviewed the principles behind the methods selected in this study, including the Direct Linear Transformation, panning camera techniques, and the software genlock. In addition, applications of these methods in skiing field research have been reviewed and some of the challenges and limitations of these types of methods were presented. In the next chapter, a detailed description is given of how the selected methods chosen for this study were implemented.

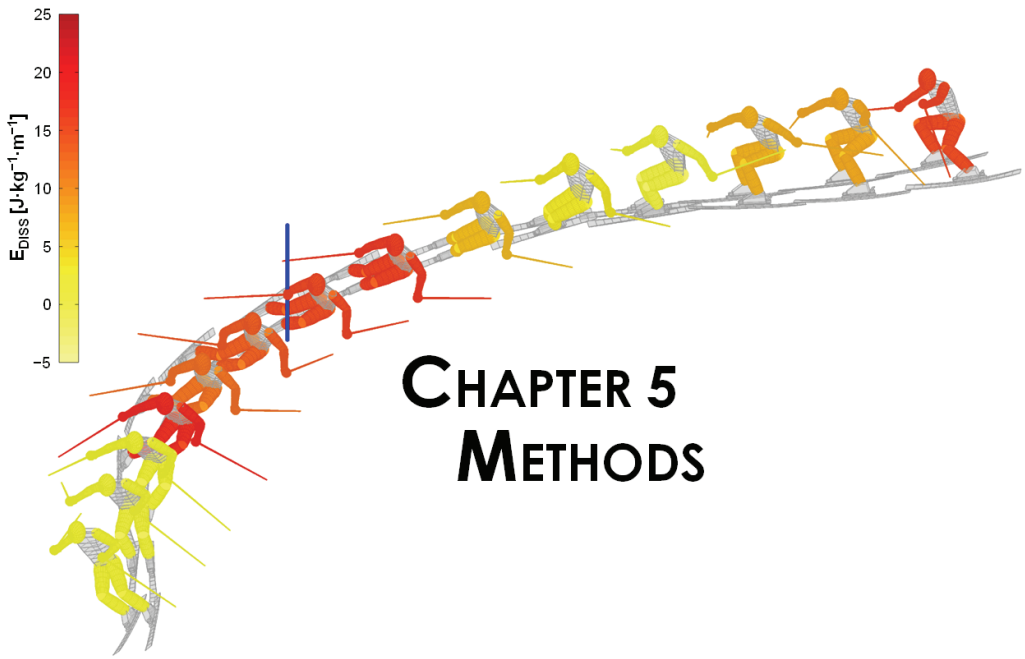

CHAPTER 5
METHODS

CHAPTER 5. METHODS

5.1 INTRODUCTION

The purpose of this chapter is to present the reader with a detailed description of the methods used in this study. A rather thorough description is given not only to give the interested reader better insight into the actual meaning of the results, but also to give researchers in the field enough detail that they are able to replicate measurements of interest for the purposes of comparison. The latter aspect is perhaps particularly important considering the infinitely variable nature of the sport of alpine ski racing. Gaining better scientific insight into the mechanics of turning technique will require numerous investigations using a large number of athletes in multiple, variable situations. Due to the intensiveness and expense of such data collections, this will require that investigators conduct studies that allow comparison with other research groups. Publication of detailed method descriptions will facilitate this process.

In the first part of this chapter, issues regarding method selection and implementation in the field environment are presented. This is followed by descriptions of the skier model, procedures for camera calibration and synchronization, and the reconstruction algorithm. A particularly detailed description of the calculation of the kinematic and kinetic parameters is then given followed by a presentation of the statistical methods. Finally, an analysis of the implemented method's accuracy is given. Limitations of the

various parameters, as well as suggestions for future investigations, are discussed in Chapter 7.

5.2 METHOD SELECTION

The purpose of this study was to quantify and describe the techniques of a group of highly-skilled skiers and to further examine the relationships between skier kinematic and kinetic characteristics and performance. To achieve this, a method was required that could measure parameters of skier and ski kinematics, including center of mass motion. Several important factors were considered during method selection.

First, we required a method that had been previously developed, validated and tested in the alpine environment as we wished to focus primarily on questions of skiing technique and not method development. Further, we wished to avoid placing any measurement devices on the skiers or their equipment that might interfere with their performances as our goal was to study them in as close to competition conditions as possible. Over the course of a season, top skiers fine tune their equipment to their individual technical styles and requirements. Even small alterations to an elite skier's equipment can be expected to have an impact on their performance (Schwameder et al., 2001). It was therefore important that athletes were free to use their own equipment just as they would in a competition. In addition, transferring measurement equipment from athlete to athlete would require time, reducing the number of athletes that could be studied under similar course conditions. Since we wished to study individual differences in how a group of athletes skied in the same situation, this was undesirable. Finally, as is almost always the case, budget constraints were a consideration in method selection. This was perhaps a particularly important requirement in the present study as it was the first of its kind for our research team. Until we have gained experience in this type of study and understand better the parameters we wish to quantify, it seemed logical to invest conservatively.

Several alternatives exist to quantify skier and ski motion, including video-based motion analysis (Klous, 2007; Mössner et al., 1996; Müller et al., 1998; Nachbauer et al., 1996; Pozzo, Canclini, Cotelli et al., 2005; Raschner et al., 1997; Raschner et al., 2001; Schiefermüller et al., 2005; Supej, Kugovnik, & Nemec, 2005b), GPS-based motion analysis (Brodie et al., 2007, 2008, 2009; Huber et al., 2009; Kruger & Edelmann-Nusser, 2008; Supej, 2009), and direct measurement using accelerometers and goniometers (Müller, 1994; Scott, Kagawa, & Yoneyama, 2006; Yoneyama et al., 2001).

While GPS-based systems certainly have the potential to completely revolutionize motion analysis in alpine skiing, these methods were still in a relatively early stage of development at the time of this study. There was, for example, no one complete "package" of hardware and software on the market that had been validated and could be used in a motion analysis study. Consequently, substantial time and resources would be required to design, implement, and validate such a system for use in skiing. Furthermore, a GPS-based system would require placing equipment on the athletes, something we wished to avoid. Direct measurement techniques such as goniometry can provide a high level of accuracy and reliability. However, these methods suffer from the same disadvantages associated with having to place equipment on the athletes as GPS-based systems. In addition, such methods do not readily allow determination of whole body center of mass motion, an important parameter that we were interested in studying.

Video-based motion analysis thus seemed to be a good alternative based on our requirements. Video-based methods have been popular in skiing field research and several approaches have demonstrated accuracy, reliability, and applicability in the challenges of the alpine environment. One difficulty of using video-based motion analysis in alpine skiing, however, lies in maintaining a sufficiently large image of the skier for accurate digitization as she moves through a very large object-space volume. Several approaches to this problem have been implemented in skiing research

including the use of overlapping kinematic subspaces (Supej et al., 2003; Supej, Kugovnik, & Nemec, 2005b), the "Repeated Calibration" method for panning cameras (Baroni et al., 1998; Mössner et al., 1996; Nachbauer et al., 1996; Pozzo, Canclini, Cotelli et al., 2005), and the Passpoint method based on the Drenk algorithm for panning cameras (Drenk, 1994; Klous, 2007; Müller et al., 1998; Raschner et al., 1999; Raschner et al., 1997; Raschner et al., 2001; Schiefermüller et al., 2005; Vodičková et al., 2005).

Despite being the method requiring by far the largest volume of manual digitization work, the Repeated Calibration method was selected for this study. Both the kinematic subspace and Passpoint methods place restrictions on camera movement that complicates implementation in the field and that we wished to avoid. The Repeated Calibration method, on the other hand, allows for a much larger degree of flexibility in terms of camera placement and motion that we chose to prioritize despite the increased digitization volume. Furthermore, the Repeated Calibration method could be implemented using previously purchased equipment and relatively little financial investment.

5.3 PILOT STUDIES

Over the course of the year prior to the primary investigation, a series of pilot studies were conducted to develop and test methods as well as to train personnel. Starting from elementary 2-dimensional single-camera tests, the methods implemented in each pilot study became progressively more sophisticated as the skill level and experience of the investigators improved, culminating in three complete mock-up training sessions in the field in the weeks prior to the data collection. Over the course of these pilot studies, investigation team members were thoroughly trained in their designated tasks. Further, various aspects of the methods were investigated including (a) control point design, placement and mapping; (b) camera number, placement, calibration and synchronization; (c) theodolite measurement; (d) software development; (e)

development of schedules and routines for on-site work; and (f) delegation of responsibilities amongst investigation team members.

5.4 SAMPLE CHARACTERISTICS

Six male members of the Norwegian national alpine ski team (European Cup Team) were invited to participate. Subjects were 17 to 20 years of age and world-ranked between 112 and 500 in the slalom discipline according to the 6th International Ski Federation (FIS) list of the 2005/2006 season (Table 5.1). Relative to their respective age group classifications, they were ranked between 1 and 6 in the world at the time of data collection.

Prior to participation, subjects were presented the study objectives and procedures as well as informed of the risks and benefits associated with participation. They received written information regarding the study objectives (Appendix A) and signed the informed consent form (Appendix B). This study was registered with the Ombudsman for Privacy in Research, Norwegian Social Science Data Services, AS (Appendix C).

While the highest caliber athletes available are desirable for studies such as this, there are some advantages to studying athletes at top developmental levels as well. In alpine ski racing, these younger athletes have grown up with more modern equipment and as

TABLE 5.1 Subject descriptive statistics.

	Age [yrs]	Height [cm]	Mass [kg]	FIS Points*	World Rank*	Age-Class World Rank*
Mean	18.3	180.8	82.7	22.35	280.0	3.5
SD	1.5	2.1	7.5	8.21	172.0	1.9
Range	17-20	178.5 - 183.5	76.3 - 94.6	13.37 - 32.41	112 - 500	1 - 6

* According to the 6th FIS points list, 2005/2006, valid from 1.4.06 - 30.4.06.

a result may have more progressive aspects of their technique than older, perhaps more conservative racers. Thus, it can be argued that while younger athletes, such as those examined in this study, may perform less consistently than more experienced ones, certain characteristics of their technique may be more representative of the future in skiing technique.

5.5 ON-HILL SET UP

A Spring-time data collection was chosen as at that time of year the alpine competitive season is ending and athletes are not only more available, they are also normally in good competitive form. Moreover, Spring conditions in Norway can be very good with competition-like snow conditions. Five days of data collection over the course of two weeks were conducted in conjunction with Norwegian national team training camps at the Ål and Varingskollen ski centers. Multiple days of data collection were planned due to the instability and unpredictability of the alpine environment with the intention of selecting the best day of data collection for further analysis. The data collection ultimately chosen for analysis was conducted with the men's European Cup team on April 11th, 2006, from 08:00 to 11:00 am at Varingskollen ski area, 15 km northwest of Oslo.

SLOPE SELECTION AND PREPARATION

The study of turning technique in skiing is complicated by the fact that how skiers solve one particular turn may not necessarily generalize to any other situations. However, some turning conditions are more generalizeable than others and our goal in defining the on-hill set-up and procedures was to create conditions that would maximize the generalizeability of results to similar competitive situations.

The particular slope on which the study would be conducted was selected on the basis of slope steepness, snow conditions, snow surface uniformity, gradient direction, and

the goal of creating conditions to maximize generalizeability to other turning situations. With this in mind, it was important to find a uniform slope long enough to set a course straight down the fall line. An investigation area was defined on the upper half of the selected slope, approximately 10 turns from the race start so that the athletes would be up to speed and making rhythmical turns when analyzed (Figure 5.1). Geodetic measurement of the snow surface later revealed that the investigation area had an average inclination of 19°.

The hill was closed off to the public one day prior to data collection. Due to forecasted mild daytime and freezing nighttime temperatures, slope preparation consisted of repeated side slipping and finally light salting on the afternoon prior to data collection. Over the course of the early evening, temperatures rapidly dropped to freezing and a solid, uniform snow surface was obtained.

COURSE SETTING

Data were collected of the athletes skiing two different course set-ups. The first course was set using a 10 m linear distance and 2 m offset between gates and the second course was set using a 13 m linear distance and 3 m offset. These values where chosen so as to span the range of values typically seen in rhythmical sections of competition courses. Although tape measures were used to control course setting, later measurement of gate positions by theodolite revealed that the actual average course linear distances and offsets were 9.89 m x 2.06 m and 12.88 m x 2.78 m for the 10 and 13 m courses, respectively. Despite these small deviations, these courses will continue to be referred to as the 10 and 13 m courses. Geodetic measurement of the snow surface revealed a slight course offset relative to the slope gradient of 15° and 13° for the 10 and 13 m courses, respectively. Thus, left-hand turns were oriented slightly more against the gradient than right-hand turns.

FIGURE 5.1. The investigation area at Varingskollen on the 11th of April, 2006. Visible are the course and the control points defining the calibration volume. The race course start was at the top of the slope visible in this image, approximately 10 turns prior to the investigation area. The fencing was removed prior to data collection.

CONTROL POINTS

The Repeated Calibration method is dependent upon having control points visible on every video image as the cameras are panned, tilted and zoomed. In order to analyze a minimum of two complete turn cycles, a calibration volume approximately 50 m long, 10 m wide and 2 m high was defined in the investigation area through the strategic placement of 208 control points. Important considerations in this regard included (a) control point design; (b) the total number of control points and their placement in the field; and (c) measurement of control point position in the 3-dimensional object-space reference frame.

CONTROL POINT DESIGN

Considerable time was used to develop control point constructions that would be, on the one hand, solidly positioned and readily digitizeable and, on the other hand, safe for the athletes should they crash. In all, three types of control point construction were used.

The first type consisted of foam rubber rolled into cylinders of precisely 4 cm radius and both 20 and 30 cm lengths. A 2 cm wide strip of white tape was affixed to the cylinder, 2 cm from the top (Figure 5.2 A). The tops of 20 % of these "Type 1" control points were painted neon orange to assist in identification. The position of the control point was defined as the center of the cylinder at the center of the white tape so that the same point could be readily digitized regardless of viewing angle. These control points were drilled with a 40 mm bit approximately 10 cm into the snow surface in a zig-zag pattern every 50 to 100 cm on both sides of the calibration volume.

The second control point type was constructed of tennis balls with a radius of 3.25 cm painted either neon orange or black (Figure 5.2 B). Two to three painted tennis balls with alternating color were mounted onto brand new slalom gates with stiff hinges.

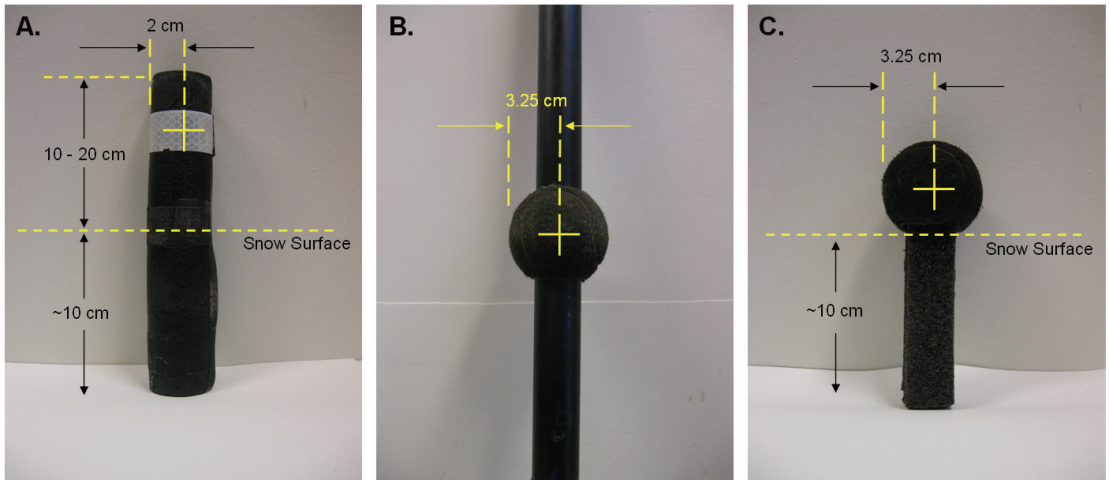

FIGURE 5.2. Type 1 (A), Type 2 (B), and Type 3 (C) control points.

The position of the control point was defined as the center of the sphere of the tennis ball. These control points were screwed into the snow surface in a zig-zag pattern every 150-200 cm on both sides of the calibration volume. The alternating color was not only for identification purposes but also to assist in control point visibility due to the varying background colors expected on the video images.

Type 3 control points, also constructed of tennis balls, were designed with the intention of being placed very close to the skiers' trajectories (Figure 5.2 C). These were painted black, mounted onto short foam rubber sticks, and placed in a zig-zag pattern on the inside of the turning gates.

CONTROL POINT NUMBER AND PLACEMENT

The 208 control points were positioned along the calibration volume in a corridor-like fashion to enclose the expected movement volume while minimizing the need to move control points when re-setting the race course (Figure 5.3). Type 1 and Type 3 control points were placed low, close to the snow surface, to calibrate the volume in which the athletes' skis would move. Type 2 control points were used to calibrate the full height of the volume to capture the skier's motions. The total number of control points placed in the field and the spacing between them was planned so as to ensure a minimum of 12 well-distributed control points on every image of each camera throughout their panning motion.

With such a large number of control points, it was anticipated that identification of individual points would be problematic during measurement and digitization. Consequently, several procedures were implemented to assist in control point identification. First, as the control points were placed on the hill, they were numbered and mapped according to a pre-defined system. In addition, every fifth Type 1 control point was painted neon orange on the tip. A bold, red stripe was also painted onto the snow surface every tenth Type 1 control point. As mentioned previously, Type 2

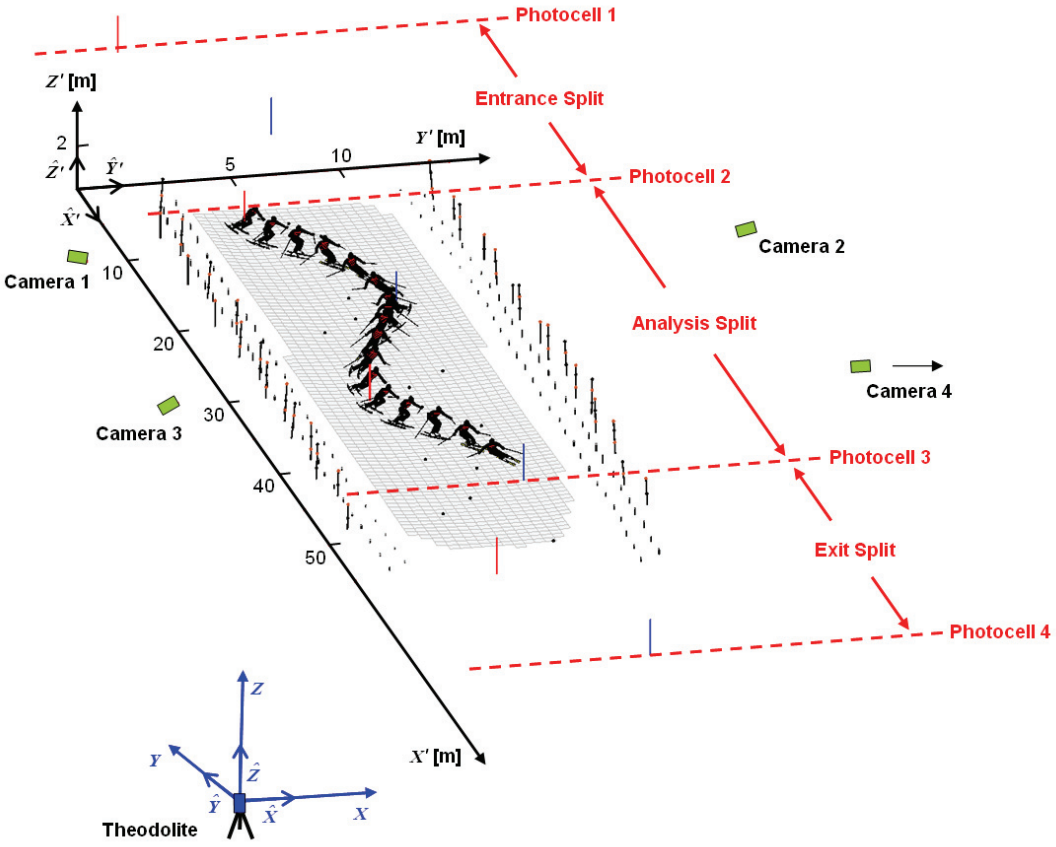

FIGURE 5.3. A graphical representation of the experimental set-up at Varingskollen on April 11th, 2006. The Theodolite Coordinate System (XYZ), Course Coordinate System (X'Y'Z'), camera positions, and timing photocell positions are indicated. The small points and poles indicate control point positions. This graphic was constructed based on actual measurements. Note that Camera 4 was actually placed approximately 30 m further to the right as seen from this perspective.

control points were mounted onto their poles in alternating colors. They were then placed on the hill such that no two poles close to each other had the same pattern of colors. Finally, a bright orange cone was placed at the base of every fourth pole of Type 2 control points.

CONTROL POINT MEASUREMENT

Control point 3-dimensional positions were measured using a theodolite (Sokkia Set 2BII, Sokkia Co. Ltd., Kanagawa, Japan) placed on a level snow surface near the track. On the afternoon of the day prior to data collection, the theodolite tripod was mounted into the snow surface and the surrounding snow subsequently watered and salted. Measurements were not started until the tripod became solidly frozen into the snow surface with the falling evening temperatures. To avoid a systematic drift of measurements over time, the theodolite height, horizontal, and vertical orientation were frequently controlled and adjustments made accordingly. An iron pillar across the hill was used to establish the reference direction.

Control point horizontal and vertical directions were measured by screwing the theodolite reticule in line with the center of the marker. The distance was then captured by holding a specifically-built reflector in front of the control point and later correcting for the known radius of the control point. Measurement data were both written manually and saved onto an electronic data logger connected to the theodolite. A total of 8 hours were required to capture all control point and snow surface measurements during the night prior to data collection.

CAMERAS

Skiers were filmed using four panning, hand-held PAL digital video camcorders (2 Sony TRV-950 and 1 Sony TRV-900, Sony Corporation, Tokyo, Japan; 1 Canon DM-XM2E, Canon, Tokyo, Japan) set to shutter priority mode and 1000 Hz shutter speed.

The PAL interlaced video sequences were later deinterlaced to obtain images at 50 Hz and 720x576 pixels resolution. All filmers were very experienced in the use of video cameras to film alpine skiers. The cameras were positioned so as to surround the investigation area with two cameras on each side (Figure 5.3) in the hope that each point of interest on the skier would be captured by at least two—and preferably three—cameras at each instant in time with a sufficient angle between them.

TIMING

A wireless photocell timing system (Microgate, S.r.l., Bolzano, Italy) was used to quantify skier performance and select trials for analysis. Four photocells were placed along the course creating three splits (Figure 5.3). The "Entrance" and "Exit" Splits consisted of the two turns prior to and after the investigation area, respectively, while the "Analysis" Split comprised of four complete turns in the investigation area. Time used in the Analysis Split was correlated to total time for all three splits to control for performance consistency when identifying the fastest trial for use in further analysis.

WEATHER CONDITIONS

Weather conditions the morning of the data collection were sunny and wind-still. Air temperatures were relatively stable, ranging from 5^{o} to 7^{o} C between 08:00 and 11:00 am. Due to the freezing nighttime temperatures (the overnight low was -5.8^{o} C registered at a nearby weather station) the snow surface was hard and grippy for the entire data collection.

PROCEDURES

Subjects completed three maximal, race simulation runs on each of the two courses. Only one of the three runs on each course was selected for further analysis on the basis of performance time and consistency. All skiers used their normal slalom competition

equipment which complied with the FIS equipment regulations for the 2005/2006 season[9].

5.6 SKIER MODEL

Twenty-three points on the skier and skis were digitized, defining an 18 segment model of the skier and equipment (Figure 5.4). The digitized points and the resulting segments are defined in Table 5.2 and Table 5.3, respectively. Shoulder (R_SJC, L_SJC), elbow (R_EJC, L_EJC), wrist (R_WJC, L_WJC), hip (R_HJC, L_HJC), knee (R_HJC, L_HJC), and ankle (R_AJC, L_AJC) joint centers were defined according to de Leva (1996a; 1996b). On the basis of the digitized shoulder and hip joint centers, mid-shoulder (MIDS) and mid-hip (MIDH) points were calculated to define the trunk segment endpoints. The ski tip (R_TIP, L_TIP) was defined as the point along the ski's longitudinal axis where the shovel begins to deflect upward, properly known as the "forward contact line" (p. 6) in the ISO Standards (International Organization for Standardization, 2003). The mid-point along the tail edge of the ski was used as the ski tail (R_TAIL, L_TAIL), also corresponding to the ISO Standards. A third point on the ski, the ski mid-point (R_MID, L_MID), was calculated as described on p. 143.

Subject segment lengths were measured for the left side of the body according to the definitions in Tables 5.2 and 5.3 to be used to quality control the digitized data (p.147) and to normalize reconstructed joint center positions according to segment length (p. 156). To accomplish this, hip joint center positions were estimated according to the method outlined by Bell, Pedersen and Brand (1990).

[9] According to the FIS Specifications for Competition Equipment and Commercial Markings 2005/2006, the men's slalom ski was limited to a maximum length of 165 cm and a minimum bredth of 60 mm while no restrictions were made for the sidecut radius. Additionally, the height of the ski/plate system and the boot sole thickness were limited to 55 mm and 45 mm, respectively.

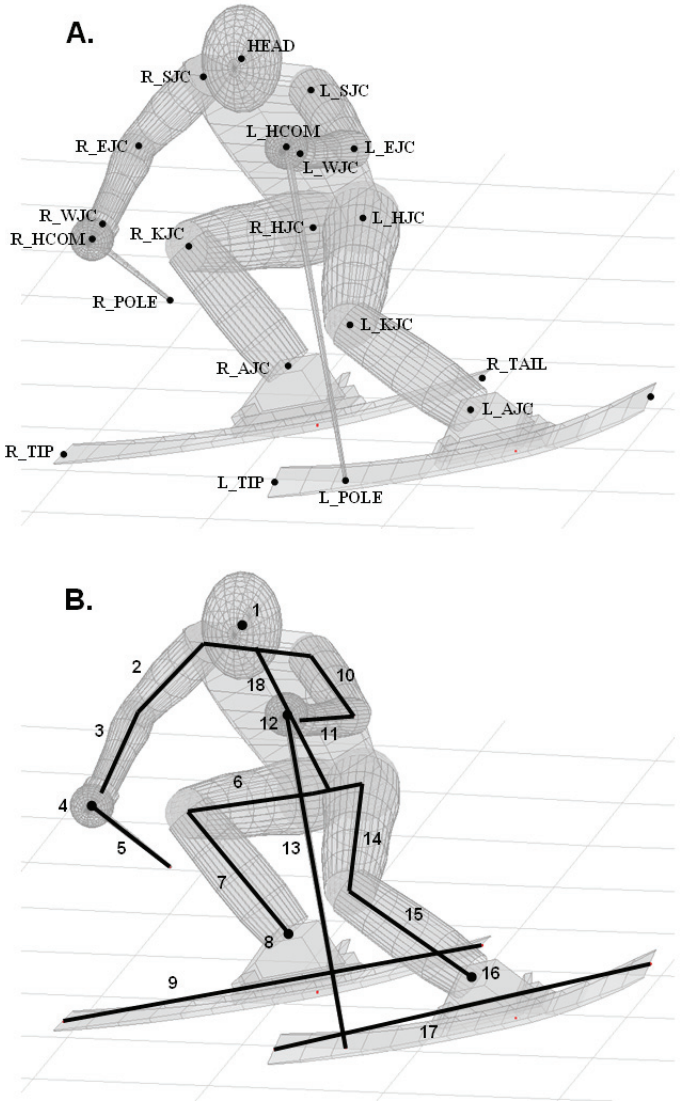

FIGURE 5.4 (A.) The digitized target points defining the skier model. (B.) The skier model segments. See Tables 5.2 and 5.3 for definitions.

TABLE 5.2. Skier model point definitions (* according to de Leva, 1996b).

Point	Abbreviation	Definition
Head COM	HEAD	Center of mass of the head, helmet and goggles.
Right Shoulder Joint Center Left Shoulder Joint Center	R_SJC L_SJC	Center of the humeral head.*
Right Elbow Joint Center Left Elbow Joint Center	R_EJC L_EJC	Center of transverse section of the humerus, at the level of greatest projection of the medial humeral epicondyle.*
Right Wrist Joint Center Left Wrist Joint Center	R_WJC L_WJC	Center of a transverse section of the capitate bone, at the level of the palpable groove between the lunate and capitate bone.*
Right Hand COM Left Hand COM	R_HCOM L_HCOM	Hand, glove, and pole grip center of mass.
Right Pole Tip Left Pole Tip	R_POLE L_POLE	Intersection of pole and basket.
Right Hip Joint Center Left Hip Joint Center	R_HJC L_HJC	Center of the femoral head.*
Right Knee Joint Center Left Knee Joint Center	R_KJC L_KJC	Midpoint between the maximum protrusions of the femoral epicondyles.*
Right Ankle Joint Center Left Ankle Joint Center	R_AJC L_AJC	Center of a transverse section of the talus, at the level of the distal tip of the fibula.*
Right Ski Tip Left Ski Tip	R_TIP L_TIP	Center point along ski longitudinal axis where the tip deflects upwards.
Right Ski Tail Left Ski Tail	R_TAIL L_TAIL	Center point along the tail edge of the ski.
Right Ski Mid Left Ski Mid	R_MID L_MID	Point along the ski longitudinal axis 20 cm directly below the AJC.
Mid Shoulder	MIDS	Mid point between R_SJC and L_SJC.
Mid Hip	MIDH	Mid point between R_HJC and L_HJC.

TABLE 5.3. Skier body segment parameter definitions.

Segment	Endpoints		Longitudinal	Regression Coefficients**			Added Mass§
	Proximal	Distal	COM Position* [%]	B0	B1	B2	[kg]
Head / Neck / Helmet	HEAD	--	--	1.296	0.0171	0.0143	0.7
Right Upper Arm	R_SJC	R_EJC	57.72	0.25	0.03012	-0.0027	--
Left Upper Arm	L_SJC	L_EJC	57.72	0.25	0.03012	-0.0027	
Right Forearm	R_EJC	R_WJC	45.74	0.3185	0.01445	-0.00114	--
Left Forearm	L_EJC	L_WJC	45.74	0.3185	0.01445	-0.00114	
Right Hand / Glove / Pole grip	R_HCOM	--	--	-0.1165	0.0036	0.00175	0.4
Left Hand / Glove / Pole grip	L_HCOM	--	--	-0.1165	0.0036	0.00175	0.4
Right Pole	R_HCOM	R_POLE	50#	--	--	--	0.2
Left Pole	L_HCOM	L_POLE	50#	--	--	--	0.2
Right Thigh	R_HJC	R_KJC	40.95	-2.649	0.1463	0.0137	--
Left Thigh	L_HJC	L_KJC	40.95	-2.649	0.1463	0.0137	
Right Shank	R_KJC	R_AJC	43.95	-1.592	0.0362	0.0121	--
Left Shank	L_KJC	L_AJC	43.95	-1.592	0.0362	0.0121	
Right Foot / Boot	R_AJC	--	--	-0.829	0.0077	0.0073	2.6
Left Foot / Boot	L_AJC	--	--	-0.829	0.0077	0.0073	2.6
Right Ski / Plate / Binding	R_TIP	R_TAIL	52+	--	--	--	3.9
Left Ski / Plate / Binding	L_TIP	L_TAIL	52+	--	--	--	3.9
Torso	MIDS	MIDH	43.10	--	--	--	--
Upper Torso	--	--	--	8.2144	0.1862	-0.0584	
Mid Torso	--	--	--	7.181	0.2234	-0.0663	
Lower Torso	--	--	--	-7.498	0.0976	0.04896	

* Center of mass longitudinal position as percentage of total segment length from the proximal endpoint (de Leva, 1996).
** Segment mass regression coefficients based on Zatsiorsky (2002).
# Pole center of mass position estimated to 50% of length between the pole tip and hand com.
+ Ski center of mass position determined from average ski balance point (n = 2).
§ Equipment masses determined from measured averages for skis and boots (n = 11) and poles, gloves, and helmet (n = 2).

CENTER OF MASS CALCULATION

Body segment parameters were calculated using Zatsiorsky's (2002) regression equations based on athlete height and weight and the de Leva (1996a) adjustments to segment endpoints. Zatsiorsky's model was selected based not only it's simplicity, but also on the similarity between the subjects used in this study and those used to develop the regression equations (Table 5.4).

Several modifications to the Zatsiorsky–de Leva model were made to account for the athlete's equipment (Table 5.3). As it was not possible to measure each athlete's equipment due to time constraints, the average characteristics of two subjects' equipment were used to modify the body segment parameters for all subjects. First, the mass of the helmet and goggles—0.7 kg—was added to the head segment. Additionally, 0.4 kg was added to each hand segment to account for the mass of the gloves, pole hand grips, and guards. Each pole without the hand grip and guard was defined as its own segment of mass 0.2 kg and its center of mass position was estimated to be 50 % of the distance between the pole tip and hand center of mass positions. Further, the mass of the boot (2.6 kg) was added to each foot segment where centers of mass were taken to be at the ankle joint centers. Finally, each ski, plate and binding

TABLE 5.4. A comparison of the current study's subject descriptives and those of the subjects used by Zatsiorsky (2002) to generate the body segment parameter regression equations.

		Current Study	Zatsiorsky 2002
n		6	100
Gender		Male	Male
Age	[years]	18.3 ± 1.5	23.8 ± 6.2
Height	[cm]	180.8 ± 2.1	174.1 ± 6.2
Weight	[kg]	82.7 ± 7.5	73.0 ± 9.1

system was taken as its own segment of mass 3.9 kg. The center of mass position of the ski, plate, and binding system along the ski's longitudinal axis was determined through balancing techniques to be 52 % of the ski length as measured from the ski forward contact line. The total mass of equipment added to the skier summed to 14.9 kg.

5.7 SKI MODEL

The TIP, TAIL and AJC position data were fit with a 15 segment model of a 14 m sidecut radius ski. To accomplish this, a third point on the ski sole ($\vec{P}_{\mathrm{MID}}$) was defined as the point between 16 and 19 cm below the $\vec{P}_{\mathrm{AJC}}$ in the direction perpendicular to the $\vec{P}_{\mathrm{TIP}}-\vec{P}_{\mathrm{TAIL}}$ vector, assuming that the ski sole to foot sole distance was close to the maximum allowable in competition (10 cm in 2006) and that the foot sole to $\vec{P}_{\mathrm{AJC}}$ distance was between 6 and 9 cm (Figure 5.5). Since the foot sole to $\vec{P}_{\mathrm{AJC}}$ distance was not measured at the time of data collection, this value was individually assigned by examining the resulting ski deformations and selecting a value that gave approximately 0 mm ski deformation at the turn transitions as has been measured in empirical studies (Kagawa et al., 2009). The resulting mean and maximum ski deformations for the turn phase were 38 mm and 67 mm, respectively and the highest instantaneous deformation across all trials was 87 mm. These values correspond reasonably well with studies where ski deformation has been experimentally measured and values have ranged from 35 to 80 mm, depending upon the loading conditions and ski characteristics (Casolo & Lorenzi, 2001; Fauve et al., 2009; Federolf et al., 2004; Lüthi et al., 2006; Tatsuno et al., 2009).

Subsequent to determining $\vec{P}_{\mathrm{MID}}$, the ski midline $\vec{M}(\mathrm{E})$, where E is the position along the ski's longitudinal axis, was then approximated by fitting $\vec{P}_{\mathrm{TIP}}$, $\vec{P}_{\mathrm{MID}}$, and $\vec{P}_{\mathrm{TAIL}}$ with a cubic spline function, constructing points at 15 evenly spaced intervals. Positions along the ski's edges $\vec{S}(\mathrm{E})$ were then approximated using the average sidecut profile of 11 slalom skis measured in another study (Laapi, 2009).

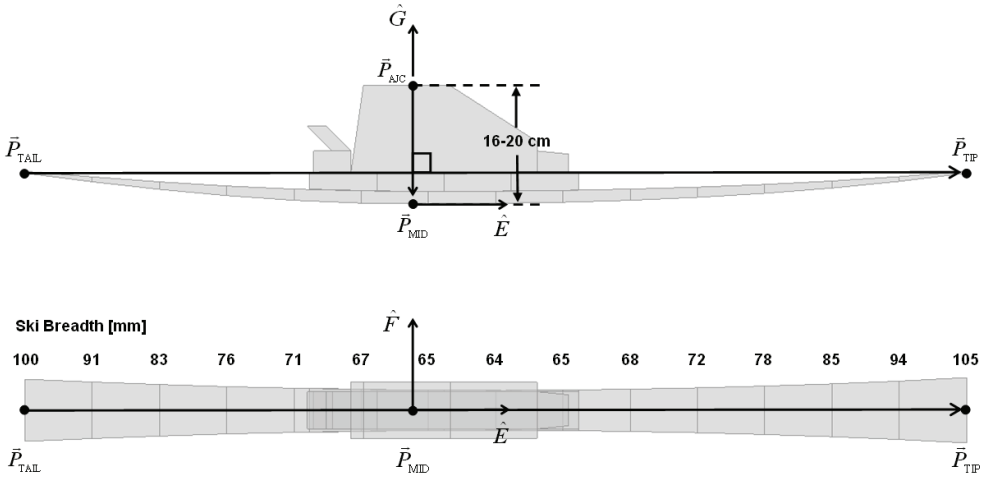

FIGURE 5.5. The 15 segment ski model fitted to $\vec{P}_{TIP}$, $\vec{P}_{TAIL}$, and $\vec{P}_{AJC}$. $\vec{P}_{MID}$ was defined as the point along the ski sole 16–20 cm below $\vec{P}_{AJC}$ in the direction perpendicular to the $\vec{P}_{TIP}$ - $\vec{P}_{TAIL}$ vector, the actual distance being chosen for each athlete based on 0 cm ski flexural deformation at turn transitions. The ski sole midline $\vec{M}(E)$ was then approximated by fitting $\vec{P}_{TIP}$, $\vec{P}_{MID}$, and $\vec{P}_{TAIL}$ with a cubic spline function. Finally, positions along the ski's edges $\vec{S}(E)$ were determined using the sidecut profile associated with the indicated ski breadths (Laapi, 2009).

5.8 DIGITIZATION

Video preprocessing was carried out using Dartfish TeamPro Version 3.0 (Dartfish, Fribourg, Switzerland). Video sequences were captured from PAL miniDV format, trimmed, deinterlaced, and saved using the Indeo 5.11 codec (Ligos Corporation, San Francisco, USA). Manual digitization of both control points and skier points was carried out in a software toolbox built specifically for that purpose in Matlab version R2006b (The Mathworks, Inc., Natick, USA) (Figure 5.6). This toolbox offered certain tools to assist the digitizer in marking both control points and skier points.

Several measures were taken to minimize the error expected in manually digitizing both control points and body landmarks (Bartlett, Bussey, & Flyger, 2006; Van Gheluwe, 1978; Walton, 1981; Wood & Marshall, 1986). First, skiers wore their tight-fitting competition suits which aided determination of joint center positions. Prior to digitizing, we were concerned that the mesh network design of the suits would make discerning target points difficult (see Appendix D for example photographs). As it turned out however, this mesh network actually assisted the digitizers in visualizing the rotational motion of body segments.

Second, substantial time was invested in training of the digitizers. Operators were first familiarized with the digitization software through a series of pilot studies (p. 127). For the main data collection, control points were digitized first as these were well-defined points and thus good practice for the digitizers. After calibration of all frames was completed, digitizers were further trained through digitizing the pole tips and hand centers of mass, the two most clearly visualized points on the skier. Prior to digitization of the more difficult skier points, a special training program was implemented. Responsibility for digitizing the different points was first delegated amongst the four main digitizers so that each would become an "expert" at digitizing his or her allotted points. A second set of data and video files was generated for training purposes and

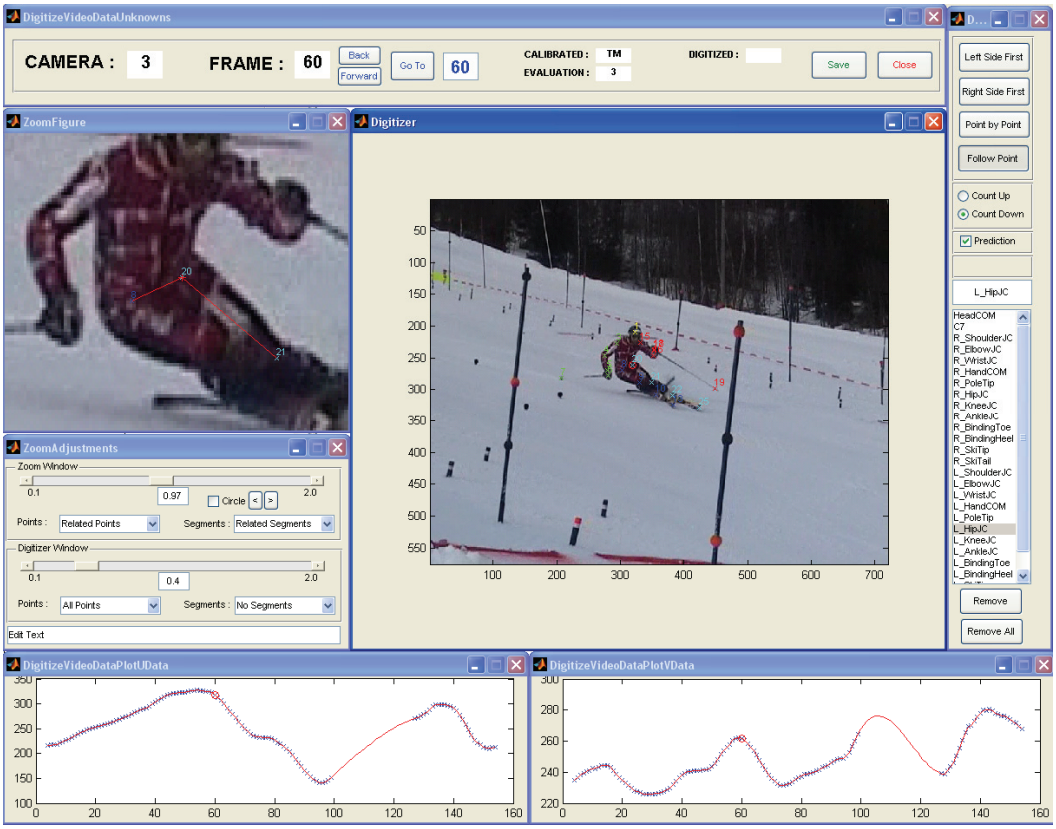

FIGURE 5.6. Screen shot showing the digitization component of the software toolbox developed for this study in Matlab version R2006b (The Mathworks, Inc., Natick, USA).

the digitizers spent a two-week period digitizing a sub-set of images taken from a wide variety of perspectives. The end of this training period was followed with a debriefing session where each point was discussed and each digitizer received feedback. Photographs of the skiers and their equipment were created to assist digitizers in visualizing their points (Appendix D). During the digitization process, digitizers held a continual discussion with each other about their perceptions of each point.

As a third measure to reduce manual digitization error, quality control checks were performed on the control point digitization. The comparator-space coordinates for control points were smoothed and, since a relatively smooth panning motion of the cameras was expected, control points with abnormally high residuals were flagged for double-checking. In addition, camera position was approximated for each calibrated frame based on the 11 DLT camera constants (Walton, 1981) and frames with abnormal camera position predictions were also double-checked.

Fourth, each operator digitized their allocated points, one at a time, tracking the same point throughout the trial. This has been shown to be both more efficient and more accurate as it enables the operator to continually track the same point (Bahamonde & Stevens, 2006). Operators often went through a trial several times, each time moving from frame to frame more rapidly, allowing the digitizer to visualize the segment in motion. Perceptual errors were often caught in this manner.

Finally, after all trials and skier points were digitized, segment lengths were calculated, compared to the known measured lengths, and used to flag sequences with large systematic errors. Using this feedback, each digitizer went through flagged sequences making corrections. Particular attention was paid to lower body segments and points whose positions would be used directly to examine research questions, such as the ankle joint centers, ski tips, and ski tails.

5.9 CAMERA CALIBRATION

Camera images were individually calibrated as per the Repeated Calibration method (Baroni et al., 1998; Mössner et al., 1996; Nachbauer et al., 1996) using the standard 11-parameter DLT algorithm (Abdel-Aziz & Karara, 1971; Walton, 1981). To reduce the digitizing work load, every other frame was calibrated initially. Subsequently, key frames where there were relatively few control points, or when control points were moving into or out of the field of view, were also calibrated. In total, 77 % of all frames were calibrated and the constants for the remaining frames were interpolated using cubic spline functions (Mössner et al., 1995). An average of 27 control points—and a minimum of 12—were manually digitized on each calibrated frame.

To calculate the camera constants, the digitized comparator-space coordinates and the corresponding measured object-space coordinates for each control point on a frame were entered into Equations [4.3] (p. 103). The resulting over-determined system of linear equations was then solved for the 11 DLT camera constants using singular value decomposition (Challis & Kerwin, 1992).

During the initial programming of the calibration algorithm, it became apparent that matrix A in Equations [4.3] became poorly conditioned during certain portions of the camera's panning, resulting in unstable estimates of the camera constants (Figure 5.7 A & B). The solution to this was to scale the control point comparator- and object-space coordinates as described by Mössner et al. (1996) and later explained in detail by Schiestl (2005). Thus, prior to being entered into matrix Equations [4.3], control point object-space coordinates were translated from the Theodolite Coordinate System (XYZ) origin to the average control point position and then scaled to an average of 0 and a standard deviation of 1 in each dimension. Additionally, the comparator-space coordinates were translated and scaled so that the origin was located at the middle of the image and the coordinates ranged from –1 to 1. This process greatly improved the condition of matrix A and the resulting solution of the camera constants (Figure 5.7 C

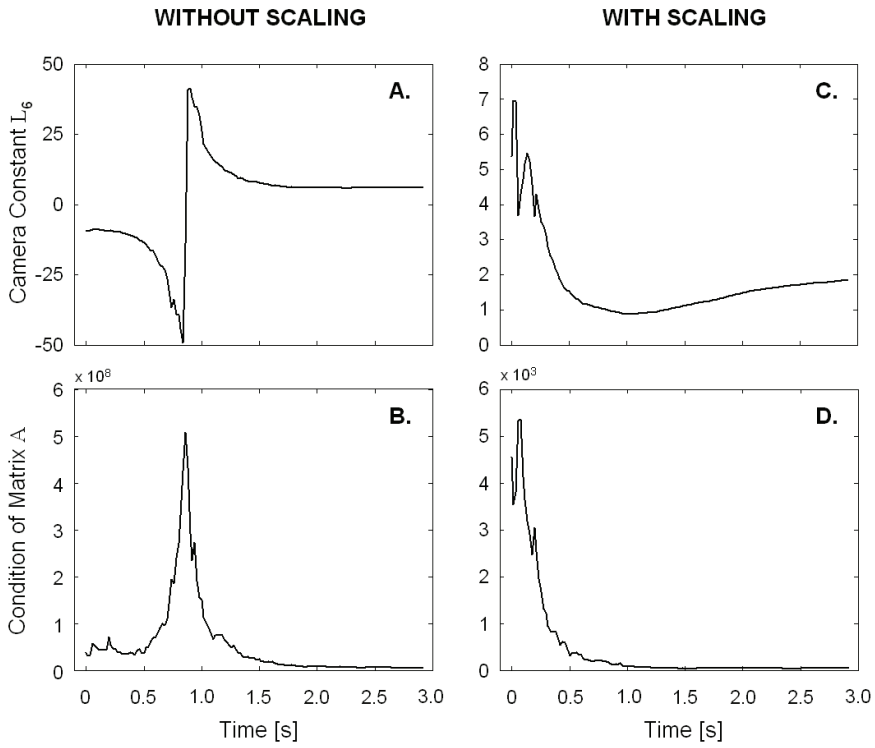

FIGURE 5.7. An example of an erroneous camera constant (A) resulting from the ill-conditioned A matrix (B) of Equations [4.3] during calculation of the camera constants without prior scaling of the comparator- and object-space coordinates. Graphs C and D show the results of the same calculations done with coordinate scaling. Note the 10^5 order difference in the Y-axis scale between graphs B and D.

& D). It is important to note that due to this scaling, object-space coordinates needed to be transformed back to the original Theodolite Coordinate System after reconstruction.

It was also discovered that during the portion of the panning of Camera 3 when the skier passed closest to the camera, there were relatively few control points and that these points had a rather poor distribution resulting in erroneous camera constants. This was due to the rather close proximity of the camera to the calibration volume. For these frames only, a special calibration algorithm consisting of two iterations was used. In the first iteration, an initial estimate of the camera constants was calculated for all frames except the affected ones using the standard DLT algorithm as explained previously. Based on this initial estimate of the DLT constants, camera position was estimated (Walton, 1981) for the entire panning motion, filtered, and then interpolated to the affected frames. Then, according to the method described by Schiestl (2005), Equations [4.3] were extended for the second iteration to include Equations [5.1]:

$$\begin{bmatrix} P_X & P_Y & P_Z & 1 & 0 & 0 & 0 & 0 & 0 & 0 & 0 \\ 0 & 0 & 0 & 0 & P_X & P_Y & P_Z & 1 & 0 & 0 & 0 \\ 0 & 0 & 0 & 0 & 0 & 0 & 0 & 0 & P_X & P_Y & P_Z \end{bmatrix} \begin{bmatrix} L_1 \\ L_2 \\ L_3 \\ L_4 \\ \vdots \\ L_{10} \\ L_{11} \end{bmatrix} = \begin{bmatrix} 0 \\ 0 \\ -1 \end{bmatrix} \qquad [5.1]$$

where P_X, P_Y, and P_Z are the estimated camera position coordinates in the Theodolite Coordinate System X-, Y-, and Z- dimensions, respectively, and $L_1 \ldots L_{11}$ are the DLT camera constants. The extended set of equations was then solved using singular value decomposition to obtain a final estimate of the camera constants for the affected frames. An example demonstrating how this procedure corrected erroneous camera constants is shown in Figure 5.8.

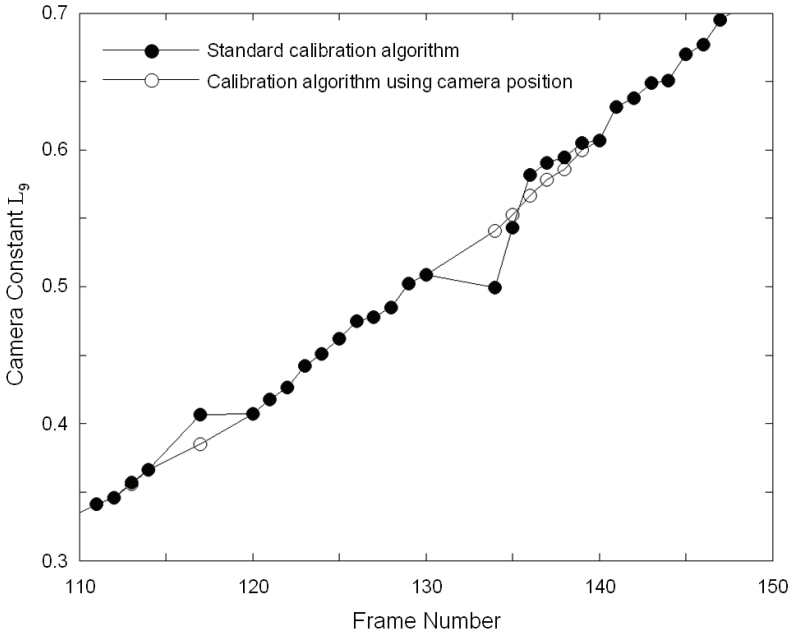

FIGURE 5.8. A comparison of the standard DLT calibration algorithm with that using camera position (Schiestl, 2005) for Camera 3 for frames with a low number of poorly distributed control points.

5.10 CAMERA SYNCHRONIZATION

Synchronization of the four cameras was achieved post-recording using an adaptation of the software genlock method described by Pourcelot et al. (2000) for use with multiple target points and panning cameras. Pourcelot's original algorithm was based on calculations tracking the motion of a single target point. However, Kwon et al. (2004) observed a trend towards improved camera synchronization accuracy when increased numbers of points were used in the phase shift calculation. Therefore, the cost function in Pourcelot's algorithm (Equation [4.8], p. 112) was modified to allow for multiple points giving Equation [5.2]:

$$\overline{\xi} = \frac{\sum_{j=1}^{2}\sum_{i=1}^{n}\sum_{k=1}^{c}\sqrt{\delta U_{jik}{}^{2} + \delta V_{jik}{}^{2}}}{2nc} \qquad [5.2]$$

where j is the camera number, n is the total number of time points, i is the time point, c is the total number of target points, k is the target point, and $\delta U_{jik}, \delta V_{jik}$ are the DLT optimization errors in the comparator-space U- and V-dimensions, respectively. The pole tips (R_TIP and L_TIP) were chosen for the phase shift calculations for two reasons. First, the accuracy of the software genlock is subject to the digitization error of the points used to determine the phase shift. The pole tips were perhaps the two most consistently digitized target points as indicated by their low DLT optimization error (see Table 5.10). Second, higher speed points are expected to exacerbate camera synchronization error and the pole tips had by far the highest speeds during portions of their motion. At the same time, however, there were times when the pole tips were stationary (i.e., when the pole is planted in the snow). As will be explained shortly, the synchronization algorithm was written so as to remove periods of time when the pole tip was stationary from the calculation of the camera phase shift.

The algorithm implementing the software genlock searched for the phase shift that minimized Equation [5.2] over three iterations consisting of progressively narrower and higher resolution searches. In the first iteration, the search included phase shifts of ± 5 frames from the expected, approximate synchronization point, stepping every 0.5 frames. Comparator-space coordinates from the slave camera were interpolated using cubic spline functions to obtain coordinates when the phase shift was between slave camera frames. Additionally, it was necessary to interpolate the 11 DLT camera constants using cubic spline functions to account for the changing constants as the cameras were panned, tilted, and zoomed (Mössner et al., 1995). The second search was conducted over ± 1 frame from the result of the first iteration, stepping every 0.1 frames. These two iterations were conducted for all camera pairs first. Using these initial estimates of the camera shifts, the pole tip trajectories were reconstructed and used to limit the third and final iteration to time points where the pole tip speed was in excess of 10 $m \cdot s^{-1}$. The final iteration searched ± 0.5 frames from the result of the second iteration, stepping every 0.025 frames. Figure 5.9 shows an example output from the third iteration of the camera synchronization subroutine. The phase shift minimizing the mean DLT optimization error in Equation [5.2] in the third iteration was taken as the shift that synchronized the cameras.

5.11 OBJECT-SPACE RECONSTRUCTION

After camera calibration and synchronization, target point object-space positions were reconstructed using singular value decomposition to solve Equations [4.5]. The reconstruction algorithm generated statistics to allow an analysis of the quality of each individual reconstruction. Tracked parameters for each reconstruction included (a) the number of cameras and which cameras were used; (b) the number of control points used to calibrate each camera; and (c) the inter-camera angles. The camera angles were calculated using the dot product of the vectors between the reconstructed target point's

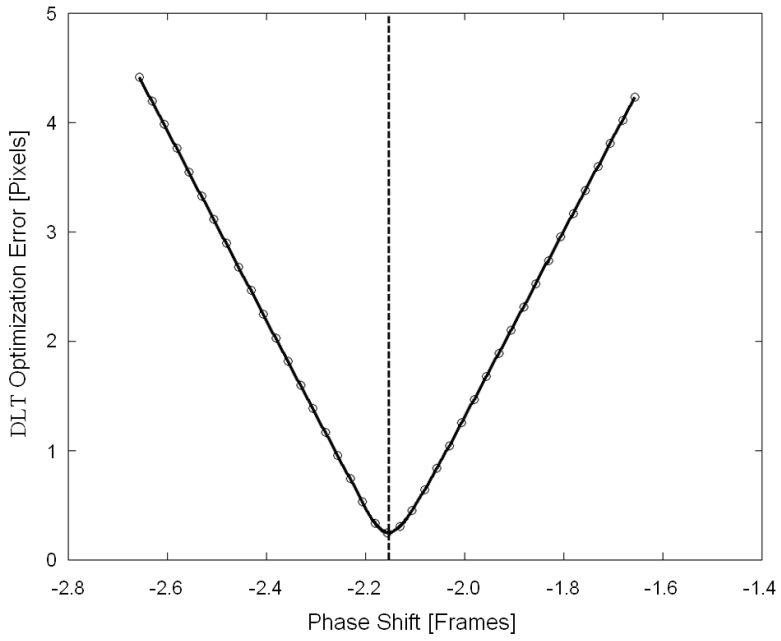

FIGURE 5.9. Example output of the final iteration in the camera synchronization subroutine showing the mean DLT optimization error ($\overline{\xi}$) of the pole tips as a function of the phase shift between two cameras. The phase shift that minimizes the mean DLT error is taken as that which synchronizes the cameras.

object-space coordinates and the object-space positions of the involved cameras as estimated from the DLT camera constants (Walton, 1981).

In all, over 35,500 points were reconstructed across the 12 analyzed trials. The majority of these reconstructions (83 %) were based on the input of three or four cameras, of which at least one camera pair had an inter-camera angle approaching 90°. Only 4 % of the reconstructions were characterized as "high risk" as indicated from the analysis of *non*-control point error (i.e., 2 cameras, poor inter-camera angle, and low number of control points) (see p. 186).

5.12 DIGITAL SIGNAL PROCESSING

INTERPOLATION

After digitization of the skier, the comparator-space coordinates for each point were examined. In cases where a point on a skier became occluded or poorly visible for a short number of frames, coordinates were interpolated using cubic spline functions. A component in the digitizing software toolbox allowed digitizers to individually examine each hole in the data and to determine whether or not interpolation was appropriate.

FILTERING

The DLT camera constants were filtered using a zero-lag, 2nd order, low-pass Butterworth filter and 20 padding points. A cut-off frequency of 15 Hz was selected based on visual inspection of the resulting residuals. In addition, *non*-control point reconstruction error was calculated for varying camera constant cut-off frequencies. Cut-off frequencies below 15 Hz resulted in large increases in *non*-control point error, presumably due to distortion of the camera constants.

Skier 3-dimensional object-space position data were similarly filtered using a zero-lag, 2nd order, low-pass Butterworth filter and 20 padding points. The Challis residual autocorrelation algorithm (Challis, 1999) was used to determine the appropriate cut off frequencies for each point. Figure 5.10 shows an example output for the elbow joint center. The Challis algorithm output and selected cut-off frequencies are given in Table 5.5. Different cut-off frequencies were selected depending on whether the data would be ultimately used to quantify position or to calculate derivatives (Giakas & Baltzopoulos, 1997). Figure 5.11 contrasts raw and filtered data for a parameter based on position filtered data (Figure 5.11. A) and a parameter based on derivative filtered data (Figure 5.11. B). The Challis algorithm output for each point is included in Appendix E.

SEGMENT LENGTH NORMALIZATION

The additional information of known segment lengths was used to correct endpoints of segments whose length remains relatively constant using a method introduced by Smith (1994). The upper arm, forearm, thigh, shank, and hip segments were length normalized using the actual measured left-side segment lengths and assuming that the left- and right-side segments were of similar length. This was accomplished using an adaptation of Smith's 2-dimensional normalization routine for use in three dimensions. An iterative procedure was implemented in which the initial reconstructed segment endpoint positions were used to calculate the vector representing the segment's longitudinal axis in 3-dimensional space. The midpoint of the segment was then calculated and new endpoint positions along the segment vector determined using the measured segment length. For joint centers connecting adjacent segments, two corrected endpoint positions were determined in this manner. These were averaged, slightly changing the length of both segments towards their measured values. With subsequent iterations, new segment vectors and midpoints were calculated using the endpoints determined in the previous iteration. Segment endpoints gradually

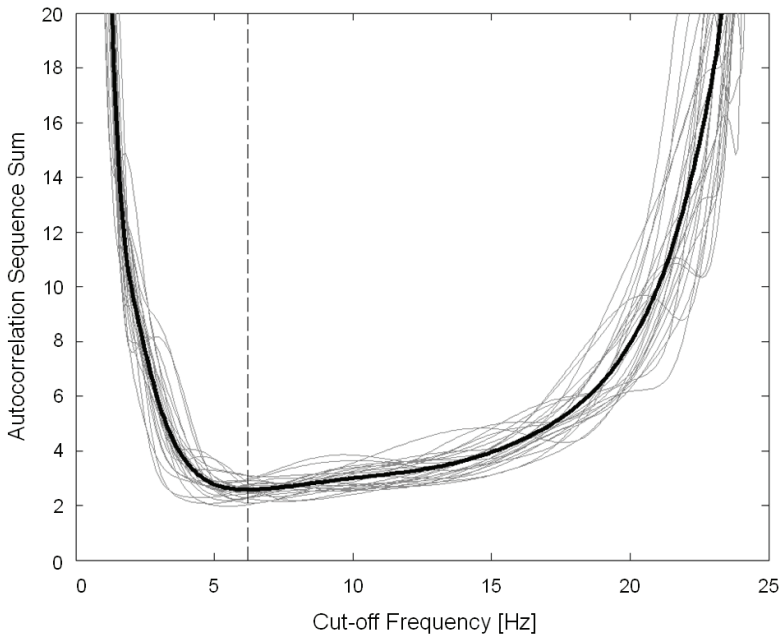

FIGURE 5.10. An example Challis algorithm (Challis, 1999) output for determining filter cut-off frequency for the elbow joint center in the Y′-dimension. The algorithm output for each of the 12 trials both left and right elbow (thin lines) and the ensemble average (thick line) are shown. The ensemble average minimum was used as an indicator of the appropriate cut-off frequency.

TABLE 5.5. Average results of the Challis (1999) residual autocorrelation algorithm for estimating filter cut-off frequency and the selected cut off frequencies for use in this investigation. Different cut-off frequencies were selected dependent upon whether the data were to be used for characterizing position or if higher order derivatives were to be calculated.

Point	Code		Challis Output			Selected	
			X' [Hz]	Y' [Hz]	Z' [Hz]	Position [Hz]	Derivatives [Hz]
Head COM	HEAD		6	5	7	5	5
Shoulder Joint Center	R_SJC	L_HJC	7	5	8	8	5
Elbow Joint Center	R_EJC	L_EJC	8	6	8	8	5
Wrist Joint Center	R_WJC	L_WJC	10	7	9	9	5
Hand COM	R_HCOM	L_HCOM	9	7	9	9	5
Pole Tip	R_POLE	L_POLE	11	8	11	11	11
Hip Joint Center	R_HJC	L_HJC	8	7	7	7	5
Knee Joint Center	R_KJC	L_KJC	8	7	9	8	5
Ankle Joint Center	R_AJC	L_AJC	8	7	9	9	5
Ski Tip	R_TIP	L_TIP	9	9	10	9	9
Ski Tail	R_TAIL	L_TAIL	8	7	9	8	8

Note: X',Y',Z' refer to the Course Coordinate System dimensions.

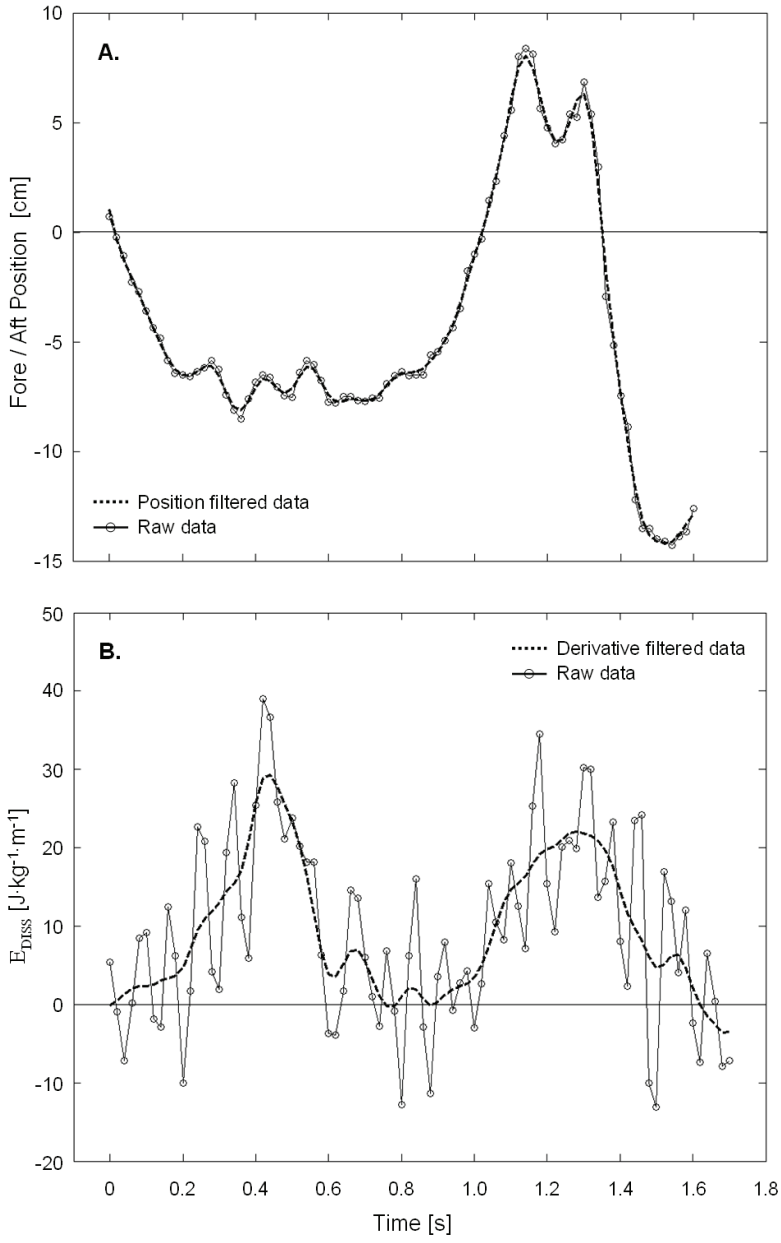

FIGURE 5.11. (A) A comparison of center of mass fore / aft position based on raw and position-filtered data. (B) A comparison of energy dissipation based on raw and derivative-filtered data.

converged on positions such that segment lengths equaled the measured lengths over the course of 10 iterations. As a part of this algorithm, the ankle joint center was additionally constrained to lie in the plane of the knee, ski tip and ski tail positions. This was done based on the dual assumptions that the lower leg and ski longitudinal axes are coplanar and that the lower leg is firmly attached to the ski (Federolf, 2005).

5.13 SNOW SURFACE QUANTIFICATION

To quantify the geomorphology of the snow surface, the positions of 82 points on the snow surface in the investigation area were captured using a theodolite (Sokkia Set 2BII, Sokkia Co. Ltd., Kanagawa, Japan). The distance to each point was measured by means of a reflector placed on the snow surface and the direction was determined by screwing the theodolite reticule to where the reflector contacted the snow. Two models of the snow surface were generated on the basis of these measurements, a planar model and a 3-dimensional surface model.

PLANAR MODEL

A least-squares plane model of the captured snow surface points was calculated using principal component analysis. The average and maximal residuals between the raw data and the planar surface were 5.7 and 27.1 cm, respectively. The planar snow model served as the basis for defining the Course Coordinate System (X'Y'Z') used in the kinematic analyses (see p. 161).

SURFACE MODEL

A more sophisticated snow surface model was generated based on the Delaunay triangulation of the captured snow points for use in analyses requiring knowledge of local snow surface orientation (Gilgien, 2008). A smooth surface model with continuous first- and second-order derivatives was obtained by computing the bi-cubic spline

function that passed through the triangulated data points. The average and maximal residuals for the triangulated model were 2.0 and 7.8 cm, respectively. This model allowed determination of local snow surface normals ($\hat{\boldsymbol{n}}_{x,y}$) and gradients ($\hat{\boldsymbol{g}}_{x,y}$) specific to a skier's location on the surface.

This modeling of the snow surface should be considered at best as a general approximation of the snow surface shape and orientation. The precise position and detail of the snow surface will progressively change with each passing skier as their skis either dig into and deform the snow surface (carving) or scrape off layers of snow (skidding). Consequently, parameters such as ski penetration depth cannot be determined with sufficient accuracy using this methodology. In addition, other parameters which depend upon surface topography such as ski edge and tilt angles should be considered as approximations with some uncertainty affected by surface variability.

5.14 PARAMETER COMPUTATION METHODS

INERTIAL COORDINATE SYSTEM DEFINITIONS

Two inertial coordinate systems were defined; the Theodolite Coordinate System and the Course Coordinate System (Figure 5.3). The origin of the Theodolite Coordinate System (XYZ) was defined by the inner structures and orientation of the theodolite. $\hat{\boldsymbol{X}}$ was defined as lying in the horizontal plane and directed towards an iron pillar across the slope from the theodolite position through both leveling of the theodolite and setting of the reference direction. $\hat{\boldsymbol{Z}}$ was defined as normal to the horizontal plane and $\hat{\boldsymbol{Y}}$ was then defined so as to obtain a right-handed, orthogonal triad.

For the majority of analyses, coordinate data were transformed from the Theodolite Coordinate System to the Course Coordinate System (X'Y'Z'), whose origin was defined at an arbitrary point on the snow surface at the top of the calibration volume. $\hat{\boldsymbol{X}}'$ was

defined as lying in the least squares plane of the snow surface and directed parallel to the average direction of the course as determined from the gate positions. $\hat{\boldsymbol{Z}}'$ was directed vertically, normal to the least squares plane of the snow surface. Finally, $\hat{\boldsymbol{Y}}'$ was defined so as to obtain a right-handed, orthogonal triad. By this definition, the X'Y' plane was contained in the least squares plane of the snow surface. The Course Coordinate Systems for the 10- and 13-meter courses differed slightly according to the average direction of each course.

PERFORMANCE TIME

While the on-hill timing system was used to identify trials for further analysis, the time skiers took to negotiate the two analyzed turns was calculated to describe skier performance. Performance time (PT) was thus calculated as the time the center of mass used to travel from the first to the third switch in the analysis (two complete turn cycles). Since the actual switch positions on the hill for a given turn transition varied slightly between skiers, virtual start and finish lines were constructed. To define the start line, the average center of mass position projected to the plane of the snow surface and the average direction of the center of mass velocity vector at the first Switch were calculated. The line passing through the average Switch point and perpendicular to the average velocity vector in the plane of the snow surface was used as a virtual start line. The time point when the center of mass crossed this line was defined as t = 0 s. A finish line was similarly constructed at the third Switch, at the end of the second turn of the analysis.

TRAJECTORY CHARACTERISTICS

TURN CYCLE STRUCTURE

As described in Chapter 3, numerous approaches have been used to define the turn cycle phase structure. The methods employed by Nachbauer (1987a, 1987b) and Müller

et al. (1998) require measurement of ground reaction forces on each ski. As forces were not measured in this study, an alternative system was used where each turn was divided into three phases based on characteristics of the center of mass motion, similar to LeMaster's (1999) approach. First, the transitions between turns, termed "Switch" in this dissertation, were defined as the intersections between the projections of the center of mass trajectory $\vec{P}_{COM}(t)$ and average ski trajectory $\vec{P}_{SKI}(t)$ on the X'Y' plane of the snow surface, according to the method outlined by Supej et al. (2003). The Turn Phase was defined as that portion of the turn cycle where the R_{COM} was less than 15 m to identify the portion of the turn cycle where the primary impetus for turning occurred. The 15 m criterion was chosen based on a qualitative inspection of the R_{COM} data. The portion of the turn cycle from the initiation Switch to the start of the Turn Phase was then defined as the Initiation Phase. Finally, the Completion Phase was defined as starting at the end point of the Turn Phase and ending at the following Switch.

TRAJECTORY LENGTH

Several parameters were calculated to characterize trajectory length. First, the cumulative displacement of the center of mass in all three dimensions X'Y'Z' from the virtual start line to the virtual finish line was used to describe the total, 3-dimensional trajectory length, L_{XYZ}. In addition, the cumulative center of mass displacements in both the Y'- and Z'- dimensions were calculated as L_Y and L_Z, respectively. In the calculation of L_Y, the start and finish lines were defined as the central, longitudinal axis of the course which was, by definition, parallel to the X' axis. The start and finish lines in the calculation of L_Z were defined as the center of mass positions in the Z'- dimension at the first and third switches, respectively.

VELOCITY AND ACCELERATION

For a point X's position as a function of time, $\vec{P}_X(t)$, the first and second time derivatives in an inertial reference frame ($\dot{\vec{P}}_X(t)$ and $\ddot{\vec{P}}_X(t)$) were calculated using the 4-

and 5-point finite central difference formulae, respectively (Gilat & Subramaniam, 2008).

TURN RADIUS

The instantaneous turn radius of a point X's trajectory at time point index i, $\vec{P}_X(i)$, parallel to the least squares plane of the snow surface, was calculated by determining the radius of the circle fitting the projections of the three points $\{\vec{P}_X(i-3), \vec{P}_X(i), \vec{P}_X(i+3)\}$ on the Course Coordinate System X'Y' plane. The turn radii for both the center of mass (R_{COM}) and ski mid points (R_{L_MID}, R_{R_MID}) were calculated in this manner. R_{L_MID} and R_{R_MID} were used to characterize the outside ski turn radius (R_{SKI}) in right- and left-hand turns, respectively.

SKI ORIENTATION CHARACTERISTICS

SKI COORDINATE SYSTEM DEFINITIONS

Two accelerated coordinate systems were defined for each ski in a manner similar to that described by Lieu (1982) and Lieu and Mote (1985) (see Figure 3.2). The Ski Coordinate System EFG originated at $\vec{P}_{MID}$ and defined the orientation of the ski within the inertial reference system. $\hat{E}$ was oriented parallel to the ski longitudinal axis, defined by $\vec{P}_{TIP} - \vec{P}_{TAIL}$, while $\hat{G}$ was directed parallel to the vector between the ankle joint center and the ski MID point ($\vec{P}_{AJC} - \vec{P}_{MID}$). Finally, $\hat{F}$ was constructed so as to define a right-handed orthogonal triad. The EF plane was thus parallel to the tangent of the deformed ski sole at $\vec{P}_{MID}$.

The E'F'G' coordinate system, also originating at $\vec{P}_{MID}$, defined both the direction of the ski motion as well as the orientation of the local snow surface. $\hat{E}'$ was defined to be parallel to the projection of the MID point velocity vector, $\dot{\vec{P}}_{MID}$, on the local plane of the local snow surface. $\hat{G}'$ was defined parallel to the local snow surface normal vector,

$\hat{\boldsymbol{n}}_{x,y}$, and $\hat{\boldsymbol{F}}'$ was defined so as to generate a right-handed orthogonal triad. Defined in this way, the E′F′ plane was parallel to the local plane of the snow surface.

Local coordinate systems were defined along the ski's edge for each of the 15 ski segments. Positions along the ski's midline $\vec{\boldsymbol{M}}(\mathrm{E})$ and interacting edge $\vec{\boldsymbol{S}}(\mathrm{E})$ were derived as described previously (p. 143). Analogous to the EFG reference frame, a coordinate system $e_E f_E g_E$ was constructed to define the local ski orientation in the inertial reference frame for each point along the ski's edge, $\vec{\boldsymbol{S}}(\mathrm{E})$. The direction of $\hat{\boldsymbol{e}}_E$ for a given edge point was thus defined according to the vector from the preceeding to the following edge point:

$$\hat{\boldsymbol{e}}_E = [\vec{\boldsymbol{S}}(\mathrm{E}+1) - \vec{\boldsymbol{S}}(\mathrm{E}-1)] / \left\| [\vec{\boldsymbol{S}}(\mathrm{E}+1) - \vec{\boldsymbol{S}}(\mathrm{E}-1)] \right\| \qquad [5.3]$$

The direction of $\hat{\boldsymbol{g}}_E$ was defined as normal to the deformed ski sole at the given point by taking the cross product between $\hat{\boldsymbol{e}}_E$ and the vector from the interacting edge point $\vec{\boldsymbol{S}}(\mathrm{E})$ to the ski midline point $\vec{\boldsymbol{M}}(\mathrm{E})$:

$$\hat{\boldsymbol{g}}_E = \hat{\boldsymbol{e}}_E \times [(\vec{\boldsymbol{M}}(\mathrm{E}) - \vec{\boldsymbol{S}}(\mathrm{E})) / \left\| \vec{\boldsymbol{M}}(\mathrm{E}) - \vec{\boldsymbol{S}}(\mathrm{E}) \right\|] \qquad [5.4]$$

Finally, $\hat{\boldsymbol{f}}_E$ was defined so as to create a right-handed orthogonal triad. In addition to the $e_E f_E g_E$ reference system, the coordinate system $e'_E f'_E g'_E$ was constructed at each edge point to quantify the point's direction of motion and the orientation of the local snow surface plane. $\hat{\boldsymbol{e}}'_E$ was directed parallel to the projection of the edge point velocity vector $\dot{\vec{\boldsymbol{S}}}(\mathrm{E})$ on the plane of the local snow surface and $\hat{\boldsymbol{g}}'_E$ was defined as normal to the local snow surface plane. $\hat{\boldsymbol{f}}'_E$ was then constructed so as to generate a right-handed orthogonal coordinate system.

SKI EDGE ANGLE

The whole ski edge angle (θ) was determined by projecting $\hat{\boldsymbol{G}}$ onto the F′G′ plane and calculating the angle between the projected $\hat{\boldsymbol{G}}$ vector and $\hat{\boldsymbol{G}}'$. Since the orientation of $\hat{\boldsymbol{G}}$ is defined by the relative positions of the ankle joint center and the ski tip and tail, θ is probably more appropriately described as a rough estimate of the ski edge angle (Müller et al., 1998). The actual edge angle can be expected to differ somewhat from this estimate depending on the individual's binding and boot set-up. In addition, the edge angle is likely to vary along the ski's length due to ski flexion and torsion deformations whose measurement is beyond the resolution of this current method. Complicating matters further is the fact that the exact nature of the local snow surface is not precisely known and can be expected to progressively change with each passing skier as the snow is scraped and deformed.

SKI ATTACK ANGLE

The whole ski attack angle (φ) was quantified to describe the angle between the ski's direction of motion and its longitudinal axis. This was calculated as the angle between $\hat{\boldsymbol{E}}'$ and the projection of $\hat{\boldsymbol{E}}$ (the ski longitudinal axis) onto the E′F′ plane, which was by definition parallel to the plane of the local snow surface.

LOCAL SKI ATTACK ANGLE

Local ski attack angles φ_E at points $\vec{\boldsymbol{S}}(E)$ along the outside ski's interacting edge were calculated by projecting $\hat{\boldsymbol{e}}_E$ onto the $e'_E f'_E$ plane, and then determining the angle between the projected $\hat{\boldsymbol{e}}_E$ vector and $\hat{\boldsymbol{e}}'_E$.

CENTER OF MASS ATTACK ANGLE

The angle of attack between the center of mass velocity vector $\dot{\vec{\boldsymbol{P}}}_{COM}$ and the longitudinal axis of the outside ski was calculated as described by Müller et al. (1998),

who referred to this parameter as the "downhill ski to movement direction angle." At each instant in time, an accelerated coordinate system ABC was constructed, originating at the center of mass position. $\hat{\boldsymbol{A}}$ was defined as parallel to the center of mass velocity vector, $\dot{\vec{\boldsymbol{P}}}_{\mathrm{COM}}$. $\hat{\boldsymbol{B}}$ was then constructed to be perpendicular to both $\dot{\vec{\boldsymbol{P}}}_{\mathrm{COM}}$ and $\hat{\boldsymbol{n}}_{\mathrm{XY}}$, the local snow surface normal vector. Finally, $\hat{\boldsymbol{C}}$ was defined so as to generate an orthogonal, right-handed triad. Note that the AB plane was not necessarily parallel to the local snow surface, as per Müller et al.'s definition. The center of mass attack angle (λ) was then calculated as the angle between the projection of the ski longitudinal axis (defined by $\hat{\boldsymbol{E}}$) on the AB plane and $\hat{\boldsymbol{A}}$. The sign of λ was defined to be negative when $\dot{\vec{\boldsymbol{P}}}_{\mathrm{COM}}$ was directed more to the inside of the turn than $\hat{\boldsymbol{E}}$ and, conversely, positive when $\dot{\vec{\boldsymbol{P}}}_{\mathrm{COM}}$ was directed more to the outside of the turn than $\hat{\boldsymbol{E}}$.

SKIER LATERAL ACTION CHARACTERISTICS

CENTER OF MASS INCLINATION

The center of mass inclination angle (ς) was calculated by constructing a local coordinate system QRS at the projection of the average ski point on the snow surface, indicated by $\vec{\boldsymbol{P}}_{\mathrm{SKI}}$ in Figure 5.12 A. $\hat{\boldsymbol{Q}}$ was oriented parallel to the projection of the outside ski longitudinal axis on the local snow surface plane. $\hat{\boldsymbol{S}}$ was directed normal to the local snow surface (parallel to the local normal vector $\hat{\boldsymbol{n}}_{\mathrm{XY}}$). $\hat{\boldsymbol{R}}$, defined so as to generate an orthogonal, right-handed triad, lay in the local snow surface plane, perpendicular to the ski longitudinal axis projection. The center of mass position ($\vec{\boldsymbol{P}}_{\mathrm{COM}}$) in the QRS reference frame was projected onto the RS plane and ς was then calculated as the angle between the projected center of mass position vector and $\hat{\boldsymbol{S}}$.

To quantify the degree to which skiers modified the ski edge angle from that given by inclination, angulation (A) was defined as the difference between the ski edge angle (θ) and the center of mass inclination (ς), according to Brown (2007):

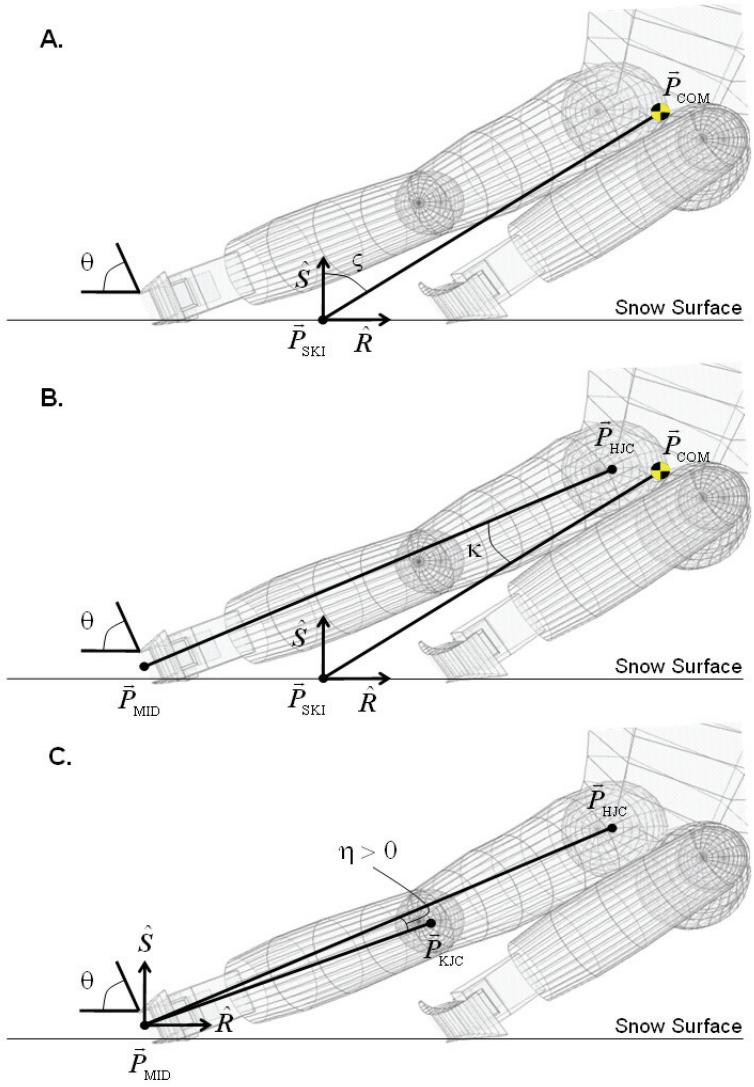

FIGURE 5.12. Definitions of skier inclination angle (ς) (A), hip angulation angle (κ) (B), and knee angulation angle (η) (C). θ is the ski edge angle. The SR plane is defined as normal to the outside ski longitudinal axis and, in the images shown above, parallel to the image plane. $\hat{\boldsymbol{S}}$ and $\hat{\boldsymbol{R}}$ are defined as perpendicular and parallel to the local snow surface plane, respectively.

$$A = \theta - \varsigma \quad [\text{deg}] \qquad [5.5]$$

Angulation was further sub-divided into components resulting from hip (κ) and knee angulation (η).

HIP ANGULATION

Hip angulation was calculated by first projecting the position vectors of the outside hip joint center and ski mid points ($\vec{P}_{\text{HJC}}$ and $\vec{P}_{\text{MID}}$, respectively) in the QRS reference frame to the RS plane and calculating the angle between the resulting vector and that of the projected center of mass position vector (Figure 5.12 B). Hip angulation thus describes the degree to which the overall inclination of the outside leg differed from the center of mass inclination, ς. When the leg inclination was greater than that of the center of mass, κ was defined as positive and acted to increase the edge angle beyond that which the center of mass inclination would have accomplished alone. Conversely, when the leg inclination was less than that of the center of mass, κ acted to reduce the edge angle from that which center of mass inclination would have created alone and was thus defined as negative.

KNEE ANGULATION

Finally, knee angulation was calculated by constructing a local coordinate system QRS in a manner identical to that for the calculation of inclination, but originating in the outside ski mid point, $\vec{P}_{\text{MID}}$ (Figure 5.12 C). The hip and knee joint center positions in the QRS reference frame, $\vec{P}_{\text{HJC}}$ and $\vec{P}_{\text{KJC}}$, were then projected onto the RS plane and the angle between the two projected position vectors was taken as knee angulation (η). Knee angulation that acts to increase the ski edge angle beyond that caused by leg inclination was defined as positive and, conversely, that which acts to decrease the edge angle was defined as negative.

It is important to point out that neither κ nor η represent actual joint angles, but instead quantify the effective change in ski edge angle due to motion about the knee and hip joints. Theoretically, the ski edge angle θ should be equal to the sum of center of mass inclination, hip angulation and knee angulation angles:

$$\theta = \varsigma + \kappa + \eta \quad [\text{deg}] \qquad [5.6]$$

This relationship was used to test the results of the aforementioned calculations for consistency. The maximum difference between the measured edge angle and the sum of inclination and angulation angles over all 12 analyzed trials was less than 0.001 degrees which is probably less than the angular resolution capability for this type of video analysis, indicating that these calculations were performing according to expectations.

SKIER VERTICAL ACTION CHARACTERISTICS

In a manner similar to that described by both Supej, Kugovnik, and Nemec (2005b) and Pozzo, Canclini, Cotelli et al. (2005), skier vertical motion was divided into the following two components: Center of mass motion normal to the snow surface and distance from the center of mass to the outside ankle joint center.

CENTER OF MASS POSITION ORTHOGONAL TO THE SNOW SURFACE

The center of mass position in the Z' dimension was used to quantify motion normal to the least squares plane of the snow surface, $Z'_{COM}(t)$. The mean peak-to-peak amplitude for the two turns ($\overline{Z}'_{AMP}$) was calculated as the cumulative vertical center of mass displacement from $\vec{P}_{COM}$ at Switch 1 to $\vec{P}_{COM}$ at Switch 3 divided by 4 (for one upwards motion and one downwards motion per turn cycle, two cycles).

CENTER OF MASS TO ANKLE JOINT CENTER DISTANCE

The center of mass to outside ankle joint center distance, $D_{AJC}(t)$, was calculated at each instant in time as the Euclidian distance between the center of mass position and the outside ankle joint center position at each instant in time, t:

$$D_{AJC}(t) = \left| \vec{\boldsymbol{P}}_{COM}(t) - \vec{\boldsymbol{P}}_{AJC}(t) \right| \quad [5.7]$$

SKIER FORE / AFT ACTION CHARACTERISTICS

To describe skier fore/aft movement relative to the outside ski, an accelerated local coordinate system (QRS) was constructed originating at the outside ankle joint center in a manner similar to Schiefermüller et al. (2005) (Figure 5.13). $\hat{\boldsymbol{Q}}$ was defined as parallel to the projection of the outside ski longitudinal axis on the local plane of the snow surface. $\hat{\boldsymbol{S}}$ was defined as normal to the local plane of the snow surface (i.e., parallel to $\hat{\boldsymbol{n}}_{x,y}$) and $\hat{\boldsymbol{R}}$ was defined so as to obtain a right-handed orthogonal triad. The QR plane was thus parallel to the local snow surface. The center of mass position in the local Q-dimension was used to characterize center of mass fore/aft position as a function of time, $Q_{COM}(t)$. Average center of mass position ($\bar{Q}_{COM}$) and range of center of mass motion (Q_{ROM}) in the Q-dimension were calculated for each turn separately.

SKIER MECHANICAL ENERGY

Total mechanical energy (E_{MECH}) at each instant in time was calculated as the sum of skier potential energy (E_{POT}) and kinetic energy (E_{POT}), knowing the center of mass altitude (Z in the Theodolite Coordinate System) and speed ($\dot{P}_{COM}$) (Equation [5.8]). Energy dissipation (E_{DISS}) was then calculated as the change in E_{MECH} per change in altitude per kilogram body mass (m) using finite central differences to give an instantaneous measure of the skier's energy behavior (Equation [5.9]) (Supej, 2008; Supej, Kugovnic, & Nemec, 2005a):

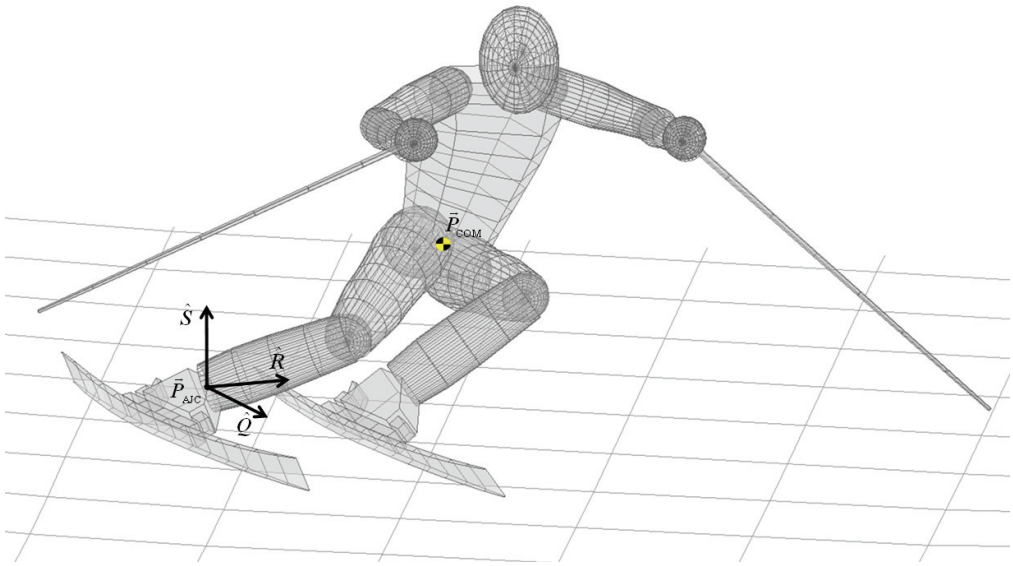

FIGURE 5.13. Application of the QRS coordinate system for determination of skier fore / aft position.

$$\begin{aligned} E_{MECH}(i) &= E_{POT}(i) + E_{KIN}(i) \\ &= mgZ(i) + \frac{1}{2}m\dot{P}_{COM}(i)^2 \quad [J] \end{aligned} \qquad [5.8]$$

$$\begin{aligned} E_{DISS}(i) &= \frac{\Delta E_{MECH}}{m\Delta Z} \\ &= \frac{[E_{MECH}(i+1) - E_{MECH}(i-1)]}{m[Z(i+1) - Z(i-1)]} \quad [J \cdot kg^{-1} \cdot m^{-1}] \end{aligned} \qquad [5.9]$$

It is important to be aware that Supej, Kugovnik, and Nemec (2005a) changed the sign of the right-hand side of Equation [5.9] so that the resulting information would be easier for coaches and athletes to understand. A similar change was not done in the current study. In this report, positive energy dissipations indicate the loss of energy to the surrounding environment and, conversely, negative dissipations represent the increase of energy due to the athlete's muscular work.

EXTERNAL FORCES

The equation representing the skier's motion was defined according to Lüthi et al. (2005) as:

$$m\ddot{\vec{P}}_{COM}(t) = \vec{F}_R(t) + \vec{F}_D(t) + \vec{F}_G \quad [N] \qquad [5.10]$$

where m is the skier and equipment mass, $\ddot{\vec{P}}_{COM}$ is the center of mass resultant acceleration, $\vec{F}_R$ is the snow reaction force, $\vec{F}_D$ is the air drag force, and $\vec{F}_G$ is the gravitational force. The following sections describe how each of these parameters was determined.

CENTER OF MASS ACCELERATION

The center of mass resultant acceleration ($\ddot{\vec{P}}_{COM}$) was calculated based on the center of mass trajectory as a function of time ($\vec{P}_{COM}(t)$) and using the 5-point finite central difference formula (Gilat & Subramaniam, 2008).

AIR DRAG FORCE

The air drag force ($\vec{F}_D$) was modeled according to an algorithm developed by Gilgien (2008) in which the magnitude of the force was determined according to the formula:

$$F_D = \frac{1}{2}\rho \cdot A \cdot C_D \cdot v^2 \quad [N] \qquad [5.11]$$

where ρ is the air density, A is the frontal surface area, C_D is the air drag coefficient and v is the speed of the athlete relative to the surrounding air (Lind & Sanders, 2004).

An air density of 1.23 $kg \cdot m^{-3}$ was calculated based on the on-site temperature measurements and the air pressure measurements taken at a nearby meteorological station. This estimate does not take into account the effect of air humidity, which was assumed to be small and thus negligible (van Ingen Schenau, 1982).

Skier frontal area (A) was estimated using an adaptation of a pixel counting function developed by Brodie (2008) for this purpose. A model of the skier and equipment was first constructed by attaching simple geometric volumes to the reconstructed landmarks. A silhouette of the skier's body was then generated by projecting the skier model onto a plane oriented normal to the center of mass velocity vector ($\dot{\vec{P}}_{COM}$). This silhouette was plotted white against a black background, allowing the algorithm to count the number of white pixels, the sum of which was taken to represent the skier's frontal area that is presented to the wind (Figure 5.14). The conversion factor from numbers of pixels to m^2 was determined through counting the number of pixels in the

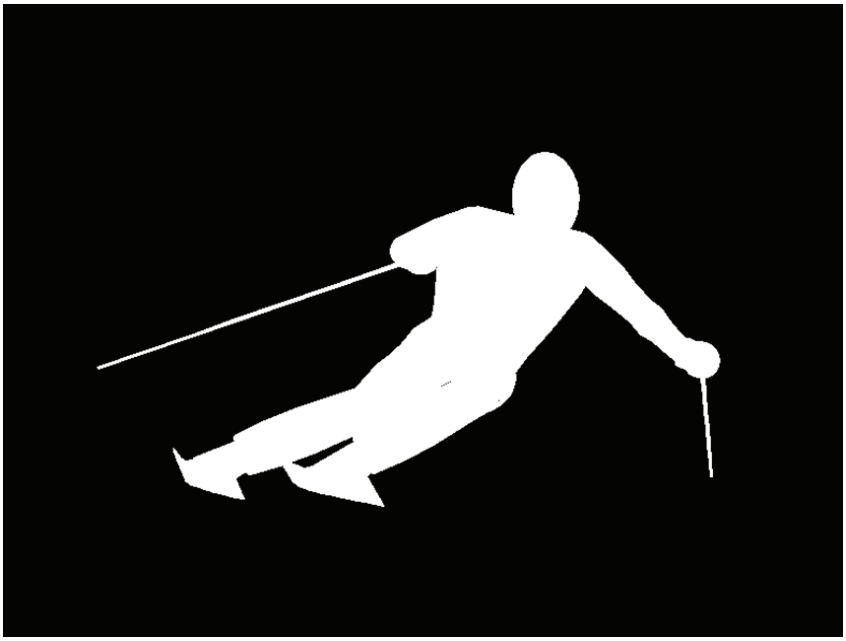

FIGURE 5.14. An example screen capture from Brodie's (2008) pixel counting algorithm for estimating skier frontal area. The plane of the image is orthogonal to the center of mass velocity vector.

plot of a 1 m side length square. The calculated frontal areas ranged from 0.52 to 0.72 m^2 and averaged 0.61 m^2 across all 12 trials.

The value of the air drag coefficient C_D was taken from experimental data in the existing literature. Since experimental measurements of drag forces and coefficients in alpine ski racing have typically focused on speed events, it was necessary to search alternative literature to find experimental data appropriate for the slalom discipline. Drag coefficient data were finally taken from a cross country study (Spring, Savolainen, Erikkila, Hamalainen, & Pihkala, 1988) where the drag areas ($C_D \cdot A$) of three male skiers were measured at speeds ranging from 5 to 12 $m \cdot s^{-1}$, speeds that are much closer to those expected in slalom. Spring et al. reported drag coefficients of 1.0 and 0.6 for upright and crouched positions, respectively, for a skier of approximately the same height and weight as the subjects in the current study[10]. A linear regression equation was developed based on these values to calculate the drag coefficient as a function of skier length at each instant in time. The resulting air drag coefficient averaged 0.82 across all trials and ranged from 0.70 to 0.95.

As stated earlier, skier speed ($\dot{P}_{COM}$) was calculated based on the center of mass trajectory using the 4-point finite central difference formula (Gilat & Subramaniam, 2008). Unfortunately, wind conditions were not measured during the data collection. Although no appreciable winds were observed, a constant uphill wind is to be expected from mid-morning to mid-afternoon in high pressure weather conditions, such as that on the day of data collection (Gilgien, 2008). Since the investigation team did not observe any appreciable wind, it was assumed that there was weak and constant 1 $m \cdot s^{-1}$ wind flowing in the uphill $-X'$ direction. The component of this wind acting opposite the

[10] Spring et al. (1988) did not, in fact, report the drag coefficients directly. They reported the so-called drag area which is the product of the drag coefficient and the frontal area. However, we were able to extract the drag coefficient by dividing the drag area by the reported frontal area.

center of mass velocity vector was thus added to the skier speed prior to entering Equation [5.11].

Finally, the line of action of the drag force was assumed to be opposite the direction of the center of mass velocity vector. Therefore, the drag force vector $\vec{\boldsymbol{F}}_D(t)$ was calculated at each instant in time t knowing the force magnitude ($F_D(t)$) and the center of mass velocity unit vector ($\hat{\dot{\boldsymbol{P}}}_{COM}(t)$) using the Equation [5.12]:

$$\vec{\boldsymbol{F}}_D(t) = -F_D(t)\hat{\dot{\boldsymbol{P}}}_{COM}(t) \quad [N] \qquad [5.12]$$

GRAVITATIONAL FORCE

The gravitational force vector $\vec{\boldsymbol{F}}_G$ was calculated knowing the skier (and equipment) mass m and the line of action of gravity:

$$\vec{\boldsymbol{F}}_G = -mg\hat{\boldsymbol{Z}} \quad [N] \qquad [5.13]$$

where g is the gravitational acceleration constant and $\hat{\boldsymbol{Z}}$ is the vertical dimension of the Theodolite Coordinate System whose orientation was defined by leveling of the theodolite.

SNOW REACTION FORCE

Finally, the snow reaction force $\vec{\boldsymbol{F}}_R$ was calculated by rearranging Equation [5.10] to obtain:

$$\vec{\boldsymbol{F}}_R(t) = m\ddot{\vec{\boldsymbol{P}}}_{COM}(t) - \vec{\boldsymbol{F}}_D(t) - \vec{\boldsymbol{F}}_G \quad [N] \qquad [5.14]$$

The vertical component of the snow reaction force was calculated by taking the dot product between the snow reaction force vector and the local snow surface normal at the average ski position:

$$F_{VERT}(t) = \vec{\boldsymbol{F}}_R(t) \cdot \hat{\boldsymbol{n}}_{X,Y} \quad [5.15]$$

POWER

To describe the instantaneous work rate of each external force on the skier center of mass, power was calculated as the dot product between the force vector and the center of mass velocity vector at each instant in time, t (Ohanian & Markert, 2007):

$$P_R(t) = \vec{\boldsymbol{F}}_R(t) \cdot \dot{\vec{\boldsymbol{P}}}_{COM}(t) \quad [W] \quad [5.16]$$

$$P_D(t) = \vec{\boldsymbol{F}}_D(t) \cdot \dot{\vec{\boldsymbol{P}}}_{COM}(t) \quad [W] \quad [5.17]$$

$$P_G(t) = \vec{\boldsymbol{F}}_G \cdot \dot{\vec{\boldsymbol{P}}}_{COM}(t) \quad [W] \quad [5.18]$$

where P_R, P_D, and P_G are the snow reaction force, air drag force, and gravitational force powers, respectively.

WORK

The total mechanical work done by each of the external forces on the athlete over the two analyzed turns was calculated as the line integral of the dot product between the force and center of mass velocity vectors:

$$W_R = \int_a^b \vec{\boldsymbol{F}}_R(t) \cdot \dot{\vec{\boldsymbol{P}}}_{COM}(t)dt \quad [J] \quad [5.19]$$

$$W_D = \int_a^b \vec{\boldsymbol{F}}_D(t) \cdot \dot{\vec{\boldsymbol{P}}}_{COM}(t)dt \quad [J] \quad [5.20]$$

$$W_G = \int_a^b \vec{\boldsymbol{F}}_G \cdot \dot{\vec{\boldsymbol{P}}}_{COM}(t)dt \quad [J] \quad [5.21]$$

where W_R, W_D, and W_G are the reaction force, drag force, and gravitational force work energies, respectively, and a and b are the start and end times, respectively, of the two analyzed turns.

COMPARISONS WITH MECHANICAL ENERGY DISSIPATION

Two approaches have been used to quantify the skiers' mechanical energy behavior. On the one hand, skier potential and kinetic energies were calculated knowing the center of mass altitude and speed. Changes in the skier's total energy were subsequently used to describe energy gains and losses made by the skier (see Mechanical Energy Dissipation p. 171). On the other hand, the work done by each of the three external forces was also calculated as described above. Both are justifiable approaches and—if modeling of the air drag force has been done accurately—should come forth to the same result in terms of skier energy behavior. Thus, as a quality control test of the two algorithms making these calculations, total skier energy gains and losses calculated from the two approaches were compared.

5.15 STATISTICAL METHODS

There are in essence four types of research objectives for this investigation. The first type involves describing skier kinematic and kinetic characteristics on the two courses. The second type involves making comparisons between courses on a selection of the quantified parameters while the third type looks at comparisons with performance time. The final type of question is concerned with identifying potential causes of mechanical energy dissipation. Different statistical approaches were used for each of these types of questions.

DESCRIPTIVE STATISTICS

To characterize the performances of the skiers as a group, standard descriptive statistics were calculated for the parameters of interest. Due to varying turn cycle durations, data were initially time-normalized as a percentage of turn cycle duration. To describe the time-course of continuous parameters, ensemble averages and standard deviations were generated and plotted for each course separately. In addition, descriptive statistics including means and standard deviations were calculated for each parameter of interest at key time points of the turn cycle including turn start, turn phase start, gate passage, turn phase end, and turn end and are presented in table format. Descriptive statistics can be deceiving, however, in that they can hide individual variations that are important. Therefore, individual examples from the data are also presented with each parameter in Appendices to allow the reader to make comparisons.

COURSE-TO-COURSE COMPARISONS

Course-to-course comparisons were made on continuous variables by initially time-normalizing data as a percentage of turn cycle duration. Data were then averaged for each 10 % of the turn cycle for each turn, and then averaged across all turns for the 10 and 13 meter courses, separately. These data are presented for the reader graphically showing means and standard deviations for each 10 % of the turn cycle. Since the groupings in the graphics are paired samples, it is sometimes difficult to visualize the magnitude of the difference. Therefore, to help the reader judge the size of the differences taking into account individual subject variability, p values from paired sample t tests are indicated on the graphics. The non-parametric Wilcoxon Signed Ranks Test for paired samples was used on the center of mass and ski turn radius data due to very large individual differences in the data around turn transitions.

RELATIONSHIPS TO PERFORMANCE

Based on the research objectives, the following parameters were selected for comparison to performance time (PT):

COM 3-dimensional trajectory length	L_{XYZ}
COM trajectory length in the Y-dimension	L_Y
COM trajectory length in the Z-dimension	L_Z
Mean COM speed	$\bar{\dot{P}}_{COM}$
Mean energy dissipation	$\bar{E}_{DISS}$
Mean wind drag force power	$\bar{P}_D$
Mean reaction force power	$\bar{P}_R$
Mean initiation ski attack angle	$\bar{\varphi}^{INIT}$
Mean COM fore/aft position	$\bar{Q}_{COM}$
COM fore/aft range of motion	Q_{ROM}
Mean vertical motion amplitude	$\bar{Z}'_{AMP}$
Mean vertical reaction force during initiation	$\bar{F}^{INIT}_{VERT}$

Comparisons to performance were made by calculating the non-parametric Spearman's correlation coefficient. But perhaps more importantly, scatter plots were generated and are presented in an Appendix P to allow the reader to make independent judgments.

RELATIONSHIPS TO MECHANICAL ENERGY LOSS

To understand the causes of skier mechanical energy loss better, Pearson's product moment correlation was calculated between skier fore/aft position (Q_{COM}), ski attack angle (φ), and reaction force power (P_R).

5.16 MEASUREMENT ACCURACY

A number of tests were conducted to assess the accuracy of the implemented methods. In particular, assessments were made of both the camera phase shifts derived using the

software genlock algorithm as well as the reconstructed object-space positions. When possible, methods similar to Klous (2007) and Lindinger (2006) were used to allow for comparisons with other similar investigations.

ACCURACY OF THE SOFTWARE GENLOCK METHOD

As no direct measurement of the shift between cameras was made, the inconsistency in phase shifts between pairs of cameras was used to estimate the accuracy of the software genlock algorithm, in a manner similar to Pourcelot et al. (2000). Average and maximum inconsistencies were 1.4 % and 3.8 % of the time interval between frames (n = 48 analyses over 12 trials), agreeing well with the values reported by Pourcelot et al. With a sampling frequency of 50 Hz, this translates to a maximum inconsistency of less than 1 ms, which also corresponds well with the results reported by both Yeadon and King (1999) and Kwon et al. (2004).

It is tempting to estimate the reconstruction error due to a 1 ms shift in camera synchronization by considering the speed of the target point and the distance that it would travel over 1 ms. In this way, one might estimate a reconstruction error of less than 13 mm for a target point travelling at 13 $m \cdot s^{-1}$. Such a calculation, however, oversimplifies the geometry of the quasi-intersecting rays from each camera and likely underestimates the actual error, depending upon the angle between these rays.

To assess the impact that a 1 ms error in camera synchronization would have on reconstruction accuracy, a simulation was programmed using the camera constants and the filtered, reconstructed object-space trajectories for all points from all 12 trials. In this manner, the effect of synchronization error under the specific conditions of this study was assessed. From the four cameras, each possible two-camera combination was evaluated for each reconstruction, where one camera was designated the master and the other the slave. To generate image-space coordinate data of the target points for the master camera, the object-space position data of the 23 digitized landmarks on the skier

and equipment were transformed back to the comparator-space coordinate system using Equations [4.1] and [4.2]. The same object-space position data were then shifted 1 ms forward in time and then transformed back to the comparator-space coordinate system of the slave camera, thus simulating a 1 ms error in camera synchronization. The comparator-space coordinates from the master camera and the time-shifted comparator-space coordinates from the slave camera were then used to reconstruct the trajectories of all points. The differences between the new, erroneous object-space coordinates and the original data were used to describe the deterioration in accuracy due to camera synchronization error.

As a pair of cameras tracked a target point's motion through the object-space, the angle between cameras changed. To assess the effect that the inter-camera angle has on the component of reconstruction error due to camera synchronization inaccuracy, the 3-dimensional camera angle was determined for each reconstruction in the simulation using the dot product between the camera-to-target point vectors and the camera positions derived from the 11 DLT camera constants (Walton, 1981). The mean and maximum speeds for the target points were 13.8 $m \cdot s^{-1}$ and 17.5 $m \cdot s^{-1}$, respectively. This resulted in mean and maximum displacements between the true trajectories and the time-shifted trajectories of 14 and 18 mm, respectively.

To ensure that the simulation truly isolated error due to the shift in camera synchronization, a simulation was conducted with a 0 ms time shift in the object-space trajectories used to generate the slave camera comparator-space coordinates. The resulting object-space reconstructions had a maximal error of 6 $x10^{-10}$ mm, indicating that the simulation did indeed isolate the error associated with the shift in camera synchronization.

Results of the simulation are presented in Table 5.6. Introducing a 1 ms error in camera synchronization caused a resultant RMSE of 17 mm and a maximal resultant error of 57 mm. The largest errors were in the Y′- dimension. The error magnitude is clearly

TABLE 5.6. Target point reconstruction error due to a simulated 1 ms error in camera synchronization. Data are based on n = 133138 reconstructions over all 2-camera combinations, all target points, and all trials.

Point	RMSE [mm]	95%-ile [mm]	Max Error [mm]
X'	9	16	34
Y'	14	25	55
Z'	1	2	9
Resultant	17	27	57

Note: X', Y', Z' refer to the Course Coordinate System dimensions.

dependent upon the angle between the two cameras, with the highest errors for angles less than approximately 40^{o} or higher than about 140^{o} (Figure 5.15). The sharp reduction in error at very low camera angles was surprising so graphics were generated to examine why this occurred. It was discovered that, at these points, the rays from the master camera and the time-shifted slave camera passed on either side of the true target point's position. Since the cameras still had a slight angle in the vertical plane, the least squares solution to Equations [4.5] in this situation resulted in accurate reconstructions.

Considering that the majority of reconstructions (83 %) used in this study involved at least one camera pair with an inter-camera angle approaching 90^{o}, and less than 4 % of the reconstructions involved only two cameras with a poor angle (see p. 153), the component of reconstruction error due to inaccuracies in camera synchronization on the order of 1 ms can be expected to be less than 15 mm for the large majority of reconstructions. As the error due to manual digitization of difficult to visualize target points is likely to be larger, this level of synchronization accuracy was deemed sufficient for the purposes of this study.

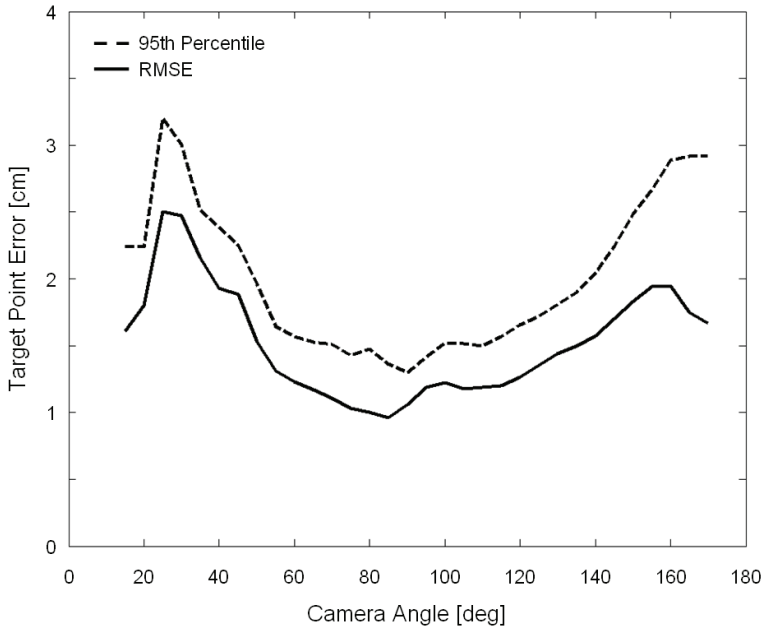

FIGURE 5.15. Target point reconstruction error due to a simulated 1 ms error in camera synchronization versus inter-camera angle. Data are based on n = 133138 reconstructions over all 2-camera combinations, all target points, and all trials.

Chapter 5

ACCURACY OF THE PANNING DLT METHOD

Object-space reconstruction accuracy was assessed using two methods. In the first, known positions of so-called "*non*-control points" were used as references in calculating measurement error. In the second, reconstructed segment lengths were compared to measured values.

NON-CONTROL POINT ERROR

It is known that points which are used to assess measurement accuracy in photogrammetry should not be the same ones that were used to derive the transformation parameters (Challis & Kerwin, 1992). A "*non*-control point" is the term used in this dissertation to refer to a marker of known object-space position that is not used for camera calibration but is instead used to assess measurement accuracy. In this study, Type 3 (Figure 5.2 C) control points were used for this purpose since they were distributed throughout the calibrated volume along the snow surface close to the skiers' trajectories. Normally, these points were in fact used in camera calibration. To generate *non*-control points, Type 3 points were rotated out of the camera calibration sequence, one at a time, and then reconstructed using the updated transformation parameters. Error in the reconstructed position relative to the geodetically measured position could then be used to assess measurement accuracy.

As the cameras panned following the skier, control points passed in and out of each camera's field of view. The calibration volume at a particular instant in time was defined in space by the configuration of the digitized control points used in camera calibration. Points extending beyond the edge of this volume were expected to be subject to extrapolation error (Angulo & Dapena, 1992; Bate, 1993; Brewin & Kerwin, 2005; Challis & Kerwin, 1992; Chen et al., 1994; Gazzani, 1993a; Hatze, 1988; Hinrichs & McLean, 1995; Levy & Smith, 1995; Walton, 1981; Wood & Marshall, 1986; Yu et al., 1993). To both avoid measuring extrapolation error and to better estimate

reconstruction accuracy of the calibration volume in the vicinity of the skier's position, only Type 3 control points that fell within 3 m of the projection of the center of mass onto the snow surface at a particular instant in time were used as *non*-control points.

Further, it was expected that in certain situations a Type 3 control point might play a particularly important role in calibration accuracy and that the removal of this point from the calibration sequence would result in a marked deterioration in reconstruction accuracy. Therefore, if the removal of a particular Type 3 control point from the calibration sequence resulted in greater than a 1 % change in the 11 DLT camera constants on average—or maximally 5 % for any one camera constant—the point was excluded from the *non*-control point error calculation.

Results of the analysis are presented in Table 5.7 and Figure 5.16. A total of 980 *non*-control point reconstructions were assessed across all 12 trials. *Non*-control point root mean squared error (RMSE) was 4, 5, and 2 mm in the Course Coordinate System X'-, Y'-, and Z'- dimensions, respectively. Less than 2 % of all reconstructions had greater than 15 mm resultant error. For each reconstruction, the number of cameras, inter-camera angles, and number of control points were determined for a more detailed analysis of the reconstruction error.

TABLE 5.7. *Non*-control point reconstruction error.

Dimension	n	RMSE [mm]	95%-ile [mm]	Max Error [mm]
X'	980	4	8	18
Y'	980	5	10	25
Z'	980	2	5	9
Resultant	980	7	12	27

Note: X', Y', Z' refer to the Course Coordinate System dimensions.

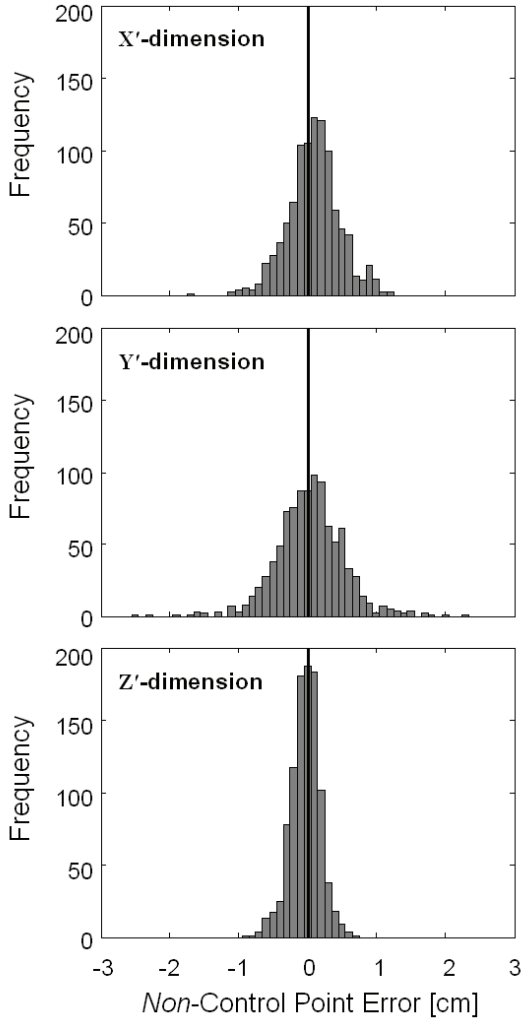

FIGURE 5.16. Frequency distributions of *non*-control point reconstruction error in the Course Coordinate System X′-, Y′-, and Z′-dimensions. n = 980 reconstructions.

Figure 5.17 shows the relationship between *non*-control point resultant error and the number of cameras used in the reconstruction. There was a trend towards increasing accuracy with increased numbers of cameras, in agreement with other published works (Levy & Smith, 1995). Interestingly, the majority of 2-camera reconstructions were as accurate as those using 3 and 4 cameras. The main improvement from increasing number of cameras seemed to come from a reduction in the most extreme errors.

The relationship between *non*-control point error and inter-camera angle for all of the 2-camera reconstructions is shown in Figure 5.18. High error reconstructions occurred when the inter-camera angle was either less than about 50° or greater than about 130°, in good accordance with earlier investigations (Bate, 1993; Chen et al., 1994; de Haan & den Brinker, 1988; Shapiro, 1978; Wood & Marshall, 1986). It is interesting to note that accurate reconstructions with two cameras at a poor angle are possible; however, the likelihood of a poor reconstruction is substantially increased. In other words, reconstructions may still be very accurate with two cameras at a poor angle, but they are more susceptible to error.

Figure 5.19 shows the relationship between the mean number of control points used in the calculation of the camera constants and the resultant *non*-control point error. Accuracy improved with increasing numbers of control points confirming the work of others (Abdel-Aziz & Karara, 1971; Challis & Kerwin, 1992; Chen et al., 1994; de Haan & den Brinker, 1988; Gazzani, 1993b; Hatze, 1988; Hinrichs & McLean, 1995; Wood & Marshall, 1986). Similar to Hinrichs and McLean (1995), accuracy seemed to continue to improve to above 60 control points. The reconstructions with the worst error (i.e, those in excess of 15 mm) were characterized as 2-camera reconstructions with a poor inter-camera angle (< 50° or > 130°) and a relatively low number of control points (< 30). Figure 5.20 shows an example of one such high-error reconstruction in which 2 cameras at a very poor inter-camera angle of 165° were used. Less than a 0.2 pixel correction in the digitized comparator-space coordinates of Camera 2 would have been sufficient to

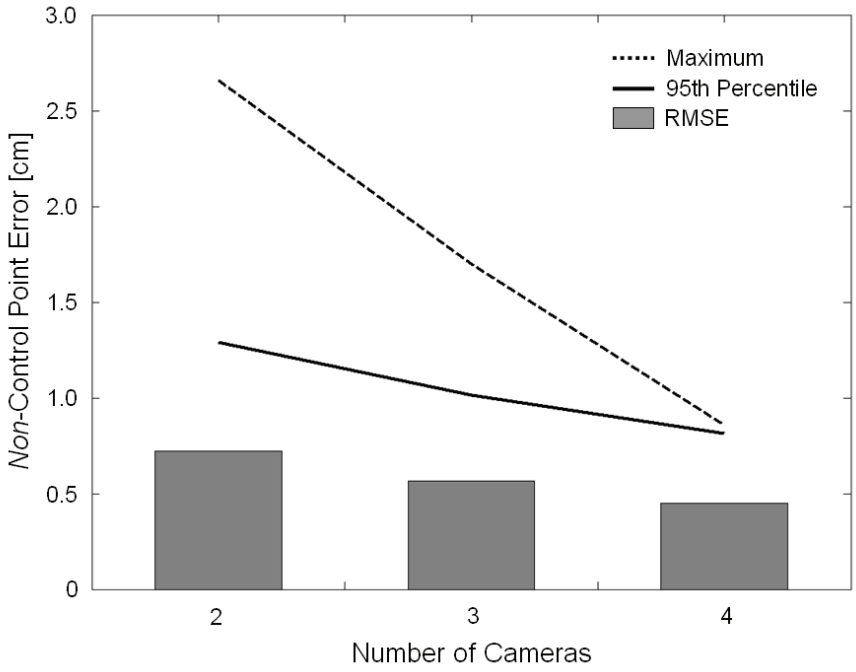

FIGURE 5.17. *Non*-control point resultant error and the number of cameras used in reconstruction (n = 980).

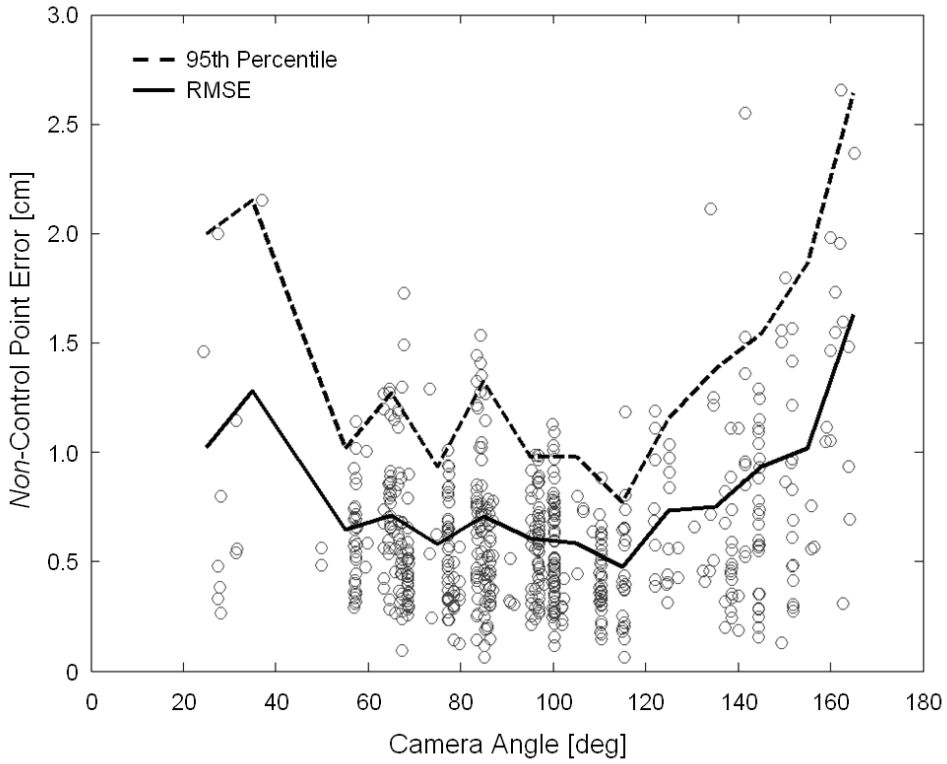

FIGURE 5.18. *Non*-control point resultant error and the inter-camera angle for two-camera reconstructions (n = 601).

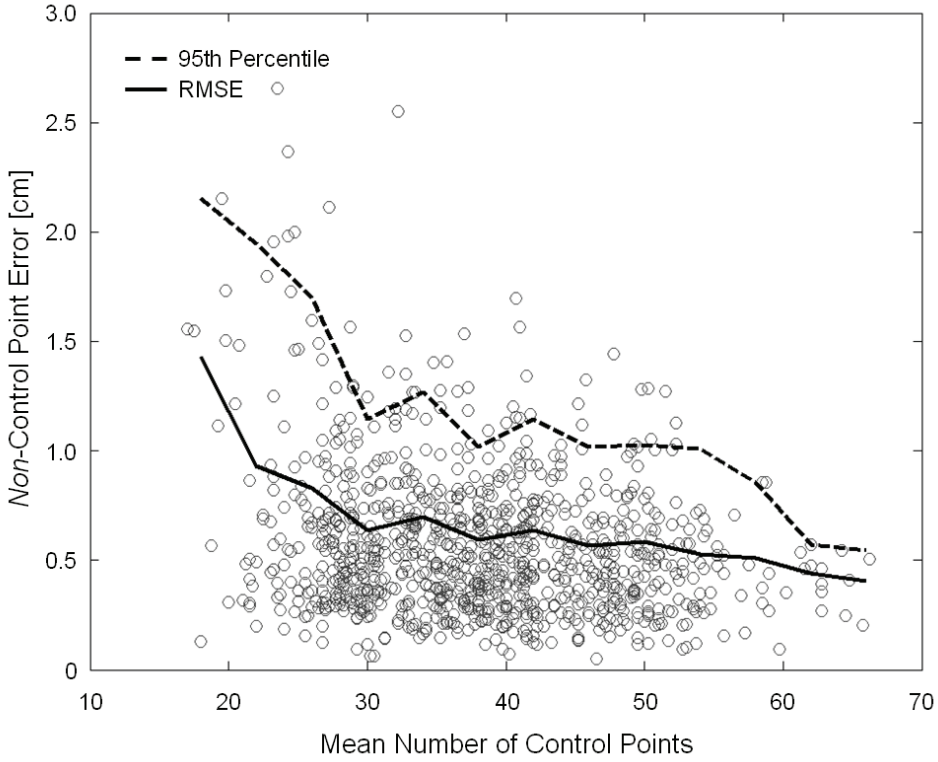

FIGURE 5.19. *Non*-control point resultant error and the mean number of control points (n = 980).

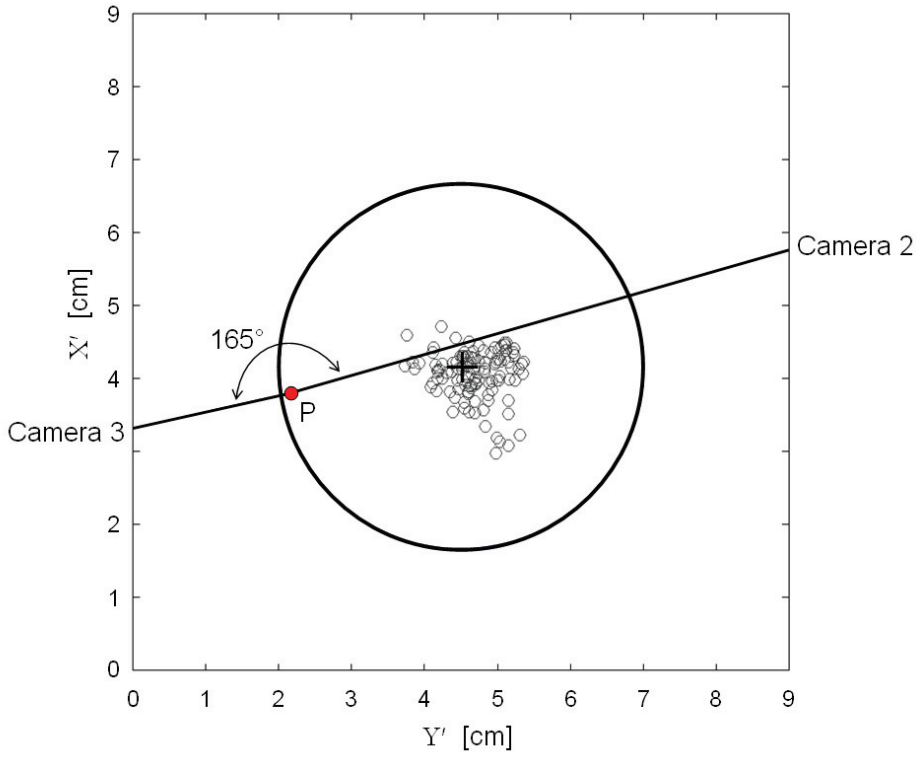

FIGURE 5.20. The reconstructions for *non*-control point number 536 (n = 115). Reconstruction P is a good example of a large error reconstruction in which two cameras were used with a very poor inter-camera angle of 165° and a rather low average number of control points of 24.5. Less than a 0.2 pixel correction in the digitized image coordinates from Camera 2 would have been sufficient to correct the resulting reconstruction to the control point center. The large circle indicates the circumference of the tennis ball defining the marker.

correct the resulting reconstruction to the control point center. This is within the resolution of the implemented digitization system since the smallest possible step in the digitization window was set to 0.3 pixels. This is a good example of how even very small digitization errors can lead to very large reconstruction errors in 2-camera reconstructions when the camera angle is poor.

SEGMENT LENGTH ERROR

While the *non*-control point error represents the accuracy of the measurement system for clearly visualized points, it underestimates the error associated with manually digitizing points which are more difficult to visualize, such as the hip joint centers. Furthermore, since *non*-control points are stationary, this error also does not reflect inaccuracies in camera synchronization. To assess measurement accuracy that includes both of these error components, segment lengths were calculated and compared to directly measured values for the left side of the body. Unfiltered, object-space coordinate data from the first turn switch to the third turn switch for all 12 trials were used to calculate segment lengths for the left upper arm, forearm, thigh, and shank, as well as the hip breadth. Segment lengths were calculated as the Euclidian distance between segment endpoints.

Table 5.8 summarizes the segment length reconstruction error for each segment. In this study, larger errors were observed for upper body segments than for lower body segments, perhaps reflecting the increased focus and quality control undertaken on the lower body segments. Compared to earlier works using similar methods, upper body segment errors were somewhat higher, while lower body segment errors were at least equivalent or even slightly improved. Since this study does not examine any questions directly related to upper body motion, upper body points are only used in determining center of mass position, a calculation which is assumed to average out at least some of the random error component of the individual point reconstructions. All of the lower

TABLE 5.8. Reconstructed segment length error relative to measured lengths for the left-hand side of the body.

Segment Type	n	RMSE [mm]	95%-ile [mm]	Max Error [mm]
Upper Arm	1085	29	64	89
Forearm	1085	15	32	49
Thigh	1085	7	14	37
Shank	1085	9	18	38
Hip Breadth	1085	9	18	38

body points, however, are used directly in the calculation of the various parameters of interest. Error in these reconstructions will therefore have a greater, more direct impact on the accuracy of the variables of interest than inaccuracies in the upper body reconstructions.

RELIABILITY OF THE PANNING DLT METHOD

Due to the very large digitization workload, reliability was not assessed through multiple digitizations of trials. Assessments using this method have been done in earlier works and it is assumed that a similar reliability was attained in this study. For instance, Müller et al. (1998) assessed inter-operator reliability by having one trial digitized by three different operators. He reported objectivity coefficients of equal to or better than 0.9 for the analyzed variables. Instead of multiple digitizations, measurement reliability in the current study was assessed indirectly through examining measurement variability and DLT optimization error.

MEASUREMENT VARIABILITY

Since each *non*-control point reconstruction was independently calibrated and reconstructed, the pooled standard deviation was taken as an indicator of measurement variability. *Non*-control point pooled standard deviations were 4, 5, and 2 mm in the X′-, Y′-, and Z′- dimensions, respectively (Table 5.9). Segment length pooled standard deviations ranged from 14 mm for the upper arm to 7 mm for the thigh segment. These are approximately equivalent to earlier field studies using similar methods (Klous, 2007; Lindinger, 2006).

DLT OPTIMIZATION ERROR

As a second, indirect assessment of measurement reliability, the DLT optimization error was calculated as described by Yeadon and King (1999) for all *non*-control point reconstructions and all target point reconstructions. Target point optimization error calculations are based on unfiltered, reconstructed object-space coordinates from the first to the third turn switch in all 12 trials.

It is important to note that the DLT optimization error is not the same as the reconstruction error and in certain situations can be very different. Rather, the DLT optimization error is a measure of how closely the camera rays come to intersecting in the object-space. This does not necessarily indicate how close their quasi-intersection is to the actual target point, however. The high-error reconstruction shown in Figure 5.19 is a good example of a reconstruction that would be expected to have a low DLT optimization error but a high reconstruction error. Conversely, it is also possible to have a high optimization error but a low reconstruction error if, for instance, the target point position were to be between the camera rays. So, for the purposes of this analysis, the optimization error is understood as a measure of how close the rays from each camera come to intersecting in space and thus a reflection of how well the digitizers

TABLE 5.9. Measurement variability in reconstructed *non*-control point positions and segment lengths.

	n	Pooled SD [mm]
Non CP Position		
X'	980	4
Y'	980	5
Z'	980	2
Segment Length		
Upper Arm	2170	14
Forearm	2170	13
Pole	2170	10
Thigh	2170	7
Shank	2170	8
Hip Breadth	1085	8
Ski Running Surface Length	2170	11

Note: X', Y', Z' refer to the course coordinate system dimensions

were able to identify the same 3-dimensional point from different 2-dimensional perspectives.

Results of the DLT optimization error calculations are summarized in Table 5.10. As might be expected, errors were higher for the more difficult to identify target points than for the readily digitized *non*-control points. The least consistent target points to digitize were the hip and ankle joint centers with RMSE's of 17 and 15 mm, respectively. The most consistent points were the pole tips with a RMSE of 6 mm. Surprisingly, the pole tips also had by far the largest maximum optimization errors, reaching in some cases as high as 10.6 cm. These highly inconsistent reconstructions represented a very small percentage of the total number of pole tip reconstructions, however, and may be due to the limited resolution of the selected camera synchronization method and the high frequency, high amplitude oscillations of the pole tip that sometimes occur when the pole impacts the gate.

TABLE 5.10. DLT optimization error for *non*-control point and target point reconstructions.

Point	n	RMSE [mm]	95%-ile [mm]	Max Error [mm]
Non CP	980	3	5	9
Head COM	1062	10	18	31
Shoulder Joint Center	2124	11	19	40
Elbow Joint Center	2124	10	18	34
Wrist Joint Center	2121	10	16	26
Hand COM	2116	8	13	27
Pole Tip	2124	6	9	106
Hip Joint Center	2124	17	27	39
Knee Joint Center	2115	10	18	44
Ankle Joint Center	2112	15	23	47
Ski Tip	2124	12	21	34
Ski Tail	2078	10	20	55

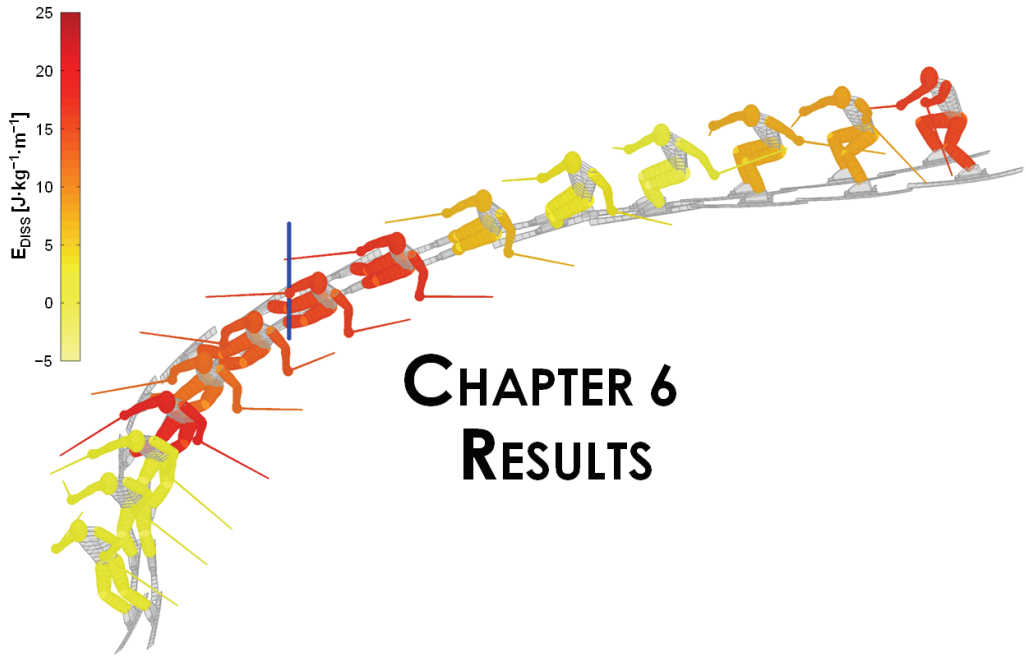

CHAPTER 6
RESULTS

CHAPTER 6. RESULTS

6.1 INTRODUCTION

This chapter presents the results of the kinematic, kinetic, and energetic analyses. To describe the general time-course of the various parameters over the turn cycle, ensemble averages and group descriptive statistics are presented. The ensemble average graphs show the group average as a bold line and the standard deviation as a white field against a gray background. The x-axis is time, normalized to turn cycle duration. The mean turn phase start and end points as well as the mean time point of gate passage are also indicated on these graphs. Unless otherwise specified, group descriptive statistics are reported as means ± standard deviations. To assist the reader in understanding the degree of variability, each skier's data are included in appendices to which the reader is periodically referred.

Course-to-course comparisons are shown using plots of interval means and standard deviations for each 10 % of the turn cycle for both courses. The p values for paired sample t-tests are given for each interval to help the reader gauge the magnitude of the mean difference relative to the extent of individual variability.

The first results to be presented provide a description of the skier and ski trajectories including the turn phase structure, trajectory length, speed, turn radius and the center

of mass angle of attack. This is followed by the results of ski orientation measures that include ski edge angle, ski attack angle, and local ski attack angles. Third, the results of skier lateral, vertical and fore/aft action parameters are presented. The results of external force calculations are then reported followed by the results of the energetic analysis. Finally, the results of the performance analyses are presented.

6.2 SKI AND SKIER TRAJECTORIES (Figure 2.1, Boxes F and G)

TURN CYCLE STRUCTURE

Turn cycle descriptive statistics are summarized in Figure 6.1. The mean turn cycle durations (± standard deviation) were 0.83 ± 0.03 and 0.94 ± 0.03 s for the 10 and 13 m courses, respectively. While the Turn Phase accounted for about 49 % of the turn cycle on both courses, the Initiation Phase represented on average 5.7 % more of the turn cycle on the 13 m course. This translated to the Completion Phase being on average 5.4 % shorter on the 13 m course. In addition, gate passage occurred later in the turn cycle on the 13 m course (52.8 ± 3.5 % versus 59.4 ± 3.2 % for the 10 and 13 m courses, respectively).

TRAJECTORY LENGTH

Descriptive statistics for ski and center of mass trajectory lengths are given in Table 6.1. On both courses, the outside ski trajectory was longer than that of the center of mass, and this difference was greater on the 13 m course.

SPEED

Figures 6.2 and 6.3 present the center of mass and outside ski speed ensemble averages, respectively. Descriptive statistics are reported in Tables G.1 and G.2 in Appendix G.

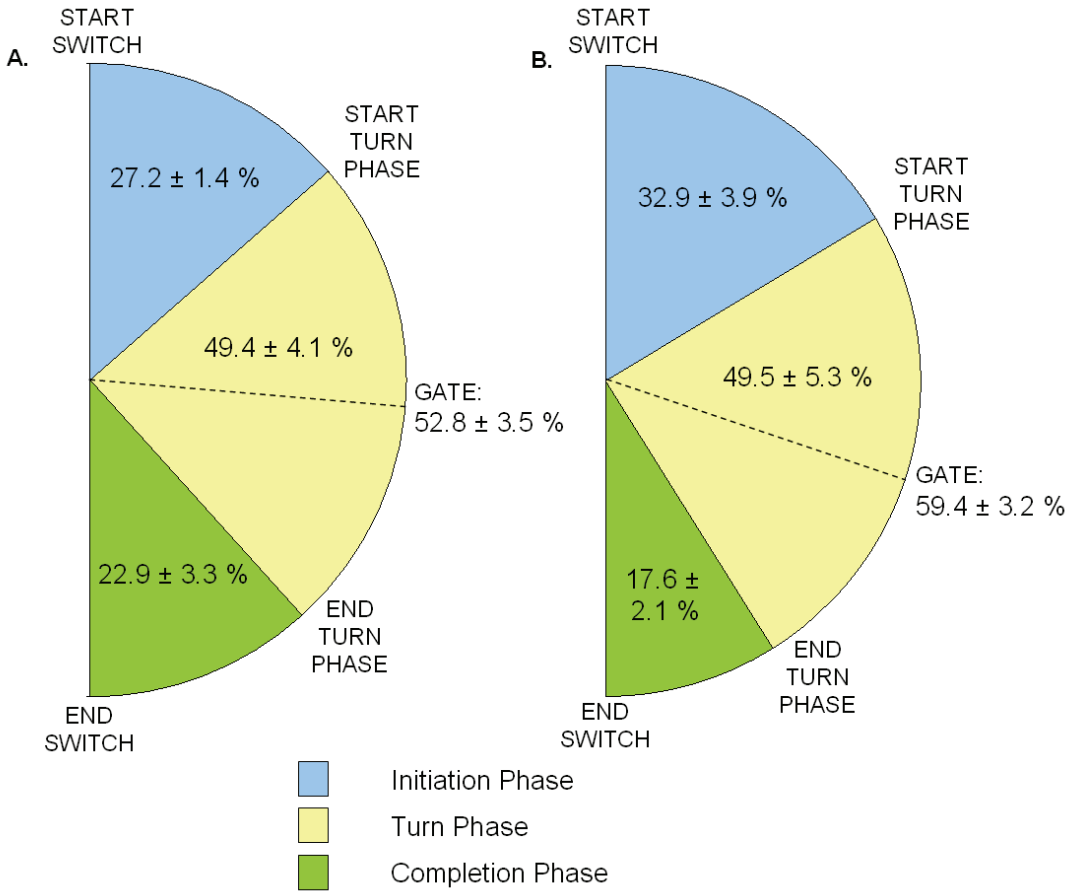

FIGURE 6.1. Turn cycle structure on the 10 m (A) and the 13 m (B) courses.

TABLE 6.1. Trajectory length descriptive statistics. Values are group means ± standard deviations.

		10 m Course	13 m Course
Center of Mass			
L_XYZ	[m]	19.99 ± 0.13	26.13 ± 0.13
L_Y	[m]	5.49 ± 0.37	7.78 ± 0.30
L_Z	[m]	1.08 ± 0.06	1.24 ± 0.06
Outside Ski			
L_XYZ	[m]	21.07 ± 0.23	27.44 ± 0.21
L_Y	[m]	8.01 ± 0.44	10.47 ± 0.28

n = 6

Both the center of mass and outside ski speed showed clear cyclic patterns associated with the turn cycle on both courses, although these patterns were shifted in time.

On the 10 m course, the center of mass increased speed through the Initiation Phase, reaching maximal speeds at on average 32.9 ± 3.5 % of the turn cycle, close to the start of the Turn Phase. The center of mass subsequently slowed down reaching a minimum speed at an average of 73.3 ± 3.7 % of the turn cycle, just prior to the end of the Turn Phase. Finally, the center of mass began picking up speed again through the Completion Phase of the turn. Outside ski speed, on the other hand, gradually increased throughout the Initiation Phase and the first portion of the Turn Phase, reaching maximal speeds at, on average, 48.8 ± 8.9 % of the turn cycle, or shortly prior to passage of the gate. Ski speed then slowed, matching center of mass speed at the turn end Switch.

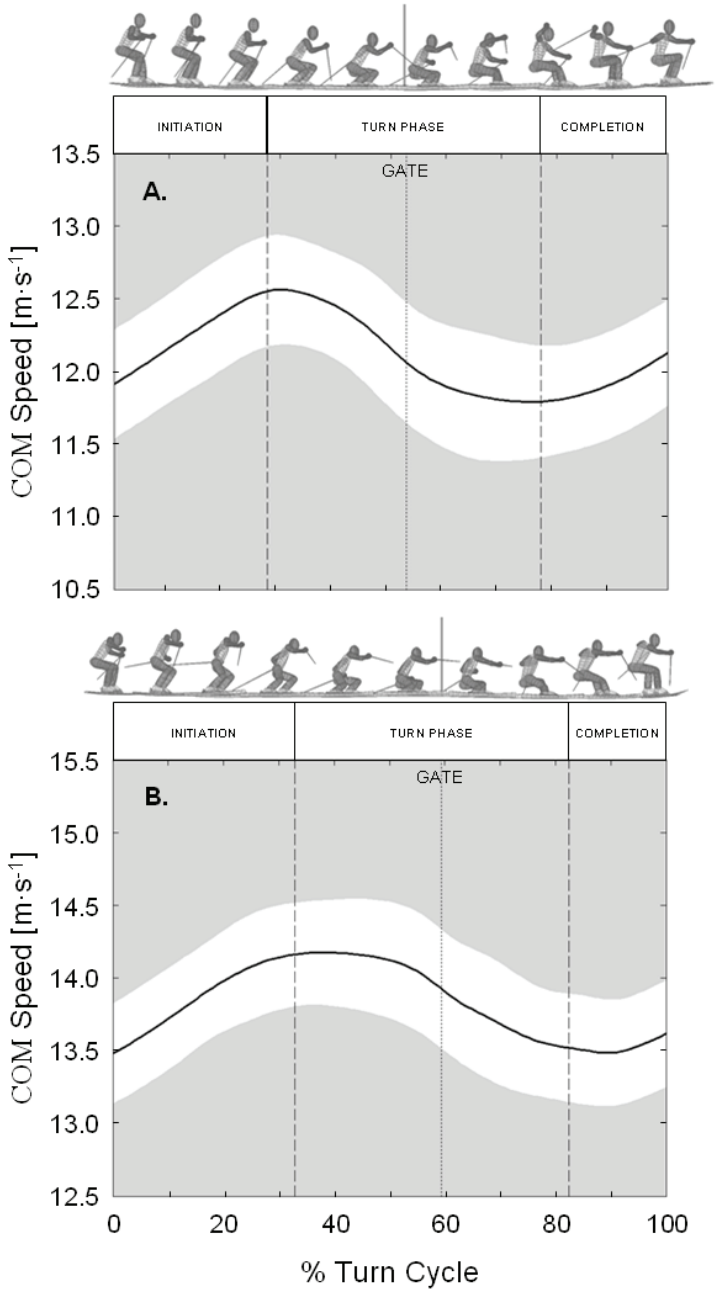

FIGURE 6.2. Ensemble average (± standard deviation) center of mass speed over the turn cycle on the 10 m course (A) and the 13 m course (B).

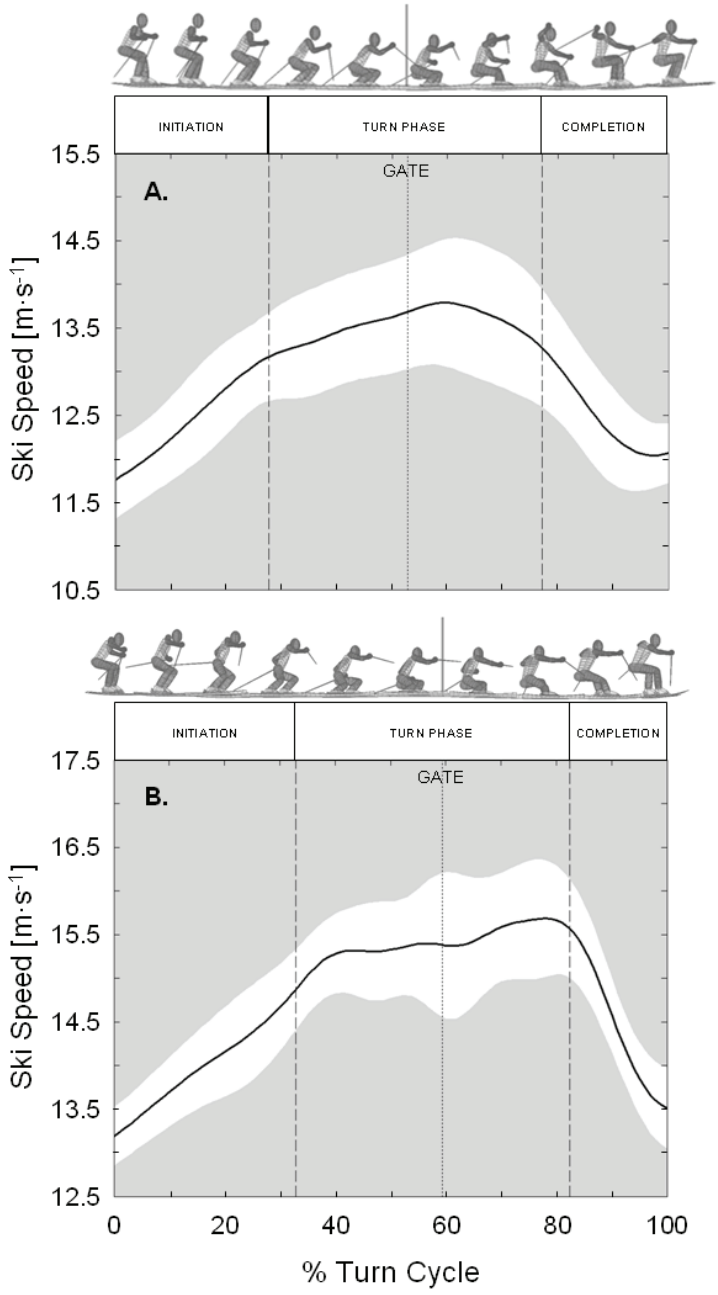

FIGURE 6.3. Ensemble average (± standard deviation) outside ski speed over the turn cycle on the 10 m course (A) and the 13 m course (B).

On the 13 m course, the center of mass speed increased through the Initiation Phase and well into the Turn Phase, reaching maximal speeds at 37.1 ± 6.6 % of the turn cycle, on average. Center of mass speed then slowed reaching a minimum speed at 88.8 ± 2.5 % of the turn cycle. Finally, center of mass speed increased again through the Completion Phase of the turn, similar to on the 10 m course. Also in a pattern similar to the 10 m course, outside ski speed increased throughout the Initiation Phase and the start of the Turn Phase. However, different from the 10 m course, outside ski speed continued to increase well past passage of the gate and into the latter portion of the Turn Phase with maximum speeds being registered at on average 71.3 ± 11.0 % of the turn cycle. Ski speed then rapidly slowed to approach center of mass speeds by the turn end Switch.

On average, the outside ski travelled at 0.86 and 0.93 $m \cdot s^{-1}$ faster than the center of mass on the 10 and 13 m courses, respectively. Comparisons between center of mass speed and outside ski speed over each 10 % of the turn cycle are made in Figures 6.4 for both the 10 and 13 m courses. On both courses, outside ski speed was similar to center of mass speed at the turn Switches. However, ski speed was substantially higher than center of mass speed in the Turn and Completion Phases. On the 10 m course, the largest differences were seen during the 60 to 70 % turn cycle interval where the skis had on average 1.86 $m \cdot s^{-1}$ higher speed than the center of mass. The largest differences on the 13 m course were registered during the 70 to 80 % interval of the turn cycle where the skis had on average 2.05 $m \cdot s^{-1}$ higher speed than the center of mass.

Peak-to-peak amplitudes in the center of mass speed fluctuations averaged 0.98 ± 0.13 $m \cdot s^{-1}$ and 0.87 ± 0.09 $m \cdot s^{-1}$ on the 10 and 13 m courses, respectively. Peak-to-peak amplitudes in outside ski speed were higher than the center of mass fluctuations on both courses (2.54 ± 0.39 $m \cdot s^{-1}$ and 3.00 ± 0.38 $m \cdot s^{-1}$ on the 10 and 13 m courses, respectively).

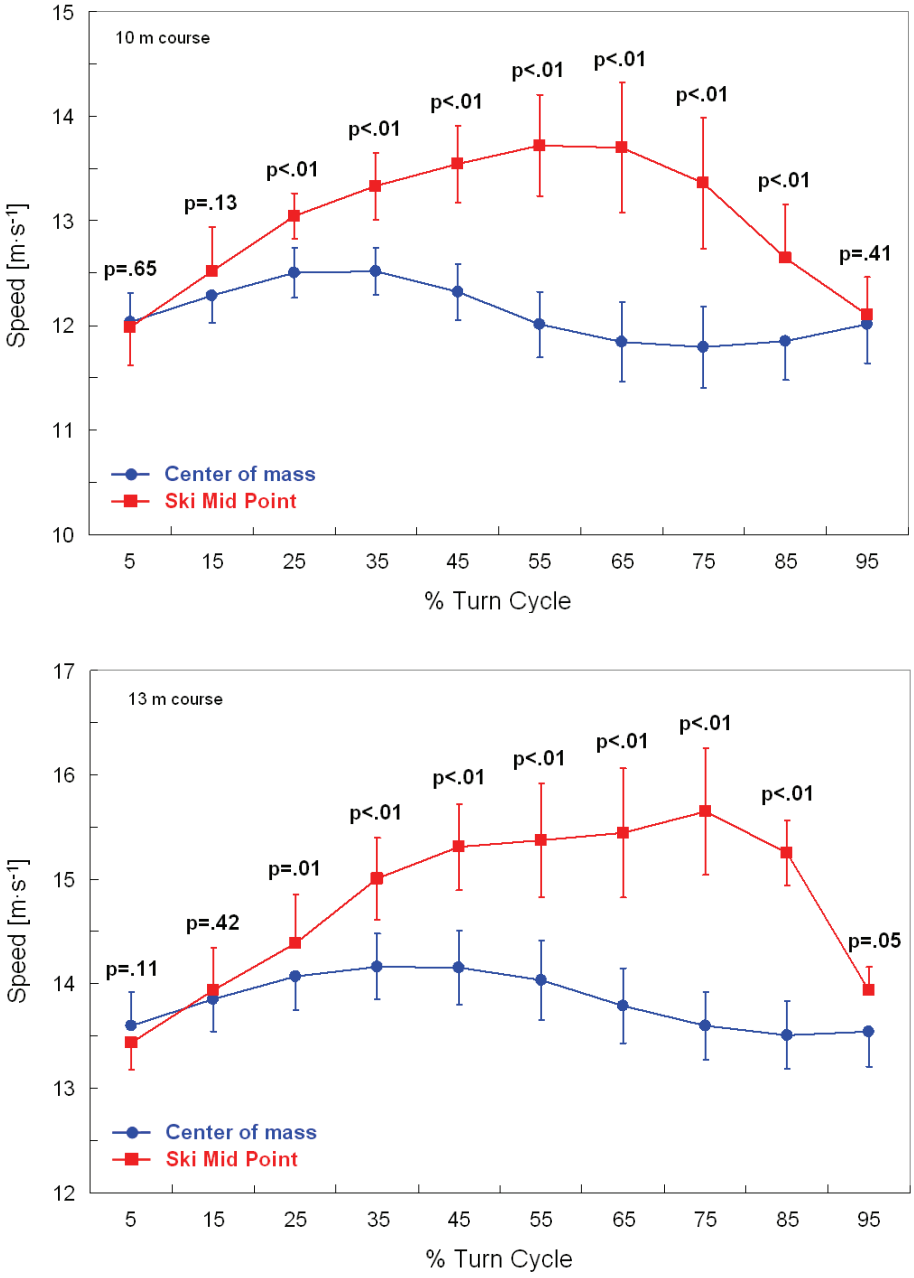

FIGURE 6.4. Outside ski versus center of mass speed over the turn cycle for the 10 and 13 m courses. Probability values are based on paired-sample t tests.

TURN RADIUS

Figures showing the center of mass turn radius (R_{COM}) and outside ski turn radius (R_{SKI}) ensemble averages are not reported due to the large variability in turn radius measures as values approached infinity around turn transitions. However, turn radius descriptive statistics are given in Table G.3 in Appendix G and a selection of individual data sets is presented in Figure 6.5. In addition, course-to-course comparisons of R_{COM} and R_{SKI} for each 10 % interval of the turn cycle are given in Figure 6.6.

Mean R_{COM} in the Turn Phase on the 10 and 13 m courses was 8.75 ± 0.36 and 9.93 ± 0.45 m, respectively. The average minimum turn radius on the 10 m course was 5.43 ± 0.33 m and occurred at 53.3 ± 6.6 % of the turn cycle, or at approximately gate passage. On the 13 m course, the average minimum turn radius was greater at 6.48 ± 0.36 m and occurred just after gate passage, at on average 63.8 ± 5.9 % of the turn cycle.

Mean R_{SKI} during the Turn Phase was also longer on the 13 m course (10.58 ± 3.03 m on the 13 m course versus 7.14 ± 0.37 m on the 10 m course). Minimum outside ski turn radius on the 10 m course was 3.96 ± 0.23 m and occurred at 57.7 ± 6.7 % of the turn cycle, on average. On the 13 m course, the average minimum outside ski turn radius was 4.94 ± 0.59 m and occurred at 69.4 ± 4.7 % of the turn cycle. In contrast to the 10 m course, fluctuations in the outside ski turn radius were common during the Turn Phase on the 13 m course (Figure 6.5, E – H). These fluctuations are part of the reason the mean turn radius in the Turn Phase is so much higher on the 13 m course.

Comparisons between R_{COM} and R_{SKI} for each 10 % interval of the turn cycle are shown in Figure 6.7 for the 10 and 13 m courses. On both courses, the ski began turning before, and ended turning after, the center of mass. During the middle of the Turn Phase there was a period of time where both the center of mass and outside ski turned at approximately the same turn radius. To help visualize this, individual graphics were

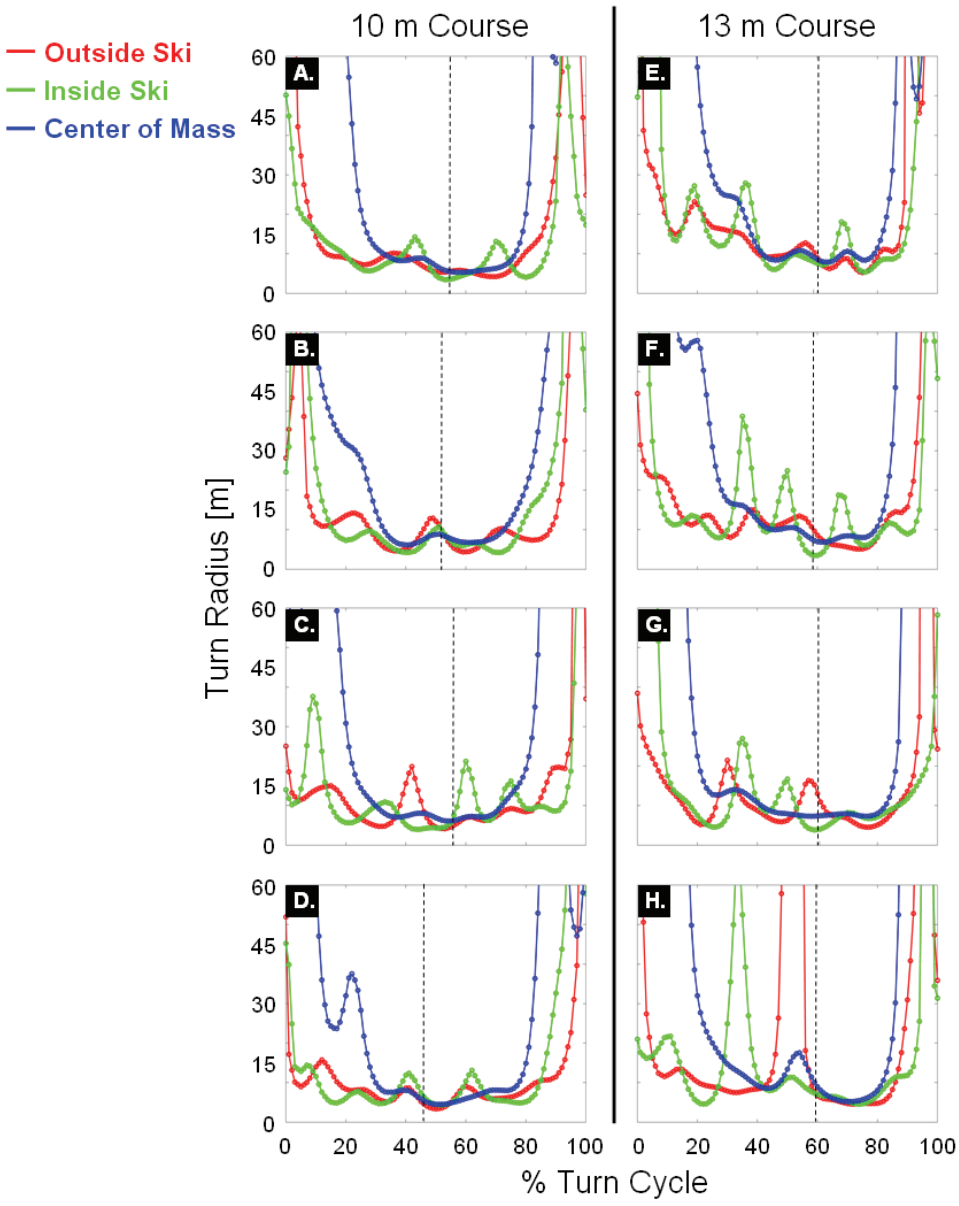

FIGURE 6.5. Example individual inside ski, outside ski, and center of mass turn radius over the turn cycle.

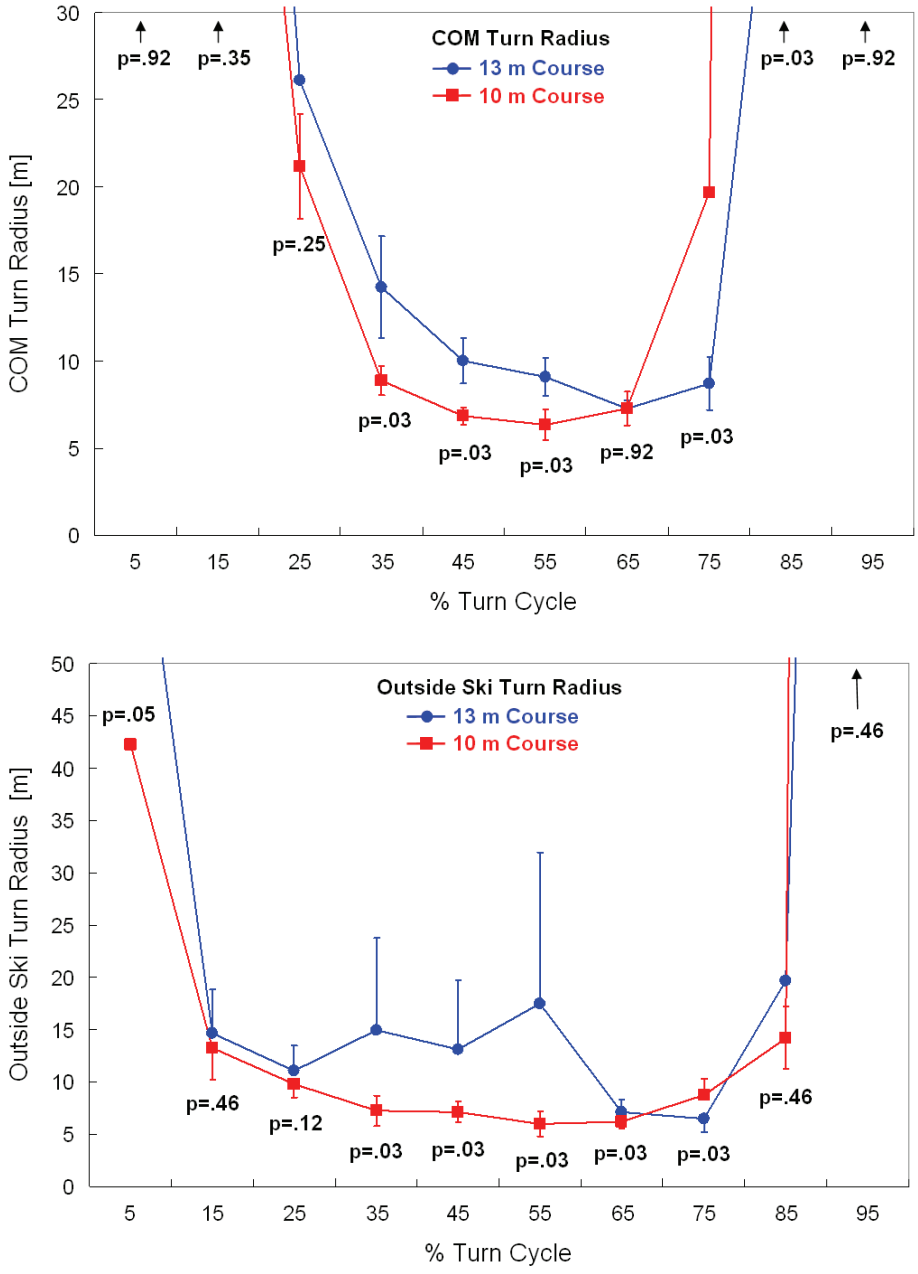

FIGURE 6.6. Course-to-course comparisons of center of mass turn radius (upper graph) and outside ski turn radius (lower graph). Probability values are based on Wilcoxon Signed Ranks tests.

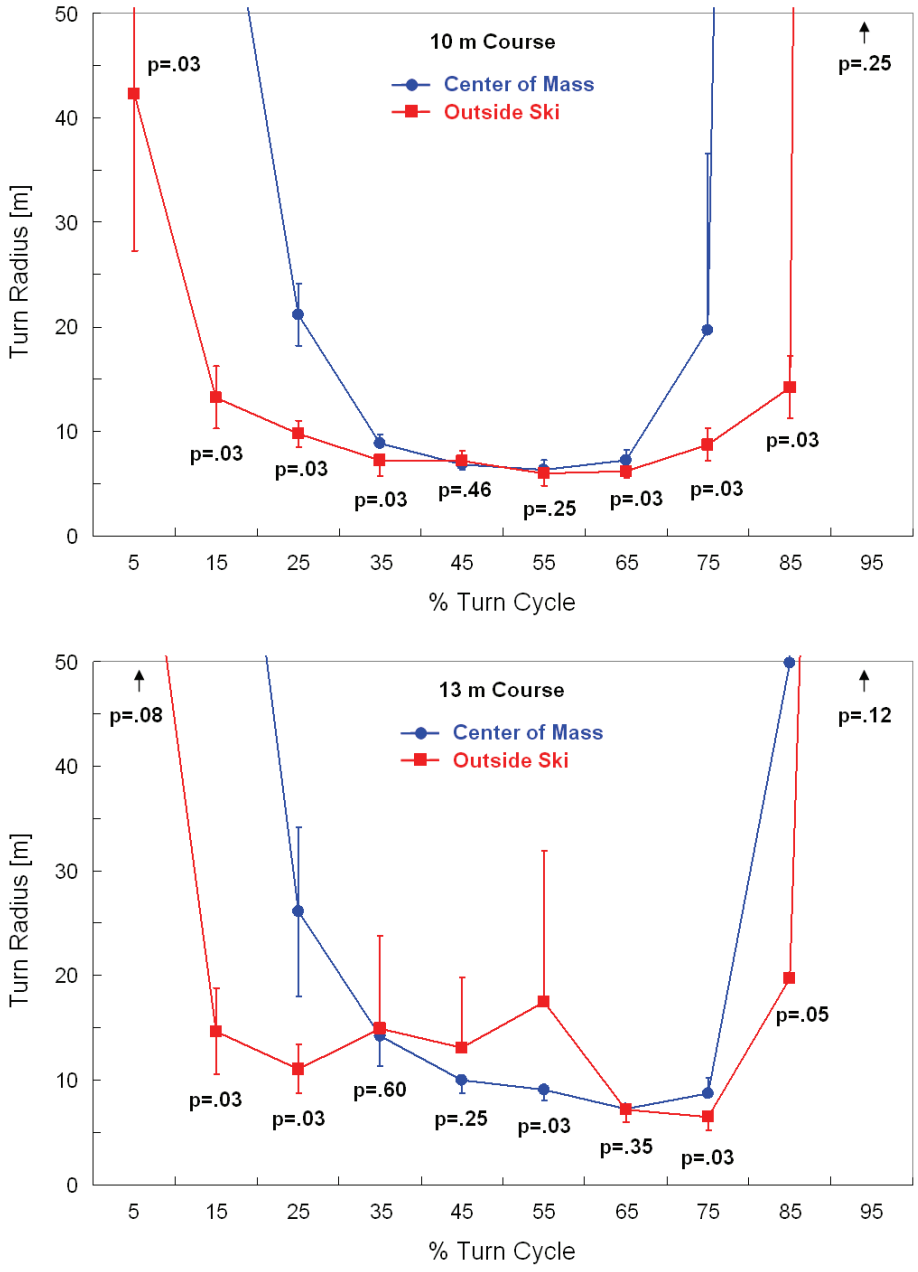

FIGURE 6.7. Comparisons between center of mass and outside ski turn radius for the 10 m course (upper graphic) and the 13 m course (lower graphic). Probability values are based on Wilcoxon Signed Ranks tests.

generated showing the center of mass and outside ski trajectories colored according to the trajectory turn radius (Appendix H).

CENTER OF MASS ATTACK ANGLE

The ensemble average center of mass attack angles (λ) for both courses are presented in Figure 6.8 and descriptive statistics are reported in Table G.4 in Appendix G. As a reminder, negative attack angles indicate that the center of mass velocity vector $\dot{\vec{P}}_{COM}$ is directed more towards the center of the turn than the outside ski longitudinal axis. Conversely, positive attack angles indicate that $\dot{\vec{P}}_{COM}$ is directed more to the outside of the turn than the ski.

With some turns being carved, and some skidded, there was a great deal of variability in the center of mass attack angle measurements, particularly in the first half of the turn cycle. At the start Switch, center of mass attack angles relative to the new outside ski were –10.9 ± 2.4° and –12.9 ± 2.8° on the 10 and 13 m courses, respectively. On the 10 m course, the center of mass attack increased rapidly in the Initiation Phase, crossing zero degrees at 21.4 ± 7.1 % of the turn cycle. Nine out of the 12 analyzed turns demonstrated an initial maximum attack angle of on average 15.3 ± 5.2° at 38.4 ± 4.5 % of the turn cycle, before leveling off during the remainder of the turn phase at about 8 degrees. The remaining 3 turns were characterized by a continual, steady increase in attack angle throughout the Turn Phase. During the Completion Phase on the 10 m course, the center of mass attack angle increased further reaching a second maximum of 16.2 ± 1.3° at 93.1 ± 3.5 % of the turn cycle. Finally, the center of mass attack angle reduced slightly to an average of 13.9 ± 2.3° by the turn end Switch as the skis were redirected for the following turn.

A similar time-course was seen on the 13 m course, with a rapid increase in center of mass attack angle during the Initiation Phase, crossing zero degrees at 23.2 ± 8.4 % of the turn cycle and reaching an initial maximum of 9.8 ± 4.0° at 39.9 ± 10.2 % of the turn

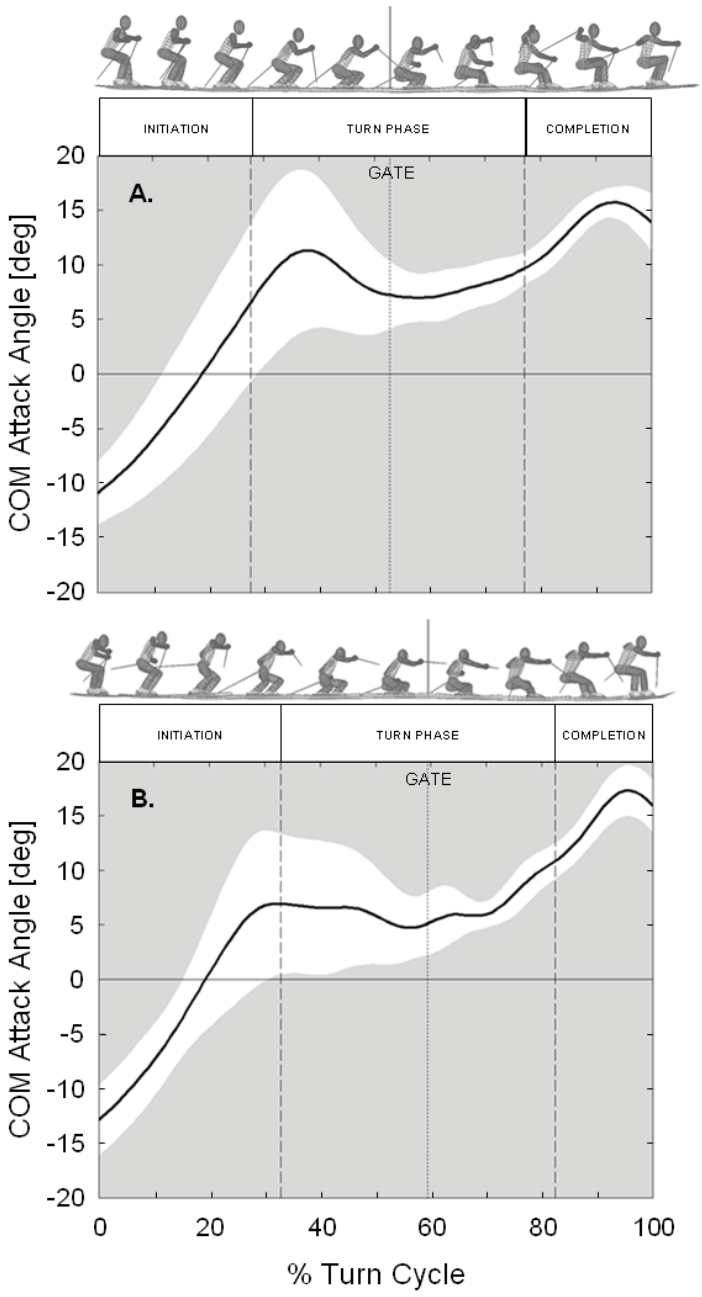

FIGURE 6.8. Ensemble average (± standard deviation) center of mass attack angle (λ) over the turn cycle on the 10 m course (A) and the 13 m course (B).

cycle on 9 of the 12 analyzed turns. During much of the Turn Phase, the center of mass attack angle was stable at about 6°, slightly lower than on the 10 m course. During the latter portion of the Turn Phase, the center of mass attack angle increased further, reaching a new maximum of 17.5 ± 2.3° at 95.4 ± 2.2 % of the turn cycle. Finally, center of mass attack angle decreased to 15.9 ± 2.1° by the end turn Switch.

Course-to-course differences in center of mass attack angle for each 10 % interval of the turn cycle are presented in Figure 6.9. During the Turn Phase, the center of mass attack angle was larger on the 10 m course, particularly over the interval from 30 to 40 % of the turn cycle where the mean difference was 3.6°. Individual turn graphs showing the center of mass attack angle are presented in Appendix I.

6.3 SKI ORIENTATION (Figure 2.1, Box D)

OUTSIDE SKI EDGE ANGLE

The outside ski edge angle (θ) ensemble averages are presented in Figure 6.10 and descriptive statistics are listed in Table G.5 of Appendix G. At the start Switch of the turn cycle, the new outside ski was already slightly edged to on average 5.1 ± 4.6° and 4.5 ± 5.1° on the 10 and 13 m courses, respectively. On the 10 m course, edge angle progressively increased through the Initiation Phase and the first portion of the Turn Phase, reaching an average maximum angle of 65.7 ± 1.7° at 58.0 ± 4.1 % of the turn cycle, or just after gate passage. On the 13 m course, there was an initial rapid rise in edge angle during initiation followed by a period of more gradual increase, reaching maximum angles of 70.2 ± 1.3° at approximately gate passage. Edge angle then declined rapidly on both courses during the latter portion of the Turn Phase and the Completion Phase. At the end of the turn, the old outside ski was on average still slightly edged at 4.7 ± 4.4° and 6.3 ± 5.5° for the 10 and 13 m courses, respectively.

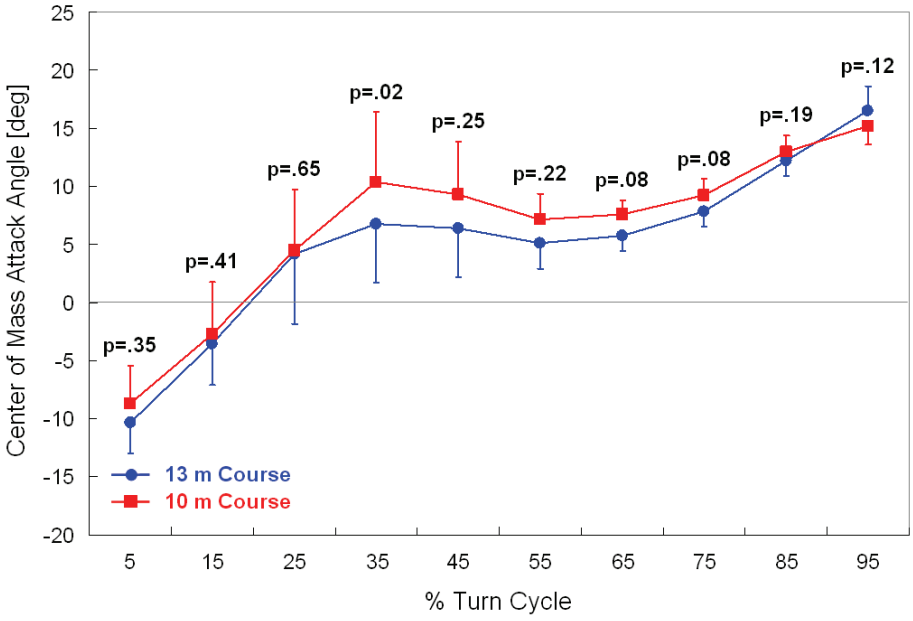

FIGURE 6.9. Course-to-course comparisons of center of mass attack angle (λ). Probability values are based on paired-sample t tests.

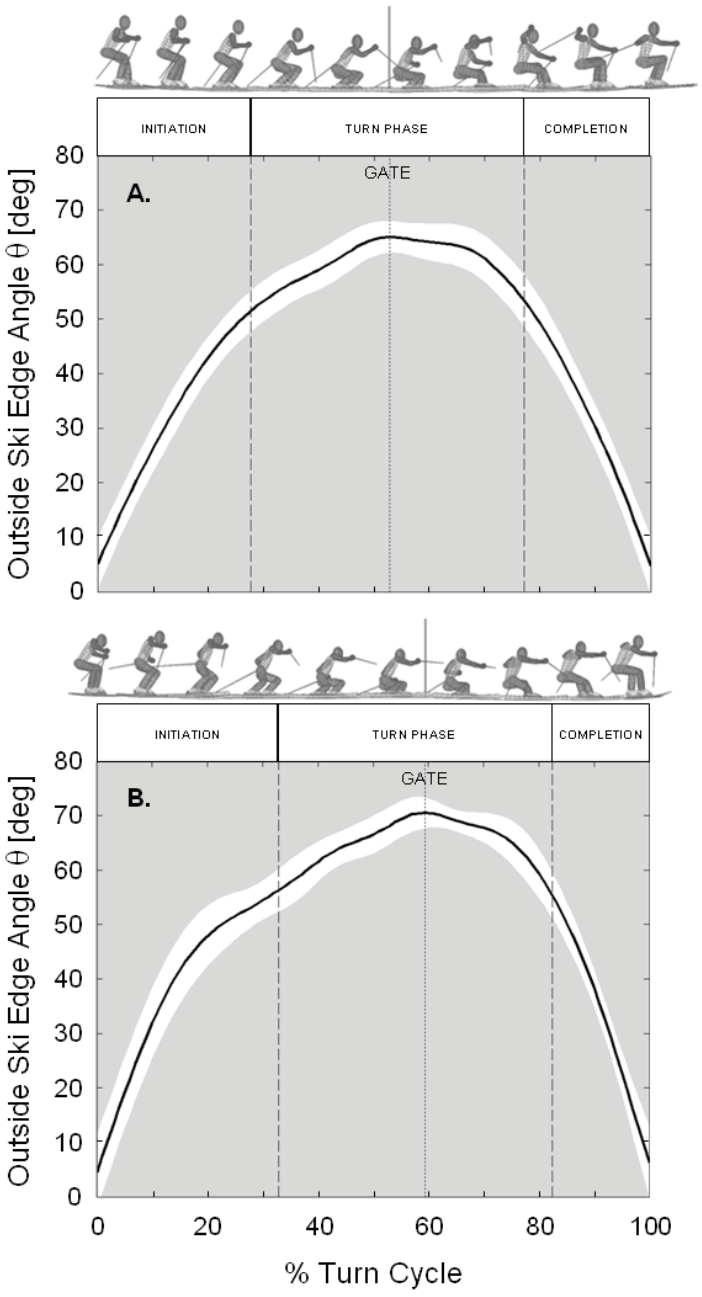

FIGURE 6.10. Ensemble average (± standard deviation) outside ski edge angle over the turn cycle on the 10 m course (A.) and the 13 m course (B.).

Course-to-course differences in outside ski edge angle at each 10 % interval of the turn cycle are summarized in Figure 6.11. Edge angles were slightly larger on the 13 m course throughout the turn cycle, but in particular in the latter half of the Turn Phase and the Completion Phase where average differences ranged from 4° to 9°.

OUTSIDE SKI ATTACK ANGLE

The outside ski attack angle (φ) ensemble averages from both courses are shown in Figure 6.12 and descriptive statistics are summarized in Table G.6 in Appendix G. Similar to the center of mass attack angle, positive ski attack angles indicate that the ski middle point velocity vector is directed more to the outside of the turn than the ski longitudinal axis.

At the start switch, the outside ski had on average a positive attack angle of 3.1 ± 2.4° and 0.5 ± 2.4° on the 10 and 13 m courses, respectively, indicating that the skis were already being oriented for the upcoming turn prior to the switch. Attack angles rose rapidly during the Initiation Phase reaching average maximums of 15.1 ± 5.3° and 12.1 ± 4.9° for the 10 and 13 m courses, respectively, by the start of the Turn Phase. There was, however, a substantial amount of variation on both courses during this part of the turn with some turns being carved and some skidded. Attack angles on both courses were then rapidly reduced during the first part of the Turn Phase, prior to gate passage. The remainder of the Turn Phase and the Completion Phase were then completed with attack angles for the most part less than 4°.

Course-to-course differences in outside ski attack angle for each 10 % interval of the turn cycle are shown in Figure 6.13. During the first half of the turn cycle, attack angles were greater on the 10 m course, in particular from 10 to 45 % of the turn cycle, indicating that there was a greater degree of skidding used on the 10 m course, on average. In addition, attack angles were lower (and negative) on the 10 meter course during the last 10 % of the turn cycle, showing that at this point the skis were already

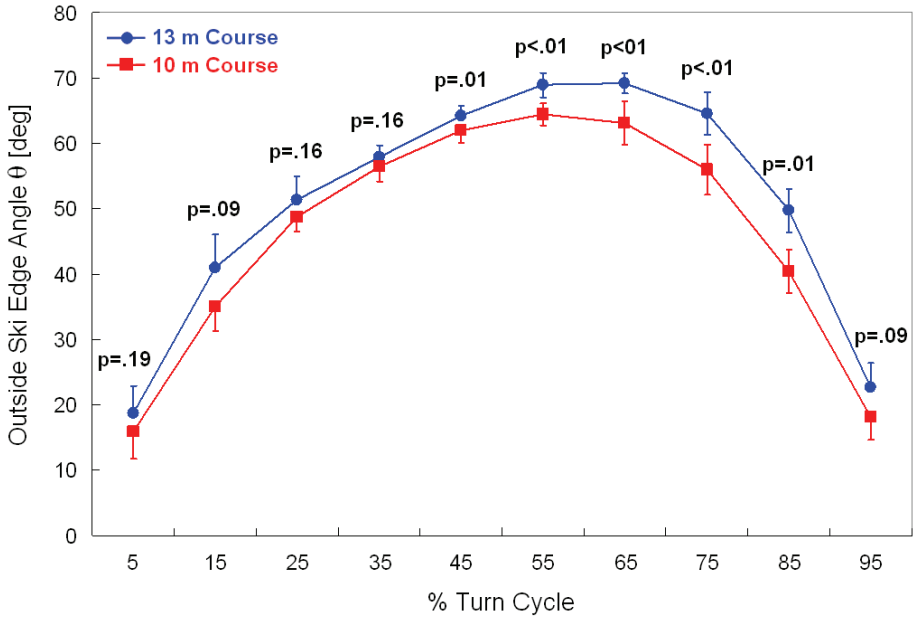

FIGURE 6.11. Course-to-course comparisons of outside ski edge angle. Probability values are based on paired-sample t tests (n = 6).

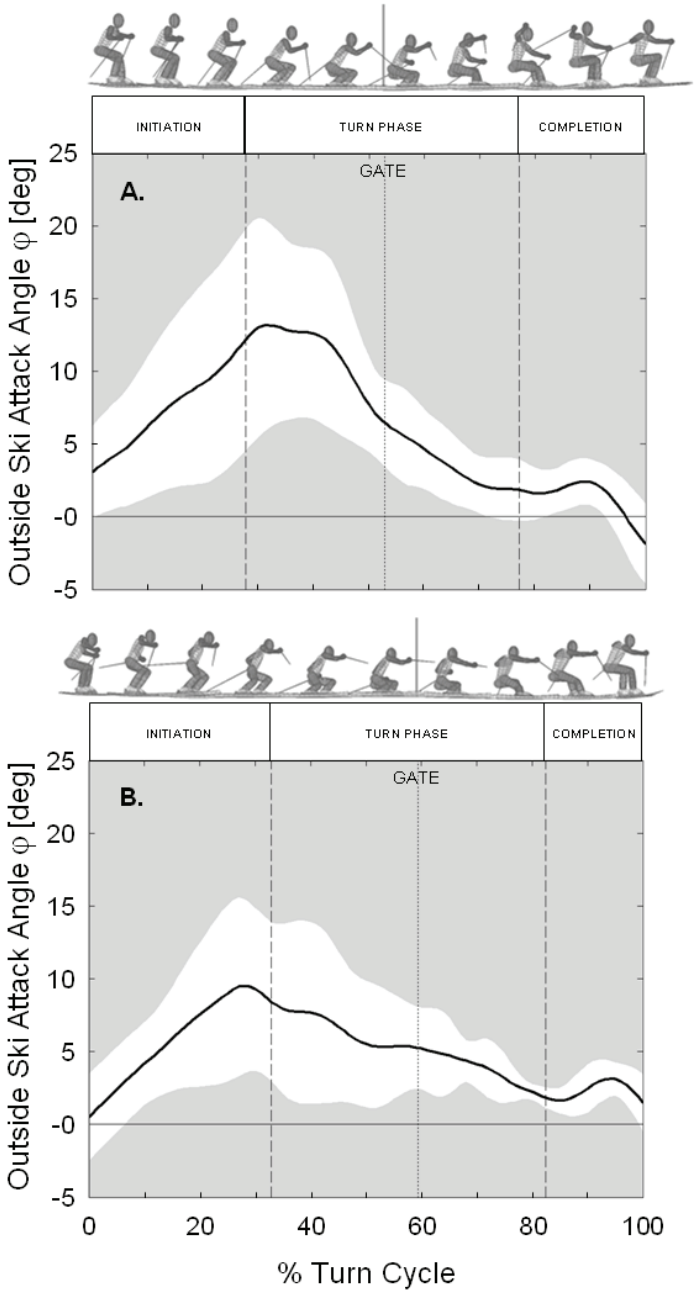

FIGURE 6.12. Ensemble average (± standard deviation) outside ski attack angle over the turn cycle on the 10 m course (A) and the 13 m course (B).

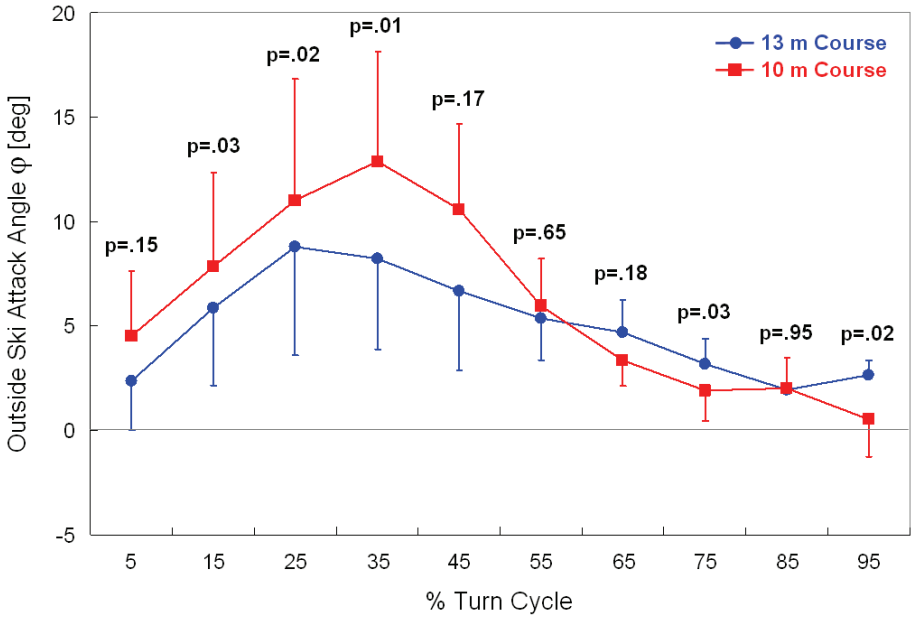

FIGURE 6.13. Course-to-course comparisons of outside ski attack angle. Probability values are based on paired-sample t tests (n = 6).

being oriented for the up-coming turn. Graphs showing individual approaches to ski edge and attack angles are shown in Appendix J.

LOCAL SKI ATTACK ANGLE

Figure 6.14 shows the local ski attack angle (φ_E) data averaged according to whole ski attack angle (φ) for the Turn Phase of the turn cycle. The coloring in the graph is indicative of the size of the local attack angle with bright colors indicating large attack angles and black indicating an attack angle of less than or equal to 0^o. To help the reader visualize the meaning the local attack angle data, sample graphics were generated showing ski edge point trajectories during the transition from skidding to carving. The red and blue lines indicate ski forebody and rearbody point trajectories, respectively.

At high ski attack angles (the top of the graphic), each point along the ski traced its own trajectory across the snow surface and points along the ski's forebody had larger local attack angles than points along the rear part of the ski. As skis transitioned into carving and the whole ski attack angle was reduced (moving down along the Y-axis of the graphic), local attack angles were reduced across the length of the ski and aftbody points reached very low attack angles, indicating that they followed in the trace of points in front of them. However, even at the highest degree of carving (at the bottom of the graphic), there was still a gradient in the local attack angles with forebody points having slightly positive angles. This can be seen in the example ski graphic where the red lines are still tracing independent trajectories.

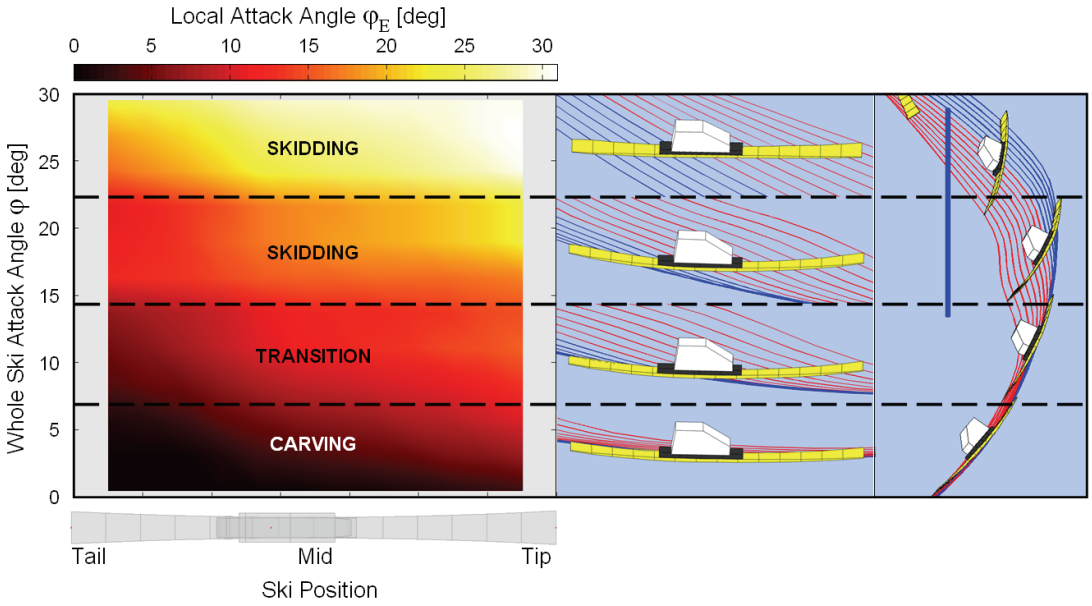

FIGURE 6.14. Mean local ski attack angle for the Turn Phase averaged across whole ski attack angle (left panel). An example ski making the transition from skidding to carving through a turn is shown in the right panels. Red and blue lines indicate ski forebody and ski aftbody trajectories, respectively.

6.4 SKIER ACTIONS (Figure 2.1, Box H)

LATERAL ACTIONS

CENTER OF MASS INCLINATION

The center of mass inclination angle (ς) ensemble averages are presented Figure 6.15 and descriptive statistics are given in Table G.7 in Appendix G. During the Initiation Phase, the center of mass rapidly inclined to the inside of the turn reaching a maximum inclination angle of 49.9 ± 1.0° just prior to gate passage on the 10 m course. On the 13 m course, the center of mass inclined rapidly during the first portion of the Initiation Phase before going into period of more gradual increase and finally reaching a maximum inclination of 56.2 ± 1.5° just prior to gate passage. After the gate, center of mass inclination was rapidly reduced on both courses, reaching zero values at the Switch.

Figure 6.16 shows the course-to-course differences in center of mass inclination angles for each 10 % of the turn cycle. The center of mass was more inclined on the 13 m course throughout the turn cycle, with the exception of turn transitions where inclination angles approached zero by definition. Differences were particularly large during the latter portion of the Turn Phase where inclination angles were on average between 7° and 9° greater on the 13 m course.

HIP ANGULATION

Figure 6.17 shows the ensemble average hip angulation angles (κ) for both courses. Table G.8 in Appendix G summarizes hip angulation descriptive statistics. Positive angles indicate that hip angulation contributed towards increasing the ski edge angle while negative angles indicate that hip angulation acted to reduce the ski edge angle.

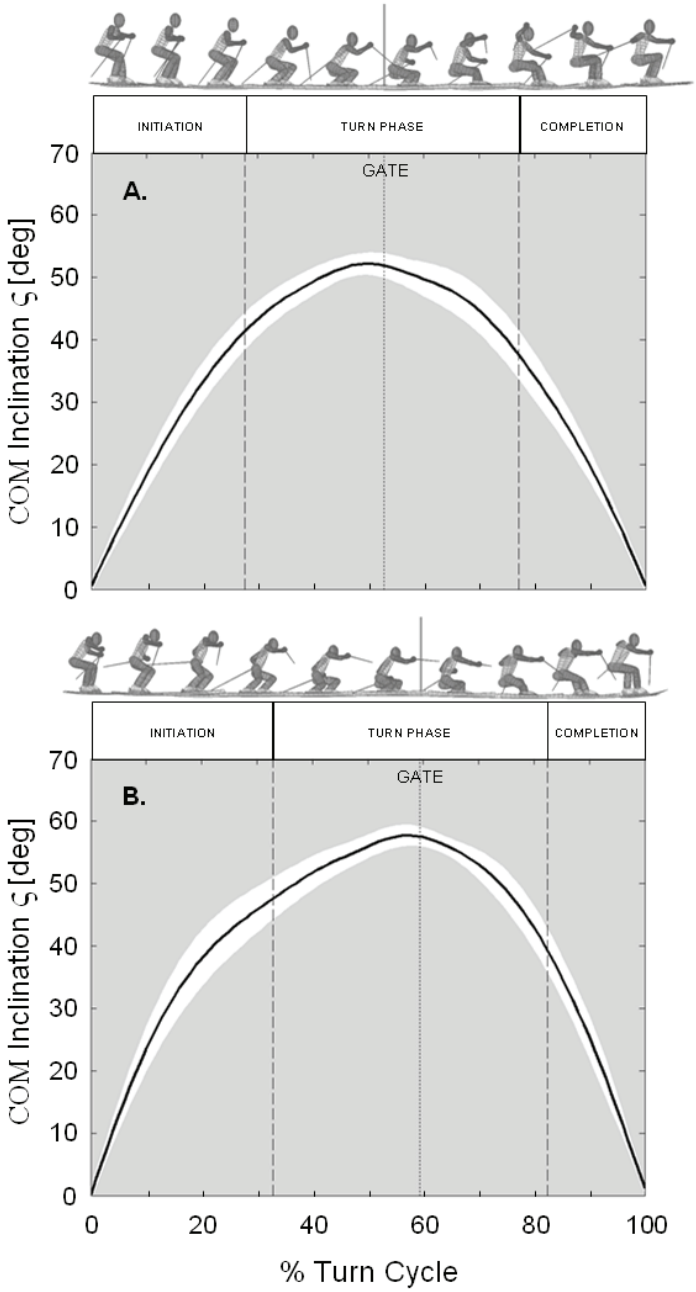

FIGURE 6.15. Ensemble average (± standard deviation) center of mass inclination over the turn cycle on the 10 m course (A) and the 13 m course (B).

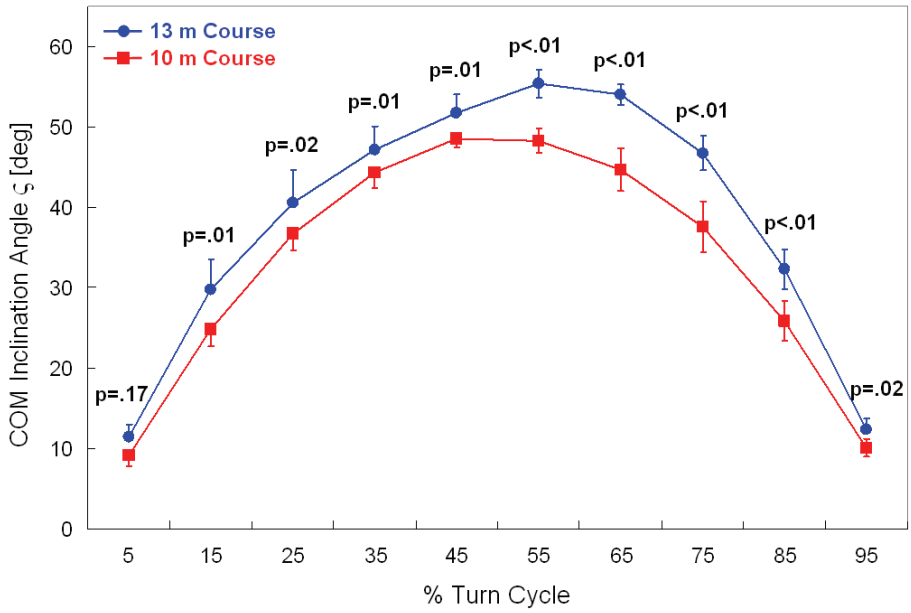

FIGURE 6.16. Course-to-course comparisons of center of mass inclination angle. Probability values are based on paired-sample t tests (n = 6).

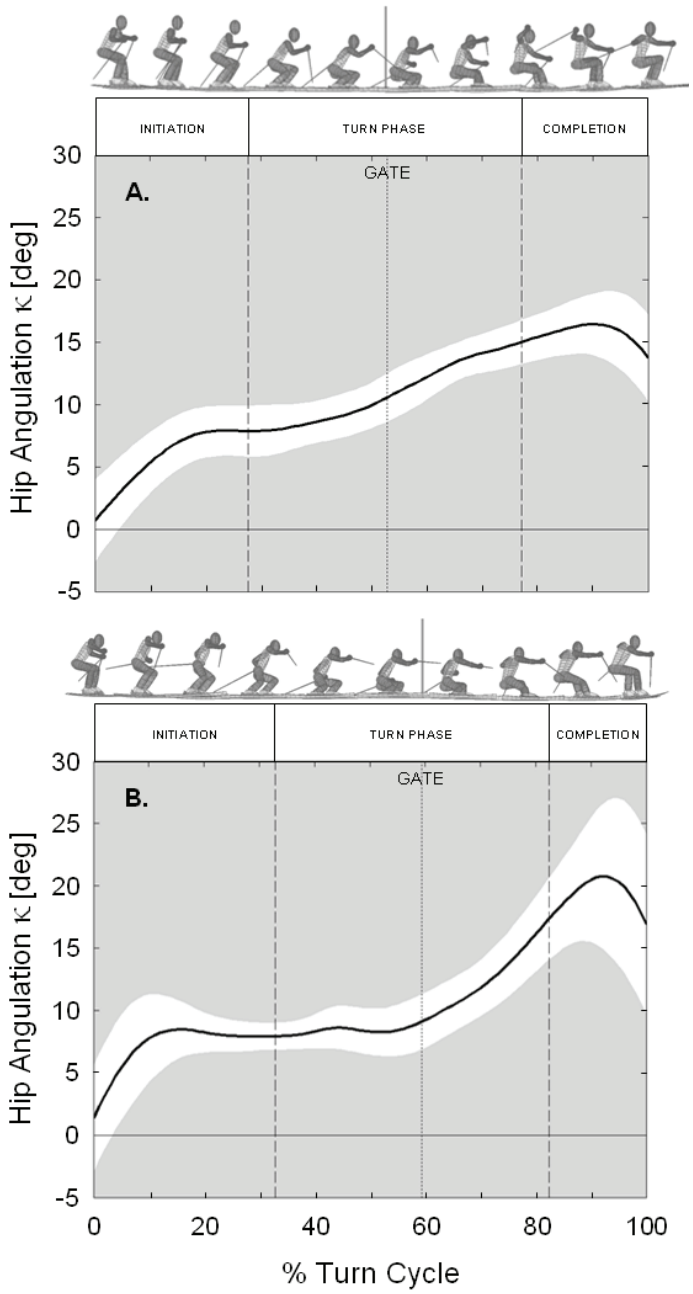

FIGURE 6.17. Ensemble average (± standard deviation) hip angulation over the turn cycle on the 10 m course (A) and the 13 m course (B).

For the first 15 to 20 % of the turn cycle, hip angulation angle increased on both courses, stabilizing at between 5° and 10° in the latter portion of the Initiation Phase. On the 10 m course, hip angulation continued to increase starting in the first part of the Turn Phase, reaching a maximum of 17.1 ± 1.9° at 88.8 ± 4.4 % of the turn cycle. On the 13 m course, the increase in hip angulation did not start until approximately gate passage, after which there was a relatively rapid increase, reaching a maximum angle of 21.6 ± 5.6° by 91.3 ± 2.2 % of the turn cycle.

Course-to-course differences in hip angulation angles for each 10 % interval of the turn cycle are shown in Figure 6.18. Initially, hip angulation was slightly greater on the 13 m course, although differences were small relative to the individual variability. During the phase of the turn where hip angulation was relatively stable, there were no course-to-course differences. Due to the earlier secondary increase, hip angulation was on average 2° to 3° greater on the 10 m course from 40 to 70 % of the turn cycle. Once the rapid increase in hip angulation was initiated on the 13 m course, values quickly exceeded those on the 10 m course during the Completion Phase, although differences were small relative to individual variability. The highest individual variability occurred at the turn transitions and was greater on the 13 m course compared to the 10 m course.

KNEE ANGULATION

Knee angulation angle (η) descriptives are presented in Table G.9 in Appendix G and ensemble averages for both courses are shown in Figure 6.19. Positive angles indicate that knee angulation contributed towards increasing the ski edge angle while negative angles indicate that knee angulation acted to reduce the ski edge angle.

By the turn start Switch, the knee angulation of the outside leg was already close to maximal values at 4.0 ± 3.3° and 3.1 ± 1.9° for the 10 and 13 m courses, respectively. Knee angulation remained relatively constant through most of the turn until almost the start of the Completion Phase. Maximal angles of 7.5 ± 1.9° and 6.7 ± 0.8° were reached

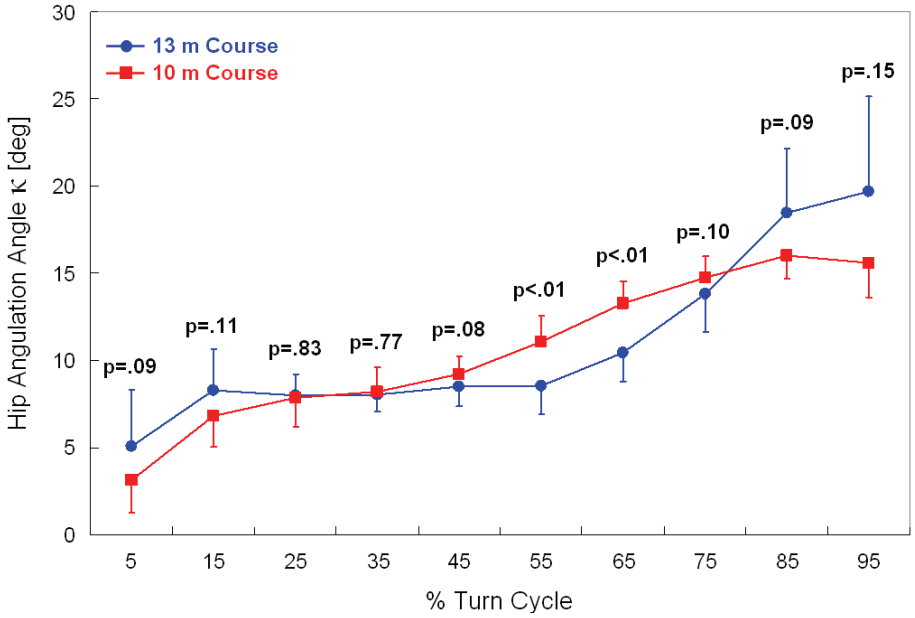

FIGURE 6.18. Course-to-course comparisons of hip angulation. Probability values are based on paired-sample t tests (n = 6).

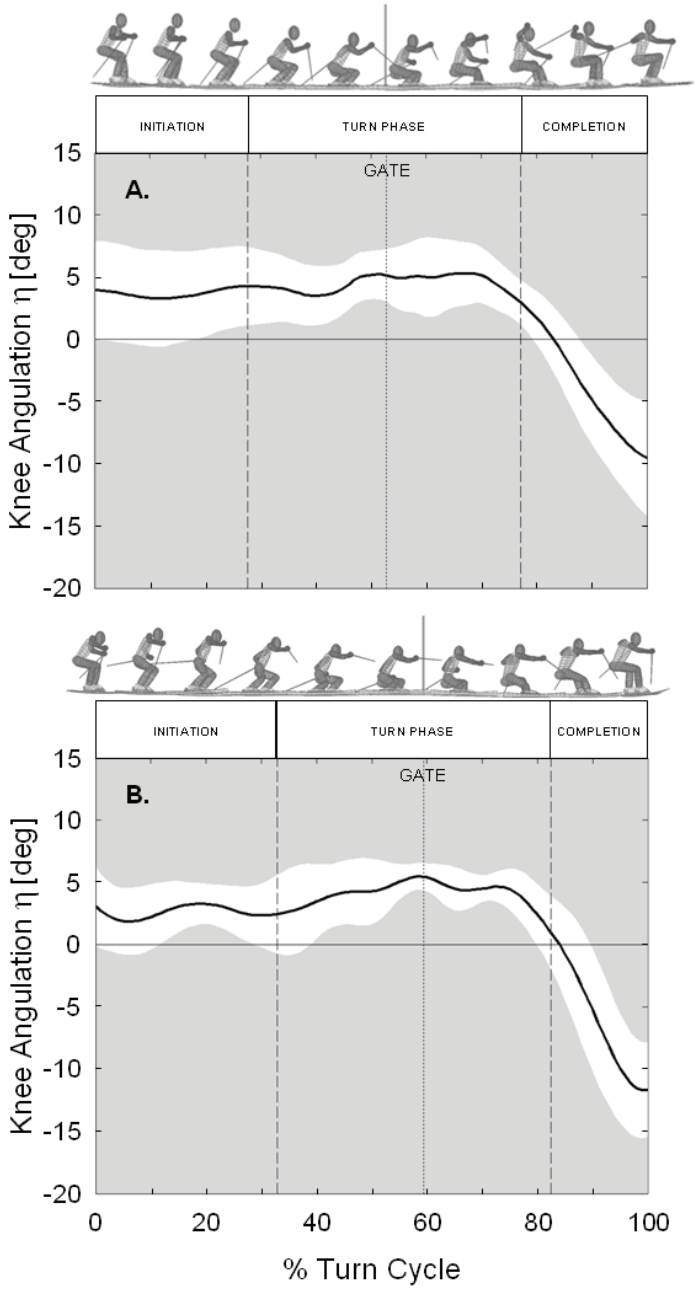

FIGURE 6.19. Ensemble average (± standard deviation) knee angulation over the turn cycle on the 10 m course (A) and the 13 m course (B).

at 42.5 ± 11.0 and 62.9 ± 6.9 % of the turn cycle on the 10 and 13 m courses, respectively. The large variability in the time points reflects the relatively stable nature of knee angulation during this portion of the turn cycle. During the latter portion of the turn, knee angulation was rapidly reduced reaching large negative values—indicating that it was functioning to reduce the ski edge angle—by the Switch to the next turn.

Course-to-course differences in knee angulation for each 10 % interval of the turn cycle are shown in Figure 6.20. There were slightly greater knee angulation values on the 10 m course during both the Initiation Phase and much of the Turn Phase. Differences, however, were small relative to the individual variability. Individual graphs showing outside ski edge angle, center of mass inclination angle, hip angulation angle, and knee angulation angle are given in Appendix K.

VERTICAL ACTIONS

CENTER OF MASS POSITION ORTHOGONAL TO THE SNOW SURFACE

Figure 6.21 presents the ensemble average center of mass position in the Course Coordinate System Z'- dimension (Z'_{COM}), where Z' is the dimension normal to the least squares plane of the snow surface. Table G.10 in Appendix G reports the Z'_{COM} descriptive statistics. On the 10 m course, skiers reached their highest positions above the snow surface of 70.9 ± 3.0 cm at approximately the Switch between turns (1.6 ± 2.5 % of the turn cycle). On the 13 m course, skiers reached the same maximal position (70.2 ± 3.9 cm) but slightly later in the turn cycle, at 8.1 ± 1.6 % of the turn cycle. During the turn, center of mass position moved closer to the snow surface as skiers inclined into the turn, reaching its lowest position at gate passage on the 10 m course (42.5 ± 1.9 cm at 53.8 ± 2.3 % of the turn cycle) and slightly after gate passage on the 13 m course (38.7 ± 1.9 cm at 62.7 ± 1.7 % of the turn cycle). The similar maximum positions but lower minimum positions on the 13 m course corresponded to a slightly larger average

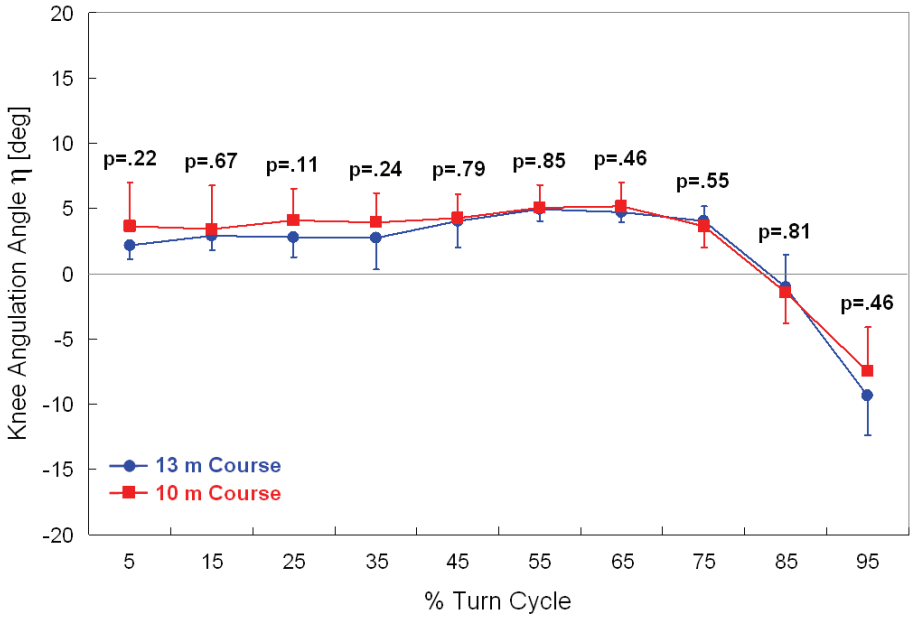

FIGURE 6.20. Course-to-course comparisons of knee angulation. Probability values are based on paired-sample t tests (n = 6).

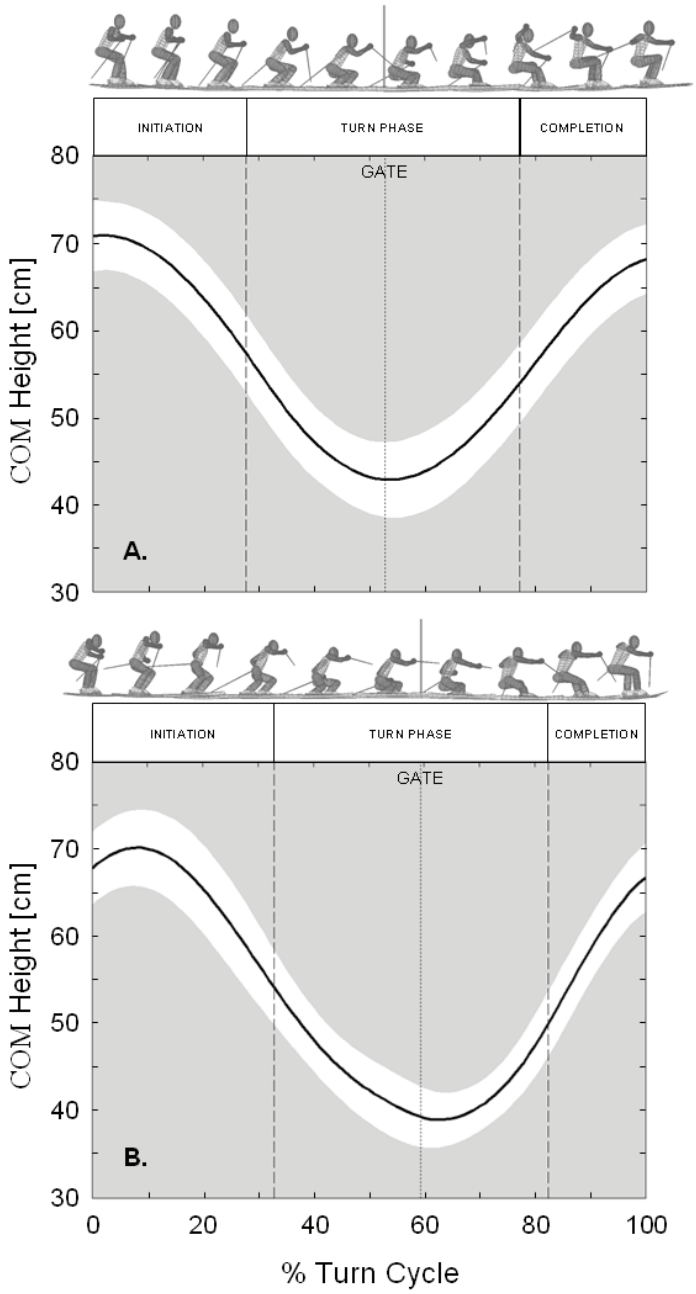

FIGURE 6.21. Ensemble average (± standard deviation) center of mass height above the snow surface over the turn cycle on the 10 m course (A) and the 13 m course (B).

peak-to-peak amplitude of vertical motion on the 13 m course (27.2 ± 1.6 versus 31.0 ± 1.6 cm for the 10 and 13 m courses, respectively).

Figure 6.22 shows the course-to-course differences in Z'_{COM} for each 10 % interval of the turn cycle. Although the highest center of mass positions were similar on both courses, relatively large differences were seen in the second half of the turn cycle where there was a clear shift in the timing of the upwards motion of the center of mass.

CENTER OF MASS TO OUTSIDE ANKLE JOINT CENTER DISTANCE

The center of mass to outside ankle joint center distance (D_{AJC}) ensemble averages are graphed in Figure 6.23 and the descriptive statistics are reported in Table G.11 in Appendix G. During the Initiation Phase, D_{AJC} increased rapidly, particularly on the 13 m course, reaching maximal distances by the start of the Turn Phase of on average 77.8 ± 2.4 and 82.6 ± 2.8 cm on the 10 and 13 m courses, respectively. From this point, D_{AJC} decreased gradually all the way to the end of the turn on the 10 m course. In contrast, D_{AJC} on the 13 m course showed a second period of increase during the latter part of the Turn Phase on some turns, but not all.

Course-to-course differences in D_{AJC} for each 10 % interval of the turn cycle are plotted in Figure 6.24. On average, D_{AJC} was slightly longer on the 13 m course with mean distances over the whole turn cycle of 69.9 ± 1.9 and 72.1 ± 2.3 cm on the 10 and 13 m courses, respectively. Skiers also moved through a greater range of motion on the 13 m course (28.7 ± 4.3 cm) compared to the 10 m course (20.7 ± 3.2 cm). The rapid increase in D_{AJC} during the Initiation Phase on the 13 m course is evident in Figure 6.25 where it can be seen that although skiers started the turn at a somewhat smaller distance than on the 10 m course, they had already achieved a greater distance by 15 % of the turn cycle. A double pattern of increasing D_{AJC} is visible on the 13 m course with particularly large inter-course differences in D_{AJC} from approximately 10 to 50 % of the turn cycle and again from about 60 to 70 % of the turn cycle. Average D_{AJC} differences

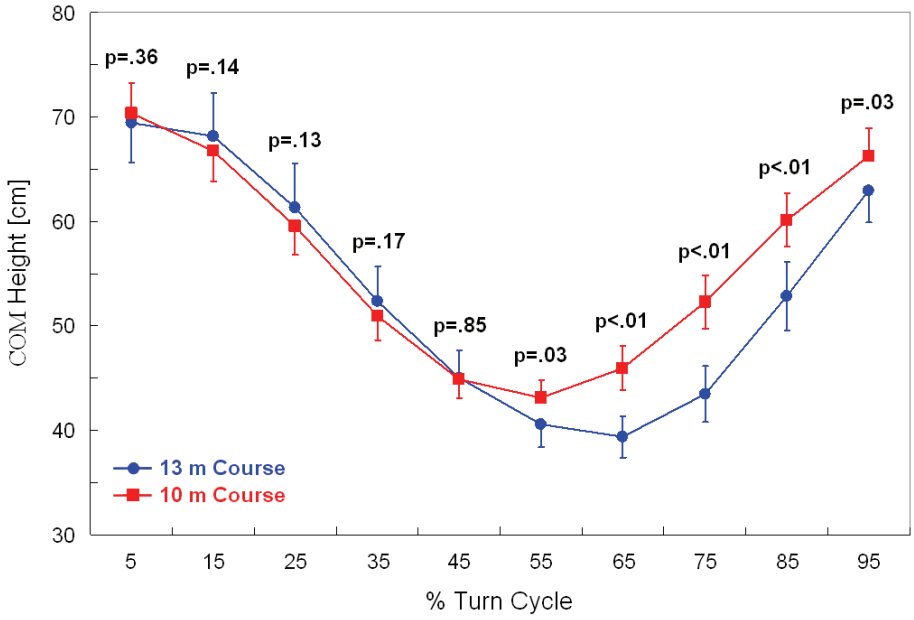

FIGURE 6.22. Course-to-course comparisons of center of mass height above the snow surface. Probability values are based on paired-sample t tests (n = 6).

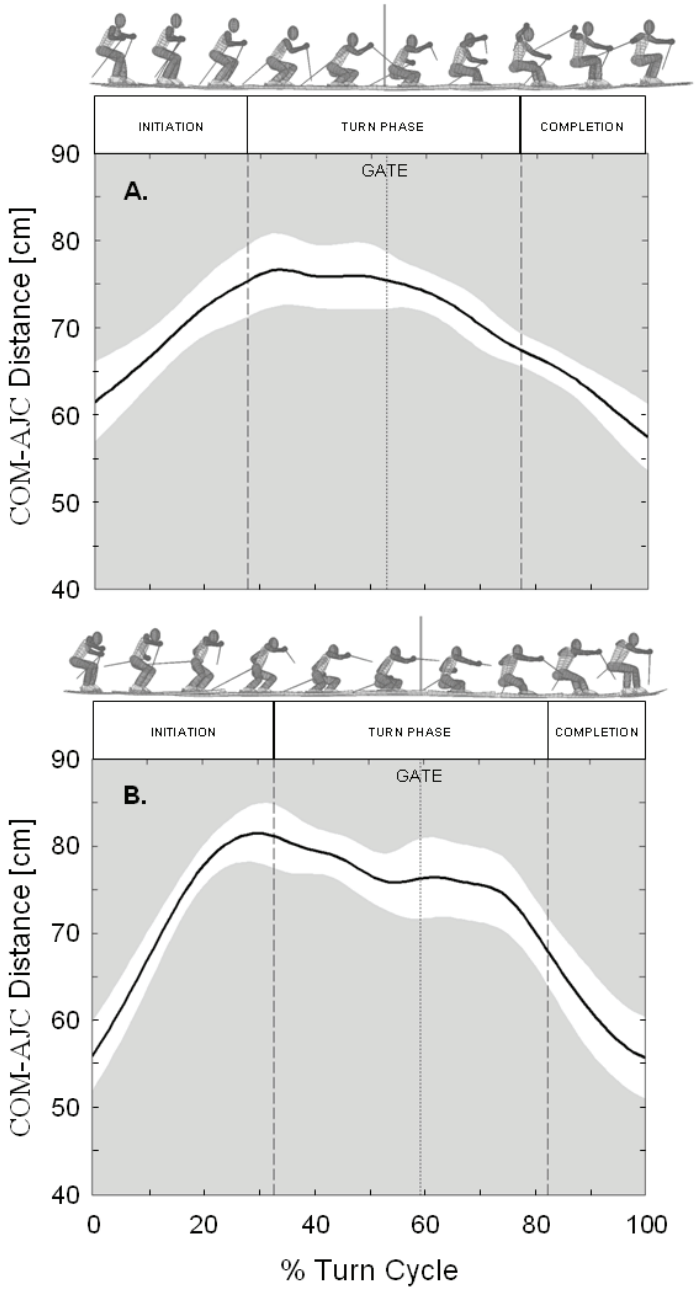

FIGURE 6.23. Ensemble average (± standard deviation) center of mass to outside ankle joint center distance over the turn cycle on the 10 m course (A) and the 13 m course (B).

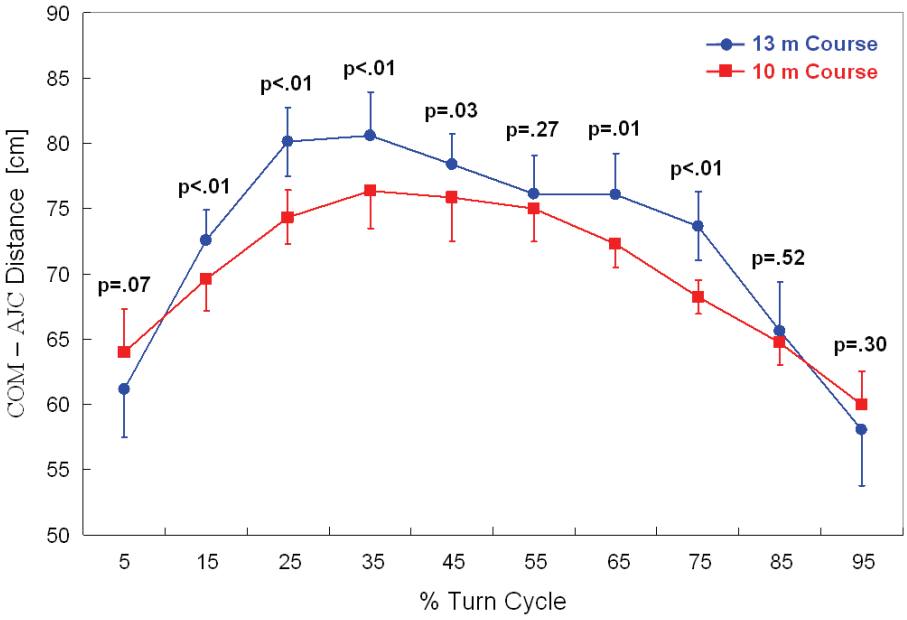

FIGURE 6.24. Course-to-course comparisons of the center of mass to outside ankle joint center distance. Probability values are based on paired-sample t tests (n = 6).

between courses in these phases ranged from 3 to 6 cm. Appendix L presents individual graphs showing both Z'_{COM} and D_{AJC}.

FORE/AFT ACTIONS

Skier fore/aft position (Q_{COM}) ensemble averages are plotted in Figure 6.25 and descriptive statistics are given in Table G.12 in Appendix G. At the start of the turn cycle, skier center of mass positions were located on average –11.4 ± 4.4 and –13.8 ± 4.3 cm behind the outside ankle joint center along the longitudinal axis of the outside ski, for the 10 and 13 m courses, respectively. On the 10 m course, the center of mass position moved forward through the Initiation Phase and the first part of the Turn Phase to reach maximal forward positions of 16.4 ± 4.1 cm prior to gate passage. The center of mass then moved gradually back reaching a position –7.8 ± 4.0 cm behind the ankle joint center by the end Switch. On the 13 m course, skier center of mass position moved quickly forward during the Initiation Phase to reach a relatively stable forward position of approximately 8 cm for the duration of the Turn Phase. However, there is a fair amount of individual variability despite the rather stable appearance of the ensemble average. This can be seen when examining the selection of individual graphs presented in Appendix M. From the end of the Turn Phase on the 13 m course, center of mass position then moved aft reaching a position –10.7 ± 3.0 cm behind the ankle joint center by the turn's end. While mean fore/aft position ($\bar{Q}_{COM}$) for the whole turn cycle was further forward on the 10 m course (2.5 ± 2.5 cm) than on the 13 m course (1.6 ± 2.8), the range of fore/aft movement (Q_{ROM}) was about the same (26.0 ± 6.3 and 26.7 ± 0.4 cm on the 10 and 13 m courses, respectively).

Figure 6.26 compares skier fore/aft position at each 10 % interval of the turn cycle on the 10 and 13 m courses. The largest average differences between courses occurred from 30 to 60 % of the turn cycle, where positions on the 10 m course were between 2.5 and 4.5 cm further forward, and again from 70 to 80 % of the turn cycle, where

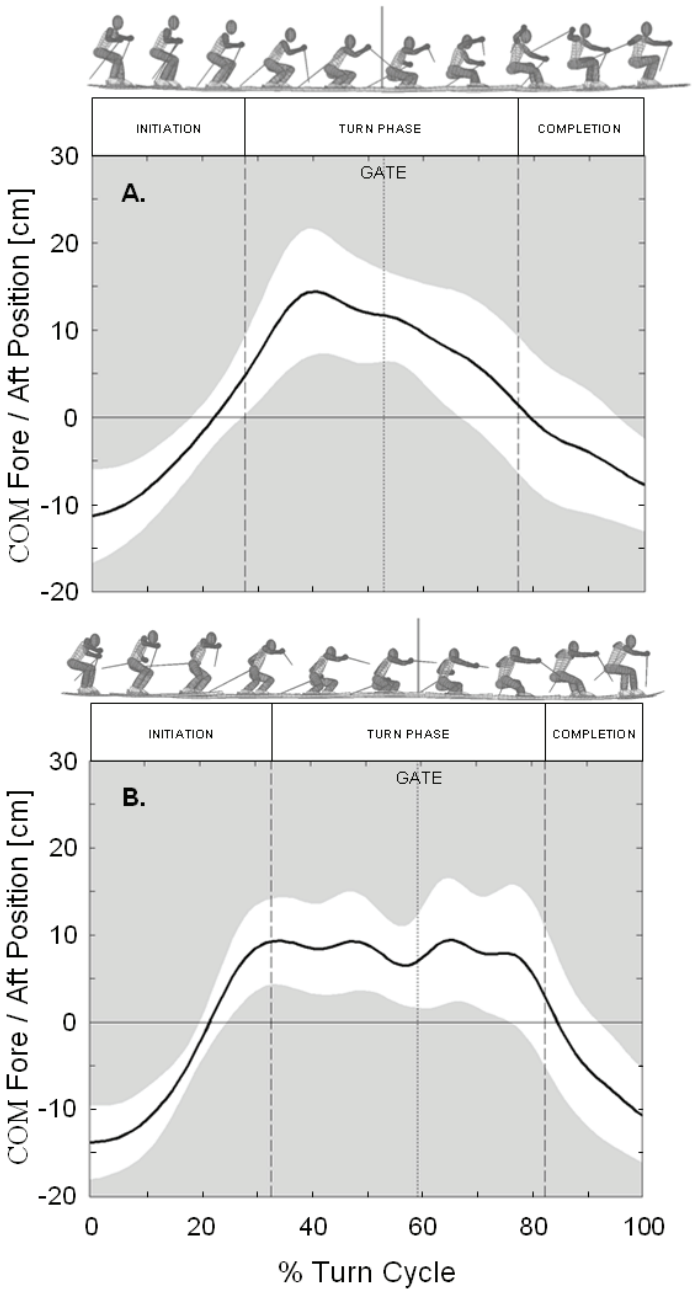

FIGURE 6.25. Ensemble average (± standard deviation) center of mass fore/aft position over the turn cycle on the 10 m course (A) and the 13 m course (B).

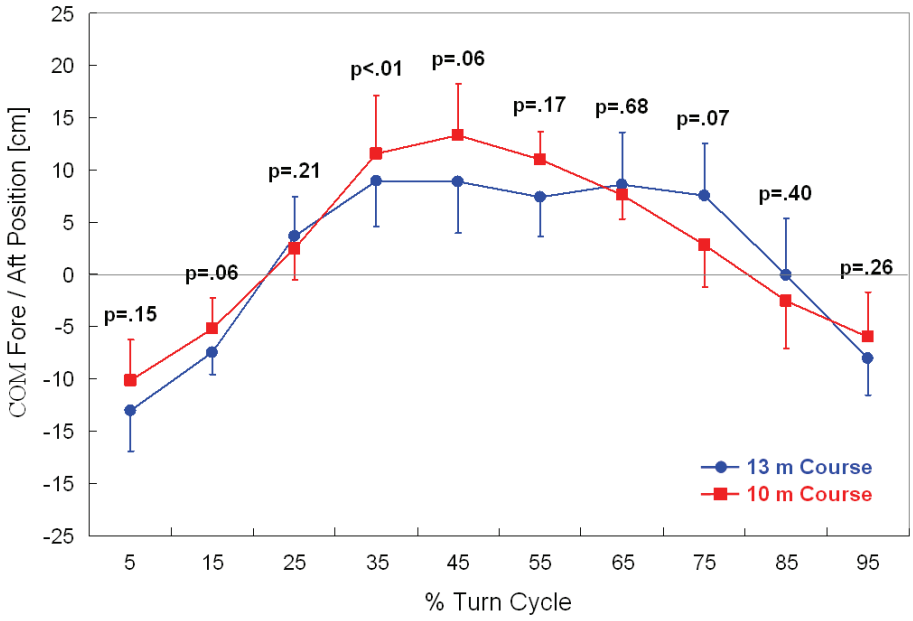

FIGURE 6.26. Course-to-course comparisons of the center of mass fore/aft position. Probability values are based on paired-sample t tests (n = 6).

positions on the 10 m course were on average 4.7 cm further aft. However, differences between courses were small relative to the individual variability.

6.5 EXTERNAL FORCES (Figure 2.1, Boxes A, I, and K)

AIR DRAG FORCE

It is important to remind the reader that the air drag force in this study was not measured, but rather modeled based on skier velocity and frontal area calculations, as well as estimated values of the air drag coefficient. Figure 6.27 presents the ensemble average wind drag force magnitudes (F_D) for both the 10 and 13 m courses. Descriptive statistics are reported in Table G.13 in Appendix G. The drag force magnitude showed a clear cyclic nature over the course of the turn cycle. Average maximum air drag forces of 62 ± 3 and 85 ± 8 N acted on the skier at 31.5 ± 3.3 and 27.0 ± 1.4 % of the turn cycle—close to the start of the Turn Phase—on the 10 and 13 m courses, respectively. The mean air drag force acting on the skiers was greater on the 13 m course (69 ± 7 N) than on the 10 m course (52 ± 1 N).

Course-to-course differences in air drag force magnitude for each 10 % interval of the turn cycle are shown in Figure 6.28. The air drag force was larger across all intervals with the largest differences of approximately 20 N occurring at the 20 to 40 % interval of the turn cycle. It is also of interest to note that the variability of the wind drag force as described by the standard deviations was much higher on the 13 m course than the 10 m course.

AIR DRAG FORCE POWER

Since the air drag force vector ($\vec{F}_D$) was defined as acting opposite the center of mass velocity vector ($\dot{\vec{P}}_{COM}$), the pattern of air drag force power (P_D) parallels that of the air drag force magnitude (F_D). Figure 6.29 presents the ensemble average air drag force

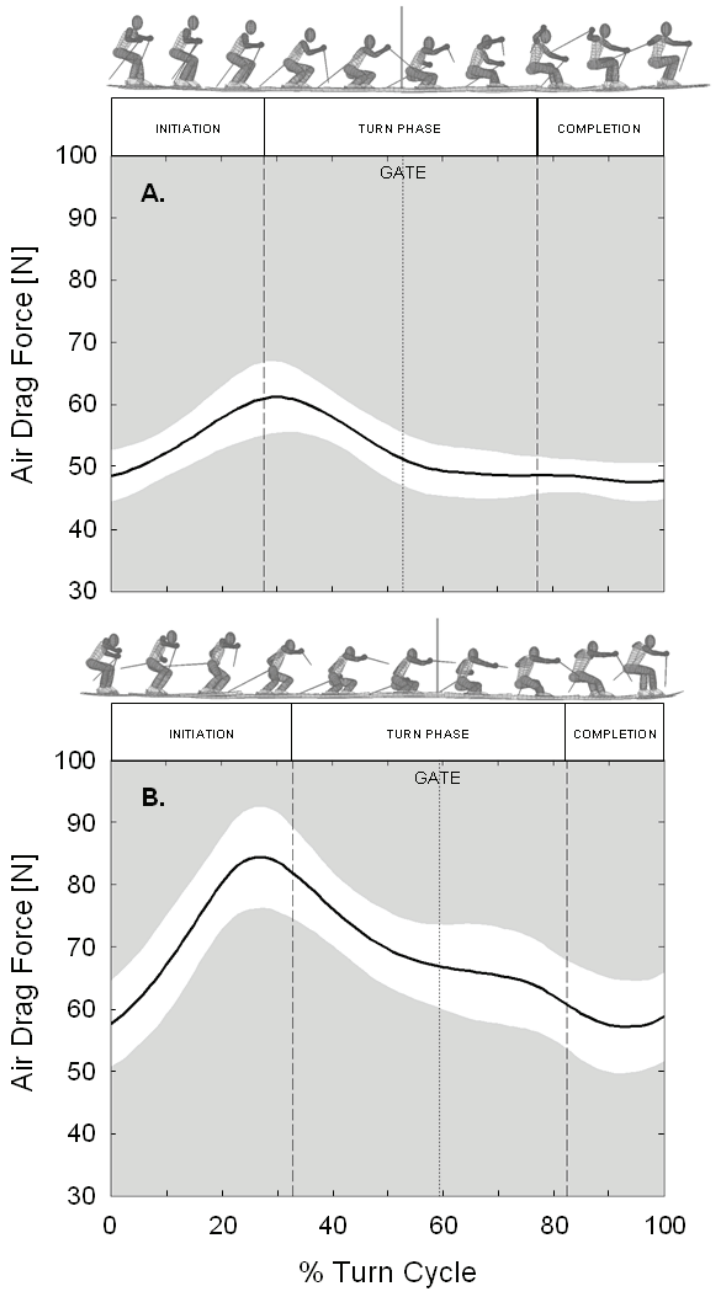

FIGURE 6.27. Ensemble average (± standard deviation) air drag force magnitude over the turn cycle on the 10 m course (A) and the 13 m course (B).

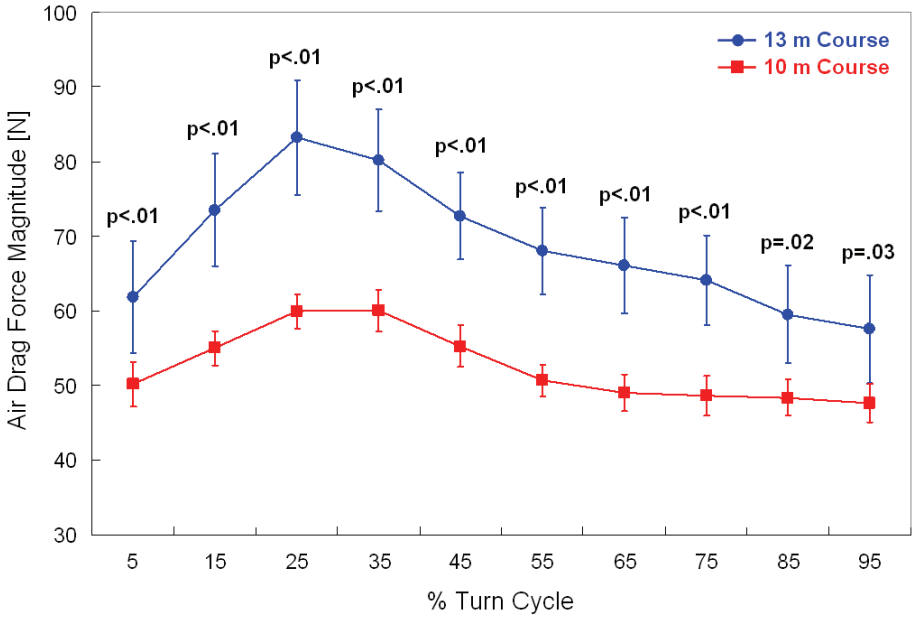

FIGURE 6.28. Course-to-course comparisons of the air drag force magnitude. Probability values are based on paired-sample t tests (n = 6).

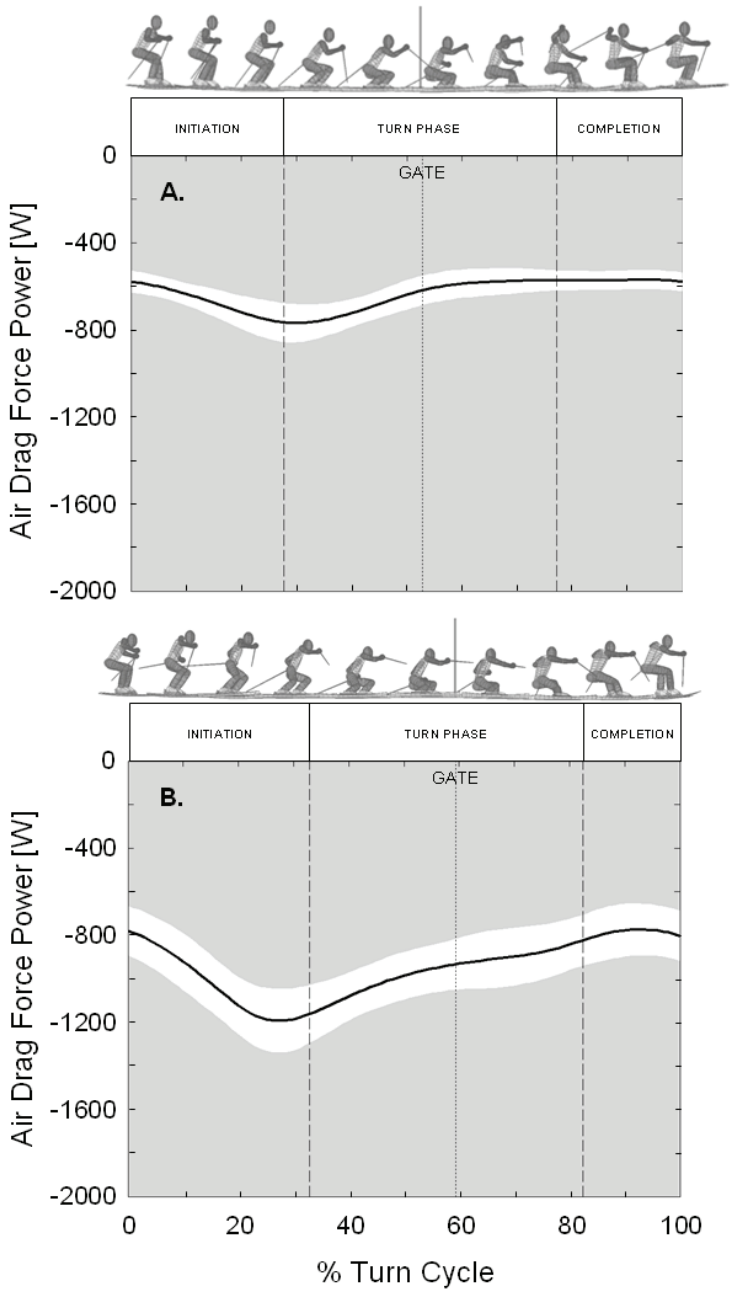

FIGURE 6.29. Ensemble average (± standard deviation) air drag force power over the turn cycle on the 10 m course (A) and the 13 m course (B).

power P_D for each course. Descriptive statistics are reported in Table G.14 in Appendix G. Mean air drag power over the whole turn cycle for the 10 and 13 m courses was –638 ± 18 and –954 ± 113 W, respectively. Peak (maximally negative) air drag powers of –779 ± 39 and –1197 ± 137 W occurred at 32.1 ± 2.5 and 28.1 ± 1.8 % of the turn cycle on the 10 and 13 m courses, respectively.

Course-to-course differences in air drag power for each 10 % interval of the turn cycle are shown in Figure 6.30. Similar to the air drag magnitude, power on the 13 m course was greater than that on the 10 m course over all intervals, with particularly large differences from 20 to 40 % of the turn cycle. Again, the larger variability in air drag force on the 13 m course was evident.

SNOW REACTION FORCE

Absolute and body weight normalized snow reaction force magnitude (F_R) ensemble averages are shown in Figures 6.31 and 6.32, respectively. Descriptive statistics are included in Table G.15 in Appendix G. Generally speaking, snow reaction forces were low at the Switches between turns and high during the Turn Phase. On the 10 m course, minimum reaction forces of 158 ± 52 N (0.17 ± 0.06 BW) occurred close to the Switch between turns (0.8 ± 6.3 % of the turn cycle). On the 13 m course, slightly lower minimum reaction forces of 85 ± 45 N (0.09 ± 0.05 BW) occurred slightly later in the turn cycle at 6.5 ± 3.7 %. An average maximum force on the 10 m course of 3212 ± 329 N (3.35 ± 0.20 BW) occurred at 50.9 ± 5.9 % of the turn cycle, or approximately gate passage. On the 13 m course, slightly higher maximum forces of 3378 ± 252 N (3.53 ± 0.16) acted on the skier after gate passage, at 66.6 ± 4.2 % of the turn cycle.

A shift in the timing of the snow reaction force is evident in the course-to-course comparison of each 10 % interval of the turn cycle presented in Figure 6.33. During the early portion of the Initiation Phase, snow reaction forces were on average 114 N greater on the 10 m course, indicating that skiers did not unweight as much during the

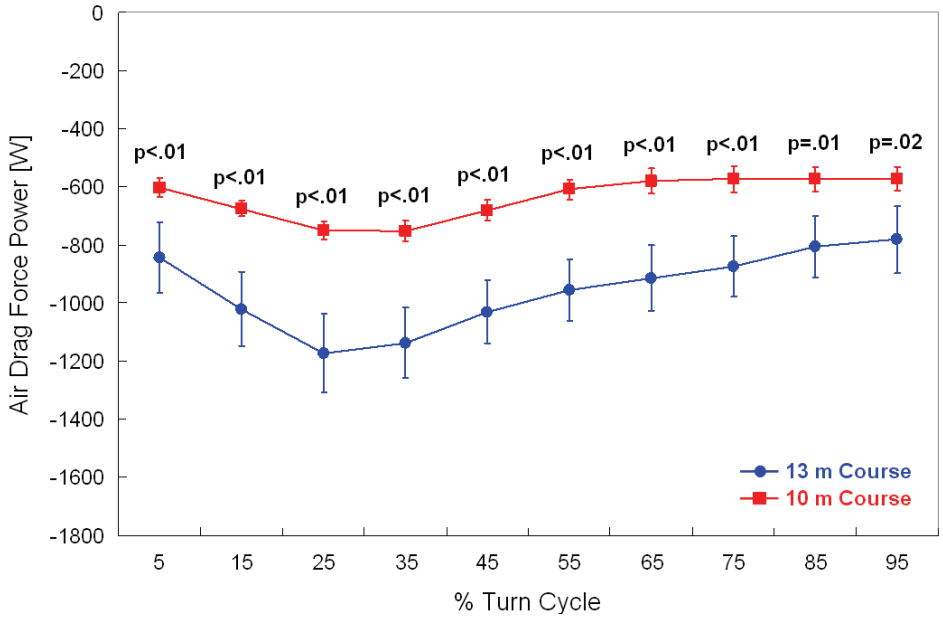

FIGURE 6.30. Course-to-course comparisons of the air drag force power. Probability values are based on paired-sample t tests (n = 6).

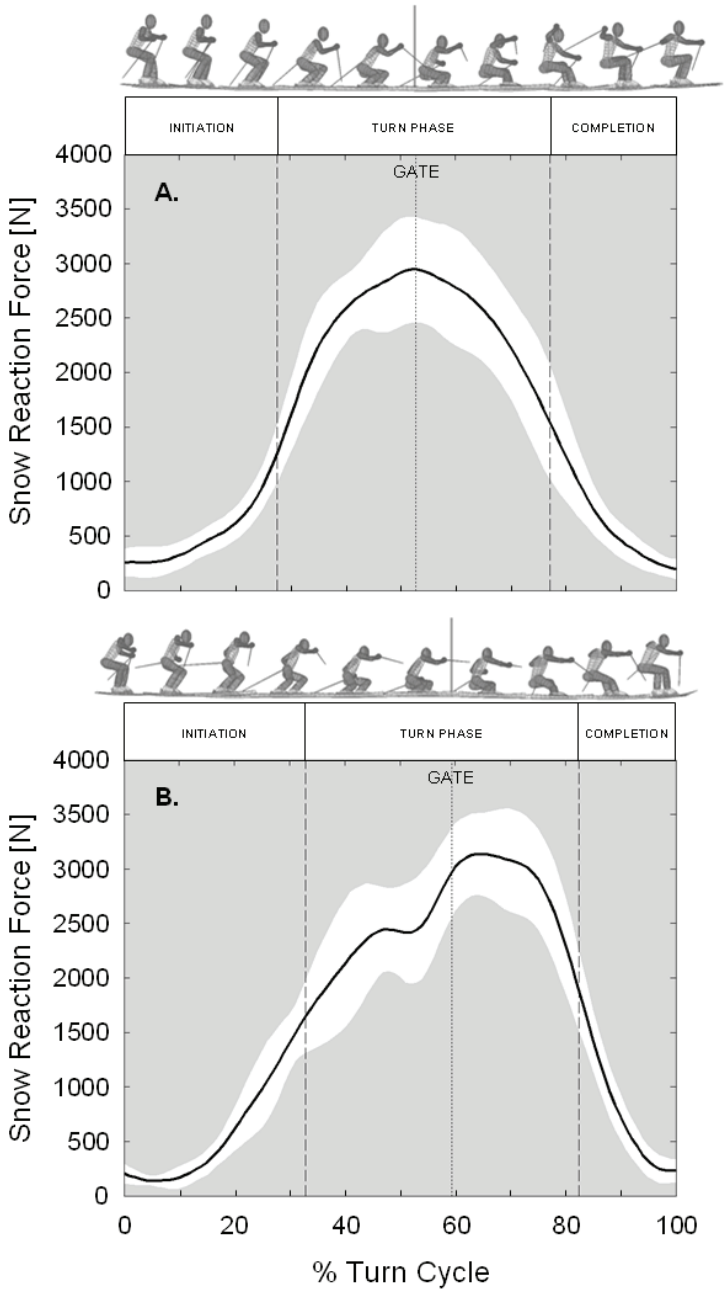

FIGURE 6.31. Ensemble average (± standard deviation) snow reaction force absolute magnitude over the turn cycle on the 10 m course (A) and the 13 m course (B).

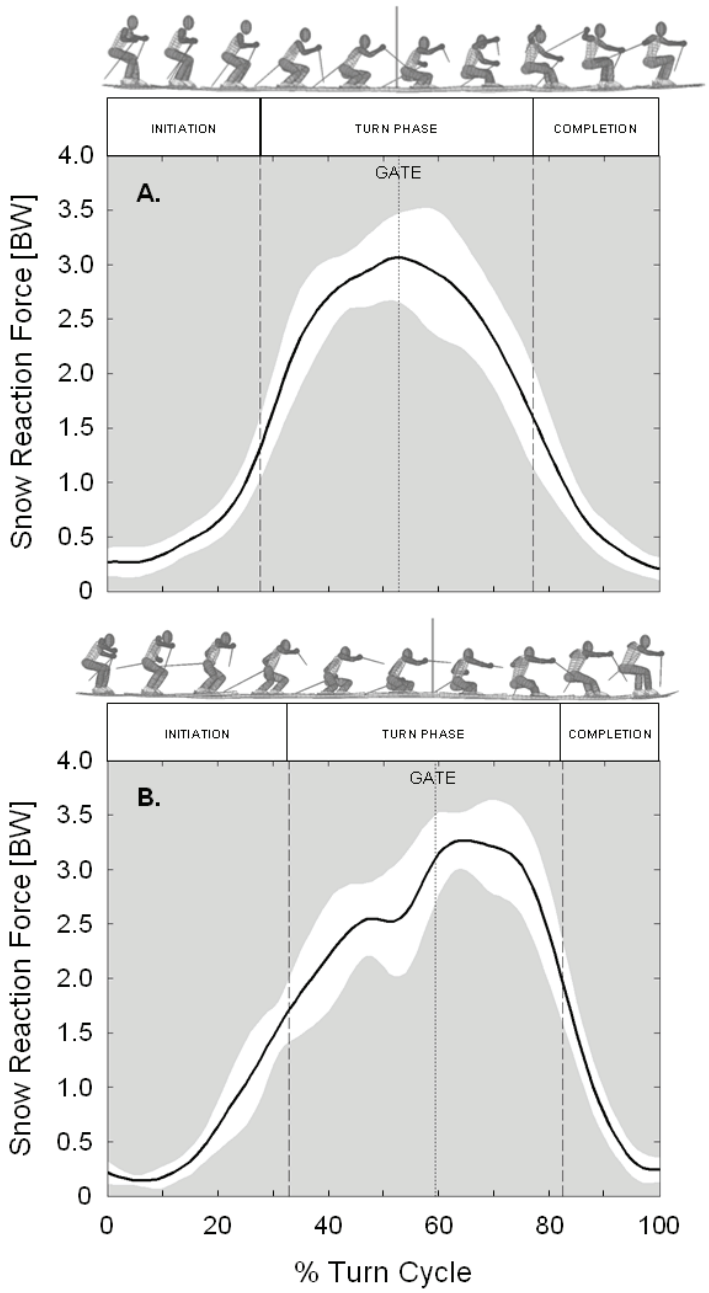

FIGURE 6.32. Ensemble average (± standard deviation) snow reaction force relative magnitude over the turn cycle on the 10 m course (A) and the 13 m course (B).

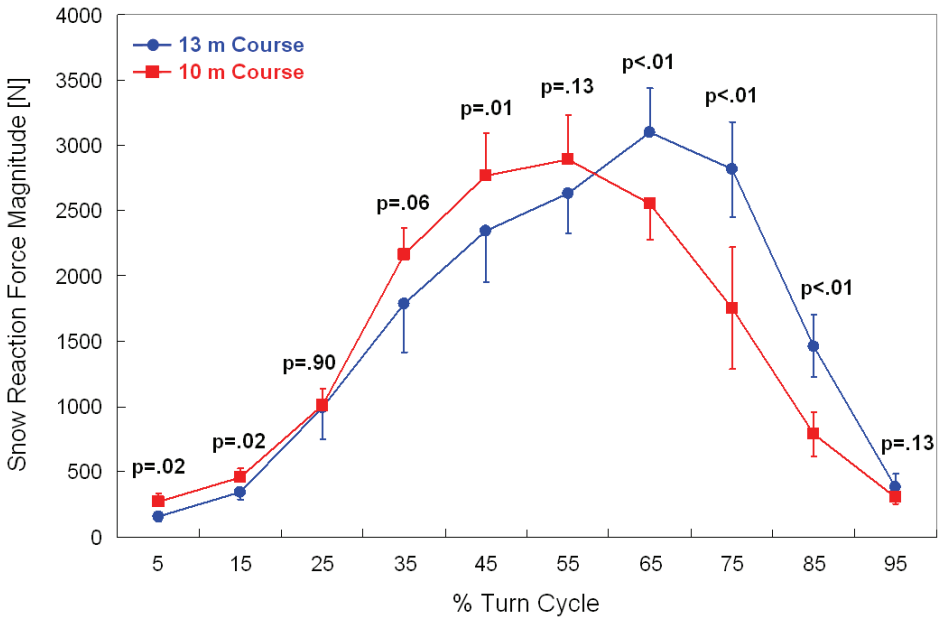

FIGURE 6.33. Course-to-course comparisons of the snow reaction force magnitude. Probability values are based on paired-sample t tests (n = 6).

transition between turns. From approximately 30 to 50 % of the turn cycle, the skiers generated on average between 374 and 418 N greater reaction forces on the 10 m course. Conversely, skiers generated on average between 551 and 1063 N greater reaction force on the 13 m course from approximately 60 to 90 % of the turn cycle.

SNOW REACTION FORCE POWER

The ensemble average reaction force power (P_R) for both courses is plotted in Figure 6.34 Descriptive statistics are included in Table G.16 in Appendix G. Positive powers indicate when the snow reaction force acted to accelerate the skier in the direction of travel while negative powers indicate when the reaction force did negative work on the skier. Maximum (positive) powers of 1123 ± 254 and 1312 ± 557 W were registered on the 10 and 13 m courses, respectively. On the 10 m course, this maximum sometimes occurred prior to the switch and sometimes shortly after the switch. In contrast, reaction force power maximums occurred almost exclusively after the switch on the 13 m course. Average minimum (maximally negative) powers of –10246 ± 1027 and –9774 ± 1718 W acted on the skier just prior to gate passage on the 10 and 13 m courses, respectively.

Figure 6.35 shows the course-to-course differences in P_R for each 10 % interval of the turn cycle. Similar to the reaction force magnitude data, the reaction force power also showed a shift in timing between the two courses, with larger negative powers on the 10 m course from 30 to 50 % of the turn cycle and larger negative powers on the 13 m course from 60 % to the end of the turn cycle.

VERTICAL COMPONENT OF THE SNOW REACTION FORCE

The ensemble averages of the component of the snow reaction force acting normal to the local snow surface (F_{VERT}) are presented in Figure 6.36. Descriptive statistics are summarized in Table G.17 in Appendix G. At the turn start Switch, average vertical

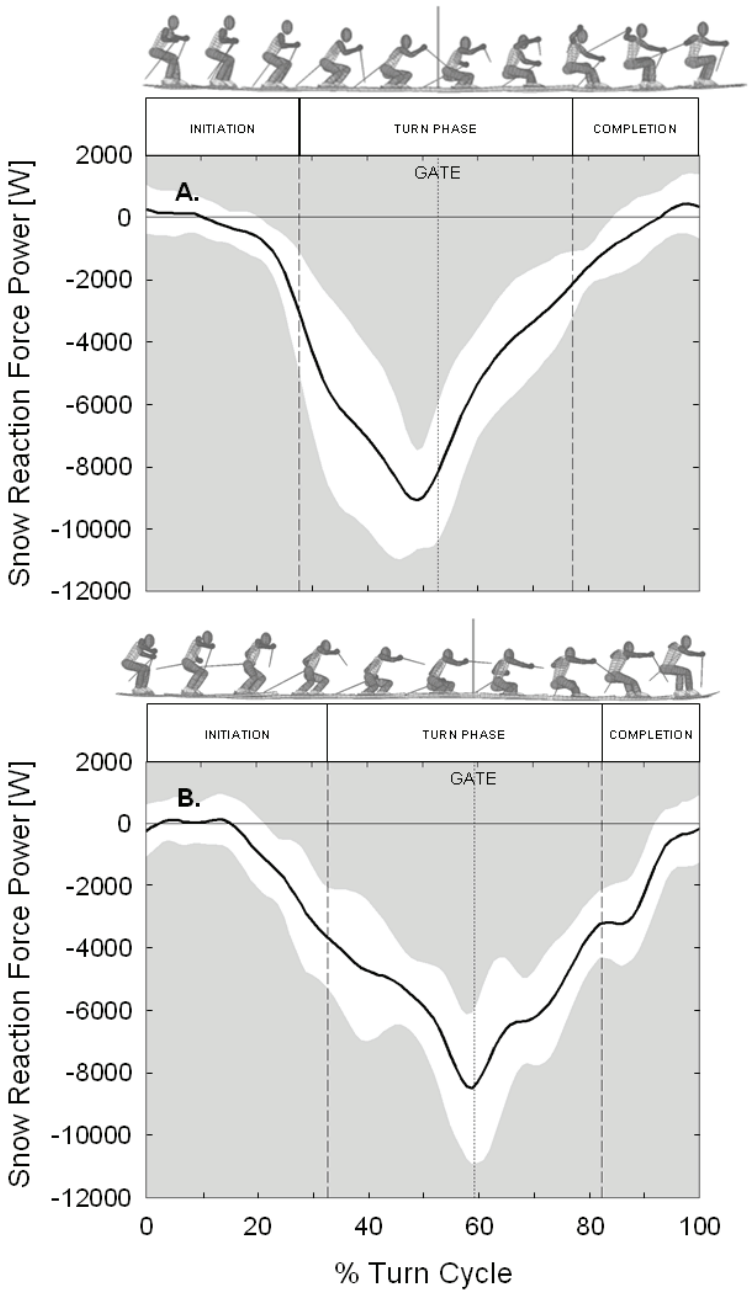

FIGURE 6.34. Ensemble average (± standard deviation) snow reaction force power over the turn cycle on the 10 m course (A) and the 13 m course (B).

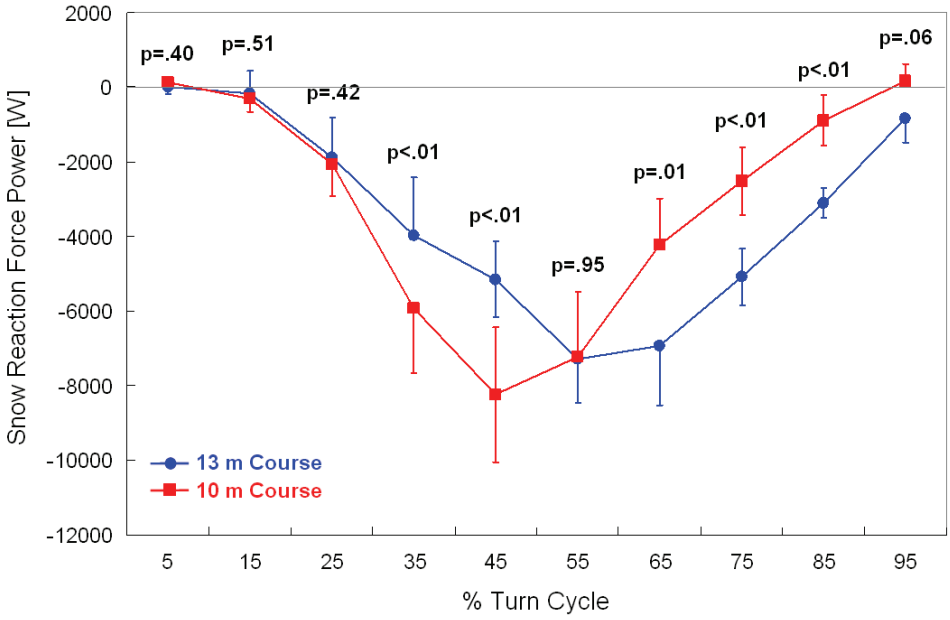

FIGURE 6.35. Course-to-course comparisons of the snow reaction force power. Probability values are based on paired-sample t tests (n = 6).

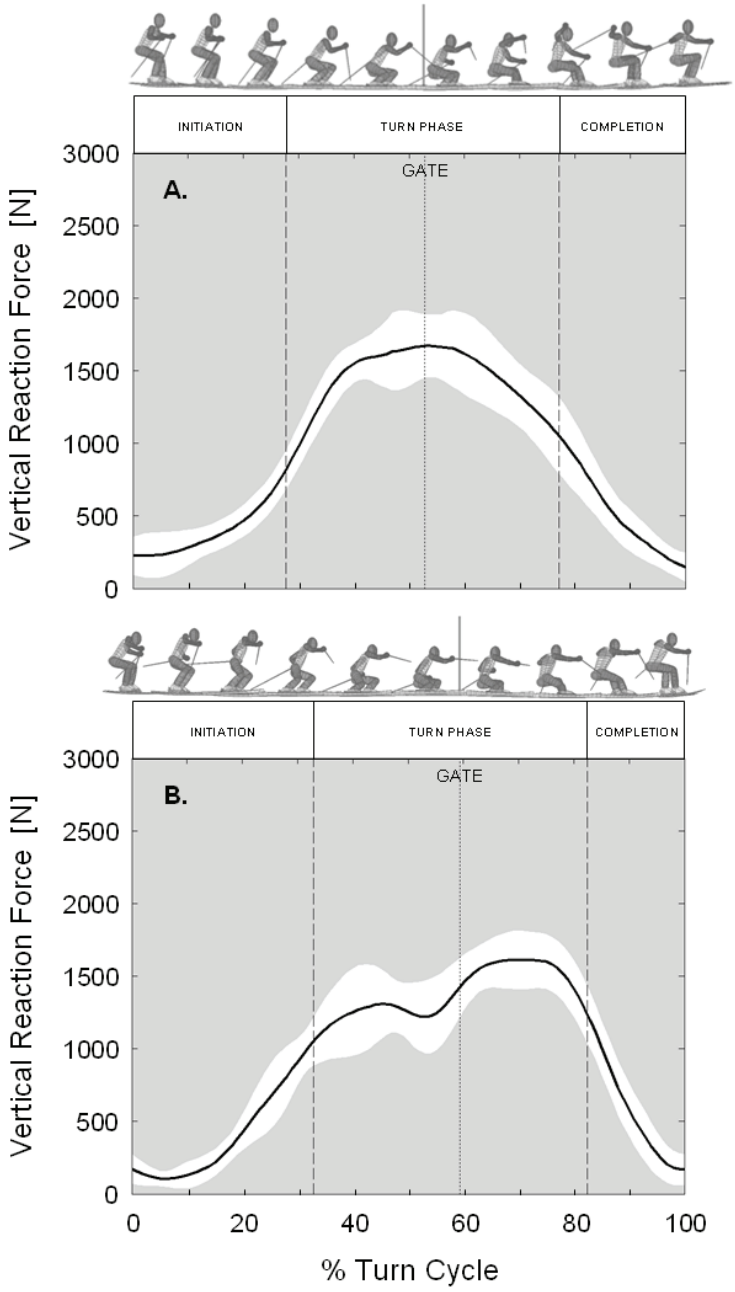

FIGURE 6.36. Ensemble average (± standard deviation) vertical component of the snow reaction force over the turn cycle on the 10 m course (A) and the 13 m course (B).

reaction forces were 226 ± 57 and 124 ± 81 N on the 10 and 13 m courses, respectively. Minimum vertical reaction forces of 130 ± 51 and 50 ± 50 N occurred at 0.8 ± 5.7 and 6.3 ± 3.5 % of the turn cycle on the 10 and 13 m courses, respectively. On the 10 m course, the vertical reaction force built up smoothly, peaking at an average 1832 ± 207 N at 52.8 ± 4.2 % of the turn cycle, or just after gate passage, on average. The vertical reaction force then progressively declined to the end of the turn. On the 13 m course, there was an initial build up of the vertical reaction force in the Initiation Phase, followed by a brief period in the first part of the Turn Phase where the vertical reaction force stabilized at just over 1000 N. Prior to gate passage, the vertical reaction force continued to increase, reaching peak values of 1716 ± 139 N at 67.3 ± 6.6 %—well into the latter portion of the Turn Phase. This was followed by a rapid decline in vertical reaction force during the Completion Phase.

Course-to-course differences in the vertical component of the snow reaction force over each 10 % interval of the turn cycle are shown in Figure 6.37. During the Initiation Phase, there was less unweighting on the 10 m course by on average between 115 and 122 N. The 10 m course showed a much earlier development of vertical reaction forces with greater forces registered between 30 and 60 % of the turn cycle. The 13 m course clearly had a delayed development of vertical reaction force with greater forces acting between the 60 and 90 % interval of the turn cycle.

GRAVITATIONAL FORCE POWER

Gravitational force power (P_G) ensemble averages are shown in Figure 6.38. Table G.18 in Appendix G presents the descriptive statistics. Mean turn cycle powers were 4046 ± 225 and 4578 ± 350 W for the 10 and 13 m courses, respectively. There was a clear cyclic pattern of gravitational force power over the turn cycle, with maximal powers of 5174 ± 354 and 5640 ± 462 W occurring at 32.2 ± 2.2 and 36.6 ± 3.6 % of the turn cycle on the 10 and 13 m courses, respectively. An average minimum power of 2909 ± 155 W occurred

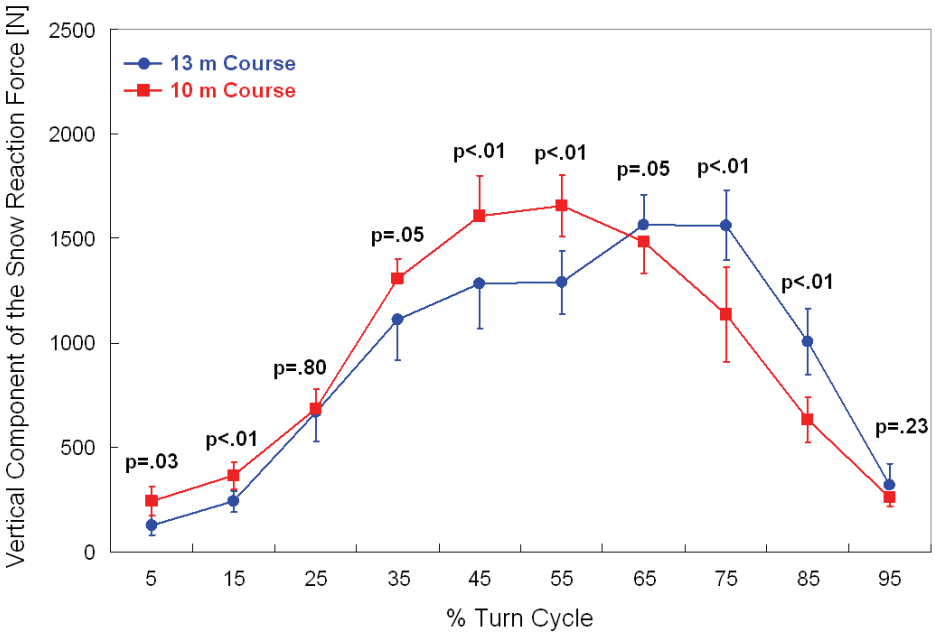

FIGURE 6.37. Course-to-course comparisons of the vertical component of the snow reaction force. Probability values are based on paired-sample t tests (n = 6).

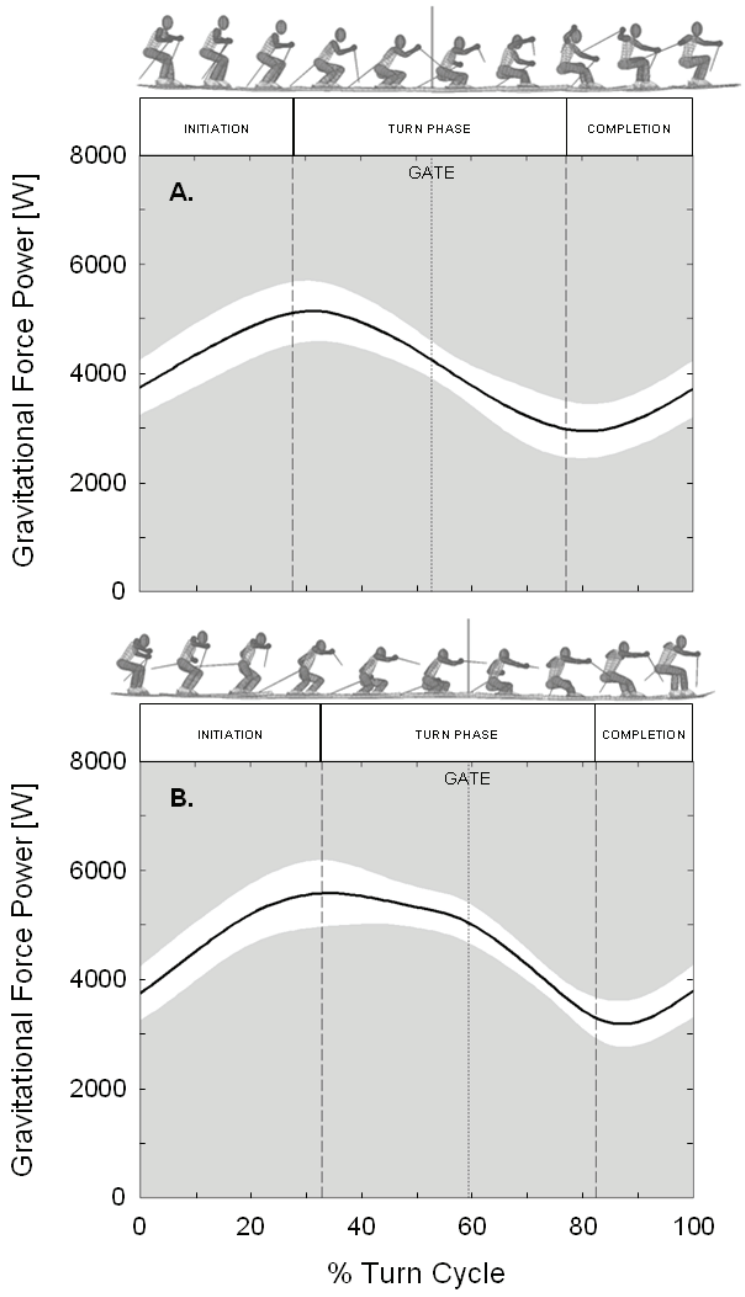

FIGURE 6.38. Ensemble average (± standard deviation) vertical component of the snow reaction force over the turn cycle on the 10 m course (A) and the 13 m course (B).

at 80.3 ± 2.2 % of the turn cycle on the 10 m course while a somewhat higher average minimum power of 3167 ± 284 W was registered at 86.9 ± 1.9 % on the 13 m course.

Course-to-course differences for each 10 % interval of the turn cycle are shown in Figure 6.39. The gravitational force acted with greater power on the skiers on the 13 m course for the majority of the turn cycle, except around the turn transitions. Individual graphs showing all three of the external force powers are shown in Appendix N.

6.6 SKIER MECHANICAL ENERGY

MECHANICAL ENERGY DISSIPATION

The ensemble averages of mechanical energy dissipation (E_{DISS}) for both courses are graphed in Figure 6.40. Descriptive statistics are summarized in Table G.19 in Appendix G. Mean turn cycle dissipations ($\overline{E}_{DISS}$) were 8.85 ± 0.71 and 9.43 ± 0.76 $J \cdot kg^{-1} \cdot m^{-1}$ on the 10 and 13 m courses, respectively, indicating that skiers were very close to an energy balance with the work of the gravitational force. There was a cyclic pattern of energy dissipation over the turn cycle with low dissipations—and in some cases negative dissipation—occurring around the transition between turns, and high dissipations taking place during the Turn Phase. Mean maximum dissipation on the 10 m course was 23.46 ± 1.79 $J \cdot kg^{-1} \cdot m^{-1}$ and occurred at 50.5 ± 6.7 % of the turn cycle, approximately at gate passage. On the 13 m course, the average maximum dissipation was 22.02 ± 2.34 $J \cdot kg^{-1} \cdot m^{-1}$ and occurred at 64.3 ± 6.67 %—slightly after gate passage.

Figure 6.41 presents the course-to-course comparisons of energy dissipation for each 10 % interval of the turn cycle. A clear shift in the time course of energy dissipation was apparent with energy being dissipated earlier in the turn cycle on the 10 m course, and later in the turn cycle on the 13 m course.

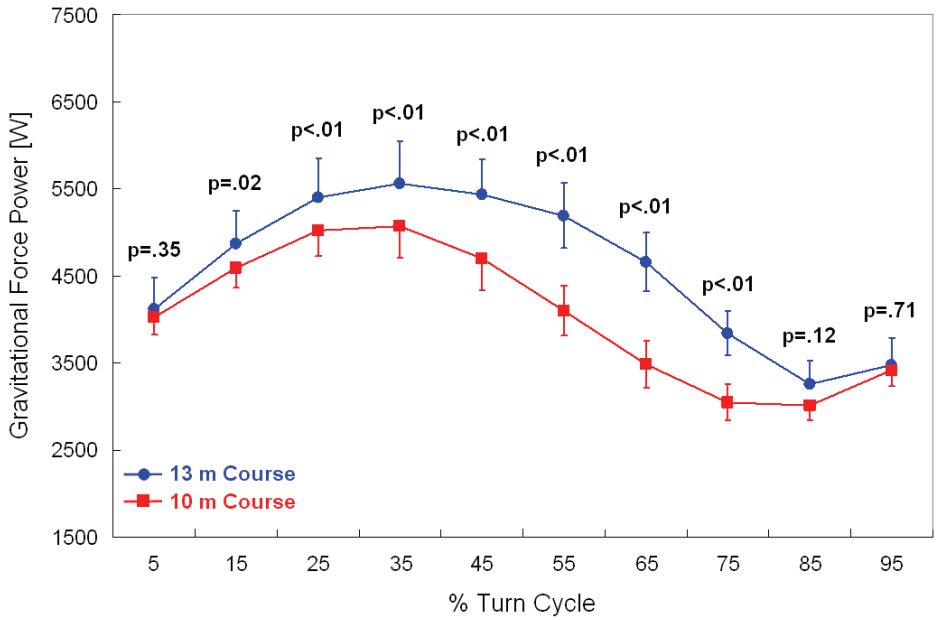

FIGURE 6.39. Course-to-course comparisons of the gravitational force power. Probability values are based on paired-sample t tests (n = 6).

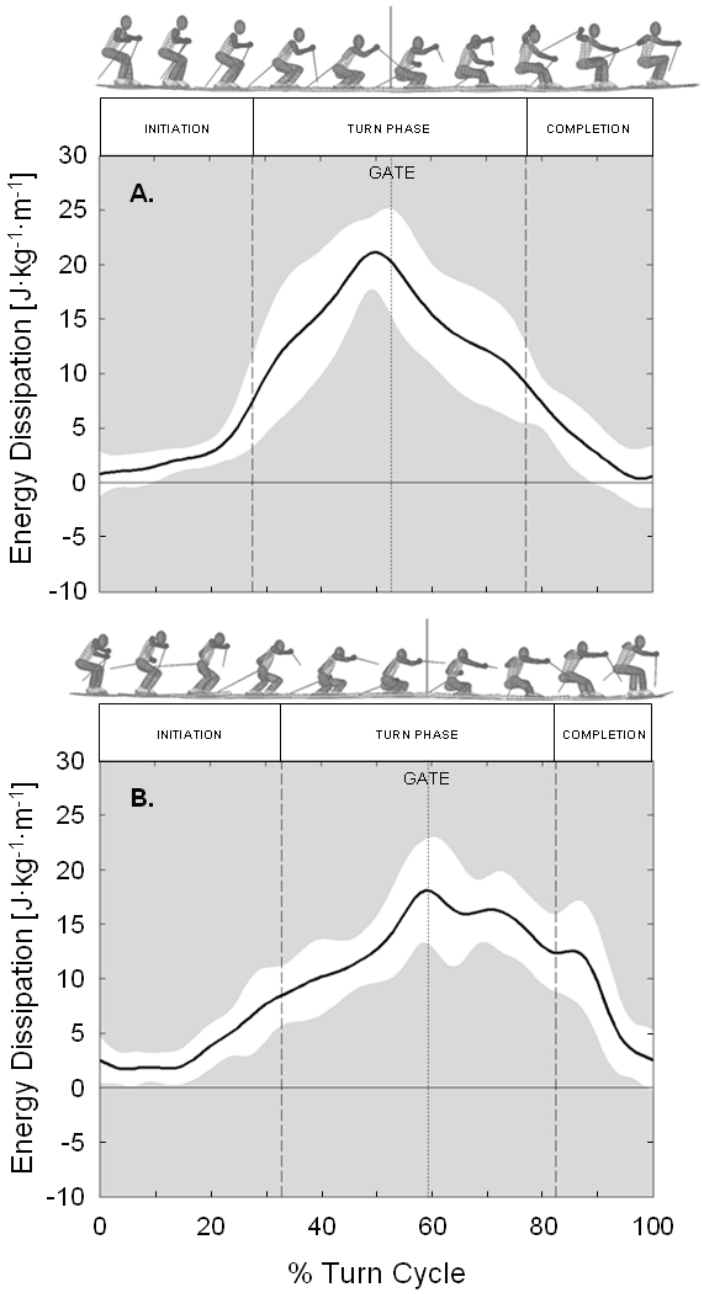

FIGURE 6.40. Ensemble average (± standard deviation) mechanical energy dissipation over the turn cycle on the 10 m course (A) and the 13 m course (B).

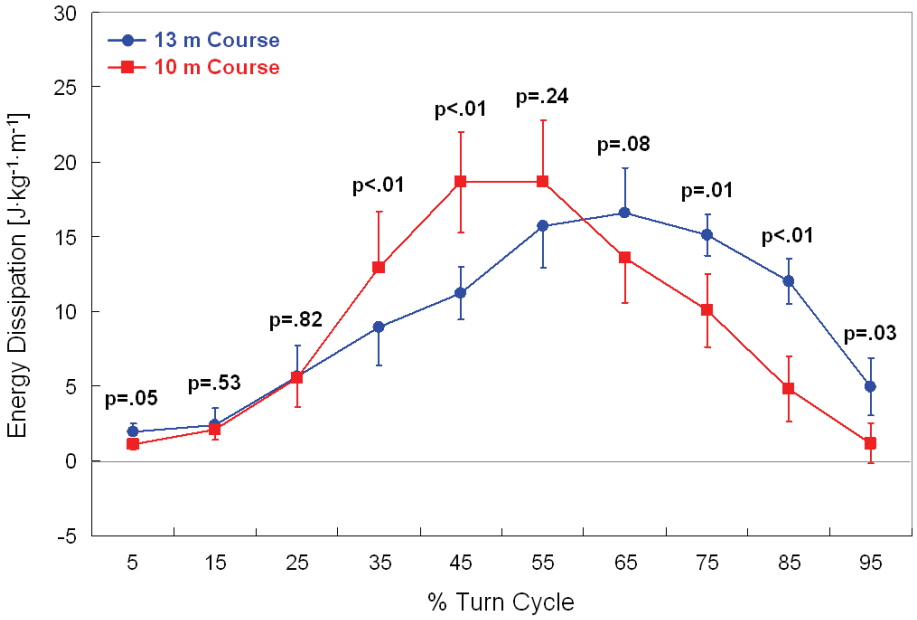

FIGURE 6.41. Course-to-course comparisons of mechanical energy dissipation. Probability values are based on paired-sample t tests (n = 6).

CAUSES OF MECHANICAL ENERGY DISSIPATION

To determine the proportion of total energy losses attributable to the air drag and snow reaction forces, the negative component of work done by each force on the skier was calculated and is presented in Table 6.2 as percentages of total energy loss. On the 10 m course, the air drag force accounted for on average 16.7 ± 1.9 %, and the snow reaction force 83.3 ± 1.9 %, of total skier energy losses. On the 13 m course, the air drag force accounted for a slightly greater proportion, and the reaction force a lower proportion, at 21.4 ± 2.2 and 78.6 ± 2.2 % of energy losses, respectively.

The gravitational force accounted for by far the majority of energy gains on both courses. Although the snow reaction force also acted at certain times to increase the skier's kinetic energy, these contributions were relatively small (2.6 ± 0.7 and 2.1 ± 0.8 % of the total kinetic energy gains on the 10 and 13 m courses, respectively).

The relationships between instantaneous measures of skier fore/aft position and reaction force power (P_R) are presented in Figures 6.42 A and B for the 10 and 13 m courses, respectively. The Pearson's product moment correlation coefficients for the 10

TABLE 6.2. Relative contributions of the external forces to changes in skier mechanical energy. W_G, W_R, and W_D are the mechanical work of the gravitational, reaction, and air drag forces, respectively, on the skier.

		10 m Course	13 m Course
ENERGY GAINED			
W_G	[%]	97.4 ± 0.7	97.9 ± 0.8
W_R	[%]	2.8 ± 0.7	2.1 ± 0.8
ENERGY LOST			
W_R	[%]	83.3 ± 1.9	78.6 ± 2.2
W_D	[%]	16.7 ± 1.9	21.4 ± 2.2

n = 6

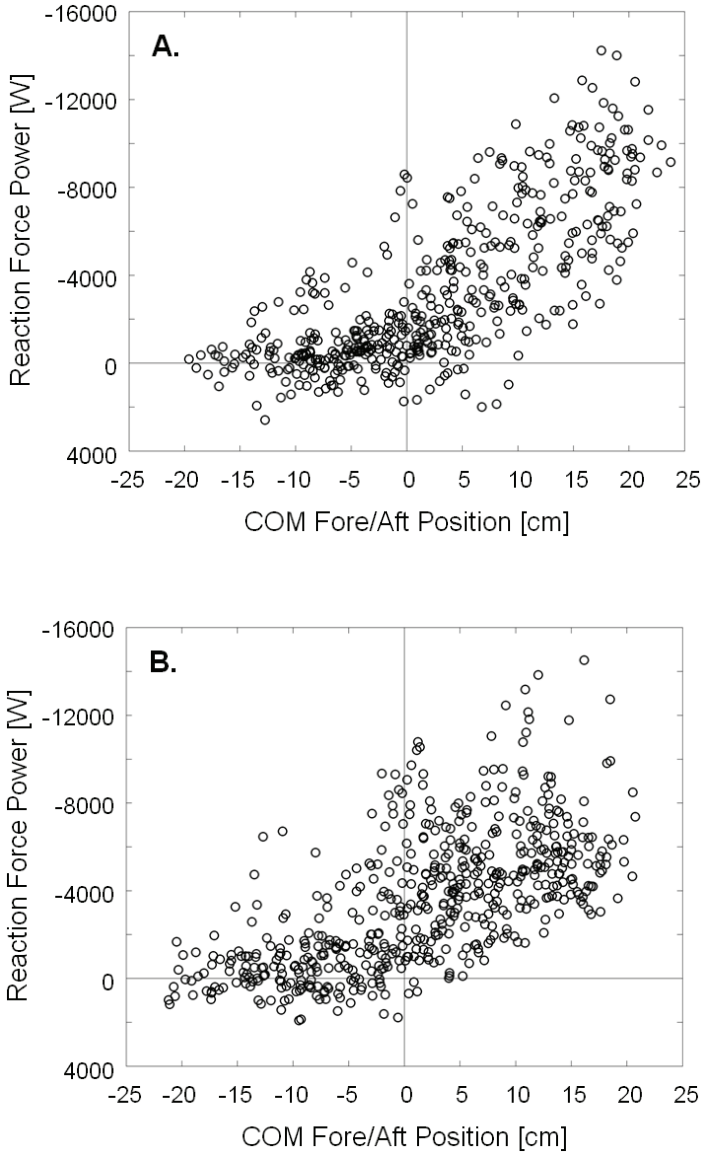

FIGURE 6.42. Center of mass fore/aft position versus snow reaction force power on the 10 m (A) and 13 m (B) courses. Note the inverted y-axis.

and 13 m courses were –.76 and –.64, respectively (Note that the direction of the Y-axes on Figures 6.42 A and B are reversed for presentation purposes).

Instantaneous measures of outside ski attack angle (φ) and reaction force power (P_R) are compared in Figures 6.43 A and B for the 10 and 13 m courses, respectively. Pearson's product moment correlation coefficients were –.49 and –.23 for the 10 and 13 m courses, respectively.

6.7 PERFORMANCE

Skier performance times (PT) through both the analyzed turns and the outer photo cells of the timing system are presented in Tables 6.3 and 6.4 for the 10 and 13 m courses, respectively. To calculate PT for the analyzed turns, virtual start and finish lines were constructed (see p. 162). Spearman's rank correlations of .81 (p=.05) and .77 (p=.07) indicate that although there was some shifting in rankings between skiers through the analyzed sequence, performances were relatively consistent and there were no extreme changes.

Table 6.5 presents the Spearman's rank correlation coefficients of the selected parameters with performance time. Due to the low number of subjects, the scatter plots are also presented for all parameters in Appendix P so that the reader may judge for themselves the possibility of a relationship.

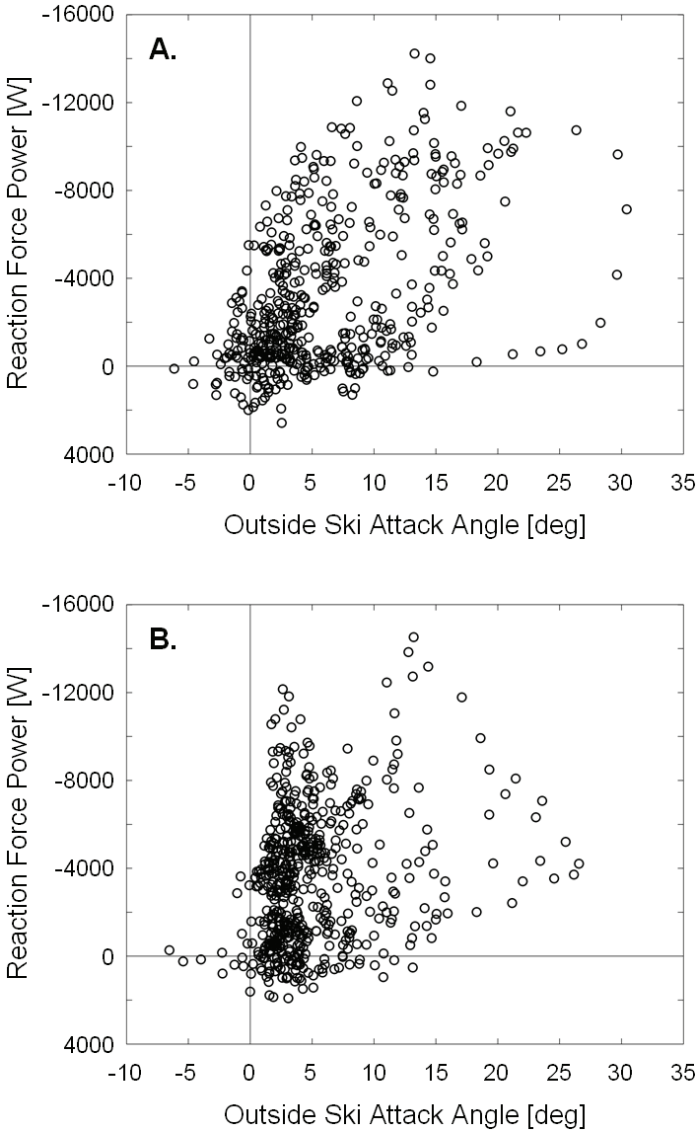

FIGURE 6.43. Outside ski attack angle versus snow reaction force power on the 10 m (A) and 13 m (B) courses. Note the inverted y-axis.

TABLE 6.3. Skier performances in terms of time on the Analysis Section and total time from the first photocell to the last (Figure 5.3) on the 10 m course.

Trial	Subject ID	Analysis Section		Total Time	
		Time [s]	Rank	Time [s]	Rank
1	6	1.85	2	7.80	4
2	7	1.92	4	7.73	3
4	5	1.81	1	7.56	1
5	8	1.93	5	8.03	6
9	9	1.91	3	7.71	2
12	10	1.93	6	7.83	5

TABLE 6.4. Skier performances in terms of time on the Analysis Section and total time from the first photocell to the last (Figure 5.3) on the 13 m course.

Trial	Subject ID	Analysis Section		Total Time	
		Time [s]	Rank	Time [s]	Rank
45	7	1.63	3	8.84	2
46	9	1.62	2	8.77	1
47	5	1,72	6	9.22	5
48	8	1,65	4	9.13	4
49	10	1,68	5	9.30	6
55	6	1,61	1	8.96	3

TABLE 6.5. Spearman's rank correlation coefficients and probability values for correlations with performance time.

Parameter	10 m Course	13 m Course
Mean Fore/Aft Position	.89 (.02)	.77 (.07)
Fore/Aft Range of Motion	.20 (.70)	.26 (.62)
Trajectory Length XYZ	.26 (.62)	.77 (.07)
Trajectory Length Y	.31 (.54)	.83 (.04)
Trajectory Length Z	.83 (.04)	.49 (.33)
Average Speed	–1.00	–.94 (<.01)
Mean Energy Dissipation	.37 (.47)	–.09 (.87)
Mean Air Drag Power	.71 (.11)	.49 (.33)
Mean Reaction Force Power	–.89 (.02)	–.14 (.78)
Mean Initiation Phase Ski Attack Angle	.03 (96)	.20 (.70)
Mean Vertical Amplitude	.83 (.04)	.71 (.11)
Mean Initiation Phase F_{VERT}	.60 (.21)	–.77 (.07)

n = 6

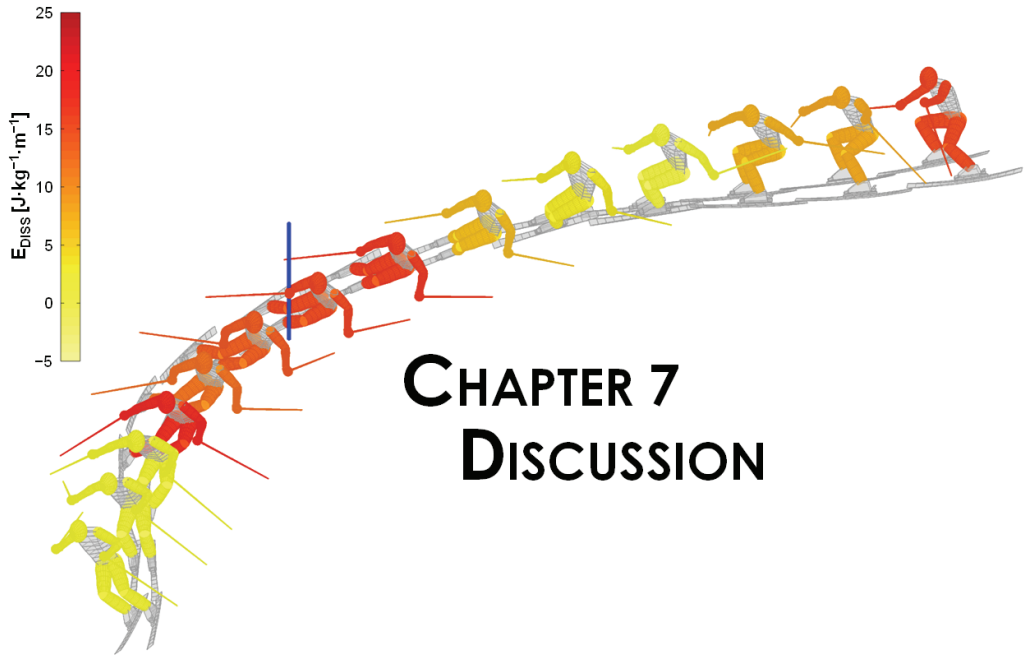

CHAPTER 7
DISCUSSION

CHAPTER 7. DISCUSSION

7.1 INTRODUCTION

In the previous chapter, much of the focus in presenting this investigation's results was on describing the general, average trends that were observed in the kinematic and kinetic data. In this chapter, the focus will now shift to discussing the practical implications of these results. In some cases, individual examples from the data will be presented to compare and contrast different types of skier actions. It is hoped that, in this way, the reader will gain a good overview of the trends seen in the results, but at the same time grasp the extent of individual variability.

In the first section of this chapter, the structure of the turn cycle is discussed and particular attention is directed towards understanding the cause of the difference in structure observed between the 10 and 13 m courses. This is followed by a discussion of outside ski and center of mass trajectory characteristics and how these trajectories interrelate. Characteristics of skier lateral, vertical and fore/aft actions are then discussed with emphasis on trying to understand how these actions may influence the interaction between ski and snow. A description of the external forces acting on the skier is then presented followed by a discussion of skier mechanical energy behaviour, where much of the focus is on identifying potential sources of energy loss as a step

towards understanding how skier technique relates to performance. In addition to identifying potential methodological limitations throughout this chapter, a general evaluation of the methods used in this investigation, along with suggestions for improvement, is presented towards the end of this chapter. Finally, potential areas for future study are proposed.

7.2 SKI AND SKIER TRAJECTORIES (Figure 2.1, Boxes F and G)

An important focus of this investigation has been to understand how the ski's and skier's trajectories interrelate. In the following sections, possible reasons for the observed difference in turn cycle structure between the 10 and 13 m courses are explored. Interesting results concerning ski motion which may have implications for both skier technique and ski design are then discussed. This is followed by a discussion of some of the relationships between ski and skier motion.

TURN CYCLE STRUCTURE

As previously described, the turn cycle was structured according to a three phase system, similar to LeMaster's (1999) approach. Turn cycle descriptive statistics are presented in Figure 6.1. According to the definition used in this study, the Turn Phase accounted for about 50 % of the turn cycle on both the 10 and 13 m courses. However, there was a clear trend of a longer Initiation Phase, and a correspondingly shorter Completion Phase, on the 13 m course. On the 10 m course, the structure of the turn cycle showed a close to symmetrical distribution about the gate which was passed at just over 50 % of the turn cycle, on average. In contrast, the turn cycle on the 13 m course had an asymmetrical distribution about the gate, with approximately 60 % of the turn cycle occurring prior to gate passage, and 40 % after. Despite this asymmetry in the turn cycle taken as a whole, the Turn Phase itself was approximately

symmetrical about the gate on the 13 m course, similar to on the 10 m course. These observations are perhaps particularly interesting since indications of similar trends have been reported by other investigators.

For instance, Müller and coworkers (Müller et al., 2004; Müller & Schwameder, 2003) reported on a kinematic and kinetic investigation where they compared the techniques used by a world class skier performing giant slalom-type turns on carving and conventional equipment. Although they defined the turn structure somewhat differently than in the current study, using Müller et al.'s (1998) system of Initiation and Steering Phases, they found that the Initiation Phase accounted for a greater portion of the turn cycle, and the second Steering Phase (out of the fall line) accounted for a correspondingly lesser portion, when the athlete skied on carving equipment. Considering Müller et al.'s (2004) finding, and that skiers used a greater degree of carving on the 13 m course in this investigation, some of the shift in turn cycle structure observed between courses might be somehow attributable to differences in carving and skidding turn mechanics.

In another example, Laapi (2009) used plantar pressure measurements with synchronized video footage to investigate the timing of snow reaction forces of skilled skiers during slalom race simulations on courses set with 10 and 13 m linear gate distances, a set-up very similar to the current study. To associate pressure measurements with the timing of the turn cycle, the synchronized video footage was was used to identify turn start and end points, as well as the time point of gate passage. In this way, the timing of gate passage as a percentage of the turn cycle could be determined, in a manner comparable to that of the current investigation. In her analysis of 9 athletes and nearly 500 turns, she found that gate passage occurred significantly later in the turn cycle on the 13 m course, concurring with the current study's findings. Although, a potential difference in turn cycle structure was not investigated, the later gate passage on the 13 m course indicates that there may very well have been one.

Why there is a difference in the turn cycle structure between the two courses is certainly an interesting question, the answer to which may help us to understand turning mechanics better. One plausible explanation is that skier trajectories may have been rounder through the Initiation Phase on the 13 m course, relative to the gate positions, a characteristic one might expect with increased carving. In order to explore this possibility, the center of mass trajectory through each turn was graphed relative to the gate position. This allowed the center of mass trajectory data as well as the Switch, Turn Phase Start, and Turn Phase End positions from both courses to be visualized on the same figure relative to the gate position (Figure 7.1).

In examining Figure 7.1, the symmetry of the center of mass trajectory on the 10 m course about the gate, and its asymmetry on the 13 m course, are readily apparent. The primary differences in trajectory appear to be during the first portion of the turn, prior to the gate. After gate passage, the trajectories on both courses are surprisingly similar. While the turn start Switch occurred much higher on the slope on the 13 m course, relative to the approaching gate, the turn end Switches occurred at almost the same location for both courses. This indicates a shift in the Switch position relative to the gates between courses. Switches on the 13 m course occurred at approximately 40 % of the distance between gates in both the X′- and Y′-dimensions. In contrast, Switches on the 10 m course occurred at about 50 % of the distance between gates. This perhaps explains, at least in part, the longer Initiation Phase on the 13 m course. Despite representing a smaller proportion of the turn cycle taken as a whole, the Completion Phase on the 13 m course took place over approximately the same absolute distance as on the 10 m course, and at almost the same position relative to the gate.

These findings naturally beg the question of why the Switches on the 13 m course are shifted relative to the gate positions. As will be seen shortly, this seems to be an important question which will come up repeatedly throughout this chapter.

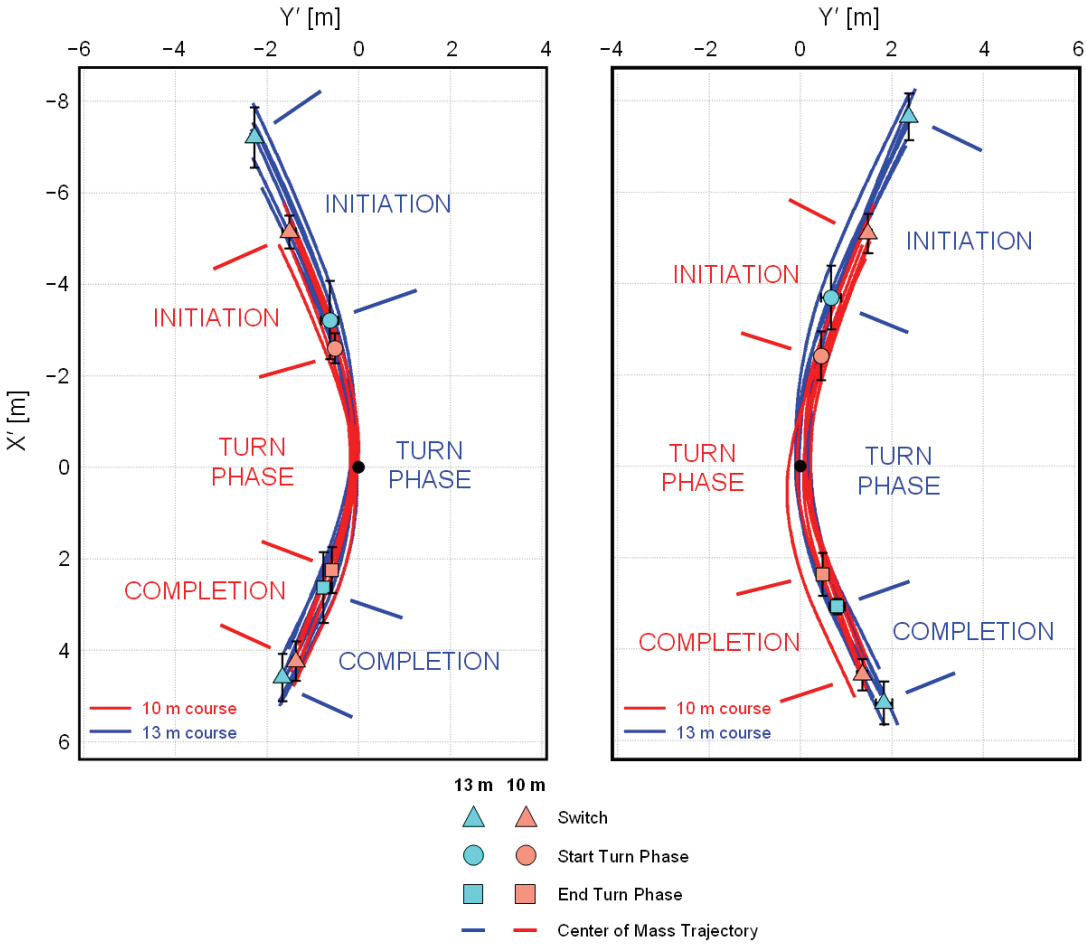

FIGURE 7.1. Center of mass trajectory relative to the gate position over both analyzed turns for the 10 m (red) and the 13 m (blue) courses. Note the elevated Switch and prolonged Initiation Phase on the 13 m course. Also note that, despite the asymmetry of the turn cycle taken as a whole on the 13 m course, the Turn Phase itself was rather evenly distributed about the gate, similar to on the 10 m course.

CARVING AND SKIDDING

In terms of ski motion, the whole ski attack angle (φ) was used in this investigation to describe the overall degree of skidding and carving used by skiers. In addition, local ski attack angles along the length of the ski (φ_E) were calculated to help further our understanding of the mechanics of the transition from skidding to carving as well as groove formation.

WHOLE SKI ATTACK ANGLE

On both courses, there was a relatively large individual variation in the outside ski attack angle, particularly in the Initiation Phase and the first part of the Turn Phase, indicating that some skiers used carving strategies while others chose skidding solutions (see Figure 6.12 and Appendix J). The majority of the analyzed turns involved some degree of outside ski skidding during the first portion of the turn, with some skiers reaching outside ski attack angles as high as 30°. The outside ski then transitioned to carving by about gate passage with all turns being completed at attack angles below 4°.

That skiers used skidding in this investigation is not surprising considering that the experimental set-up was on moderately steep terrain. Sjøstrand (2006) used video recordings to subjectively categorize the top three finishers' turns from eight World Cup slalom races during the 2005/2006 season according to the degree of skidding. Of the over 3000 turns that were evaluated, only 26.8 % were classified as carved, the majority of which took place on either flat terrain or transitions from steep to flat. Seventy-five percent of the turns in medium terrain, which probably corresponds best to the terrain used in the current investigation, involved some form of skidding.

There was a slightly greater degree of skidding on the 10 m course, primarily in the first portion of the turn. However, the average maximum attack angles of 15° and 12°

seen on the 10 and 13 m courses, respectively, are perhaps best described as moderate compared to what can often be observed in typical competition conditions.

LOCAL SKI ATTACK ANGLES

Since the majority of analyzed turns involved a transition from skidding to carving, it is interesting to examine how the pattern of local ski attack angles through this transition changed and to see how well these patterns correspond to the predictions of previous investigations. Using models based on metal cutting theory, Lieu, Mote, and Renshaw (Lieu, 1982; Lieu & Mote, 1985; Renshaw & Mote, 1989) predicted that carving is initiated first at the tail of the ski during the transition from skidding. Their model further predicted that even in its most advanced form, carving is limited to the ski after-body. More recently, there has been a growing body of evidence indicating that the deformation of the ski forebody does not correspond to the ski's trajectory during carving, as thought earlier (Casolo & Lorenzi, 2001; Federolf, 2005; Mössner et al., 2009). This phenomenon has been related to the mechanics of groove formation where the current understanding is that the ski forebody does not carve as it ploughs through the snow surface, generating the groove in which the remainder of the ski will follow (Kagawa et al., 2009; Tatsuno et al., 2009; Yoneyama et al., 2008). These are concepts which, if true, have important implications for skiing technique and equipment development yet are poorly understood amongst practitioners.

To understand the mechanics of the transition between skidding and carving better, the reconstructed ski position data were fit with a 15 segment model of 14 m sidecut radius ski, the dimensions for which were determined from measurements of competitive slalom skis from another study (Laapi, 2009). The trajectories of points along the ski's interacting edge were tracked, and the local ski attack angles at each point were calculated. Local ski attack angle data were averaged according to whole ski attack

angle across all trials and subjects for the Turn Phase of the turn cycle and are presented in Figure 6.14.

Some variability in local ski attack angle patterns was evident, likely due to variation in the mechanical and geometrical properties of the skis used by the athletes as well as irregularities in the ski's motion. In general, however, local attack angles were high along the entire ski when whole ski attack angles were greater than about 15°, indicating that skidding processes dominated. Below this level, local attack angles in the aft-most ski segments reduced while those of the forebody segments remained elevated. Local attack angles of the aft-most segments reached 2° to 5° as whole ski attack angles approached 8°, indicating that these points began carving, in good accordance with Lieu and Mote's predictions (Lieu, 1982; Lieu & Mote, 1985). Further decreases in the whole ski attack angle were associated with increasing numbers of tail segments carving, along with the reduction of forebody segment attack angles. The ski reached an advanced carving stage at whole ski attack angles of approximately 3°, although local forebody segment attack angles remained slightly elevated, indicating that this part of the ski was still machining new snow, also in good accordance with Lieu and Mote's predictions.

These results support the current understanding of ski forebody function (Kagawa et al., 2009; Tatsuno et al., 2009; Yoneyama et al., 2008) and help to explain why the geometry of the deformed ski edge may not correspond directly to the ski's turn radius as predicted in Howe's (2001) equations, a trend which has been seen in several studies (Federolf, 2005; Mössner et al., 2009; Wimmer, 2001). These results also confirm that there is a gradient in local attack angles along the ski's edge, even in advanced stages of carving, a phenomenon thought to be the basis for the ski's self-steering effect (Hirano, 2006; Hirano & Tada, 1996; LeMaster, 1999; Tada & Hirano, 2002).

The reader should bear in mind that the estimates of local ski attack angles reported in this study are limited by the fact that they were not measured directly. Instead, the

trajectories of points along the ski's edge were modelled according to the reconstructed ski tip, ski tail, ski mid and ankle joint center positions as well as average measurements of ski dimensions. Since the ski motion data presented here are perhaps somewhat unique to this investigation, this method's limitations are explored in greater detail here so that the reader is aware of these and thus may better interpret the results.

One limitation is that the reconstructed ski's accuracy is directly dependent upon the accuracy of the reconstructed tip, tail, mid and ankle joint center positions. Digitization of the tail points was at times challenging due to snow spray. Fortunately, the tail was visibile from at least two cameras in the majority of cases. And when visible, the tail was a relatively well-defined point that was readily digitized. At time points where the tail could not be digitized, the object-space coordinates were interpolated using cubic spline functions. As described in the methods chapter (p. 143), the ski mid point was calculated using an estimate of the distance from the ankle joint center to a point on the ski sole. This distance estimate was made based on FIS regulations and obtaining approximately 0 cm ski deformations during the turn transition. However, errors in this estimate will affect the shape of the deformed ski. Despite these difficulties, the relatively low running surface length pooled standard deviation of 11 mm across all trials is a good indication that the reconstructed ski positions were reasonable. Improved accuracy can be obtained in future investigations through the inclusion of an extra camera filming the skis from an overhead view as well as measurement of each individual's skis and the ankle joint center to ski sole distance.

A second limitation is related to the fact that points along the ski's length were constructed using the positions of the aforementioned three points and interpolation. In reality, it is possible for the deformed ski to take on numerous configurations and still pass through the measured points. To give an example of how this might be a problem, using the current investigation's methods vibrations occuring in the ski tip will affect the entire ski's configuration. In reality however, such vibrations may be

limited to the ski shovel. Furthermore, it is known that the configuration of the deformed ski can be influenced by a number of factors including, for example, skier fore/aft positioning (Fauve et al., 2009). When the skier is positioned more foreward, one expects greater ski forebody deformation which would increase the local attack angles along this portion of the ski. Conversely, when the skier is balanced aft, ski forebody deformation should decrease. The method employed in this study is likely to be limited in capturing these subtle changes to the ski's configuration. However, the relatively low running surface length standard deviation does seem to indicate that the reconstructed ski configurations were reasonable, although this is certainly not conclusive evidence.

Although the relatively low sampling rate of 50 Hz used in this investigation (based on the deinterlaced PAL video) may have been adequate to characterize skier motion, it may not have been sufficient to fully capture ski motion. According to the sampling theorem (Robertson, Caldwell, Hamill, Kamen, & Whittlesey, 2004), the 50 Hz sampling rate would have been limited in characterizing components of ski motion exceeding a frequency of 25 Hz. The target point on the ski most likely to be affected by this is the tip which is likely to vibrate as the ski moves across the snow surface.

A fourth limitation is that the employed method did not capture ski torsional deformations since the only points on the ski that were digitized, the tip and tail, were by definition aligned along the ski's longitudinal axis. This is important since torsional deformations will change ski edge point positions from those constructed using this method and will therefore impact calculations of local attack angles along the ski's interacting edge. The size of this error and the degree to which it impacts local attack angle measurements is not known and requires further investigation.

A final limitation of the ski motion data is that it is not known precisely where the ski is in fact in contact with the snow surface. For instance, it is expected that as the ski transitions from skidding to carving, the ski will tilt slightly upwards and some points

along the shovel may lose contact with the snow surface (Lieu & Mote, 1985). To determine more accurately the area of contact between ski and snow, however, would require a more sophisticated method of quantifying the snow surface, perhaps even to the extent of creating new terrain models specific to every trial since the snow surface can be expected to permanently change with each passing skier.

SPEED

Both the outside ski and center of mass speeds demonstrated cyclic fluctuations over the turn cycle. Center of mass speed had average peak-to-peak amplitudes of 0.98 and 0.87 $m \cdot s^{-1}$, on the 10 and 13 m courses, respectively, which corresponds well with Supej et al. (2004) who reported fluctuations in center of mass speed ranging between 0.5 to 1.0 $m \cdot s^{-1}$ in slalom. The skis demonstrated much greater range of speeds than the center of mass (2.54 and 3.00 $m \cdot s^{-1}$ on the 10 and 13 m courses, respectively), confirming Witherell & Evrard's (1993) contention that the skier's feet experience larger speed fluctuations than the center of mass.

Although both the outside ski and center of mass speeds fluctuated in a cyclic manner, the timing of this pattern was slightly shifted between the two (Figure 6.4). While the center of mass reached maximal speeds late in the Initiation Phase, the skis reached peak speeds later, during the middle of the Turn Phase. Additionally, the center of mass typically reached minimum speeds late in the Turn Phase and increased through the Completion Phase. The skis, in contrast, decelerated through the Completion Phase to match center of mass speed by the end of the turn.

This difference in speed pattern between the skis and center of mass unveils an aspect of turning mechanics that, while not complicated, is not immediately apparent either. First, during a turn, both the skis and skier rotate about an axis at the turn's center. For a given angular velocity, points closer to the axis of rotation will have a lower tangential speed than points further away. So, as the skier inclines into the turn, and

the skis take a trajectory further away from the axis of rotation, they can be expected to have a higher tangential speed. Conversely, as the skis come in under the skier's body, and the entire system stops turning, the ski and center of mass speeds should coincide, a pattern that was clearly observed in this study. Furthermore, in addition to rotating about the turn's center, the skis also rotate about the skier's center of mass through the turn. Thus, the ski's tangential speed is a function of both the ski-skier system rotation about the turn center as well as the ski's rotation about the ski-skier system center of mass.

This difference in ski and center of mass speed patterns has important methodological implications. For example, it can be tempting to use ski speed to describe skier performance in order to simplify data collection procedures. The results from this study indicate that careful consideration should be taken when inferring skier performances based upon changes in ski speed, particularly at time points when the center of mass and skis are on different trajectories.

That being said, the time course of ski speed observed in this study was strikingly similar to data reported by other investigators. In their 2-dimensional study of ski kinematics, Nachbauer and Förg-Rob (Förg-Rob & Nachbauer, 1988; Nachbauer, 1987a, 1987b) reported peak ski speeds occurring shortly after the start of the steering phase and minimum speeds at the turn transitions. Although Goodwin (1990a; 1990b) only reported the results of a part of a turn, the pattern of ski speed increase through turn initiation and the middle of the turn reported in his study seems to correspond well with the current study's results, as well. Sahashi and Ichino (1998) also observed a pattern of ski speed similar to the current investigation's, with minimum speeds at turn transitions and peak speeds occurring at about the apex of the turn.

Not all reports show this trend in ski speed, however. Wimmer (2001) used video-based motion analysis to examine the ski speeds of world cup skiers performing giant slalom turns. His data showed increasing outside ski speed through turn transitions

with a peak relatively early in the turn cycle—a pattern more reminiscent of this study's center of mass speed pattern. Considering this result, it may be that outside ski and center of mass trajectories follow each other more closely in long-radius turns, and therefore have more similar speed patterns in comparison to short-radius, slalom turns.

There were also some more subtle differences of interest in ski and center of mass speeds between the 10 and 13 m courses. While the center of mass speed fluctuation amplitudes were similar between courses, the skis had a larger amplitude on the 13 m course. This greater disparity between center of mass and ski speeds on the 13 m course might be indicative of a greater divergence between the ski and skier trajectories. This would make some sense considering the greater center of mass inclination angles measured on the 13 m course and the longer distances measured between center of mass and the outside ankle joint center (D_{AJC}).

TURN RADIUS

On the 10 m course, the center of mass turn radius (R_{COM}) rapidly decreased through the Initiation Phase as skiers began turning. During the middle of the turn cycle, the center of mass traced a somewhat circular trajectory with R_{COM} ranging between 6 and 8 m for a period of about 28 % of the turn cycle duration, or about 0.23 s. This corresponds well with Supej et al. (2004) who also described relatively constant R_{COM} during the middle of the turn. On the 13 m course, a more gradual decrease in R_{COM} was seen, accompanied by a somewhat delayed onset of the Turn Phase relative to the turn cycle, as described previously. Despite the Turn Phase accounting for similar proportions of the turn cycle on both courses, the center of mass trajectory was circular for only 14 % of the turn cycle on the 13 m course (or about 0.13 s) but with similar R_{COM} to the 10 m course, ranging between 6.5 and 8.5 m.

In studying the individual graphs of turn radii (Appendix H), it is readily apparent that the outside ski begins high intensity turning prior to the center of mass, confirming

both LeMaster's (1999) and Morawski's (1973) observations that the skis turn before the skier. During the middle of the Turn Phase, both the center of mass and skis have approximately the same turn radius, indicating that they turned at about the same rate, corroborating Sahashi and Ichino's (1998) prediction. At the end of the Turn Phase, the skis continued to turn after the center of mass trajectory straightened, which may correspond with the need to generate the ski and center of mass trajectory divergence required for the skier to cross over and incline into the following turn (Bear, 1976; Joubert, 1978/1980; LeMaster, 1999; Major & Larsson, 1979/1979; Morawski, 1973; Witherell, 1972; Witherell & Evrard, 1993).

While the outside ski experienced high intensity turning over the majority of the turn cycle (and in some instances starting prior to the Switch), the center of mass experienced high intensity turning for only about the middle 50% of the turn cycle. This can be seen in Figure 7.2 and in Appendix H where the outside ski and center of mass trajectories are plotted and colored according to turn radius. While the center of mass went straight for significant portions of the turn cycle, as indicated by the black portions of the trajectory, the outside ski turned relatively intensely from almost Switch to Switch. Taken together, these results suggest that during the Completion and Initiation Phases, the skier and skis are to a certain extent uncoupled as the skis turn and the skier travels in a straight trajectory. Conversely, during the Turn Phase, the skier and skis are linked and, for at least a portion of the Turn Phase, turn as a single unit.

When examining the individual plots of outside ski turn radius, large intermittent fluctuations are apparent, particularly on the 13 m course (see Figure 6.5 and Appendix H). That these disturbances in ski trajectory did not occur to the same degree on the 10 m course seems counter-intuitive knowing that there was a greater degree of skidding on the 10 m course. This result is perhaps particularly striking considering that other researchers have also observed possibly related phenomena when studying carved

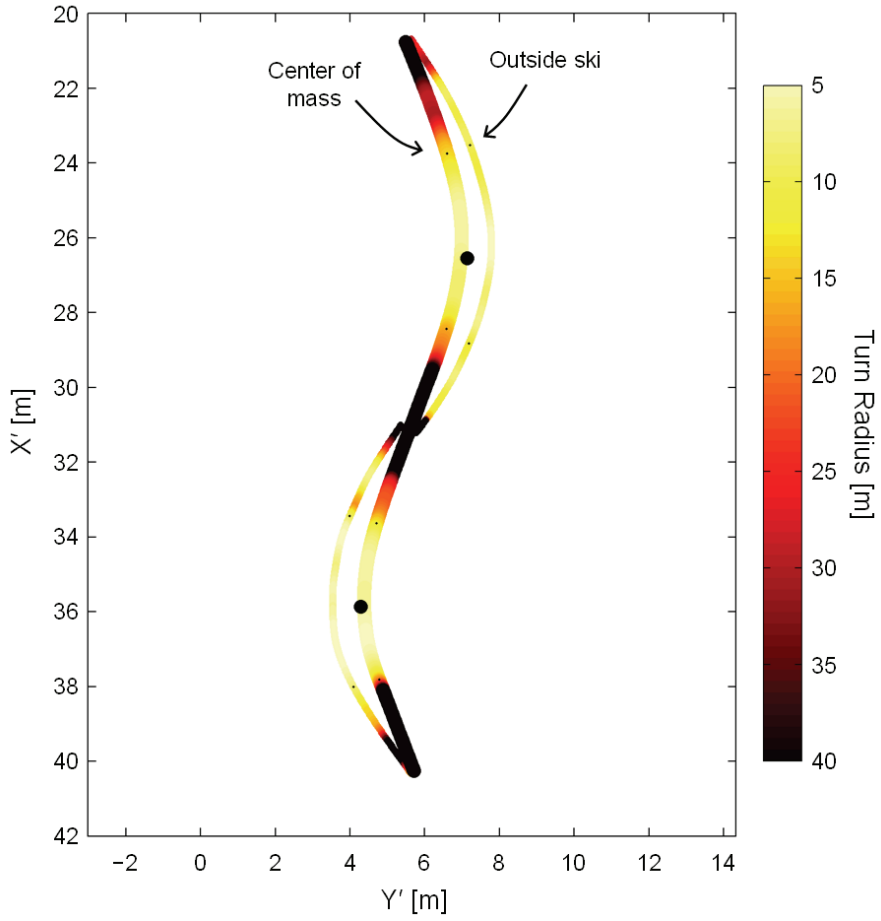

FIGURE 7.2. Example center of mass and outside ski trajectories through the two analyzed turns taken from a trial on the 10 m course. Trajectories are colored to indicate turn radius parallel to the snow surface. Note that while the outside ski turns nearly continuously, the center of mass has a prolonged phase with little or no turning.

turns. Of particular note, Federolf (2005) observed times where the outside ski reduced turning in the first portion of the turn in his kinematic analysis of carving ski trajectories. Furthermore, in their comparison of an athlete skiing on carving and conventional equipment, Raschner and colleagues (Müller et al., 2004; Müller & Schwameder, 2003; Raschner et al., 2001; Schiefermüller et al., 2005) reported irregular force-time curves when skiing on the carving equipment, in contrast to when skiing on the conventional equipment, a finding that they attributed to repeated lateral skidding. Understanding the cause of this phenomenon, and why it occurred to a greater extent on the 13 m course than the 10 m course in the current investigation, can give insight into not only skiing technique but also ski design issues.

One obvious explanation for these occurrences could simply be that irregularities in the snow surface interfered with the ski's trajectory. If this were the case, then one might expect these intermittent disturbances to occur at approximately the same location on the slope, i.e., skiers hitting the same bump on the snow surface. To examine this possibility, outside ski trajectories were plotted for the analyzed turns and colored according to turn radius in Figures 7.3 and 7.4.

One of the first things to notice when examining these figures is the absence on the 10 m course of the dark black coloring during the turn that indicates the ski has reduced turning substantially. When examining the 13 m course graphs, it appears that the positions associated with reduced turning were grouped around two locations in each of the analyzed turns; one grouping at approximately the transition from the Initiation Phase to the Turn Phase and the other grouping just prior to gate passage. Within each grouping, these occurrences are certainly close enough in space that they could be associated with snow surface irregularities. Unfortunately, the method employed to measure the snow surface geomorphology did not have sufficient resolution to capture this level of detail in the snow surface characteristics. Although this explanation cannot be ruled out, the spacing between the affected portions of the ski trajectories is also

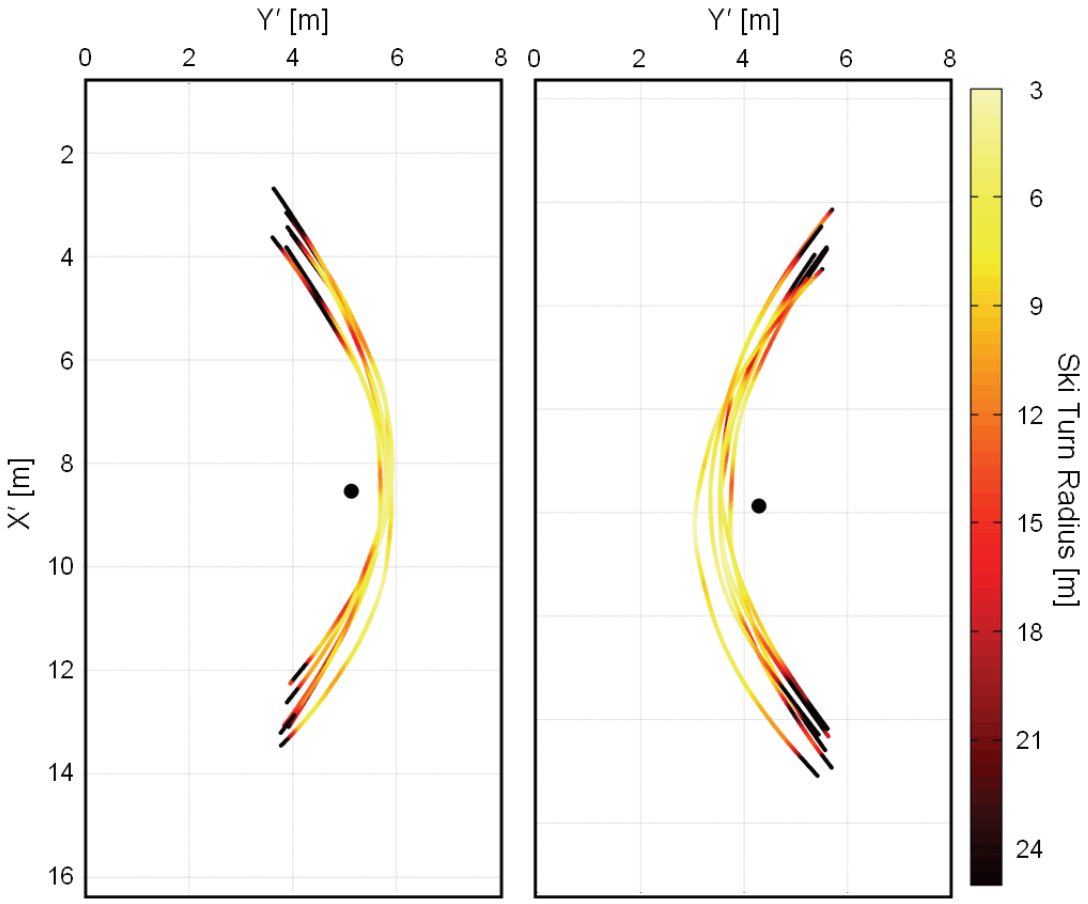

FIGURE 7.3. Outside ski trajectories on the 10 m course for all six trials and both turns. The trajectories are color coded to indicate ski turn radius. The black dot indicates the gate position.

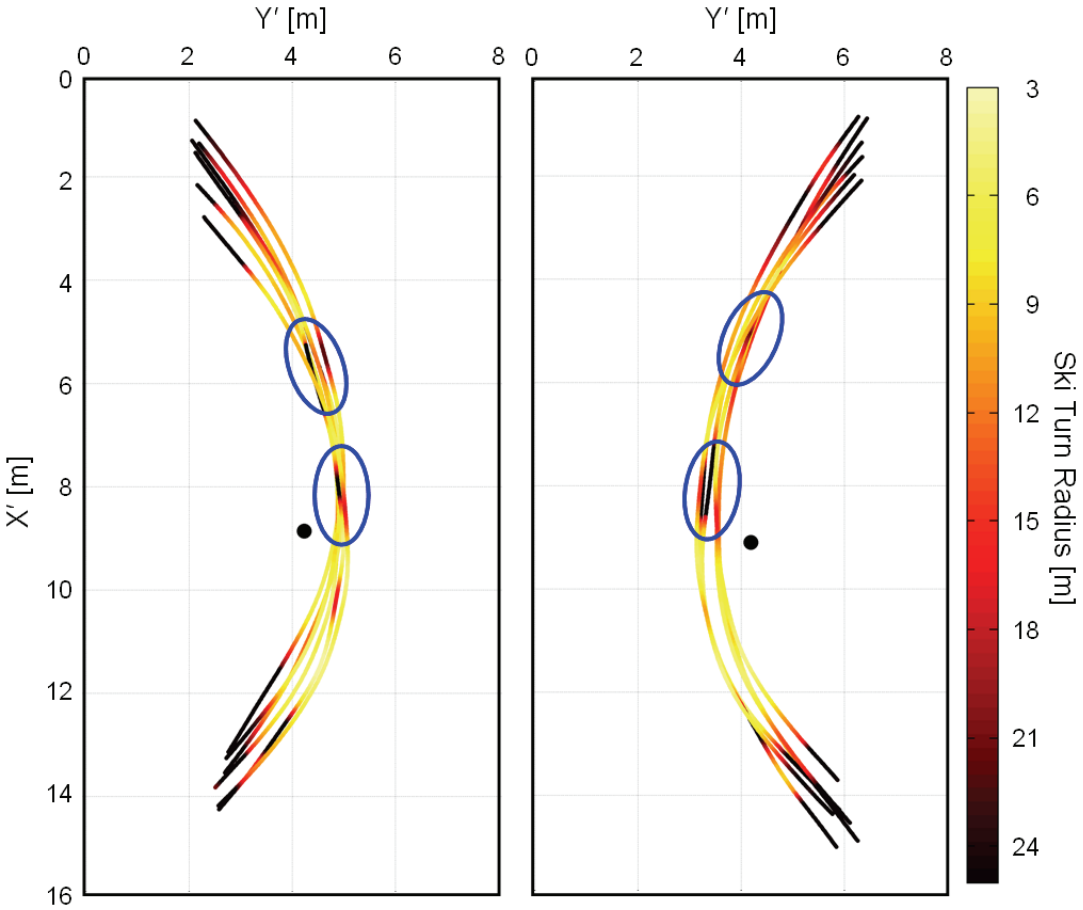

FIGURE 7.4. Outside ski trajectories on the 13 m course for all six trials and both turns. The trajectories are color coded to indicate ski turn radius. The black dot indicates the gate position. Note the two groupings of disturbances indicated by the blue ovals.

large enough (between 5 and 50 cm) that there may be other explanations worth exploring.

For instance, the fact that these disturbances occured to a greater extent on the 13 m course seems to suggest that differences in carving and skidding ski-snow interaction mechanics may help to explain their occurrence. An important difference between carving and skidding ski mechanics is the process of groove formation. When carving, the relatively soft ski shovel vibrates back and forth in flexion and torsion as it digs the groove in which the remainder of the ski will follow.

During the first, Immersion Phase of this project, high-speed video was used to help visualize this ski motion. Certain situations were observed where the shovel of the ski could be seen vibrating and then, when on a swing towards the outside of the turn, catching in the snow and redirecting groove formation towards the outside of the turn. The remainder of the ski continued to carve, following in the redirected groove. Such a mechanism might explain why the ski momentarily increases turn radius as well as why this phenomenon may occur to a larger degree during carved turns.

An example of this phenomenon for a carving ski is given in Figure 7.5 which shows a photo sequence generated from high-speed video taken during a women's World Cup giant slalom. In Frame A, the outside ski is carving and a portion of the shovel is not in contact with the snow. From Frame A to C, the ski shovel vibrates and swings towards the outside of the turn. The shovel reaches the snow surface in Frame C and engages in the snow. The ski then resumes carving along a new trajectory in Frames D and E. It is interesting to note that the increased distance between the skier's feet over the course of the sequence may also be an indication that the outside ski has come onto a new trajectory.

An important prerequisite for this mechanism is that some portion of the shovel must disengage from the snow surface so that it is free to vibrate. This can be seen in Figure

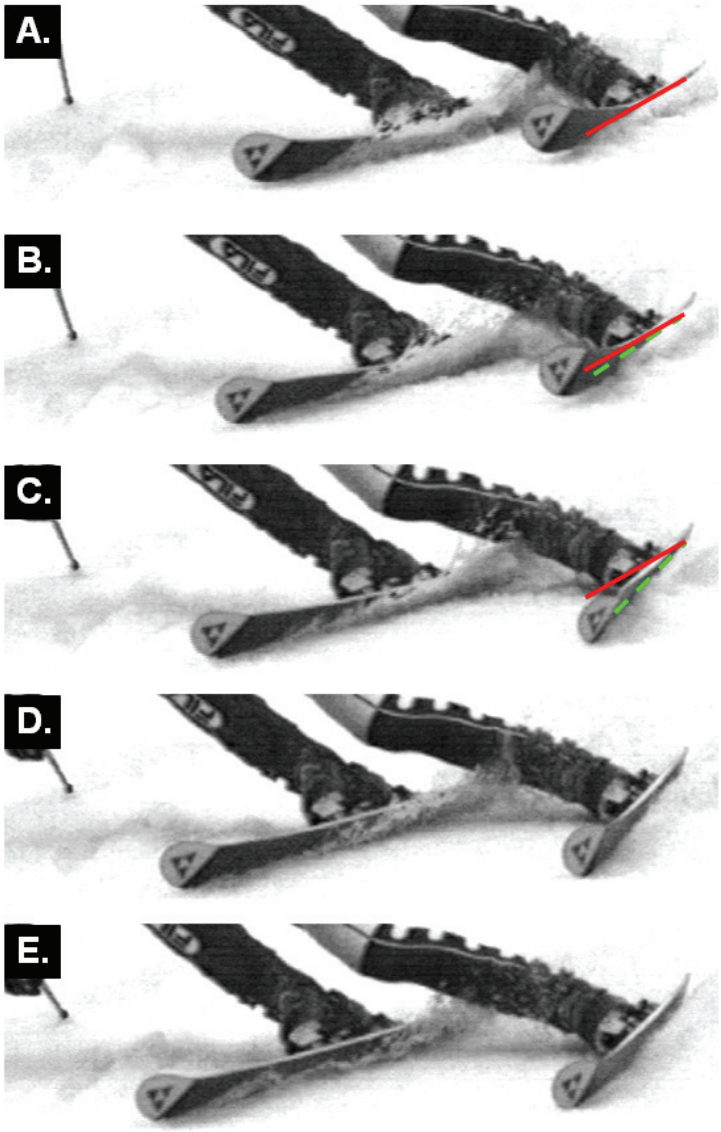

FIGURE 7.5. High-speed video footage of a carving ski experiencing a disturbance possibly similar to that oberved in this investigation. This video, taken during the women's World Cup giant slalom at Åre in March, 2006, was filmed using an Olympus i Speed camera (Olympus Corporation, Tokyo, Japan) at 1500 fps. The solid red line indicates the approximate ski orientation in Frame A, while the dashed green line is used to help the reader visualize the change in ski orientation.

7.5, Frames A and B. According to the work of Lieu and Mote (Lieu, 1982; Lieu & Mote, 1985), one mechanism for this loss of contact might be that in the process of groove formation, the ski tail is expected to penetrate deeper into the snow surface than the ski shovel. Lieu and Mote predicted that this would tilt the ski slightly, lifting some portion of the shovel away from the snow surface. This portion of the shovel is then free to vibrate in flexion and torsion.

That there are two groupings of disturbances in each turn, and the fact that these groupings appear very similar in both turns on the 13 m course, also suggest that these disturbances may be due to something other than merely irregularities in the snow surface. To further explore the disturbances occurring early in the turn, graphics were generated of the ski's motion from two examples on the 13 m course which are described here.

Figure 7.6 shows the motion of a carving ski that experienced a substantial increase in turn radius at about the 30 to 40 % increment of the turn cycle (indicated by marker A on Figure 7.6) on the 13 m course. This disturbance in ski motion was accompanied by an increase in center of mass turn radius and an associated unloading in the vertical component of the snow reaction force. The ski's attack angle first reduced and then increased as the ski resumed turning. Similarly, the rate of ski edge angle increase during the Initiation Phase slowed during the disturbance and then increased again as the ski resumed turning. Interestingly, this change in ski motion occurred right at the transition from the Initiation Phase to the Turn Phase and was associated with a decrease in ski deformation, as can be seen in Figure 7.6 at the 38 % mark. That a number of parameters showed changes associated with the ski's disturbance, some of which were characteristics of skier actions, opens the possibility that the increase in the ski's turn radius may have been purposefully induced by the skier, although probably not at a conscious level considering the short time frame over which these actions took place. For instance, the timing of the disturbance immediately prior to the start of the

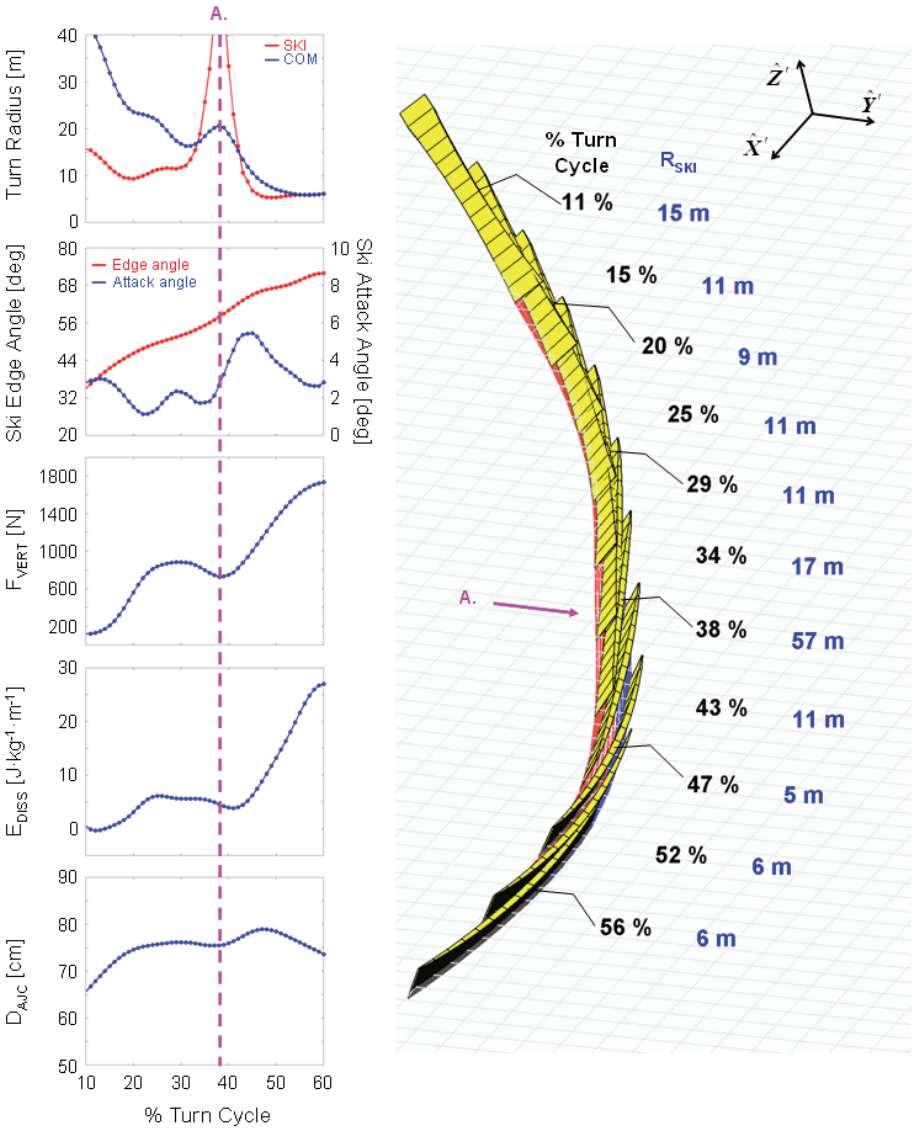

FIGURE 7.6. An example of a carving ski on the 13 m course that experiences a disturbance in its trajectory early in the turn (in the early grouping). The point marked A indicates the location of the disturbance. Note how the ski loses its deformation at about the 38 % point of the turn cycle, corresponding well with the high speed video images shown in Figure 7.5.

Turn Phase might indicate that the skier intentionally reduced the ski's self-steering effect to time the start of the high intensity turning of the Turn Phase to the desired position on the hill relative to the up-coming gate. That the center of mass trajectory was not disturbed to an equal extent as the outside ski seems to suggest that the skier may have been supporting himself at least partially on the inside ski. The role of the inside ski in these occurences is therefore in need of further investigation.

Figure 7.7 shows a second example of a ski that experienced a disturbance over the 35 to 45 % interval of the turn cycle (indicated by marker A). The disturbance in this example also occurred at the transition from the Initiation Phase to the Turn Phase. In this case however, the ski was skidding slightly when the disturbance occurred. The increase in ski turn radius was much smaller than in the previous example, and was accompanied by an increase in the vertical component of the snow reaction force (as opposed to the decrease observed in the previous example). In this turn, the disturbance did not seem to interfere with the center of mass trajectory.

That this disturbance was accompanied by a decrease in ski attack angle as well as mechanical energy dissipation, suggests the possibility that it may somehow be associated with the mechanics of transitioning from skidding to carving. In practice, a skidding outside ski can sometimes be observed to rotate towards the outside of the turn, presumably aligning its longitudinal axis with its velocity vector. The reduction in ski attack angle observed in this example may be indicative of such a mechanism where the ski aligned itself with its velocity vector during the transition to carving, and that during this process its turn radius was temporarily increased.

Figure 7.8 shows an example taken from high speed video of a ski possibly undergoing a similar mechanism while making the transition from skidding to carving. In Frame A, the outside ski is skidding and the vibrating tip has swung towards the inside of the turn. Over the course of Frames A to C, the shovel swings back to the outside of the turn and engages in the snow at Frame C. Note again the loss of ski deformation in

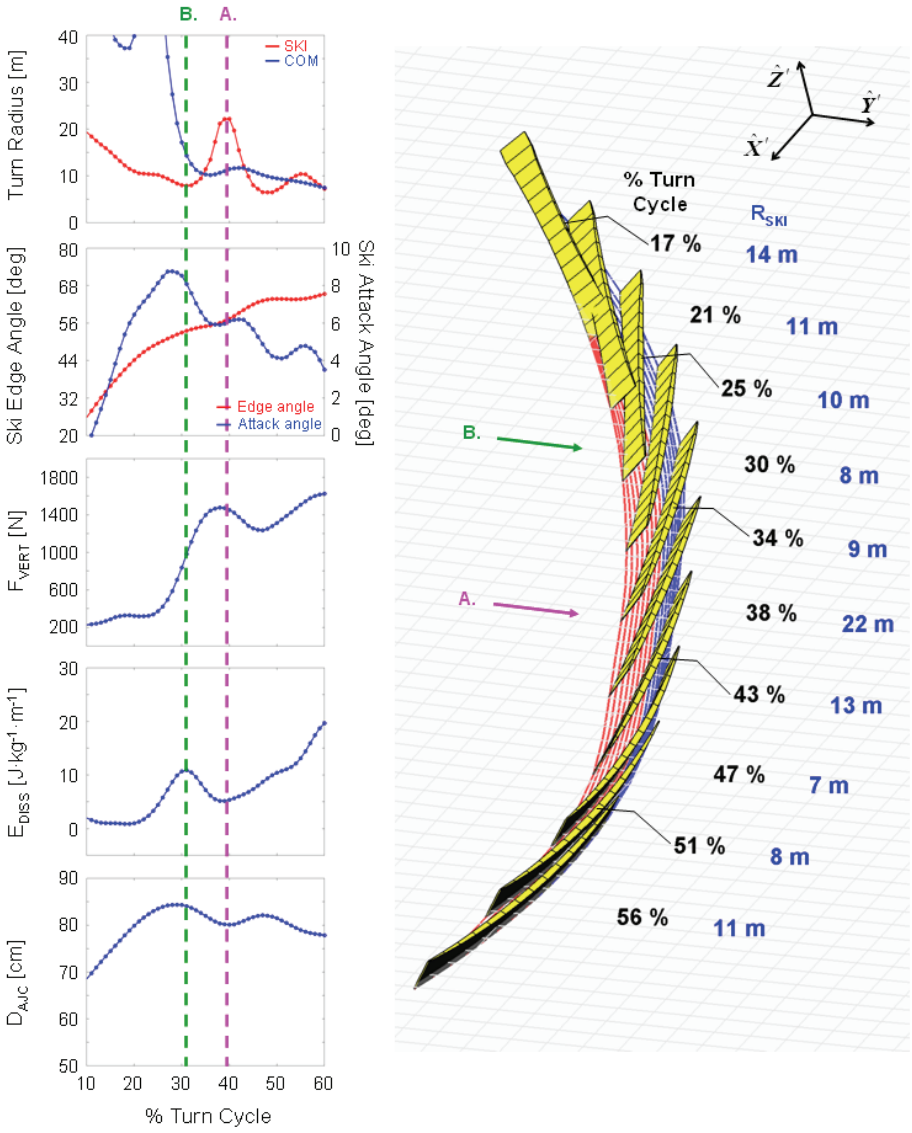

FIGURE 7.7. Example of a skidding ski on the 13 m course that experiences a disturbance in its trajectory early in the turn (in the early grouping). The point marked A indicates the location of the disturbance. The point marked B indicates the location of increased energy dissipation. Note the loss of ski deformation at the 38 % mark.

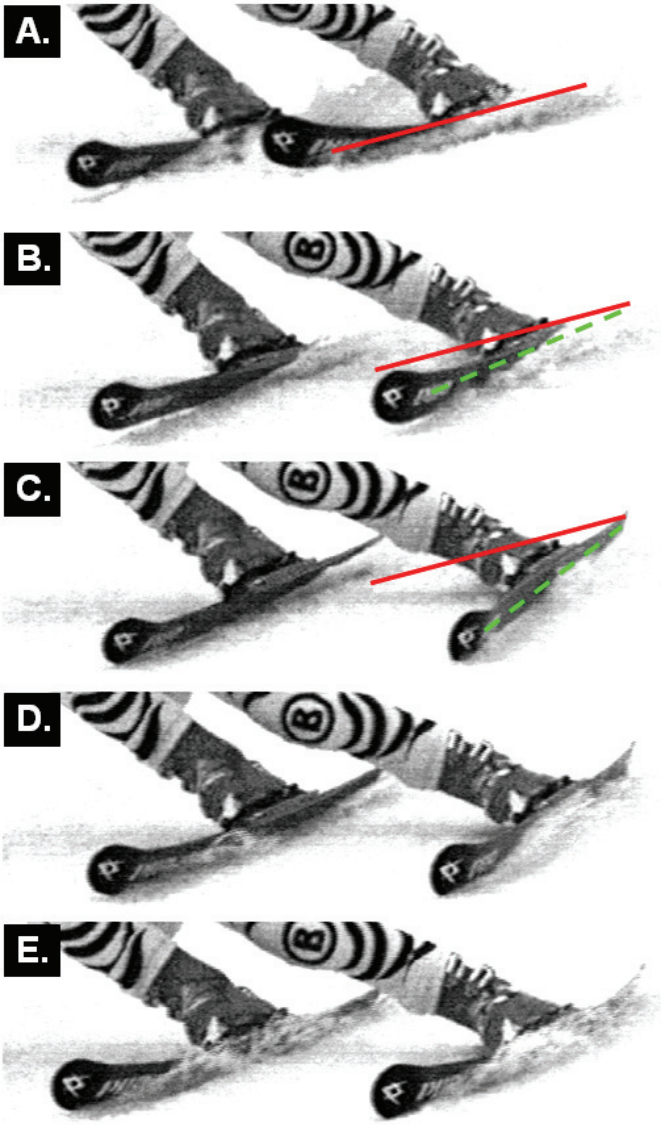

FIGURE 7.8. High speed video footage of a skidding ski (Frame A) making the transition to carving (Frame D). The video was taken from the women's World Cup giant slalom at Åre in March, 2006 using an Olympus i Speed camera (Olympus Corporation, Tokyo, Japan) and filming at 1500 fps. The solid red line indicates the approximate ski orientation in Frame A, while the dashed lines are used to help the reader visualize the change in ski orientation.

Frame C and how this could correspond to the loss of deformation at the 38 % mark of Figure 7.7. In Frames D and E (Figure 7.8), the ski then begins carving along a new trajectory.

The latter grouping of disturbances occurred well into the Turn Phase, just prior to gate passage on both turns of the 13 m course. While the aforementioned mechanisms could certainly also be the cause of these disturbances, their proximity to the gate is interesting. In fact, of the 12 analyzed turns on the 13 m course, all of them showed some form of disturbance at gate passage (Appendix H) which seems to suggest that somehow interference associated with passage of the gate is certainly another plausible mechanism worthy of further investigation.

An example of this type of disturbance taken from the 13 m course is shown graphically in Figure 7.9, where the ski reduces turning over approximately the 40 to 60 % interval of the turn cycle. In this case, a rather large increase in outside ski turn radius was associated with an increase in center of mass turn radius as well. This increase was also reflected in an unloading in the vertical component of the snow reaction force. It is likely that this reduction in loading was associated with the skier's vertical actions as indicated by the decrease in the center of mass to outside ankle joint center distance (D_{AJC}), although on the basis of this investigation it is not possible to clarify to what extent this was intentional on the athlete's part. Note as well the loss of ski deformation at about the 52% mark.

The significance of the positioning of this occurrence relative to the gate becomes apparent if one compares this ski's trajectory, relative to the gate, with the ski trajectories from the 10 m course. To help visualize this, the trajectories of the outside skis from the second, left-hand turn on the 10 m course were translated and rotated to allow plotting in Figure 7.9 (the thin black lines). Viewed in this way, it is apparent that

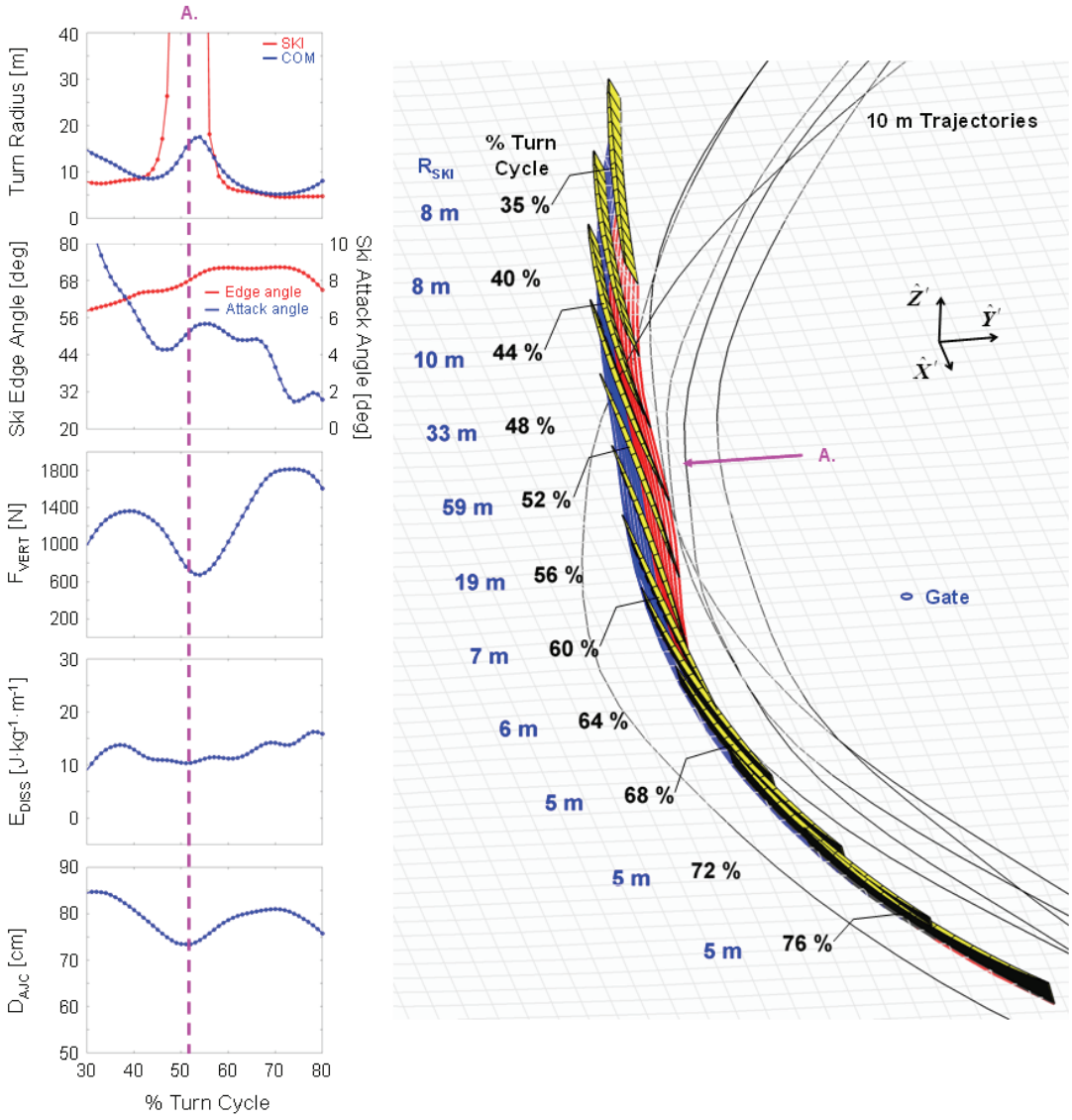

FIGURE 7.9. Example of a ski on the 13 m course that experiences a disturbance in the lower grouping, near the gate. Note how the change in ski deformation during the disturbance is similar to that observed with high speed video (Figures 7.5 and 7.8). The thin black lines indicate ski trajectories from the 10 m course, relative to the gate.

the disturbance in the 13 m course ski's trajectory occurred about where its trajectory met the "virtual" trajectories[11] from the 10 m course.

This phenomenon is not unique to this particular example. Figure 7.10 shows the outside ski trajectories from all trials and both courses relative to the gate. The timing of the lower grouping of ski disturbances, indicated by the green ovals, matches well the position where the 13 m course trajectories meet those from the 10 m course. Again, of the 12 analyzed turns on the 13 m course, all of them showed some form of disturbance at this "meeting" point, although not all to the same extent as that in the example given in Figure 7.9.

The possibility that these ski disturbances occurred at the trajectory "meeting" point by coincidence cannot be ruled out in this investigation. However, there is some further evidence that suggests that this is a topic for further research. Upon examining Figure 7.10, the asymmetrical nature of the outside ski trajectories during the first part of the turn on the 13 m course is readily apparent when compared to the trajectories of skis from the 10 m course. At the same time, the similarity of their trajectories in the latter portion of the turn is also noticeable. The disturbances to the skis on the 13 m course appear to occur during the transition from the asymmetrical portion of the turn to that which matches the 10 m course trajectories. This is perhaps a significant observation if one considers that skiers used the same skis on both courses, as will be explained.

Figure 7.11 contrasts the outside ski edge angle and turn radius of two turns taken from the 10 and 13 m courses. The x-axis in this case is distance relative to the gate in the X′-dimension (parallel to the average direction of the course). As an indicator of

[11] The term "virtual" is used here to emphasize that the trajectories did not actually "meet" in the object-space. In these graphics, the 10 m course ski position data have been translated and rotated to the 13 m course reference frame, using the gate as a common reference point, to allow for comparisons of ski trajectories between courses. In fact, not only was the 10 m course skied after the 13 m course, the analyzed turns were placed at an entirely different location in the object space.

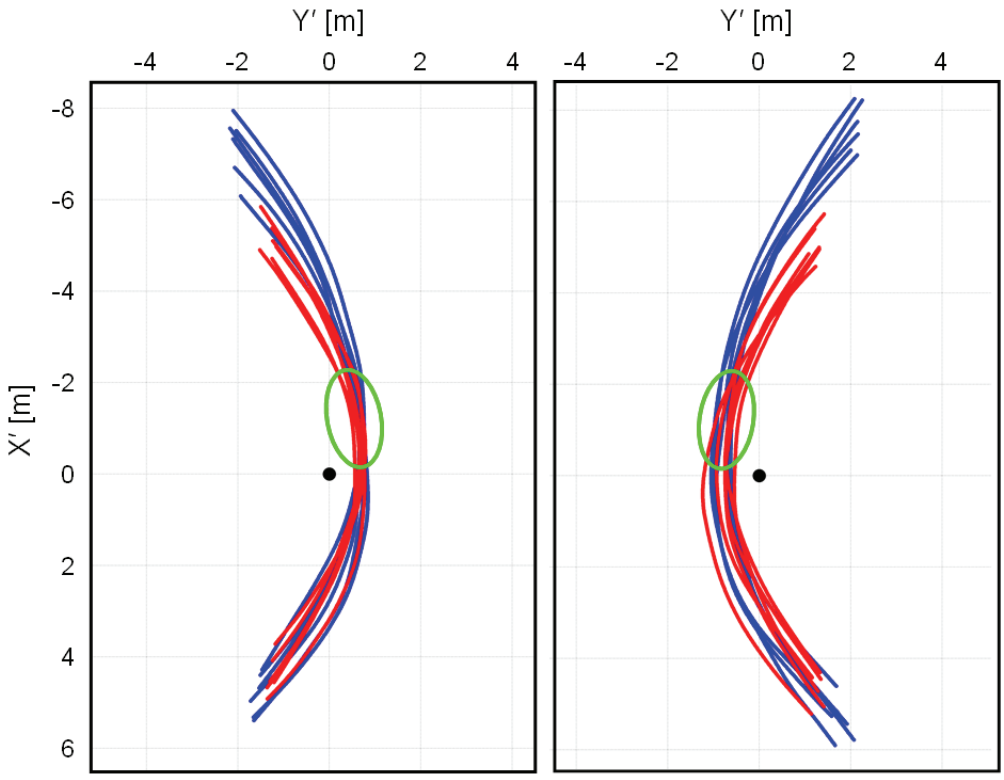

FIGURE 7.10. Outside ski trajectories from both the 10 m (in red) and the 13 m (in blue) courses. The green oval indicates the location of the lower grouping of trajectory disturbances on the skis from the 13 m course. Note the asymmetry in the upper half of the turn for skis on the 13 m course and how the disturbances appear to occur at the shift to a trajectory that is similar to that on the 10 m course.

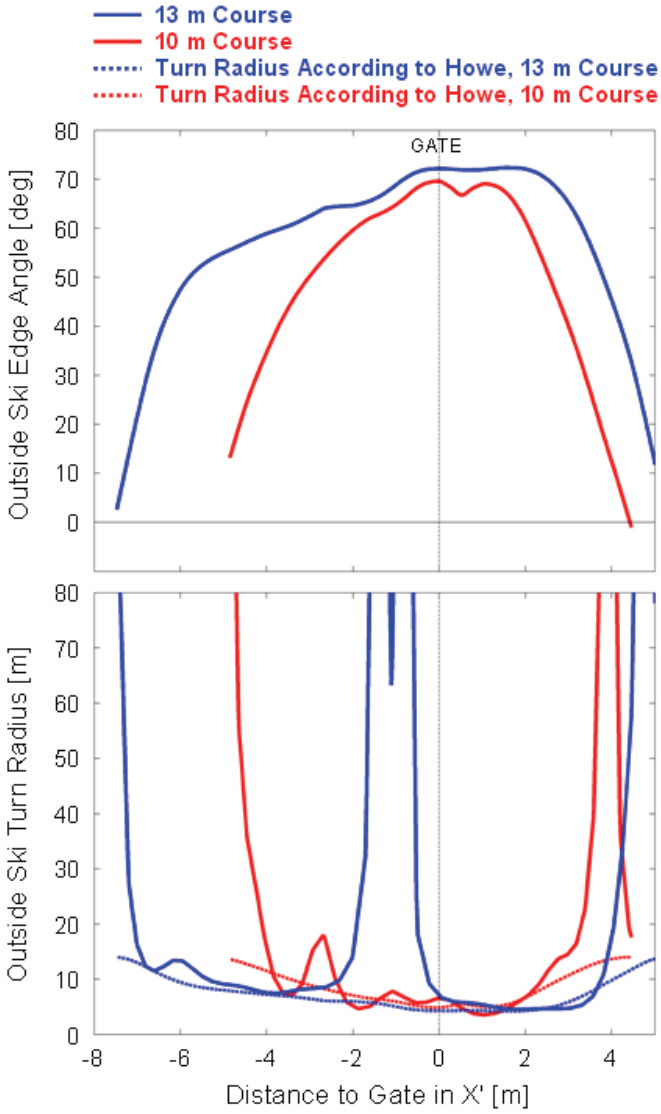

FIGURE 7.11. Outside ski edge angle (upper panel) and turn radius (lower panel) for sample turns from the 10 m and 13 m courses in red and blue, respectively. The dashed lines indicate ski turn radius estimated according to Howe's (2001) Equation [3.6].

how the ski might be expected to turn according to its geometric properties alone, turn radius derived from Howe's (2001) equation relating edge angle, sidecut radius, and turn radius (Equation [3.6]) is also shown. Note how much higher on the slope relative to the approaching gate that the outside ski is edged and turning on the 13 m course. That the measured turn radius was relatively close to that predicted by Howe's equation seems to indicate that the ski turned close to its potential given its edge angle and geometry. It may be that the 13 m ski in Figure 7.11 (which, coincidentally, is the same ski shown in Figure 7.9) turned too much, too early, and that the disturbance measured in ski turn radius was actually a result of having to reorient the ski onto a new trajectory to avoid skiing on the wrong side of the gate.

That the ski seems to be re-oriented "en masse," as opposed to evenly down-regulated over the entire Initiation Phase, is perhaps a significant observation that may have implications for ski design. In fact, it may be that down-regulating the ski's self-steering effect is more limited than traditionally thought and that the observed increases in turn radius actually occurred as a result of the ski being re-directed onto a new orientation and trajectory so as to avoid turning too much, too soon, relative to the gate.

Another possibility is that the second grouping of disturbances may correspond with the transition from down-regulating the ski to allowing it turn to its full potential as determined to a large degree by its physical characteristics and deformed shape on the snow surface. Such an explanation may also explain why the ski trajectories on both courses are similar during the latter portion of the turn. Taking this line of thinking further, the reason why these disturbances do not occur on the 10 m course to the same extent as on the 13 m course may be because the ski's trajectory on the 10 m course more closely matches its physical characteristics so that the skier does not have to down-regulate the ski as much.

The earlier Switch relative to the approaching gate on the 13 m course is perhaps a factor to consider in this discussion. It may be that the elevated Switch forced skiers onto trajectories that did not match their skis' physical and geometrical characteristics. An important question in this connection is if the elevated Switch is the result of an error on the skier's part or a consequence of the situation (gate positions, speed, ski and snow characteristics, etc). In other words, if more skilled skiers had been analyzed, would they have had lower Switches compared to the investigated group on the 13 m course? This question obviously cannot be answered based on this investigation's results and points to an important limitation of this study. However, even if better skilled skiers were able to place the Switch at the halfway point between gates (such as was the case on the 10 m course), the absolute distance to the approaching gate would still be greater on the 13 m course. This means that it is likely that, even with a lower placement of the Switch, skiers would still have been forced to somehow down-regulate the ski during the Initiation Phase on the 13 m course, albeit probably to a lesser extent. This is clearly a topic requiring further investigation.

7.3 SKIER ACTIONS (Figure 2.1, Box H)

In this investigation, aspects of skier lateral, vertical and fore/aft actions were examined. The remaining category, skier rotary actions, was not examined in this study and is therefore not discussed here.

LATERAL ACTIONS

One important goal of skier lateral actions is to regulate the ski edge angle (Howe, 2001; Joubert, 1978/1980; LeMaster, 1999; Lind & Sanders, 2004; Witherell, 1972). In general, the outside ski edge angle (θ) increased rapidly through the Initiation Phase and the first portion of the Turn Phase, reaching maximum values as high as 76^{o} at, or just after, gate passage. Edge angles were greater throughout the turn cycle on the 13 m

course, particularly in the latter half of the turn where differences averaged between 4° and 9°. Raschner et al. (2001) reported maximum edge angles of between 65° and 70°, but in longer radius turns than the ones examined in this study. Interestingly, they observed greater edge angles in the carving technique, a finding that seems to correspond to this investigation's findings on the 13 m course where there was a greater degree of carving.

Center of mass inclination (ς), hip angulation (κ), and knee angulation (η) are skier lateral actions that regulate the ski edge angle. Figure 7.12 provides an individual example showing the relationship between angulation, inclination, and ski edge angle. In a number of the analyzed turns, knee angulation accounted for the majority of the ski's edge angle at the Switch and the first moments of the turn cycle, corresponding to Supej, Kugovnik, and Nemec's (2005b) measurements as well as LeMaster's (1999) observations. However, hip angulation and center of mass inclination almost immediately assumed greater roles, with inclination appearing to be the primary contributor to ski edge angle over the majority of the turn cycle, confirming Witherell's (1972) view and Morawski's (1973) findings. The regulatory role of knee angulation was readily apparent in some turns, such as in Figure 7.12, where small changes in knee angulation are reflected in ski edge angle changes.

From a practitioner point-of-view, a somewhat surprising result in terms of skier lateral actions was the pattern of hip and knee angulation actions during the latter portion of the turn cycle. From about gate passage, there was a general trend of increasing hip angulation, with a particularly rapid increase during the Completion Phase on both courses. Knee angulation, which remained relatively constant at about 5° throughout the Turn Phase, rapidly decreased during the Completion Phase, reaching negative values as large as –20° by the end of the turn cycle, indicating that knee angulation acted to reduce ski edge angle.

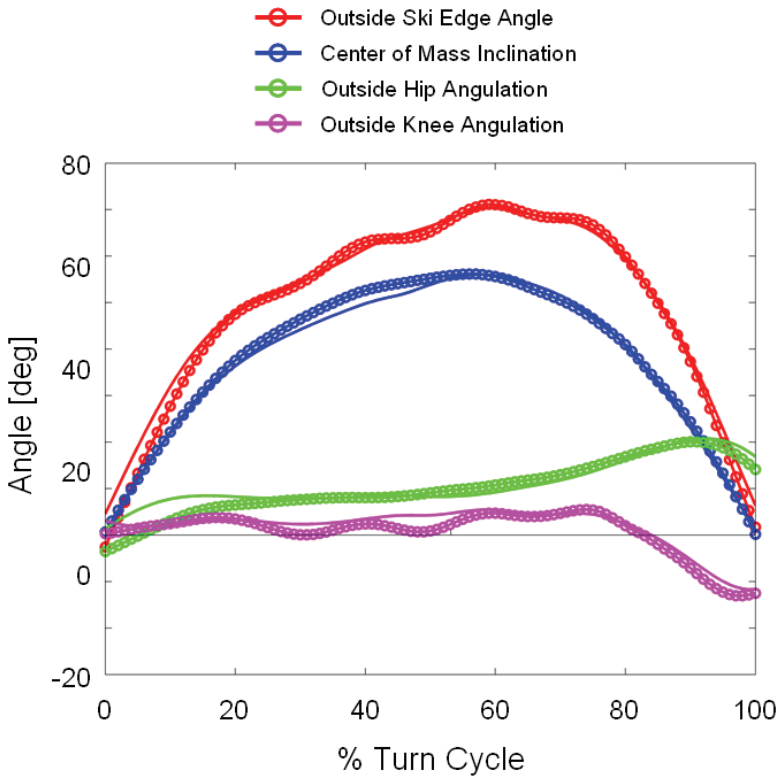

FIGURE 7.12. An example of skier lateral actions and ski edge angle. Lines with markers indicate the individual skier's data while solid lines show the group ensemble average. Notice that while the center of mass inclination accounts for the majority of the ski edge angle, knee angulation appears to function to fine-tune edge angle.

To help visualize this mechanism, graphics of one of the skiers were generated through the Completion Phase of a turn on the 13 m course and are presented in Figure 7.13. Image A was taken just prior to the end of the Turn Phase. At that moment, both the skis and center of mass turned at approximately the same rate ($R_{COM} = R_{SKI} = 10.6$ m). Center of mass inclination (ς) and ski edge angle (θ) were still quite high and both hip angulation (κ) and knee angulation (η) contributed to increase the ski edge angle as indicated by their positive values. From Images B to D, the center of mass stopped turning while the skis continued with high intensity turning. This resulted in the ski and skier trajectories gradually becoming divergent, as indicated by the increase in the center of mass attack angle (λ). This divergeance is a prerequisite for the skier to cross over to the other side of the skis for the following turn (LeMaster, 1999; Morawski, 1973; Takahashi & Yoneyama, 2001; Takahashi & Yoneyama, 2002). As the skier's inclination rapidly reduced in this phase, so did the ski edge angle. Hip angulation, however, began to increase as the skis turned in under the skier's body and the skier came into a "vissage" position (Joubert, 1978/1980). In Images E to G, the skier counteracts the effect of increased hip angulation to stop the ski from turning through reducing knee angulation.

It thus appears that in this investigation, knee angulation may have played three important roles, at least in relation to regulating the ski edge angle. At the Switch, knee angulation was responsible for establishing the initial ski edge angle. Although this initial angle was small (~ 5^{o}), it may be significant considering the attention knee angulation during the Initiation Phase receives from practitioners. During the turn, knee angulation acted to fine-tune the ski edge angle, confirming earlier literature (Howe, 2001; Joubert, 1978/1980; LeMaster, 1999; Lind & Sanders, 2004; Witherell, 1972). And finally, during the Completion Phase, knee angulation counteracted the effect of increased hip angulation to reduce edge angle. The role of knee angulation in reducing ski edge angle during the Completion Phase is interesting since it has not been emphasized in either the practitioner or scientific literature.

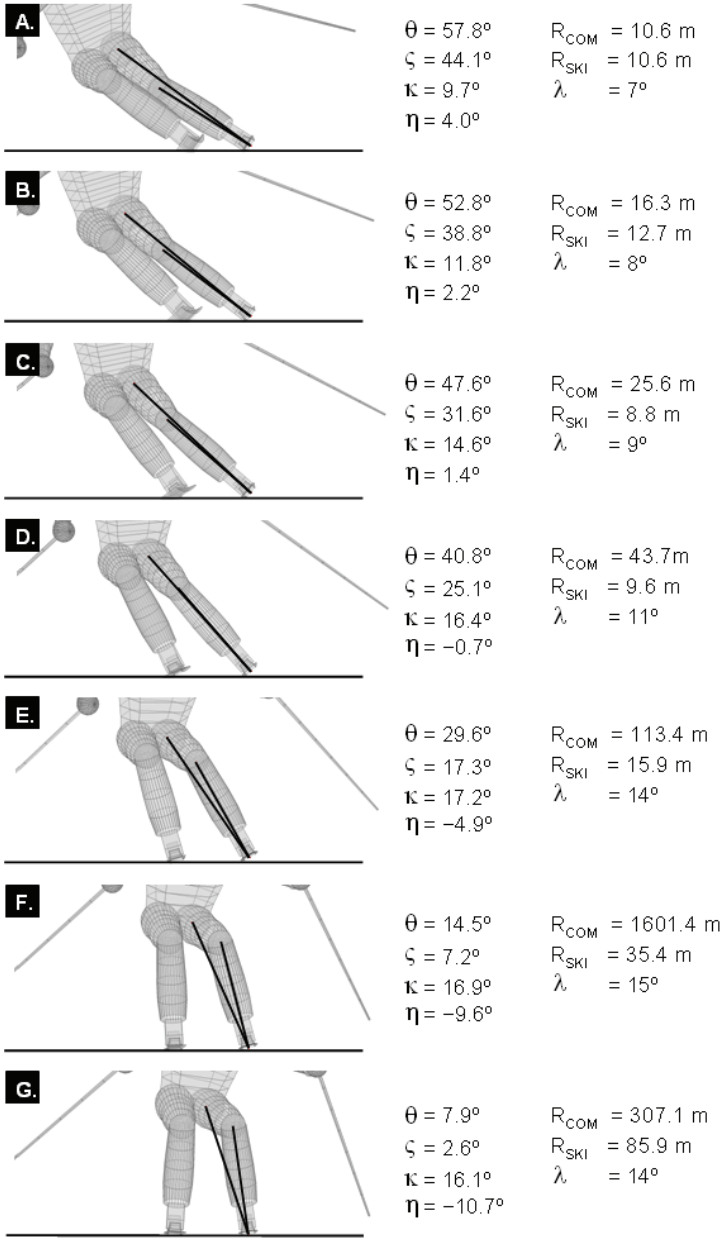

FIGURE 7.13. An example from the 13 m course demonstrating reduction in knee angulation during the Completion Phase of the turn. The camera angle is defined for each image so that the longitudinal axis of the outside ski ($\hat{\boldsymbol{E}}$) is orthagonal to the image plane.

As Bear (1976) suggested, there was a considerable amount of individual variation in the relative contributions of knee, hip and inclination angles to ski edge angle. This individual variation was relatively large compared to course-to-course differences, making comparisons of skier lateral actions between courses difficult. However, one difference between courses of interest was that skiers on the 13 m course were consistently more inclined and had greater hip angulation during the Completion Phase of the turn. This was not counteracted by a larger reduction in knee angulation, thus resulting in greater ski edge angles on the 13 m course during the Completion Phase. This increased edge angle might have been associated with the increased ski turning measured at that point which, in turn, may very well have resulted in both the greater ski and center of mass trajectory divergence as well as the earlier Switch seen on the 13 m course. Following this line of reasoning a step further, an interesting question is if the Switch would have occurred lower on the slope if the investigated skiers had been more active in using knee angulation to reduce the ski edge angle during the Turn Completion phase on the 13 m course.

When evaluating these results, it is important to bear in mind that the actual ski edge angle will vary somewhat from that measured here. In this study, ski edge angle was determined knowing the knee, ankle, ski tip and ski tail positions, which were assumed to be coplanar (p. 166). The deformed ski sole was then defined to be normal to this plane. Ski edge angle was then calculated as the angle between the ski sole at the ski mid point and the plane of the local snow surface. There are a couple of limitations to this method of which the reader should be aware.

First, as Müller et al. (1998) suggest, the actual ski edge angle is likely to vary along the ski's length according to the ski's characteristics and its interaction with the snow. Reporting a single edge angle to represent the entire ski's orientation relative to the snow surface is, in itself, an oversimplification.

Second, this method assumes that the plane of the knee, ankle, tip and tail points is orthogonal to the ski sole. In reality, this is probably not the case as this is a parameter skiers regulate in their equipment set-up. The actual angle will be individual and defined according to the set up of the athlete's boots, bindings, and plates. Although these adjustments are small, improved accuracy of ski edge angle measurements could be obtained through measurement of this angle at the time of data collection.

A final limitation worth mentioning is the fact that the precise orientation of the local snow surface was not known in this investigation. Further complicating matters is the likelihood that the orientation of the snow will change slightly with each passing skier as they either carve a groove into the surface or scrape off a layer of snow, depending on snow hardness.

VERTICAL ACTIONS

Two aspects of skier vertical actions were examined in this investigation. The first consisted of center of mass motion orthogonal to the least squares plane of the snow surface (Z'_{COM}). This component of skier vertical motion is thought to play an important role in determining the penetration component of the force that the skier applies to the snow. The second aspect of skier vertical actions examined was the distance between the skier's center of mass and the outside ankle joint center (D_{AJC}) (Pozzo, Canclini, Cotelli et al., 2005; Supej, Kugovnik, & Nemec, 2005b) which is thought to be important in terms of skier regulation of the snow reaction force magnitude.

CENTER OF MASS MOTION ORTHOGONAL TO THE SNOW SURFACE

There was a clear, cyclical pattern to skier center of mass motion relative to the least squares plane of the snow surface (Z'_{COM}) (Figure 6.21). The peak-to-peak amplitudes of center of mass motion orthogonal to the snow surface (Z'_{AMP}) observed in this study

(27.2 ± 1.6 and 31.0 ± 1.6 cm on the 10 and 13 m courses, respectively) were similar to those reported by Pozzo, Canclini, Cotelli, and Baroni (2001) in a study of skiers during a world cup slalom, but somewhat less than those reported by both Supej, Kugovnik, and Nemec (2005b) in slalom and Pozzo and colleagues. (Pozzo, Canclini, Casasola et al., 2005; Pozzo, Canclini, Cotelli et al., 2005) in giant slalom.

The fact that the highest center of mass positions on both the 10 and 13 m courses were similar (70.9 ± 3.0 and 70.2 ± 3.9 cm above the snow surface on the 10 and 13 m courses, respectively) while the lowest points were lower on the 13 m course (42.5 ± 1.9 and 38.7 ± 1.9 cm on the 10 and 13 m courses, respectively), suggests that the increased amplitude on the 13 m course was associated with the increased inclination observed during the turn, a finding that corresponds well with data described by Supej, Kugovnik, and Nemec (2005b).

Also of interest is the timing of the center of mass top point during the turn. The top point in the skier's vertical motion occurred approximately at the Switch on the 10 m course, but was somewhat delayed on the 13 m course, occurring at about 8 % of the turn cycle. However, when viewed in absolute distances relative to the approaching gate, the vertical-motion top point was further up the hill on the 13 m course, as shown in Figure 7.14. Why this is so is not clear, but is perhaps related to the fact that the gravitational force is the only external force acting to accelerate the skier's mass towards the snow surface. Since the component of gravity acting normal to the snow surface is the same on both courses, and since the skiers had higher speeds on the 13 m course, one might expect the top point in the skier's vertical motion on the 13 m course to occur further up the hill in absolute distances relative to the approaching gate. This would suggest that the timing of the top point in the skier's vertical motion between turns is not only a function of the Switch, but also of the skier's speed, the component of gravity accelerating the skier to the snow surface, and the location at which the skier desires to begin pushing on the snow to generate a reaction force. In other words, the

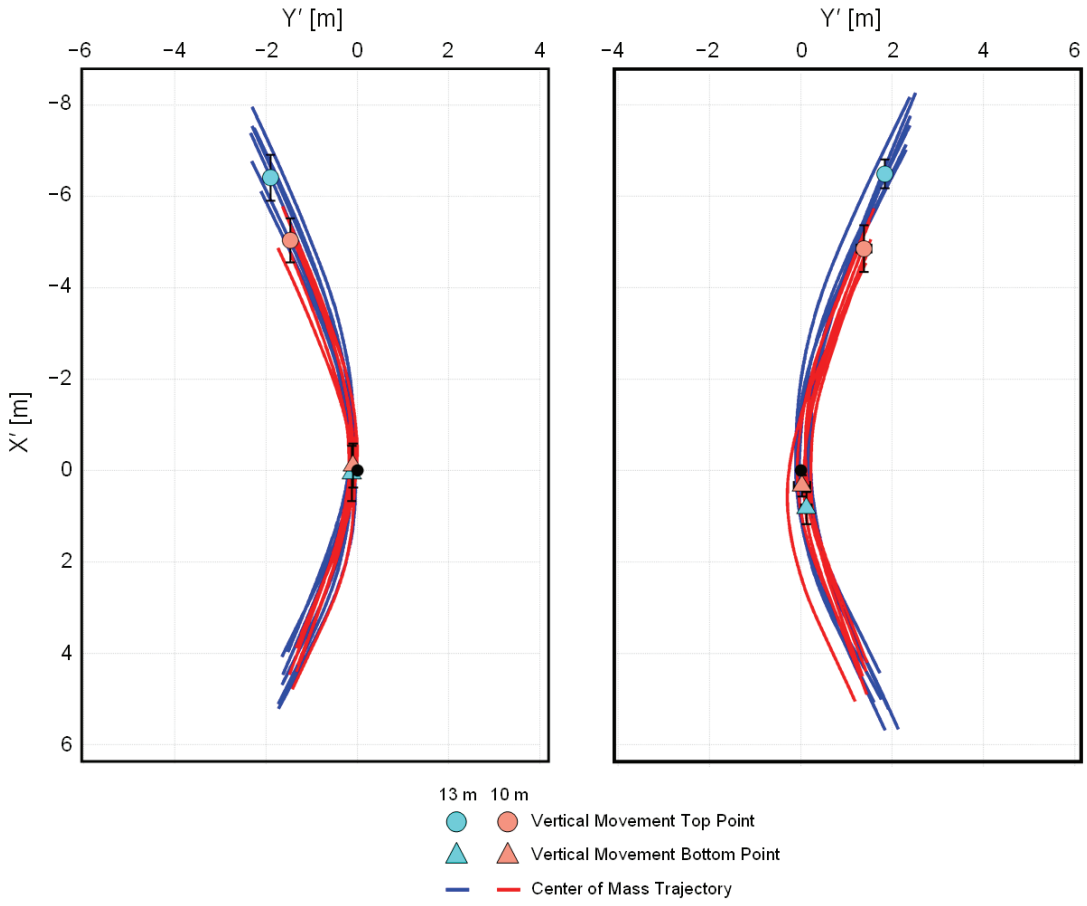

FIGURE 7.14. Center of mass trajectory relative to the gate on the 10 m (red) and 13 m (blue) courses. Indicated are the vertical motion (orthogonal to the snow surface) top points and bottom points.

timing and height of the top point of the skier's vertical motion between turns is likely to be an important factor in determining the timing of snow reaction forces in the following turn, at least in continuous turning situations such as those examined in this study.

The bottom points of the center of mass vertical motion were reached at about gate passage on both courses. However, in absolute distances, this bottom point was closer to the turn end Switch on the 13 m course than on the 10 m course. Considering the increased speed on the 13 m course, and the fact that the center of mass must rise a certain, minimum distance to allow the ski and center of mass trajectories to cross at the Switch, one might expect a more rapid vertical acceleration of the center of mass during the Completion Phase and, consequently, a greater degree of unloading during the Initiation Phase of the following turn on the 13 m course. This trend is indeed apparent when comparing the vertical component of the snow reaction force between courses in Figure 6.37.

Given that there was a greater degree of carving on the 13 m course than on the 10 m course in this study, this finding seems to be somewhat in contrast with Raschner and coworkers' results from a comparison of a world cup skier's technique using carving and conventional skis (Müller et al., 2004; Müller & Schwameder, 2003; Raschner et al., 2001; Schiefermüller et al., 2005). They observed similar vertical movement amplitudes between techniques, but a more rapid rise in center of mass position in the conventional technique, which they suggested was necessary to generate the increased unloading required to rotate the skis during the initation of the subsequent turn.

A limitation of the findings from this study is that the center of mass position was tracked relative to the least squares plane of the snow surface. Although the snow surface was relatively planar and uniform, it did curve slightly up on either side of the object space, a fact which may systematically affect the measures of skier vertical

motion (Z'_{COM}). A more sophisticated approach in the future should define skier vertical motion relative to a 3-dimensional surface model of the snow.

CENTER OF MASS TO OUTSIDE ANKLE JOINT CENTER DISTANCE

Center of mass to outside ankle joint center distance (D_{AJC}) also showed a cyclical pattern over the turn cycle, in some ways out of phase with Z'_{COM}. While Z'_{COM} was maximal at approximately the Switches, D_{AJC} was at a minimum. And conversely, when D_{AJC} was maximal during the turn, Z'_{COM} was low. This general pattern of motion can be readily observed looking at the individual data graphs in Appendix L.

In general, skiers increased D_{AJC} through the Initiation Phase, reaching initial maximal distances at about the start of the Turn Phase on both courses. On the 13 m course, some skiers reduced or stabilized D_{AJC} for a brief moment before increasing again just prior to gate passage, thus exhibiting a pattern similar to what Supej, Kugovnik and Nemec describe as the double-motion technique (Kugovnik et al., 2005; Supej, Kugovnik, & Nemec, 2005b; Supej et al., 2004). In contrast to the 13 m course, all turns on the 10 m course appeared to be of the single-motion type with a single peak in D_{AJC}.

Skiers had on average a greater range of motion in D_{AJC} on the 13 m course than on the 10 m course (28.7 ± 4.3 versus 20.7 ± 3.2 cm, respectively). Further, skiers were on average in more extended positions throughout the turn on the 13 m course, except at the Switch where they were in slightly more flexed positions (see Figure 6.24). The slightly shorter D_{AJC} at the Switch on the 13 m courses corresponds well with the lower center of mass positions orthogonal to the snow surface at the Switch and the delayed timing of the vertical motion top point observed on the 13 m course.

In contrast to the results of Kugovnik et al. (2004) and Supej et al. (2004), the double-motion in D_{AJC} observed on the 13 m course in this investigation did not seem to correspond to poor performance since both fast and slow skiers used both the double-

and single-motion approaches. This, however, is not a conclusive result. For instance, it may very well be that if more highly skilled skiers had participated in this study, that they would have demonstrated a single motion.

There are a couple possible explanations for the double-motion techniques in D_{AJC} on the 13 m course. One explanation is that the second increase was associated with pumping actions as described by Louie and Mote (Louie & Mote, 1982; Mote & Louie, 1983) and Lind and Sanders (2004). The timing of the second increase in D_{AJC} seems to coincide with about when one would expect a pumping motion. However, for reasons which will be discussed shortly, this explanation seems unlikely.

Another, perhaps more likely possibility is that the reduction in D_{AJC} in the middle of the turn is associated with the previously described irregularities observed in outside ski trajectories. If this reduction is intentional, it could represent a technique skiers use to down-regulate the ski's—and possibly the center of mass's—turning. In this case, the second increase in D_{AJC} might correspond to the skier actively provoking an increase in the snow reaction force once trajectory adjustments have been completed.

FORE/AFT ACTIONS

The fore/aft center of mass position along the outside ski's longitudinal axis (Q_{COM}) was quantified in a manner similar to that described by Schiefermüller et al. (2005). Despite a fairly large degree of individual variability, center of mass position relative to the outside ankle joint center demonstrated a cyclical pattern of fore/aft movement. During the Initiation Phase, the center of mass moved forward relative to the outside ankle joint, reaching maximal forward positions by about the start of the Turn Phase. After gate passage, skiers moved steadily back reaching the most aft positions by the turn's end. This pattern is similar to the findings of numerous kinematic (Raschner et al., 2001; Schiefermüller et al., 2005) and kinetic studies (Federolf, 2005; Gufler, 2001;

Lafontaine et al., 1998; Nigg et al., 2001; Schwameder et al., 2001; Scott, 2004; Yamagish et al., 2003; Yoneyama et al., 2006).

Despite similar ranges of fore/aft movement, skiers were on average positioned slightly further aft on the 13 m course relative to the 10 m course. That skiers were balanced further aft may be associated with the increased use of carving seen on the 13 m course. For instance, Schiefermüller and co-workers (2005) compared the fore/aft positioning of a world-class athlete skiing on carving and conventional equipment and found that the skier positioned himself further aft on the carving equipment. In addition, Gufler (2001) measured the forces acting between ski and boot for two skilled skiers while performing a selection of turn types typical of ski school teaching progressions. She observed that the skiers were balanced further aft in turns characterized by increased carving.

Contact with the slalom gate may at times interfere with skier fore/aft positioning. For example, times when the gate impacts the skier's lower legs may cause them to lose balance forward. In examining the individual graphs in Appendix M, some irregularities in skier fore/aft positioning are apparent at approximately gate passage. In a number of turns, particularly on the 13 m course, skiers appear to move aft just prior to gate passage. This is perhaps done in anticipation of the forthcoming impact of the gate with their legs.

One limitation of this study's measurements of skier fore/aft position is that the binding position along to the ski's longitudinal axis was not known. There is some evidence indicating that this may be a factor that influences skier fore/aft actions. Schwameder et al. (2001) examined the effect of varying binding position on kinetic variables in a group of skiers, including a former World Cup racer. They found that changing the fore/aft position of the binding systematically affected the fore/aft position of the force application point and that this change was more systematic for the more skilled athletes in their sample. In particular, they reported that the World Cup

racer seemed to change his fore/aft actions to maintain a constant relative position between body and skis as binding position was changed. Interestingly, while changing the binding position did affect how the elite skier positioned himself, the time course of his fore/aft movement appeared to change very little. Quantifying the position of the skier's boot relative to the ski's sidecut geometry in future investigations may help us to gain further insight into the purposes of skier fore/aft actions.

7.4 EXTERNAL FORCES (Figure 2.1, Boxes A, I, and K)

AIR DRAG FORCE

The air drag force was not measured in this study but instead modelled based on center of mass speed, frontal area calculations, and assumptions concerning the air drag coefficient and environmental conditions. The original purpose of estimating the air drag force was not to study the air drag force itself, but rather to allow estimation of the snow reaction force as well as the relative contributions of air and snow drag to skier mechanical energy dissipation. However, since the air drag force has been calculated, it is interesting to examine its magnitude and time course.

The air drag force magnitude demonstrated a clear cyclic pattern over the turn cycle associated with changes in center of mass speed and skier frontal area on both courses. Maximum air drag forces acted on the skiers at the end of the Initiation Phase, when center of mass speed was close to maximum and skiers were in extended, open positions. The air drag force was small during the transition between turns as skiers crouched into low positions at the Switch. The mean air drag force was greater on the 13 m course (69 ± 7 N) than on the 10 m course (52 ± 1 N), with the largest differences occurring between 20 and 40 % of the turn cycle.

There are several possible sources of error in the air drag force estimation which are important to discuss. The estimation of the drag coefficient, which was based on the

drag area measurements of three cross-country skiers during straight gliding in upright and crouched positions (Spring et al., 1988), is perhaps the parameter most likely to include error. Experimental determination of the drag coefficient in slalom situations could considerably improve this calculation in future work.

Another potential source of error is the estimated head wind. Unfortunately, wind conditions were not measured at the time of data collection. However, based on the geographical location of the ski area and the recorded environmental conditions, a so-called valley wind was expected to act in the uphill direction (Gilgien, 2008). Since the investigators did not register any appreciable wind, it was assumed that a weak, constant head wind of 1 $m \cdot s^{-1}$ acted in the uphill direction. The actual wind conditions may have differed substantially from this estimate, resulting in error in the air drag force calculations. This emphasizes the importance of measuring wind conditions in future investigations.

It is also possible that inaccuracies in either the estimate of air density, or the determination of skier frontal area, could have caused error in the air drag force estimate, although that errors in these parameters would have a small impact on the air drag force calculation compared to the previously mentioned facts. One final source of error could be related to the fact that the air drag force vector was defined as acting on the center of mass and in the direction opposite the center of mass velocity vector.

SNOW REACTION FORCE

Based on the resultant center of mass acceleration, the modelled air drag force, and the known gravitational force vector, the total snow reaction force acting on the center of mass was estimated. An interesting aspect of this investigation's findings is the course-to-course comparison of the reaction force magnitude and time course.

Mean and peak reaction force magnitudes were similar on both of the analyzed courses. Mean turn cycle reaction forces were 1494 ± 128 N (1.56 ± 0.05 BW) and 1600 ± 147 N (1.67 ± 0.05 BW) on the 10 and 13 m courses, respectively, and mean maximum reaction forces were 3212 ± 329 N (3.35 ± 0.20 BW) and 3378 ± 251 N (3.53 ± 0.16 BW) on the 10 and 13 m courses, respectively. These values are similar to those reported in studies of skilled skiers performing slalom turns while using skis instrumented with force measurement systems between the boot and ski (Babiel, Hartmann, Spitzenpfeil, & Mester, 1997; Nachbauer, 1987a, 1987b).

Although the reaction force magnitude was similar between the investigated courses, the time pattern of force over the turn cycle was different (see Figure 6.33). During the early portion of the Initiation Phase, the ground reaction force was significantly greater on the 10 m course, indicating that skiers did not unload as much during the transition between turns on the 10 m course. As discussed previously, this might have been associated with the increased tempo of the 10 m course and the need for skiers to more quickly begin generating a reaction force. Indeed, there was a more rapid build-up of force on the 10 m course with maximum reaction forces occurring at approximately gate passage or at 50.9 ± 5.9 % of the turn cycle, on average. In contrast, there was a delayed build-up of reaction force on the 13 m course with maximum forces occurring after gate passage at on average 66.6 ± 4.2 % of the turn cycle. Interestingly, a similar shift in the timing of the snow reaction force was also observed in Laapi's (2009) study of plantar pressure measurements taken of skilled athletes skiing 10 and 13 m courses in slalom, although in her study the shift was not as large.

It may be that the shift in timing of the snow reaction force was somehow inter-related with both the higher Switch relative to the approaching gate and the disturbances seen in the outside ski's turning trajectory on the 13 m course. This connection would make sense if, as previously discussed, skiers were required to down-regulate the outside ski's self-steering effect during the first portion of the turn as a result of the shifted

Switch position. Unloading would be one way of accomplishing this. Along these lines, it is interesting to note that the timing of the largest snow reaction forces on the 13 m course appears to follow just after the point at which the outside ski transitioned from an asymmetric trajectory about the gate to one corresponding to that of skis on the 10 m course. Furthermore, both a reduction in the center of mass to outside ankle joint center distance as well as either a decrease or levelling off of the vertical component of the snow reaction force were observed in each of the three examples of ski disturbances given earlier (Figures 7.6, 7.7, and 7.9).

The reader should be aware of a couple of limitations to the method implemented here to quantify the snow reaction force. First, this method involved modelling the air drag force vector which, in turn, was subject to a number of error sources. Using this approach, any error in the air drag force estimate would also be reflected in the snow reaction force vector. However, it appears that the air drag force was very small (less than 100 N in all cases) relative to the resultant force and gravitational force, so that even relatively large errors in the air drag force calculation would probably not affect the calculation of the reaction force to any appreciable extent. An exception to this might be during the transition between turns when the resultant force was relatively small.

Second, since the resultant center of mass acceleration was used to calculate the snow reaction force, the extent to which target point position data were filtered could potentially have a large impact on force calculations. For instance, if data were filtered at too high of a cut-off frequency, random error components in position measurement would be allowed to pass. These errors would then be amplified when the center of mass position data were twice differentiated to calculate acceleration. On the other hand, if data were filtered at too low of a cut-off frequency, systematic errors in force calculations would be likely to result (Lüthi et al., 2005). Despite these limitations, Lüthi et al. did demonstrate that with appropriate filtering the overall, general time

pattern and magnitude of forces could be measured reasonably well using video-based motion analysis.

7.5 SKIER MECHANICAL ENERGY

Understanding how elements of a skier's technique relate to changes in skier mechanical energy may give us valuable insight into how these elements relate to performance. Two approaches were used in this investigation to understand skier mechanical energy behavior. First, Supej et al.'s approach (Supej, 2008; Supej, Kugovnik, & Nemec, 2005a) of calculating mechanical energy dissipation (E_{DISS}) was used to obtain an instantaneous measure of skier energy behavior relative to potential energy changes. The second approach was based on estimating the work done on the skier by each of the external forces.

Both methods should give the same results in terms of total skier mechanical energy changes. However, the force work approach can be expected to be less accurate than E_{DISS} due to the estimates associated with modelling of the air drag force as well as the amplification of measurement error associated with the numerical differentiation used to calculate the center of mass acceleration. The advantage of the force work approach is that the relative contributions of the air drag force and snow reaction force to skier energy losses can be estimated. In addition, this method allows determination of the relative contributions of the gravitational force and the snow reaction force to skier kinetic energy gains.

The results of both approaches were compared to test the consistency of the programming routines used to make the calculations. Figure 7.15 compares mechanical energy dissipation (E_{DISS}) with the external force powers for an example turn taken from the 10 m course. Note how time points when the sum of the reaction

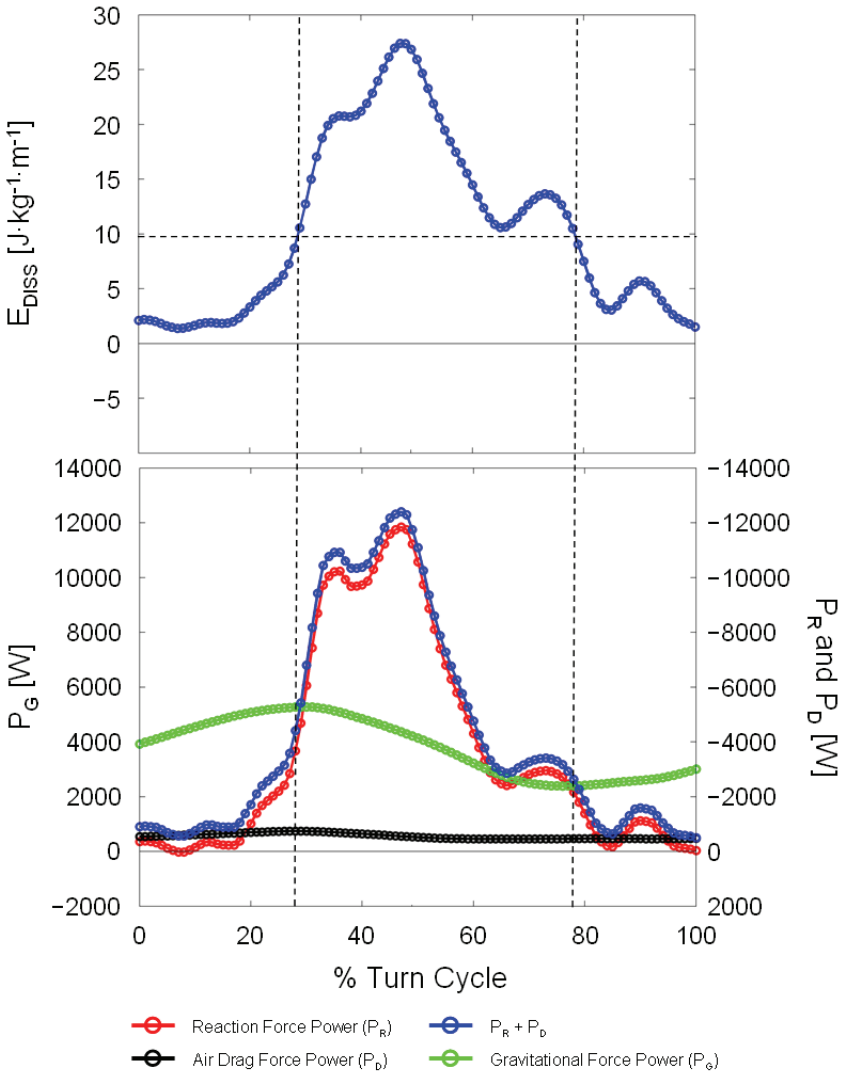

FIGURE 7.15. A comparison between mechanical energy dissipation (upper panel) and external force powers (lower panel) for a turn on the 10 m course. Note how when the sum of the reaction force and air drag force powers exceeds the gravitational force power coincides with when E_{DISS} exceeds 9.8 $J \cdot kg^{-1} \cdot m^{-1}$.

force and air drag force powers exceeds the gravitational force power coincides very well with when E_{DISS} is greater than 9.8 $J \cdot kg^{-1} \cdot m^{-1}$. The root mean squared differences between approaches in the net mechanical energy changes were less than 5 J for both of the courses. These very small differences are a good indication that the algorithms were performing as expected. However, looking at the net change does disguise an important difference of which one should be aware. Using the force work approach, the total mechanical energy gains and losses were systematically more than 100 J larger on each course compared to the dissipation method. So, although the net changes in energy were similar, the "flux" of energy using the force work approach was different.

One explanation for why this might be is if the magnitude of the air drag force was overestimated. Using the E_{DISS} approach, the true work of the air drag force is accounted for since this calculation is based on the center of mass motion alone. In contrast, the air drag force is estimated based on a number of assumptions in the force work approach. The estimated air drag force vector and the known gravitational force vector are then subtracted from the resultant force vector to obtain the snow reaction force vector. Using this approach, any overestimation of the air drag force would be compensated for in the snow reaction force to maintain the same resultant force. This would explain why the net change in energy was the same between methods despite a systematic shift in the gains and losses of energy. If this shift in energy behaviour was in fact due to an overestimation of the air drag force, it should be pointed out that this error is remarkably small. The differences in energy losses between the two approaches represent less than 3 % of total energy losses across all trials.

Due to their relative strengths and weaknesses, both the E_{DISS} and force work approaches were used in this investigation to characterize skier energy behavior. To describe skier total energy changes, the E_{DISS} approach was used as this is likely to be the most accurate. Estimating the work of each of the external forces was used to describe sources of energy loss and gain.

SKIER MECHANICAL ENERGY DISSIPATION

In the following discussion, general patterns of skier mechanical energy dissipation over the turn cycle are described first. This is followed by an examination of the relative contributions of the air drag force and snow reaction force to skier energy losses. Finally, how characteristics of skier actions that are thought to influence the drag component of the snow reaction force relate to the snow reaction force power are explored.

PATTERNS OF MECHANICAL ENERGY DISSIPATION

E_{DISS} is a measure of skier energy behaviour that describes the changes in skier total mechanical energy per change in potential energy at each instant in time. A positive E_{DISS} indicates that the skier is dissipating mechanical energy due to the work of non-conservative external forces. An E_{DISS} of 9.8 $J \cdot kg^{-1} \cdot m^{-1}$ indicates that all of the potential energy gained by the skier as he progresses down the slope is lost to his surroundings. E_{DISS} greater than this threshold indicates that not only are all of the potential energy gains being lost, but the skier also is dissipating kinetic energy. Negative E_{DISS} indicates that the skier's kinetic energy has increased more than what potential energy changes can explain. This may occur, for example, as a result of either a tail wind or skier muscular work.

The cyclical nature of E_{DISS} over the turn cycle observed in this investigation (see Figure 6.40)—with low E_{DISS} around the Switches, and high E_{DISS} during the Turn Phase—corresponds well with the results described by Supej and colleagues (Supej, 2008; Supej, Kugovnik, & Nemec, 2005a, 2005c). Mean turn cycle dissipations of 8.85 and 9.43 $J \cdot kg^{-1} \cdot m^{-1}$ on the 10 and 13 m courses, respectively, were near to the threshold of 9.8 $J \cdot kg^{-1} \cdot m^{-1}$, indicating that skiers were very close to an energy balance with the work of the gravitational force. This was an expected result since the experimental set-up was

designed so as to capture skier performances when up to speed in uniform, rhythmical turns.

Negative E_{DISS}, indicating that skiers contributed to their mechanical energy through muscular work, occurred around the transition between turns on the 10 m course and just after the transition on the 13 m course. It is perhaps significant to note that the time points of negative E_{DISS} coincided closely with the time points where the vertical center of mass motion orthogonal to the snow surface reached its top point. Potential mechanisms of negative E_{DISS} will be discussed shortly.

AIR DRAG AND SNOW REACTION FORCE DRAG

During normal skiing, both the air drag force ($\vec{F}_D$) and snow reaction force ($\vec{F}_R$) may do negative work on the skier. To estimate the relative contribution of each of these forces to total energy losses, the negative work done by each on the center of mass motion through the analyzed turns was calculated from the force powers.

The air drag force accounted for 16.7 and 21.4 % of the total energy losses through the two analyzed turns on the 10 and 13 m courses, respectively. This corresponds well with Supej's results who attributed the majority of skier energy losses in slalom to friction occurring at the ski-snow interaction (Supej, Kugovnik, & Nemec, 2005a). However, this contribution of air drag to skier energy losses is substantially less than the 70 to 80 % estimated by Savolainen and Visuri (1994) for straight cross-country skiing and speed skating at similar speeds. At the same time, however, this difference is not surprising as one would expect a marked increase in the drag component of the snow reaction force during turning. It is worthy to note that although the snow reaction force accounts for the large majority of skier energy dissipation in slalom, a sizeable proportion of energy losses are also attributable to air drag, even though this is the alpine discipline with the slowest skier speeds. This is perhaps particularly important in light of the small overall performance differences between skiers in alpine

skiing. One would also expect the importance of air drag to increase with higher skier speeds—and possibly reduced ski-snow friction due to increased carving—associated with the giant slalom, super-g and downhill disciplines.

Upon studying the individual graphs of E_{DISS} (Appendix O) and snow reaction force power (Appendix N), another potential source of energy loss became apparent; the energy cost of deforming and accelerating the gate shaft out of the skier's path. In many situations, this energy is considered negligible, and in steep terrain where the positive work of the gravitational force is very large, it probably is. But there are some coaches who have suggested that the energy cost of passing through slalom gates could be important on flat courses and some have even been able to cite observational evidence in support of this idea.

As a consequence of this investigation's measurement and calculation methods, any energy transferred from the athlete to the gate shaft would be disguised in the reaction force power and energy dissipation calculations. Interestingly, 19 of the 24 analyzed turns showed some form of local peak in both the reaction force power (Appendix N) and energy dissipation measures (Appendix O) close to gate passage. To what degree this peak in energy loss occurs as a result of the gate interfering with the skier's performance so that there is an increase in ski-snow friction, or as a result of the work done to actually accelerate the gate shaft out of the way, cannot be ascertained in this study. However, based on estimates of the acceleration the athlete impresses upon the gate from high speed video, the gate shaft's moment of inertia, and an estimate of the deformation caused to the gate shaft upon impact, a rough estimate places the energy cost of clearing the gate shaft on the order of 100 to 200 J. This would translate to between 2 to 5 % of the total energy loss per turn in the investigated situation. This seemingly small proportion of total energy losses associated with gate clearance may still be of importance, however, considering the very small margins in competitive

alpine skiing. This is an issue certainly worthy of further investigation to obtain more accurate estimates of the actual energy cost to accelerate and deform the gate shaft.

SKIER FORE/AFT POSITION

To further understand possible causes of energy losses, parameters of skier actions thought to have an impact on the ski snow interaction were related to the reaction force power. In particular, skier fore/aft position and ski attack angle were chosen on the basis of Renshaw and Mote's (1989) initial work in this area.

The relatively strong relationship between instantaneous measures of skier fore/aft position and reaction force power ($r = -0.76$ and -0.64 on the 10 and 13 m courses, respectively) indicate that the time-courses of these two parameters over the turn cycle coincided well. These results correspond with Renshaw and Mote's (1989) finding that more forward skier positioning required a greater thrust force to maintain a constant speed, constant radius turn (compare Figure 6.42 with Figure 3.16).

Although the relationships described in this study are correlational, and thus do not establish cause and effect, there may be a theoretical basis connecting skier fore/aft position and mechanical energy losses. The current understanding of the carving ski-snow interaction is that points along the shovel machine the snow surface as they generate the groove in which the remainder of the ski will ride (Casolo & Lorenzi, 2001; Lieu, 1982; Lieu & Mote, 1985; Sahashi & Ichino, 1998). Because the tail of the ski rides in the groove cut by the forward portion of the ski when carving, it is thought that the principal ski-snow interaction forces are distributed along the forward and center portions of the ski, a phenomenon that has been demonstrated in some numerical simulations of the RSPD (Lieu, 1982; Lieu & Mote, 1985; Renshaw & Mote, 1989) as well as in experimental measurement of the ski snow contact pressure during carved turns (Kagawa et al., 2009; Scott et al., 2007; Tatsuno et al., 2009).

Furthermore, it has been hypothesized that skiers can regulate the RSPD and ski deformation through their fore/aft positioning along the ski's longitudinal axis (Howe, 2001; Joubert, 1978/1980; LeMaster, 1999; Lind & Sanders, 2004; Major & Larsson, 1979/1979). There is experimental evidence supporting this hypothesis as well. Fauve et al. (2009) reported increased ski deformation along the ski shovel when the skier was balanced forward as opposed to back. This shift forward of the pressure distribution to the already heavily loaded portion of the ski that is cutting the snow surface may result in increased friction and energy dissipation. If this were to prove to be the case, it might help explain the surprisingly strong relationship between mean fore/aft position and performance time observed in this investigation.

A limitation in this analysis is the fact that the reaction force power is a resultant calculation reflecting a net change in skier energy. Therefore, there may be factors not associated with the snow reaction force that are included in the reaction force power results. For instance, the energy associated with gate clearance may be one such factor, as mentioned previously. To visualize the potential confounding effect that gate clearance may have on the measured relationship between skier fore/aft position and reaction force power, scatter plots were regenerated with data points that were within ± 5% of the turn cycle to gate passage marked by coloring (see Figure 7.16 A and B.). On both the 10 and 13 m courses, these points do seem to separate themselves from the rest of the data, particularly on the 13 m course where the correlation coefficient increases from $r = -.64$ to $r = -.69$ when these data points are removed from the analysis. This indicates that in future studies it will be important to be able to separate the energy loss associated with gate clearance from the work of the snow reaction force so that one can correctly identify the causes of these peaks in energy dissipation at gate passage.

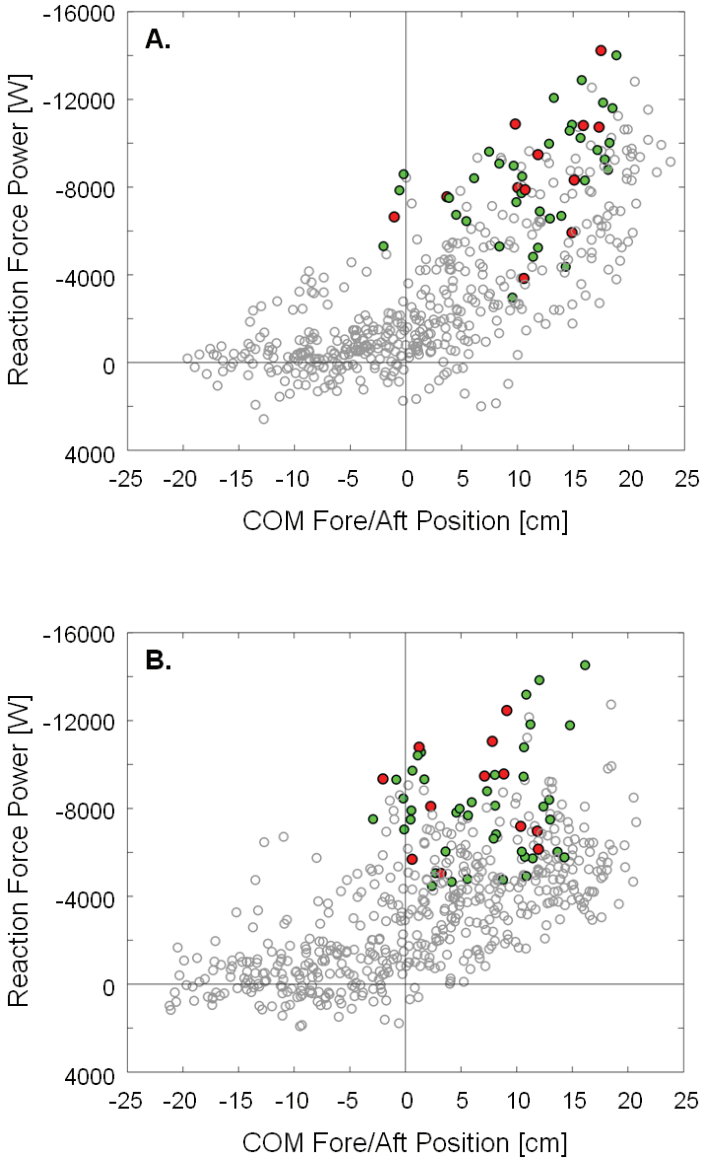

FIGURE 7.16. Center of mass fore/aft position and reaction force power on the 10 m (A) and 13 m (B) courses. Gate passage and ± 5 % of the turn cycle from gate passage are indicated by the red and green markers, respectively.

SKI ATTACK ANGLE

The second parameter analyzed in terms of its relationship to the snow reaction force power was the outside ski attack angle (φ). Based on the results of both Renshaw and Mote (1989) and Tada and Hirano (2002), one might expect a rather strong relationship where the reaction force power was proportional to the ski attack angle. Surprisingly however, this was not the case. The relationship between ski attack angle and reaction force power was more complicated, as the scatter plots clearly show (Figure 6.43).

The reason for this somewhat complex relationship can perhaps be understood by considering the mechanics of the ski snow interaction. In skidding, the snow reaction force arises out of friction and the snow's resistance to penetration, shear, and acceleration (Brown, 2009; Federolf, 2005; Hirano & Tada, 1996; Lieu, 1982; Lieu & Mote, 1985; Mössner et al., 2009; Tada & Hirano, 1998, 2002). To develop large reaction forces, the ski must penetrate the snow to a depth sufficient enough to cut the upper layer of the snow surface and accelerate the resulting loose snow out of the path of the ski (Hirano & Tada, 1996). A skidding ski that does not penetrate into the snow, but rather slides across the surface, is thus not expected to generate large forces. This is the basis for Brown's (2009) differentiation between drifting, where the ski merely skids across the snow surface, and chip formation, where the ski penetrates into the snow and machines the snow surface generating potentially large snow reaction forces.

To help illustrate how these phenomena may help explain the pattern of data in the scatter plots of ski attack angle and snow reaction force power, the plots in Figure 6.43 are regenerated in Figure 7.17 and zones are identified to indicate different forms of ski snow interaction. The green zone indicates carving and is defined as ski motion where the whole ski attack angle is less than 4^{o}. Based on the predictions of Lieu and Mote (Lieu, 1982; Lieu & Mote, 1985), as well as the results of this investigation, skis at this point are in an advanced stage of carving. It is interesting to note however, that even carving skis can be associated with high energy losses.

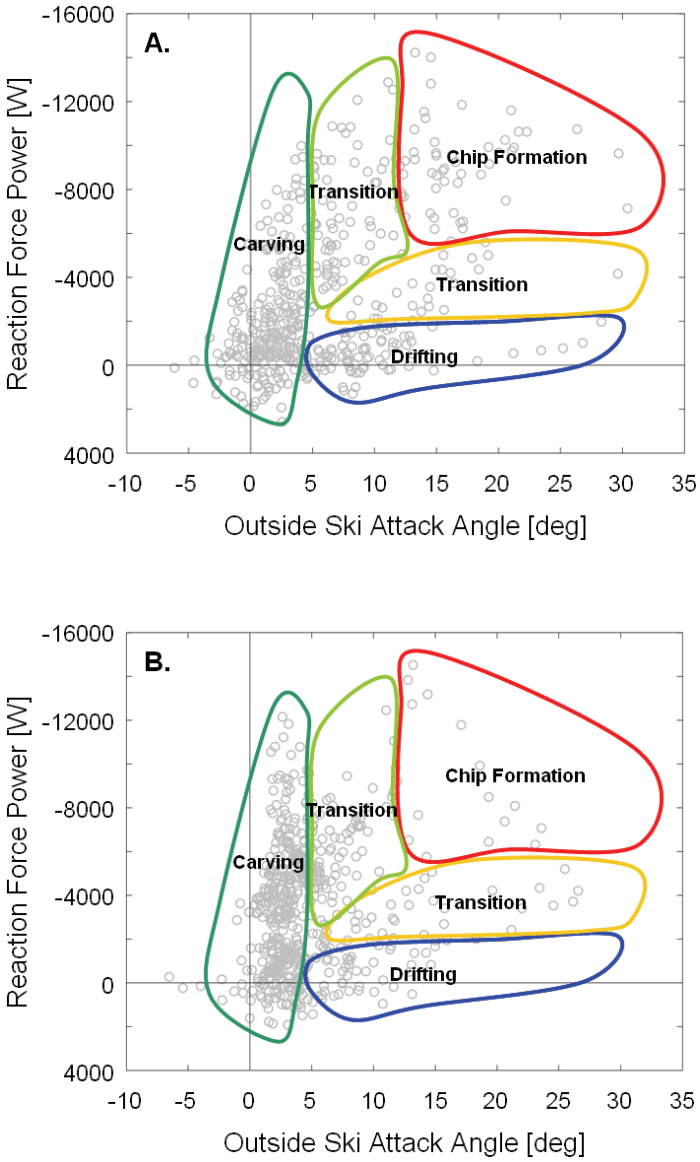

FIGURE 7.17. Outside ski attack angle and reaction force power on the 10 m (A) and 13 m (B) courses. Zones of carving, drifting, and chip formation are indicated. Note the reversed direction of the y-axis.

The blue zone across the bottom of Figure 7.17 indicates ski drifting where whole ski attack angles can be quite large but the reaction force power is low. The red zone identifies ski motion where the whole ski attack angle is greater than approximately 10^{o}, this being the point above which all points along the ski's edge can be expected to machine new snow (Lieu & Mote, 1985), and the snow reaction force power is high. The remaining areas indicate transition zones to emphasize that the shift from one form of ski motion to the other is not black and white, but rather a gradual transition.

There are some limitations to this anlaysis of the relationship between reaction force power and ski attack angle which are worthy of note. Again, reaction force power is a resultant calculation that may reflect factors that are not necessarily associated with the snow reaction force. As previously mentioned, gate impact is one potential confounding factor. To examine this possibility, the scatter plots were regenerated, this time colouring data points that were within ± 5% of the turn cycle duration to gate passage (Figure 7.18). Similar to the scatter plots with fore/aft position, data points associated with gate impacts do seem to differentiate themselves from the rest of the data, particularly on the 13 m course. This again emphasizes the importance of being able to separate out the energy cost of clearing the gate in future studies.

In addition, the fact that none of the analyzed turns were skidded during the latter portion of the turn cycle means that the relationships shown in Figure 7.16 do not completely characterize the relationship between skidding and reaction force power. For example, if one of the skiers had skidded during the latter portion of the turn, where there were large forces acting, it is likely that this would have resulted in large negative reaction force powers, perhaps much larger than those observed in this study. This, in effect, would have expanded the red, "chip formation" zone indicated in Figure 7.17 to include much larger reaction force powers.

A further limitation of this method is that only the outside ski is considered. This was done based on the assumption that the outside ski bore the majority of the load. In

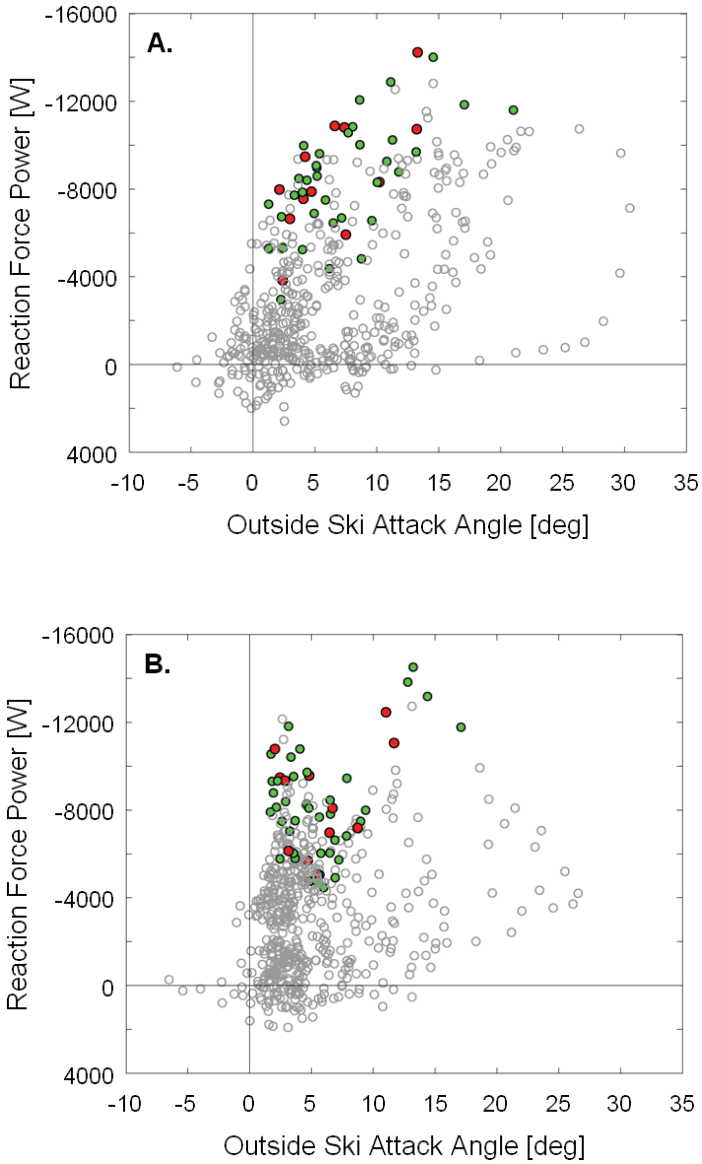

FIGURE 7.18. Outside ski attack angle and reaction force power on the 10 m (A) and 13 m (B) courses. Gate passage and ± 5 % of the turn cycle from gate passage are indicated by the red markers and green markers, respectively.

certain situations however, the inside ski may also have contributed significantly to snow drag. In her plantar pressure study of highly-skilled skiers in slalom, Laapi (2009) reported that the inside-to-outside ski force impulse ratio was, on average, 0.63 and 0.59 for courses with 10 and 13 m linear gate distances, respectively. These results suggest that although the outside ski probably did bear the majority of the load in the current investigation, it is also likely that the inside ski carried enough that its role in energy dissipation needs to be considered in future investigations.

Finally, using a single measure of ski attack angle to describe the whole ski's motion may be an oversimplification where pertinent information regarding the ski's motion is not considered. Local attack angles along the ski's interacting edge do vary. Perhaps a parameter that can better characterize the pattern of local attack angles would be a more appropriate measure.

SKIER KINETIC ENERGY GAINS

In normal skiing conditions, both the gravitational force and snow reaction force may act to increase skier kinetic energy. To estimate the relative contributions of each of these forces towards skier kinetic energy gains, the positive work of each force was calculated from the force powers.

Increases in skier kinetic energy were primarily a function of gravitational force power, with the reaction force contributions being less than 3 % on both courses. This is not a surprising result taking into consideration the moderately steep terrain (19^{o}) and the fact that the experimental set-up was designed so as to capture the skiers when they were up to speed and making uniform, rhythmical turns.

Despite the small contributions to skier kinetic energy, it is interesting to try and understand the situations in which skier energy gains are greater than that contributed by the gravitational force. These small energy gains, indicated by negative energy

dissipation (E_{DISS}) and associated with positive snow reaction force powers, occurred at the Switch on the 10 m course and just following the Switch on the 13 m course. This finding is similar to Supej (2008) who reported that negative energy dissipations[12] typically occur about the transition between turns. It is perhaps significant to note that these time points coincide approximately with the top points in the center of mass vertical motion orthogonal to the snow surface (Z'_{COM}). This timing may provide evidence as to the mechanism.

There are several possible mechanisms whereby skier muscular work could have contributed to an increase in kinetic energy at this portion of the turn cycle. One possibility could be related to skier fore/aft actions through the transition between turns. Using the base of support that his boots and skis provide against the snow surface to actively pull himself forward may be one explanation for the small increases in skier energy not accountable for by gravity. This mechanism could take place even when center of mass inclination is low, such as during the Switch, and might therefore be an explanation for the positive reaction force powers observed on the 10 m course. With the increased movement tempo associated with the shorter turn cycle duration on the 10 m course, it would not be surprising if skiers were required to be more active in their fore/aft movement than on the 13 m course.

Once the skier is inclined into the turn during the Initiation Phase, a second mechanism of skier induced energy increase could be associated with the skier pushing on the snow surface as he extends into the turn. This is a similar mechanism to the skating motion described by Takahashi & Yoneyama. (2001, 2002) and Brodie et al. (2008). Such a mechanism might explain the positive reaction force powers observed on the 13 m

[12] The reader is reminded that Supej (2008) inverts the sign of E_{DISS} so that in his reports positive values indicate increases in mechanical energy that exceed what can be accounted for by changes in potential energy. In describing his results here, the sign is changed back to maintain consistency with the rest of the dissertation.

course during the Initiation Phase. Interestingly, this does seem to correspond well with the particularly rapid increases in the center of mass to outside ankle joint center distances (D_{AJC}) observed on the 13 m course during this part of the turn cycle (see Figure 6.23).

A third possible mechanism for skier induced mechanical energy increases is pumping as described by Louie and Mote (Louie & Mote, 1982; Mote & Louie, 1983) and Lind and Sanders (2004). However, pumping would normally be expected to occur when the centripetal component of the snow reaction force is large, much later in the turn cycle than when the positive reaction force powers were observed in this investigation. The timing of the double motion observed in D_{AJC} during the Turn Phase on the 13 m course coincides better with the pumping action described by Louie and Mote. However, only large, negative reaction force powers were measured during this portion of the turn cycle. This is in contrast to Brodie et al. (2008) who measured positive reaction force powers through the Turn Phase in a study of giant slalom.

The fact that skiers were in balance energetically through the analyzed turns suggests that pumping may not have been advantageous in the investigated situation where gravity dominated the energy interactions. One might expect the contribution of pumping to be greater on flatter courses than the one investigated here, where the contribution of gravity to increases in skier kinetic energy are reduced. Skier contributions to kinetic energy gains, through actions such as pumping, are an aspect of technique in need of further investigation.

A limitation in this discussion is the fact that wind conditions were not measured during the data collection, although the investigators subjectively reported wind-still conditions. As described earlier, it was assumed that there was a small, constant head wind for the air drag force calculation based on the local environmental conditions during data collection. Despite this assumption, one plausible mechanism explaining the negative energy dissipations, which can not be ruled out in this study, is that a tail

wind acted to increase skier kinetic energy. This problem points to the importance of measuring wind conditions in future investigations.

7.6 PERFORMANCE

As previously pointed out, a limitation of this type of investigation in studying relationships to performance is that only a small portion of the course can be analyzed. This is problematic in that performance on any particular combination of turns will be intricately related to performance both prior to and subsequent to the analyzed sequence, thus making it problematic to appropriately quantify performance.

To minimize the challenges associated with this problem, the experimental set-up was defined so that skiers would be up-to-speed and making rhythmical, uniform turns before, through, and after the analyzed sequence. To control this, a photocell timing system was set-up to define intervals before, during, and after the calibration volume. The results from the timing system were used to select trials on the basis of both performance time and performance consistency as defined by the relationship between the skier's overall time and his time on the analyzed sequence. In this way, we hoped to capture turns representative of the athlete's "average" performance over this rhythmical portion of the course.

A second limitation in this investigation is the fact that a small, rather homogenous sample was used. Care needs to be taken when evaluating statistical measures, such as correlation coefficients, when there are such small numbers. To this end, the focus in the following discussion is directed towards the general trend of the various parameters in relation to performance time. To assist with this, scatter plots of all parameters with performance time are given in Appendix P, to which the reader will be referred. According to performance time, skiers fell naturally into faster and slower groups. The fast skiers are identified in the scatter plots using red markers. In addition,

the axes on the 10 and 13 m scatter plots are scaled similarly, where possible, to allow comparisons of variability between courses. To help the reader judge the strength of the relationship, the non-parametric Spearman's rank correlation coefficient and corresponding probability value are given.

TRAJECTORY LENGTH

Performance time is a function of average speed and trajectory length. In this investigation, center of mass three-dimensional trajectory length (L_{XYZ}), as well as cumulative displacements in the Y′- and and Z′- dimensions (L_Y and L_Z, respectively), were correlated to performance time. On both courses, the faster skiers were indeed on the shorter end of the spectrum on all three parameters (Appendix P, Figures P.3 – P.5). At the same time, however, it is clear that trajectory length was not the only performance variable.

The importance of trajectory length may be different between the two courses. On the 10 m course, L_{XYZ} and L_Y correlated poorly (Appendix P, Figure P.3). Two of the fast skiers did, in fact, have the shortest lines. However, one of the fast skiers, Subject 6, also had one of the longest trajectories. It is perhaps significant to note that the trial selected for analysis for Subject 6 took place later in the training session than the others. It is possible that he selected a longer trajectory due to changes in the snow surface conditions. This would correspond well with the work of Supej, Nemec, and Kugovnik (2005) who found that skiers increased trajectory length with deteriorating snow surface conditions in slalom. On the 13 m course, L_{XYZ} and L_Y seem to have been more important, with rank correlations of .77 ($p = .07$) and .83 ($p = .04$), respectively. It may be that the increased distance between gates allowed skiers to vary their approach more in terms of trajectory length. If this is the case, then trajectory length may be a more important performance factor in the other alpine disciplines where gate distances are larger.

L_Z correlated very well with performance time on the 10 m course, despite only 17 cm separating the shortest and longest L_Z (Appendix P, Figure P.5). This includes Subject 6 who, in spite of having a long total trajectory, had a short L_Z. The small range of distances seems to suggest that it was not the distance travelled in L_Z that was of importance for performance time, but perhaps other aspects of skier vertical actions instead. On the 13 m course, L_Z did not show the same importance. This may have been due to the rather homogeneous performances of skiers on this parameter; with the exception of one subject, skiers were all within a 5 cm range of each other on L_Z (Appendix P, Figure P.5).

SPEED

As one might expect, average speed correlated very well with performance time on both courses where rho = −1 ($p < .01$) and −.94 ($p < .01$) on the 10 and 13 m courses, respectively. Without exception, the skiers with the shortest performance times had the highest average speeds (Figure P.6). This seems to suggest that average speed may have been more important for performance, measured in elapsed time, than trajectory length in the investigated situation. This may be related to the relatively small differences in trajectory length used by the selected skiers. How skier trajectory, speed, and mechanical energy behaviour interact to determine performance in terms of elapsed time is an important topic for future work.

VERTICAL ACTIONS

In terms of skier vertical actions, mean center of mass vertical movement amplitude ($\bar{Z}'_{AMP}$) and mean Initiation Phase vertical reaction force amplitude ($\bar{F}^{INIT}_{VERT}$) were correlated with performance time. Relationships with performance appear to differ between courses.

On the 10 m course, $\overline{Z}'_{AMP}$ showed a rather strong relationship to performance (rho = .83, p = .04) where all three of the fast skiers clearly had lower vertical movement amplitudes than the slower skiers (Appendix P, Figure P.11). Surprisingly, this did not correspond to less unloading as quantified by $\overline{F}^{INIT}_{VERT}$. In fact, two of the fastest skiers (Subjects 6 and 7) demonstrated greater unloading during the Initiation Phase than the rest of the skiers, despite lower $\overline{Z}'_{AMP}$ (Appendix P, Figure P.12).

On the 13 m course, the relationship between $\overline{Z}'_{AMP}$ and performance was not as clear. Although the two fast skiers (Subjects 5 and 6) were, in fact, on the lower end of the distribution, there was less variability in the group taken as a whole on this parameter (Appendix P, Figure P.11). Subject 9 clearly differentiated himself, having the lowest $\overline{Z}'_{AMP}$. While Subject 9 had one of the best times on the 10 m course, he did not on the 13 m course. Perhaps there were some qualities in his skiing that would normally be associated with fast skiing (such as a low $\overline{Z}'_{AMP}$), but that in this case he made some kind of mistake affecting his performance time. Interestingly, while the trend on the 10 m course was that the fastest skiers had greater unloading in the Initiation Phase, the opposite was true on the 13 m course. Here, the two fastest skiers had the highest $\overline{F}^{INIT}_{VERT}$ (Appendix P, Figure P.12).

The reason for this difference in trends between courses is not clear. One plausible explanation may be that on the 13 m course, the distance between gates was sufficiently large that there was enough time for the gravitational force to pull the skier back to the snow surface in time to generate reaction forces, despite the increased speed. In contrast, the tempo on the 10 m course may have been high enough—indicated by the shorter turn cycle times—that increased movement away from the snow surface had a detrimental effect on performance. The fact that the fastest skiers on the 10 m course had less vertical movement, yet greater unloading in the Initiation Phase may have been a consequence of their higher speed.

FORE/AFT ACTIONS

Mean fore/aft center of mass position ($\bar{Q}_{COM}$) and mean fore/aft range of motion ($\bar{Q}_{ROM}$) were calculated to characterize skier fore/aft actions for comparison with performance time. On both courses, $\bar{Q}_{COM}$ seemed to be an important performance factor with rank correlations of .89 (p=.02) and .77 (p=.07) on the 10 and 13 m courses, respectively. In spite of the lower correlation coefficient on the 13 m course, the fastest skiers were centred the furthest aft on both courses (Appendix P, Figure P.1). This finding seems to correspond well with the rather strong relationship between skier fore/aft position and reaction force power discussed previously. Moreover, the slightly weaker relationship on the 13 m course might be expected in light of Renshaw and Mote's (1989) work showing that the effect of fore/aft positioning on mechanical energy dissipation should be expected to be less with increased carving, such as was observed on the 13 m course.

It is important to keep in mind that $\bar{Q}_{COM}$ is the skier's mean position over the turn cycle and does not indicate that skiers were static at this position. In fact, skiers were normally not static in their fore/aft positioning; instead demonstrating clear, cyclic patterns of forward movement during the Initiation Phase and aft movement during the Completion Phase (see Figure 6.25 and Appendix M). Furthermore, this finding can not be extrapolated to conclude that the further aft a skier is positioned, the better it is for performance. This finding does, however, indicate that being excessively forward can be detrimental for performance. Figure 7.19 contrasts examples of fast and slow skier fore/aft positioning on both the 10 and 13 m courses.

MECHANICAL ENERGY DISSIPATION

Mean mechanical energy dissipation correlated poorly with performance time on both courses with rank correlations of .37 (p=.47) and –.09 (p=.87) for the 10 and 13 m courses, respectively (Appendix P. Figure P.7). This is not surprising considering the

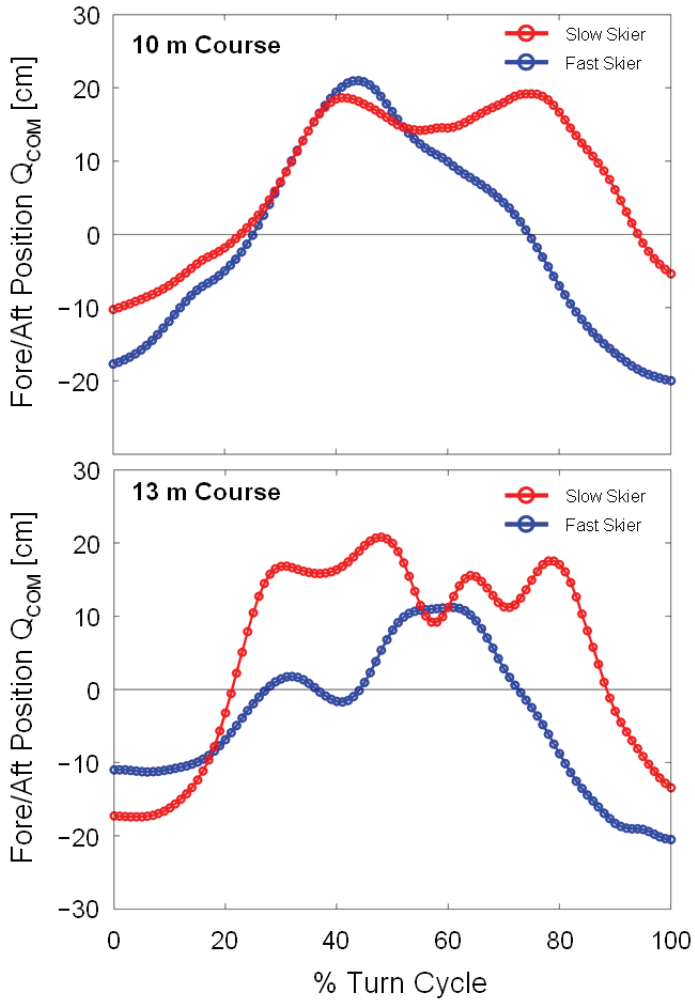

FIGURE 7.19. A comparison of a fast and a slow skier's fore/aft position on the 10 m (upper panel) and 13 m courses (lower panel).

experimental set-up where the intention was to capture skiers far enough after the start that they were up to speed while making even, rhythmical turns. In such a situation, one might expect skiers to perform in balance with the energy input of the gravitational force. This proved to be the case with average energy dissipations on all trials close to the balance point of 9.8 $J \cdot kg^{-1} \cdot m^{-1}$.

Supej and coworkers (Supej, 2008; Supej, Kugovnik, & Nemec, 2005a) originally proposed E_{DISS} as an instantaneous measure of the quality of a skier's performance. However, as this study shows, even fast skiers must dissipate excess energy at times. This complicates the interpretation of E_{DISS} since at any given time point, a high E_{DISS} could in fact represent a good performance. Nonetheless, understanding how and when fast skiers dissipate excess energy will help further our understanding of technique as it relates to racing performance.

7.7 GENERAL LIMITATIONS

Throughout this chapter, specific limitations associated with each parameter have been identified to assist the reader in gaining insight into this study's results. Several general limitations are worth emphasizing as well. First, it should be pointed out that this investigation is based on the analysis of a small, rather homogenous group of skiers in only two situations. Moreover, only two turns were analyzed for each skier on each of the two courses studied. Although this is in fact a rather large study in comparison to many previous works utilizing similar approaches, it is still limited in that ski racing is a sport of highly variable conditions and where a large diversity of technical approaches can be used to achieve successful performances. With this limitation in mind, the experimental set-up for this study was designed so as to capture skiers in conditions often encountered in competition. Furthermore, efforts were taken to capture "average" skier performances by setting rhythmical courses on even terrain and using a photocell timing system to identify consistent trials for analysis.

Another limitation is that while the group of athletes studied in this investigation were highly skilled, it is by no means certain that better skiers, had they participated, would have performed according to the trends seen in this study. For instance, the skiers analyzed in this study placed the Switch between turns higher on the slope, relative to the approaching gate, on the 13 m course compared to the 10 m course. Without having the performances of better skiers to compare with, it is difficult to know to what degree this was a sub-optimal performance or a consequence of the conditions.

A third limitation is that a number of parameters calculated in this study involve some level of estimation. For instance, the air drag coefficient is estimated in the calculation of the air drag force. Future investigations can improve upon the accuracy of this study by measuring these parameters at the time of data collection or by making more precise estimates.

A final limitation, is that much of this investigation's results are correlational and consequently do not provide sufficient evidence to identify causal relationships. In this regard, perhaps the most important contribution of this study has been to provide a theoretical basis upon which research questions can be defined and to identify parameters in this model which are likely to affect mechanical energy dissipation and skier performance and are therefore important to investigate further.

7.8 FUTURE DIRECTIONS

Based on the experiences gained in this investigation, several recommendations can be made for future studies. First, the accuracy of this investigation can be improved upon through either the careful measurement or more precise estimation of a number of the variables used in calculating the parameters of interest. For instance, more accurate estimates of the variables used in calculating the air drag force should be made. A more individualized approach to calculating center of mass should also be used. And careful

measurement of ski physical and geometrical properties at the time of data collection might not only provide information important for understanding skier actions but would also help to improve measurement accuracy of ski motion characteristics.

Second, considering the effort and investment involved in motion analysis studies of this type in the field in alpine skiing, and the large diversity of potential competition conditions, it is important that future investigations are designed to allow comparisons of results across international research groups and projects. It is only through appreciating how different skiers adapt their actions to varying conditions and situations that we, as an international research community, will be able to develop a fuller understanding of turning mechanics in alpine skiing. Detailed presentation of the experimental and numerical methods in published materials will facilitate this process. In this regard, making theses and dissertations available to the international research community can play a particularly important role.

Third, while this study provides a conceptual framework upon which to define research questions, and has further identified parameters which are likely to have important relationships with skier mechanical energy behavior and performance, its observational design limits its findings to correlation. Future investigations should be designed to allow inference as to the causal nature of these relationships. In particular, investigations should explore further the relationships between skier actions and their effects on the interaction between ski and snow, including the running surface pressure distribution, ski deformation, and ski motion characteristics.

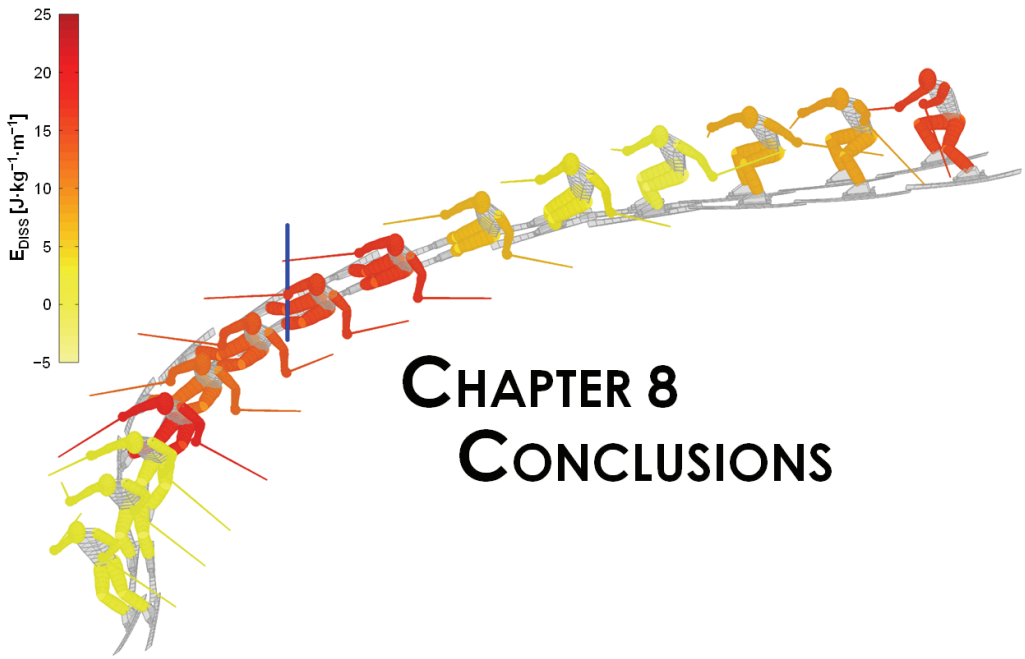

CHAPTER 8
CONCLUSIONS

CHAPTER 8. CONCLUSIONS

During the initial phase of this project, a theoretical model of turning technique in alpine ski racing was developed (Figure 2.1). The purpose of this investigation was to describe the various components of this model and to explore their interrelationships with the aim of further developing our understanding of how turning mechanics relate to skier performance. Towards this end, a 3-dimensional, video-based photogrammetric method utilizing multiple panning cameras was used to capture the performances of a group of highly-skilled athletes during slalom race simulations on courses with 10 and 13 m linear gate distances. Kinematic, kinetic, and energetic questions were examined using these data. This chapter reviews the original research questions and summarizes the study's main findings.

8.1 KINEMATIC OBJECTIVE AND QUESTION

Describe ski and skier kinematic characteristics concerning trajectory, speed, ski orientation, and skier actions.

How do ski and skier trajectories interact?

Are ski and skier kinematic characteristics different for slalom turns on courses with 10 and 13 m linear gate distances?

This investigation provides evidence indicating that the skis and skier travel on inter-related but separate trajectories. At the Switch between turns, the center of mass and skis were on divergeant trajectories, a prerequisite for their crossing during the transition between turns and the establishment of center of mass inclination (LeMaster, 1999; Morawski, 1973; Takahashi & Yoneyama, 2001, 2002). Early in the Initiation Phase, the skis began turning sharply while the center of mass continued to travel straight, leading to a convergeance of trajectories. This provides evidence in support of LeMaster's description of how the skis must turn before the skier can turn (LeMaster, 1999). While the skis and center of mass turned at similar rates during the Turn Phase, the center of mass stopped turning earlier than the skis in the Completion Phase, once again resulting in a divergeance of trajectories.

There was a difference in turn cycle structure between the 10 and 13 m courses. While the Turn Phase accounted for approximately 50 % of the turn cycle on both courses, the Initiation Phase represented a greater portion, and the Completion Phase a lesser portion, on the 13 m course—a finding reminiscent of differences observed in turn structure between skiing on conventional and carving skis (Müller et al., 2004; Müller & Schwameder, 2003). In this investigation, the difference in turn structure was at least in part due to a higher Switch on the slope relative to the up-coming gate on the 13 m course. The higher Switch, in turn, appears to have been associated with asymmetric center of mass and outside ski trajectories about the gate on the 13 m course.

A greater degree of outside ski skidding was observed during the first half of the turn cycle on the 10 m course, although the outside ski transitioned to carving by approximately gate passage on all of the analyzed turns. The analysis of local ski attack angles showed that it was the tail segments that transitioned to a carving mode first and that true carving was limited to the ski afterbody, both findings confirming numerical simulation studies of ski motion (Lieu, 1982; Lieu & Mote, 1985; Renshaw & Mote, 1989) and supporting our current understanding of carving ski-snow interaction

mechanics (Kagawa et al., 2009; Tatsuno et al., 2009; Yoneyama et al., 2008). There was also a greater degree of ski edging on the 13 m course, at least in part associated with greater center of mass inclination.

Disturbances in the outside ski's turning motion were observed similar to that reported by Federolf (2005), particularly on the 13 m course. While this study cannot isolate the cause of these irregularities, there is enough evidence to propose several mechanisms—which may be inter-related—for further investigation. One possibility is that the skis' trajectories were disturbed by irregularities in the snow surface. A second possibility may be that the ski reduced turning during the transition from skidding to carving. Skier's actively down-regulating the ski's self-steering effect is a third possibility. A final possibility may be that down-regulating the ski's self-steering effect is more limited than traditionally thought and that these disturbances are actually the result of having to re-orient and place the ski onto a new trajectory relative to the gate. Whether these changes to ski trajectory are intentional or not, it is apparent that even relatively small adjustments to ski edge angle, attack angle, and loading can lead to surprisingly large changes in the ski's turn radius.

In terms of skier actions, there was a greater range of center of mass vertical motion, measured orthogonal to the snow surface, on the 13 m course compared to the 10 m course. Considering that there was also a greater degree of center of mass inclination on the 13 m course, and the fact that the highest points of center of mass motion relative to the snow surface were equal on both courses, the increased amplitude of vertical motion on the 13 m course was likely associated with the need for increased inclination.

Center of mass inclination and hip angulation were the two main contributors to outside ski edge angle, confirming Witherell's (1972) and Morawski's (1973) work. Knee angulation appeared to play the following three roles: (1) Establishment of the initial edge angle during the transition between turns, (2) Fine-tuning of the edge angle

during the Turn Phase, and (3) Reduction of the edge angle during the Completion Phase.

A cyclical pattern of center of mass fore/aft motion was observed, similar to the findings of numerous other investigators (Federolf, 2005; Gufler, 2001; Lafontaine et al., 1998; Nigg et al., 2001; Raschner et al., 2001; Schiefermüller et al., 2005; Schwameder et al., 2001; Scott, 2004; Yamagish et al., 2003; Yoneyama et al., 2006). Despite similar ranges of fore/aft movement, skiers were positioned further aft on the 13 m course compared to the 10 m course, a finding reminiscent of differences seen between skidding and carving (Gufler, 2001; Schiefermüller et al., 2005).

8.2 KINETIC OBJECTIVES AND QUESTIONS

> Describe the timing and magnitude with which the snow reaction force and air drag force act on the skier during slalom turns on courses with 10 and 13 m linear gate distances.
>
> Are snow reaction force and air drag force characteristics different for slalom turns on courses with 10 and 13 m linear gate distances?

The simulated air drag force demonstrated a cyclic behavior over the turn cycle with maximum forces occurring at approximately the transition from the Initiation to the Turn Phase on both courses. The mean air drag force was greater on the 13 m course (69 ± 7) than on the 10 m course (52 ± 1), corresponding to the increased center of mass velocity.

Maximal snow reaction forces on both the 10 and 13 m courses were high, averaging 3212 ± 329 N (3.35 ± 0.20 BW) and 3378 ± 252 N (3.53 ± 0.16 BW) on the 10 and 13 m courses, respectively. There was a clear difference in the timing of the snow reaction force between courses relative to the turn cycle. While on the 10 m course large forces were distributed during the middle of the turn cycle at about gate passage, they occurred slightly later on the 13 m course.

8.3 ENERGETIC OBJECTIVES AND QUESTIONS

Describe the patterns of mechanical energy dissipation during slalom turns on courses with 10 and 13 m linear distances.

Are mechanical energy dissipation patterns during a turn cycle different for 10 and 13 m courses?

What are the relative contributions of the snow reaction force and air drag force work to the total mechanical energy dissipated by the skier?

A cyclic pattern of energy dissipation relative to the turn cycle was observed on both courses, corresponding well with earlier reports (Supej, 2008; Supej, Kugovnik, & Nemec, 2005a, 2005c). Low energy dissipation occurred at the transition between turns. High energy dissipation occurred at approximately gate passage on the 10 m course and just after gate passage on the 13 m course. Negative dissipations—situations where the increase in skier kinetic energy was greater than the associated change in potential energy—occurred at the Switch on the 10 m course and during the Initiation Phase on the 13 m course.

The snow reaction force accounted for 83.3 ± 1.9 % and 78.6 ± 2.2 % of total energy losses on the 10 and 13 m courses, respectively. Energy losses due to the negative work of the air drag force were not insignificant however, accounting for as much as 16.7 ± 1.9 % and 21.4 ± 2.2 % of total energy losses on the 10 and 13 m courses, respectively. These numbers should be interpreted with some caution, however, as there are indications that some energy loss may be associated with the work of clearing the gate shafts. Changes in gravitational potential energy accounted for over 97 % of skier kinetic energy gains. The remaining energy gains—corresponding to the negative energy dissipations registered during the transitions between turns—are possibly a result of skier muscular work.

8.4 INTERACTION OF PERFORMANCE AND MECHANICAL CHARACTERISTICS QUESTIONS

Are ski and skier kinematic characteristics related to mechanical energy losses during slalom turns on courses with 10 and 13 m linear gate distances?

Are ski and skier kinematic characteristics related to performance time on slalom courses with 10 and 13 m linear gate distances?

Is mechanical energy dissipation related to performance time on courses with 10 and 13 m linear gate distances?

The relationships of outside ski attack angle and skier fore/aft position with the snow reaction force power were examined to help understand their role in skier mechanical energy losses. Center of mass fore/aft position correlated well with the snow reaction force power on both the 10 m ($r = -.76$) and the 13 m courses ($r = -.64$), indicating that the time-courses of these two parameters coincided well. Although this finding does not provide evidence of a cause and effect relationship, it does indicate that such a relationship is possible, as Renshaw and Mote's (1989) work predicted. The relationship between outside ski attack angle and the snow reaction force power was complex and appeared to change over the course of the turn cycle. This is reflected in the low correlations observed on both courses ($r = -.49$ and $-.23$ for the 10 and 13 m courses, respectively).

Although the 3-dimensional, resultant center of mass trajectory length through the analyzed turns correlated poorly with performance time on the 10 m course (rho = .26, $p = .62$), the vertical component of this motion correlated strongly (rho = .83, $p = .04$). The opposite was true on the 13 m course where the resultant trajectory length correlated well (rho = .77, $p = .07$) and the vertical component correlated poorly (rho = .49, $p = .33$). Average center of mass speed through the analyzed turns correlated very well with performance time on both courses (rho = –1.00 and –.94, $p < .01$, on the 10 and 13 m courses, respectively).

While the range of skier fore/aft movement correlated poorly with performance time on both courses—rho = .20 (p = .70) and .26 (p = .62) on the 10 and 13 m courses, respectively—mean fore/aft position correlated strongly, particularly on the 10 m course—rho = .89 (p = .02) and .77 (p = .07) on the 10 and 13 m courses, respectively. This may be a further indication that center of mass fore/aft position somehow influences the drag component of the snow reaction force.

The mean Initiation Phase outside ski attack angle correlated poorly with performance time on both the 10 (rho = .03, p = .96) and 13 m (rho = .20, p = .70) courses. This perhaps corresponds to the rather complex relationship observed between outside ski attack angle and reaction force power.

Mean energy dissipation correlated poorly with performance time on both the 10 (rho = .37, p = .47) and 13 m (rho = –.09, p = .87) courses, a finding that was perhaps expected given the experimental set-up. This indicates that although E_{DISS} may be an important parameter to understand a skier's performance, it should not be interpreted as a measure of performance quality. Dissipating excessive mechanical energy in a controlled manner is a component of good ski racing technique.

8.5 CONCLUDING REMARKS

In summary, this project has provided a conceptual model of turning technique in alpine ski racing that is based on both scientific and practitioner knowledge and that can be used to guide future research efforts. This model is based on the concept that turning is a result of an interaction between the snow, skis, and skier. Seen in this way, the skier controls his trajectory and speed by manipulating the ski's orientation and loading characteristics, thereby regulating the direction and magnitude of the snow reaction force.

The results of this investigation are limited in that generalization from a single situation, and a single group of athletes, to other circumstances needs to be considered very carefully, particularly in light of the infinitely variable conditions possible in alpine ski racing. Moreover, the observational design of this study does not provide evidence of cause and effect relationships.

In light of these limitations, perhaps the most important scientific contribution of this study lies in the identification of turning technique parameters which need to be better understood to further develop our knowledge of how the mechanics of turning technique relates to performance. Of particular importance in future work will be the development of our understanding of how skier actions influence the interaction between ski and snow and, ultimately, how this interaction then determines ski and skier motion.

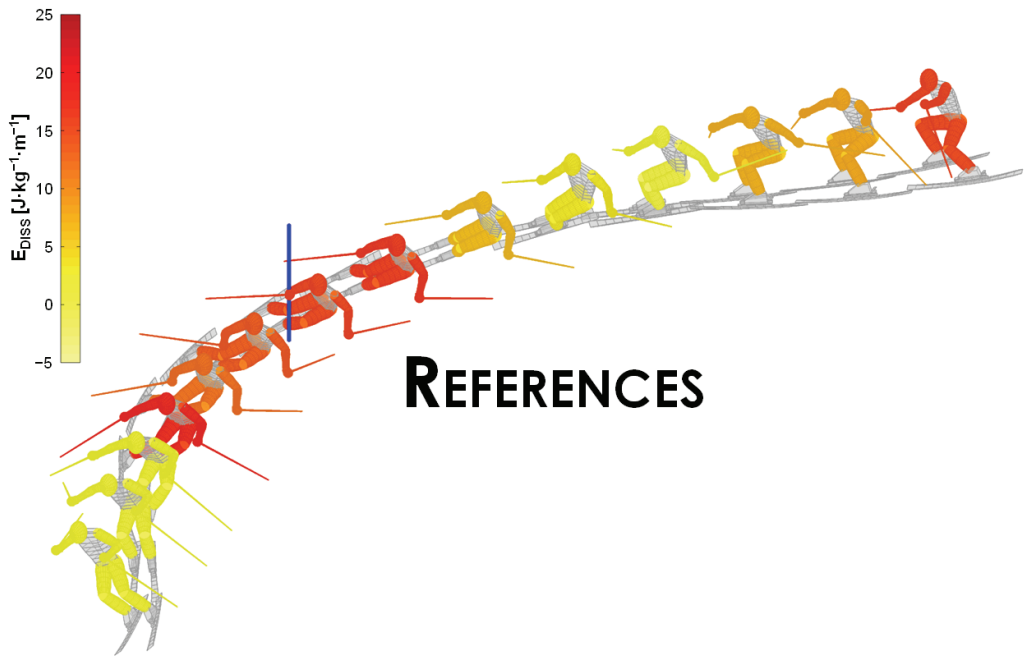

REFERENCES

REFERENCES

Abdel-Aziz, Y. I. & Karara, H. M. (1971). Direct linear transformation from comparator coordinates into object space coordinates in close-range photogrammetry. *Proceedings of the American Society of Photogrammetry Symposium on Close-Range Photogrammetry* (pp. 1-18). Falls Church, VA: American Society of Photogrammetry.

Angulo, R. M. & Dapena, J. (1992). Comparison of film and video techniques for estimating three-dimensional coordinates within a large field. *International Journal of Sport Biomechanics, 8,* 145-151.

Bahamonde, R. & Stevens, R. (2006). Comparison of two methods of manual digitization on accuracy and time of completion. In H. Schwameder, G. Strutzenberger, V. Fastenbauer, S. Lindinger, & E. Müller (Eds.), *Proceedings of the 24th International Symposium on Biomechanics in Sports* (pp. 650-653). Salzburg, Austria. [On-line]. Available: www.isbs.org

Babiel, S., Hartmann, U., Spitzenpfeil, P. & Mester, J. (1997). Ground-reaction forces in alpine skiing, cross-country skiing and ski jumping. In E. Müller, H. Schwameder, E. Kornexl, & C. Raschner (Eds.), *Science and Skiing* (pp. 200-207). London: E & FN Spon.

Baroni, G., Ferrigno, G., Rodano, R., Canclini, A., Cotelli, C., Fantino, M., Minotti, D., & Pozzo, R. (1998). Three-dimensional sport movement analysis by means of free floating TV cameras with variable optics. In H. J. Riehle & M. M. Vieten (Eds.), *Proceedings of the 16th International Symposium on Biomechanics in Sports*. Konstanz, Germany. [On-line]. Available: www.isbs.org

Barros, R. M. L. & Brenzikofer, R. (1993). Synchronization of registers for 3d description of human movement. In *Proceedings of the International Society of Biomechanics XIVth Congress* (pp. 150-151). Paris, France.

Bartlett, R., Bussey, M., & Flyger, N. (2006). Movement variability cannot be determined reliably from no-marker conditions. *Journal of Biomechanics, 39,* 3076-3079.

Bate, P. (1993). Accuracy of the peak motion measurement system. *Proceedings of the International Society of Biomechanics XIVth Congress* (pp. 156-157). Paris, France.

Bear, R. (1976). *Pianta Su: Ski like the best*. Boston: Little, Brown and Company Ltd.

Bell, A. L., Pedersen, D. R., & Brand, R. A. (1990). A comparison of the accuracy of several hip center location prediction methods. *Journal of Biomechanics, 23,* 617-621.

Blievernicht, D. L. (1967). A multidimesional timing device for cinematography. *Research Quarterly, 38,* 146-148.

Brewin, M. A. & Kerwin, D. G. (2005). Accuracy of scaling and DLT reconstruction techniques for planar motion analyses. *Journal of Applied Biomechanics, 19,* 79-88.

Brierley, H. & Bartlett, R. (1991). A three-dimensional video analysis of the kinematic differences between experienced and novice skiers performing two types of parallel ski turn. *Journal of Sport Sciences, 9,* 395.

Brodie, M. (2008). Pixel counting algorithm to estimate the frontal area in determination of the wind drag force magnitude [Computer Program: Matlab m-file]. Massey University, Wellington, New Zealand: Author.

Brodie, M., Walmsley, A., & Page, W. (2007). Fusion motion capture: The biomechanics of alpine ski racing. *Journal of Biomechanics*, *40* (Suppl. 2), S399.

Brodie, M., Walmsley, A., & Page, W. (2008). Fusion motion capture: a prototype system using inertial measurement units and GPS for the biomechanical analysis of ski racing. *Sports Technology, 1,* 17-28.

Brodie, M., Walmsley, A., & Page, A. (2009). How to ski faster: Art or science? In E. Müller, S. Lindinger, & T. Stöggl (Eds.), *Science and Skiing IV* (pp. 162-174). Maidenhead: Meyer & Meyer Sport (UK), Ltd.

Brown, C. (2007, December). *Modelling edging forces in skiing using Merchant's theory for metal cutting*. Paper presented at the 4th International Congress on Science and Skiing, St. Christoph, Austria.

References

Brown, C. & Outwater, J. O. (1989). On the skiability of snow. In R. J. Johnson, C. D. Mote, & M. Binet (Eds.), *Skiing trauma and safety: Seventh international symposium* (pp. 329-336). Philadelphia, PA: American Society for Testing and Materials.

Brown, C. A. (2009). Modelling edge-snow interactions using machining theory. In E. Müller, S. Lindinger, & T. Stöggl (Eds.), *Science and Skiing IV* (pp. 175-182). Maidenhead: Meyer & Meyer Sport (UK), Ltd.

Bruck, F., Lugner, P., & Schretter, H. (2003). A dynamic model for the performance of carving skis. In R. J. Johnson, M. Lamont, & J. E. Shealy (Eds.), *Skiing Trauma and Safety: Fourteenth Volume* (pp. 10-23). West Conshohocken, PA: American Society for Testing and Materials International.

Burtscher, M., Raschner, C., Zallinger, G., Schwameder, H., & Müller, E. (2001). Comparison of cardiorespiratory and metabolic responses during conventional and carving skiing. In E. Müller, H. Schwameder, C. Raschner, S. Lindinger, & E. Kornexl (Eds.), *Science and Skiing II* (pp. 552-565). Hamburg: Verlag Dr. Kovač.

Cappozzo, A., Leo, T., & Macellari, V. (1983). The CoSTEL kinematics monitoring system: Performance and use in human movement measurements. In H. Matsui & D. Kobayashi (Eds.), *Biomechanics VIII-B: Proceedings of the Eighth International Congress of Biomechanics* (pp. 1067-1074). Champaign, IL: Human Kinetics Publishers.

Casolo, F. & Lorenzi, V. (2001). Relevance of ski mechanical and geometrical properties in carving technique: A dynamic simulation. In E. Müller, H. Schwameder, C. Raschner, S. Lindinger, & E. Kornexl (Eds.), *Science and Skiing II* (pp. 165-179). Hamburg: Verlag Dr. Kovač.

Challis, J. H. (1999). A procedure for the automatic determination of filter cutoff frequency for the processing of biomechanical data. *Journal of Applied Biomechanics, 15,* 317.

Challis, J. H. & Kerwin, D. G. (1992). Accuracy assessment and control point configuration when using the DLT for photogrammetry. *Journal of Biomechanics, 25,* 1053-1058.

Chen, L., Armstrong, C. W., & Raftopoulos, D. D. (1994). An investigation on the accuracy of three-dimensional space reconstruction using the direct linear transformation technique. *Journal of Biomechanics, 27,* 493-500.

Chiari, L., Croce, U. D., Leardini, A., & Cappozzo, A. (2005). Human movement analysis using stereophotogrammetry Part 2: Instrumental errors. *Gait & Posture, 21,* 197-211.

Dapena, J. (1978). Three dimensional cinematography with horizontally panning cameras. *Sciences et Motricite, 1,* 3-15.

Dapena, J. & Chung, C. S. (1988). Vertical and radial motions of the body during the take-off phase of high jumping. *Medicine & Science in Sports & Exercise, 20,* 290-302.

De Cecco, M. & Angrilli, F. (1999). Testing ski stability. *Measurement Science and Technology, 10,* N38-N43.

de Haan, T. & den Brinker, B. (1988). Direct linear transformation method for 3d movement registration using 'subject tracking' cameras. In G. de Groot, A. P. Hollander, P. A. Huijing, & G. J. van Ingen Schenau (Eds.), *Biomechanics XI-B* (pp. 1051-1056). Amsterdam: Free University Press.

de Leva, P. (1996a). Adjustments to Zatsiorsky-Seluyanov's segment inertia parameters. *Journal of Biomechanics, 29,* 1223-1230.

de Leva, P. (1996b). Joint center longitudinal positions computed from a selected subset of Chandler's data. *Journal of Biomechanics, 29,* 1231-1233.

de Leva, P. (2008, April). *Summary: Stereophotogrammetric error sources.* [On-line]. Available: http://listserv.surfnet.nl/archives/Biomch-L.html.

Drenk, V. (1994). Photogrammetric evaluation procedures for pannable and tiltable cameras of variable focal length. In A. Barabás & G. Fábián (Eds.), *Proceedings of the 12th International Symposium on Biomechanics in Sports* (pp. 27-30). Budapest-Siófok, Hungary. [On-line]. Available: www.isbs.org

Fauve, M., Auer, M., Lüthi, A., Rhyner, H., & Meier, J. (2009). Measurement of dynamical ski behaviour during alpine skiing. In E. Müller, S. Lindinger, & T. Stöggl (Eds.), *Science and Skiing IV* (pp. 195-206). Maidenhead: Meyer & Meyer Sport (UK), Ltd.

Federolf, P. (2005). *Finite element simulation of a carving snow ski.* Unpublished doctoral dissertation, Swiss Federal Institute of Technology Zurich, Zürich, Switzerland.

Federolf, P., JeanRichard, F., Fauve, M., Lüthi, A., Rhyner, H., & Dual, J. (2006). Deformation of snow during a carved ski turn. *Cold Regions Science and Technology, 46,* 69-77.

Federolf, P., Scheiber, P., Rauscher, E., Schwameder, H., Lüthi, A., Rhyner, H., & Müller, E. (2008). Impact of skier actions on the gliding times in alpine skiing. *Scandinavian Journal of Medicine and Science in Sports, 18,* 790-797.

Federolf, P., Fauve, M., Lüthi, A., Rhyner, H., Ammann, W., & Dual, J. (2004). Finite element simulation of a carving alpine ski. In D. Bacharach & J. Seifert (Eds.), *Abstract Book of the 3rd International Congress on Skiing and Science* (pp. 11-12). Aspen, CO.

References

Ferrario, V. F., Sforza, C., Michielon, G., Dugnani, S., & Mauro, F. (1997). A mathematical method for the analysis of trajectories in giant slalom. In E. Müller, H. Schwameder, E. Kornexl, & C. Raschner (Eds.), *Science and Skiing* (pp. 107-115). London: E & FN Spon.

Förg-Rob, W. & Nachbauer, W. (1988). The use of spline functions in the smoothing of film data for slalom ski racers. *International Journal of Sport Biomechanics, 4,* 166-177.

Frick, U., Schmidtbleicher, D., Raschner, C., & Müller, E. (1997). Types of muscle action of leg and hip extensor musles in slalom. In E. Müller, H. Schwameder, E. Kornexl, & C. Raschner (Eds.), *Science and Skiing* (pp. 262-271). London: E & FN Spon.

Gazzani, F. (1993a). A new algorithm for calibrating stereophotogrammetric systems devoted to motion analysis. *Human Movement Science, 12,* 403-425.

Gazzani, F. (1993b). Comparative assessment of two algorithms for calibrating stereophotogrammetric systems. *Journal of Biomechanics, 26,* 1449-1454.

Giakas, G. & Baltzopoulos, V. (1997). Optimal digital filtering requires a different cut-off frequency strategy for the determination of the higher derivatives. *Journal of Biomechanics, 30,* 851-855.

Gilat, A. & Subramaniam, V. (2008). *Numerical methods for engineers and scientists*. Hoboken, NJ: John Wiley & Sons, Inc.

Gilgien, M. (2008). *External forces acting in direction of travel and their relation to energy dissipation in slalom.* Unpublished master's thesis, Norwegian School of Sport Sciences, Oslo, Norway.

Glenne, B. & Larsson, O. (1987, Winter). Mechanics of a giant slalom turn. *The Professional Skier, 3,* 23-26.

Glitsch, U. (2001). Computer simulation of alpine skiing. In E. Müller, H. Schwameder, C. Raschner, S. Lindinger, & E. Kornexl (Eds.), *Science and Skiing II* (pp. 141-154). Hamburg: Verlag Dr. Kovač.

Goodwin, D. A. (1990a). Alpine slalom ski racers. In J. Hamill, T.R. Derrick, & E.H. Elliott (Eds.), *Proceedings of the XI Symposium of the International Society of Biomechanics in Sports* (pp. 154-158). Amherst, MA. [On-line]. Available: www.isbs.org

Goodwin, D. A. (1990b). *Kinematic considerations of elite alpine slalom ski racers.* Master's thesis, Western Michigan University. (University Microfilms No. AAT 1341564)

Gufler, V. (2001). *Dreidimensionale Kraft- und Momentanalyse bei verschiedenen Schwungformen im alpinen Skilauf.* Unpublished Diplomarbeit, Leopold-Franzens-Universität Innsbruck, Innsbruck, Austria.

Hatze, H. (1988). High-precision three-dimensional photogrammetric calibration and object space reconstruction using a modified DLT-approach. *Journal of Biomechanics, 21,* 533-538.

Heinrich, D., Kaps, P., Mössner, M., Schretter, H., & Nachbauer, W. (2009). Calculation of the pressure distribution between ski and snow. In E. Müller, S. Lindinger, & T. Stöggl (Eds.), *Science and Skiing IV* (pp. 229-241). Maidenhead: Meyer & Meyer Sport (UK), Ltd.

Heinrich, D., Mössner, M., Kaps, P., Schretter, H., & Nachbauer, W. (2005). Influence of ski bending stiffness on the turning radius of alpine skis at different edging angles and velocities - a computer simulation. *Proceedings of the International Congress Mountain & sport: Updating study and research from laboratory to field* (pp. 44). Rovereto, Italy.

Heinrich, D., Mössner, M., Kaps, P., Schretter, H., & Nachbauer, W. (2006). Influence of ski bending stiffness on the turning radius of alpine skis at different edging angles and velocities. In E.F. Moritz & S. Haake (Eds.), *The engineering of sport 6* (Vol.2, pp. 207-212). New York, NY: Springer Science+Business Media, LLC.

Hinrichs, R. N. & McLean, S. P. (1995). NLT and extrapolated DLT: 3-D cinematography alternatives for enlarging the volume of calibration. *Journal of Biomechanics, 28,* 1219-1223.

Hintermeister, R. A., O'Connor, D. D., Dillman, C. J., Suplizio, C. L., Lange, G. W., & Steadman, J. R. (1995). Muscle activity in slalom and giant slalom skiing. *Medicine & Science in Sports & Exercise, 27,* 315-322.

Hirano, Y. (2006). Quickest descent line during alpine ski racing. *Sports Engineering, 9,* 221-228.

Hirano, Y. & Tada, N. (1996). Numerical simulation of a turning alpine ski during recreational skiing. *Medicine & Science in Sports & Exercise, 28,* 1209-1213.

Hoff, J. (1997). Timing muscle forces to enhance velocity in competitive alpine slalom skiing. Unpublished manuscript, University of Trondheim, Norway.

Howe, J. (2001). *The new skiing mechanics* (2nd ed). Waterford, ME: McIntire Publishing.

References

Huber, A., Waibel, K. H., & Spitzenpfeil, P. (2009). Description of race courses and estimation of ground reaction forces by GPS-data and video. In E. Müller, S. Lindinger, & T. Stöggl (Eds.), *Science and Skiing IV* (pp. 260-271). Maidenhead: Meyer & Meyer Sport (UK), Ltd.

International Organization for Standardization. (2003). *International Standard: Skis - Vocabulary* (Reference No. ISO 6289:2003(E/F)). Geneva, Switzerland: Author.

Joubert, G. (1980). *Skiing. An art. A technique.* (J. Major, S. Thomas, & D. Smith, Trans.). LaPorte, CO: Poudre Publishing Company. (Original work published 1978)

Kagawa, H. & Yoneyama, T. (2001). Effective action of skier's center of mass in skiing. In E. Müller, H. Schwameder, C. Raschner, S. Lindinger, & E. Kornexl (Eds.), *Science and Skiing II* (pp. 129-140). Hamburg: Verlag Dr. Kovač.

Kagawa, H., Yoneyama, T., Tatsuno, D., Scott, N. W., & Osada, K. (2009). Development of a measuring system on ski deflction and contacting snow pressure in turns. In E. Müller, S. Lindinger, & T. Stöggl (Eds.), *Science and Skiing IV* (pp. 281-291). Maidenhead: Meyer & Meyer Sport (UK), Ltd.

Kaps, P., Mössner, M., Nachbauer, W., & Stenberg, R. (2001). Pressure distribution under a ski during carved turns. In E. Müller, H. Schwameder, C. Raschner, S. Lindinger, & E. Kornexl (Eds.), *Science and Skiing II* (pp. 180-202). Hamburg: Verlag Dr. Kovač.

Karlsson, E., Eriksson, A., Forsberg, A., Kallberg, L., & Tesch, P. (1978). *The physiology of alpine skiing*. Park City, UT: The United States Ski Coaches Association.

Kennedy, P. W., Wright, D. L., & Smith, G. A. (1989). Comparison of film and video techniques for three-dimensional dlt repredictions. *International Journal of Sport Biomechanics, 5,* 460.

Klous, M. (2007). *Three-dimensional joint loading on the lower extremities in alpine skiing and snowboarding*. Unpublished doctoral dissertation, University of Salzburg, Salzburg, Austria.

Klous, M. & Schwameder, H. (2003). New method for 3D kinematic analysis in skiing. In E. Müller, H. Schwameder, G. Zallinger & V. Fastenbauer (Eds.), *Book of Abstracts of the 8th Annual Congress of the European College of Sport Science* (pp. 344-345). Salzburg, Austria.

Knünz, B., Nachbauer, W., Mössner, M., & Schindelwig, K. (2000). Track analysis of giant slalom turns of world cup racers. In J. Avela, P.V. Komi, & J. Komulainen (Eds.), *Book of Abstracts of the 5th Annual Congress of the European College of Sport Science* (pp. 399). Jyväskylä, Finland.

Kruger, A. & Edelmann-Nusser, J. (2008). Comparison of a full body inertial measurement system and an optical camera based system in alpine skiing. In E. Zinzen, P. Clarys, R. Meeusen, K. Huts, & W. Van den Broecke (Eds.), *Abstract Book of the First International Low Lands Congress on Science and Skiing* (pp. 24-25). Brussels, Belgium.

Kugovnik, O., Supej, M., & Nemec, B. (2004). Time advantage using the improved slalom technique. In D. Bacharach & J. Seifert (Eds.), *Abstract Book of the 3rd International Congress on Skiing and Science* (pp. 67-68). Aspen, CO.

Kugovnik, O., Supej, M., & Nemec, B. (2005). Time advantage using an improved slalom technique. In E. Müller, D. Bacharach, R. Klika, S. Lindinger, & H. Schwameder (Eds.), *Science and Skiing III* (pp. 87-95). Oxford: Meyer & Meyer Sport, Ltd.

Kvale, S. (1996). *Interviews*. London: Sage Publications.

Kwon, Y. H., Yoon, S., & Sung, R. J. (2004). Accuracy of the software genlock with digital camcorders. In M. Lamontagne, D. Gordon, E. Robertson, H. Sveistrup (Eds.) *Proceedings of the 22nd International Symposium on Biomechanics in Sports* (pp. 64). Ottowa, Canada. [On-line]. Available: www.isbs.org

Laapi, M. (2009). *The kinetic characteristics in competitive slalom skiing*. Unpublished master's thesis, Norwegian School of Sport Sciences, Oslo, Norway.

Lafontaine, D., Lamontagne, M., Dupuis, D., & Diallo, B. (1998). Analysis of the distribution of pressure under the feet of elite alpine ski instructors. In H.J. Riehle & M.M. Vieter (Eds.), *Proceedings of the XVI International Symposium on Biomechanics in Sports* (Vol. 1, pp. 485-488). Konstanz, Germany. [On-line]. Available: www.isbs.org

LeMaster, R. (2008, January 30). Skid with finesse to be fast. *Ski Racing*, 42-43.

LeMaster, R. (1999). *The Skier's Edge*. Champaign, IL: Human Kinetics.

LeMaster, R. (2009). *Ultimate skiing*. Champaign, IL: Human Kinetics.

Lešnik, B. & Žvan, M. (2003). Comparison of centre of mass trajectories in modern giant slalom techniques. *Kinesiology, 35,* 191-200.

Lešnik, B. & Žvan, M. (2007). The best slalom competitors - kinematic analysis of tracks and velocities. *Kinesiology, 39,* 40-48.

References

Levy, M. & Smith, G. A. (1995). Validation of Macreflex motion analysis system for three-dimensional coordinate prediction. In K. Häkkinen, K. L. Keskinen, P. V. Komi, & A. Mero (Eds.), *Book of Abstracts XVth Congress of the International Society of Biomechanics* (pp. 552-553). Jyväskylä, Finland.

Lieu, D. (1982). *Mechanics of the turning snow-ski.* Doctoral dissertation, University of California, Berkeley. (University Microfilms No. AAT 8312725)

Lieu, D. K. & Mote, C. D. (1985). Mechanics of the Turning Snow Ski. In R. J. Johnson & C. D. Mote (Eds.), *Skiing Trauma and Safety: Fifth International Symposium* (pp. 117-140). Philadelphia, PA: American Society for Testing and Materials.

Lind, D. & Sanders, S. P. (2004). *The physics of skiing: Skiing at the triple point* (2nd ed). New York, NY: Springer-Verlag New York, Inc.

Lindinger, S. (2006). *Biomechanische Analysen von Skatingtechniken im Skilanglauf.* Aachen: Meyer & Meyer Sport, Ltd.

Louie, J. K. & Mote, C. D. (1982). Acceleration induced by snow skier body motions. In W. Hauser, J. Karlsson, & M. Magi (Eds.), *Ski Trauma and Skiing Safety IV* (pp. 15-24). Munich, Germany: Technischer Überwachungs-Verein.

Luhmann, T., Robson, S., Kyle, S., & Harley, I. (2006). *Close range photogrammetry: Principles, techniques, and applications*. Dunbeath, UK: Whittles Publishing.

Lüthi, A., Federolf, P., Fauve, M., Oberhofer, K., Rhyner, H., Ammann, W., Stricker, G., Schiefermüller, C., Eitzlmair, E., Schwameder, H. & Müller, E. (2005). Determination of forces in carving using three independent methods. In E. Müller, D. Bacharach, R. Klika, S. Lindinger, & H. Schwameder (Eds.), *Science and Skiing III* (pp. 96-106). Oxford: Meyer & Meyer Sport (UK), Ltd.

Lüthi, A., Federolf, P., Fauve, M., & Rhyner, H. (2006). Effect of bindings and plates on ski mechanical properties and carving performance. In E. F. Moritz & S. Haake (Eds.), *The engineering of sport 6* (Vol. 1, pp. 299-304). New York, NY: Springer Science+Business Media, LLC.

Magill, R. A. (2007). *Motor learning and control: Concepts and applications*. New York, NY: McGraw-Hill.

Major, J. & Larsson, O. (1979). *World cup skiteknikk: Lær og bli bedre.* (B. Müller, Trans.). Oslo: Gyldendal Norsk Forlag A/S. (Original work published 1979)

Mann, R. W., Rowell, D., Dalrymple, G., Conati, F., Tetewsky, A., Ottenheimer, D., & Antonsson, E. (1983). Precise, rapid, automatic 3-D position and orientation tracking of multiple moving bodies. In H. Matsui & K. Kobayashi (Eds.), *Biomechanics VIII-B: Proceedings of the Eighth International Congress of Biomechanics* (pp. 1104-1112). Champaign, IL: Human Kinetics Publishers.

Margane, J., Trzecinski, L., Babiel, S., & Neumaier, A. (1998). A mechanical apparatus (skiing model) executing turns on carver skis. In H. J. Riehle & M. M. Vieten (Eds.), *Proceedings of the XVI International Symposium on Biomechanics in Sports.* Konstanz, Germany. [On-line]. Available: www.isbs.org

Marzan, G. & Karara, H. M. (1975). A computer program for direct linear transformation solution of the colinearity condition, and some applications of it. *Proceedings of the Symposium on Close-Range Photogrammetric Systems* (pp. 420-476). Falls Church, VA: American Society of Photogrammetry.

Miura, T. & Miura, M. (2004). Analysis of inside leaning motions of male junior ski racers in giant slalom. In D. Bacharach & J. Seifert (Eds.), *Abstract Book of the 3rd International Congress on Science and Skiing* (pp. 107-108). Aspen, CO.

Moger, T. (2007). *Kan en ved hjelp av en 3 dimensjonal kinematisk analyse beskrive tyngdepunktsbanen til SL-løpere nøyaktig nok til å belyse viktige prestasjonskarakteristika til tyngdepunktsbanen?* Unpublished master's thesis, Norwegian School of Sport Sciences, Oslo, Norway.

Morawski, J. M. (1973). Control systems approach to a ski-turn analysis. *Journal of Biomechanics, 6,* 267-279.

Mote, C. D. & Louie, J. K. (1983). Accelerations induced by body motions during snow skiing. *Journal of Sound and Vibration, 88,* 107-115.

Mössner, M., Heinrich, D., Kaps, P., Schretter, H., & Nachbauer, W. (2009). Effects of ski stiffness in a sequence of ski turns. In E. Müller, S. Lindinger, & T. Stöggl (Eds.), *Science and Skiing IV* (pp. 374-388). Maidenhead: Meyer & Meyer Sport (UK), Ltd.

Mössner, M., Heinrich, D., Schindelwig, K., Kaps, P., Lugner, P., Schmiedmayer, H. Schretter, H., & Nachbauer, W. (2006). Modeling of the ski-snow contact for a carved turn. In E. F. Moritz & S. Haake (Eds.), *The engineering of sport 6* (Vol. 2, pp. 195-200). New York, NY: Springer Science+Business Media, LLC.

Mössner, M., Heinrich, D., Schindelwig, K., Kaps, P., Schiedmayer, H. B., Schretter, H. & Nachbauer, W. (2005). Modelling of the ski-snow contact for a carved turn. *Proceedings of the International Congress Mountain & Sport: Updating study and research from laboratory to field* (pp. 64). Rovereto, Italy.

References

Mössner, M., Kaps, P., & Nachbauer, W. (1995). Smoothing the DLT parameters for moved cameras. In K. Häkkinen, K. L. Keskinen, P. V. Komi, & A. Mero (Eds.), *Book of Abstracts of the XVth Congress of the International Society of Biomechanics* (pp. 642-643). Jyväskylä, Finland.

Mössner, M., Kaps, P., & Nachbauer, W. (1996). A method for obtaining 3-D data in alpine skiing using pan-and-tilt cameras with zoom lenses. In C. D. Mote, R. J. Johnson, W. Hauser, & P. S. Schaff (Eds.), *Skiing Trauma and Safety: Tenth Volume* (pp. 155-164). Philadelphia, PA: American Society for Testing and Materials.

Müller, E. (1994). Analysis of the biomechanical characteristics of different swinging techniques in alpine skiing. *Journal of Sport Sciences, 12,* 261-278.

Müller, E., Bartlett, R., Raschner, C., Schwameder, H., Benko-Bernwick, U., & Lindinger, S. (1998). Comparisons of the ski turn techniques of experienced and intermediate skiers. *Journal of Sport Sciences, 16,* 545-559.

Müller, E., Schiefermüller, C., Kröll, J., Raschner, C., & Schwameder, H. (2004). Keynote: Skiing with carving skis - what is new? In D. Bacharach & J. Seifert (Eds.), *Abstract Book of the 3rd International Congress on Skiing and Science* (pp. 1-2). Aspen, CO.

Müller, E., Schiefermüller, C., Kröll, J., Raschner, C., & Schwameder, H. (2005). Skiing with carving skis - what is new? In E. Müller, D. Bacharach, R. Klika, S. Lindinger, & H. Schwameder (Eds.), *Science and Skiing III* (pp. 15-23). Oxford: Meyer & Meyer Sport (UK), Ltd.

Müller, E. & Schwameder, H. (2003). Biomechanical aspects of new techniques in alpine skiing and ski-jumping. *Journal of Sport Sciences, 21,* 679-692.

Nachbauer, W. (1987a). Fahrlinie in Torlauf und Riesentorlauf. *Leistungssport, 6,* 17-21.

Nachbauer, W. (1987b). Skiing line and ground reaction forces of ski racers over various distances between gates. In E. Kornexl (Ed.), *Spektrum der Sportwissenschaften*. Wien: ÖBV.

Nachbauer, W., Kaps, P., Nigg, B., Brunner, F., Lutz, A., Obkircher, G., & Mössner, M. (1996). A video technique for obtaining 3-D coordinates in alpine skiing. *Journal of Applied Biomechanics, 12,* 104-115.

Nachbauer, W., Rainer, F., Schindelwig, K., & Kaps, P. (2004). Effects of ski stiffness on ski performance. In M. Hubbard, R. D. Mehta, & J. M. Pallis (Eds.), *The engineering of sport 5* (Vol. 1, pp. 472-478). Sheffield: International Sports Engineering Association.

Niessen, W., Müller, E., Schwameder, H., Wimmer, M. A., & Riepler, B. (1998). Force and moment measurements during alpine skiing depending on height position. In M. M. Vieter & H. J. Riehle (Eds.), *Proceedings of the XVI International Symposium on Biomechanics in Sports* (Vol.1, pp. 544-547). Konstanz, Germany. [On-line]. Available: www.isbs.org

Nigg, B., Schwameder, H., Stefanyshyn, D., & v. Tscharner, V. (2001). The effect of ski binding position on performance and comfort in skiing. In E. Müller, H. Schwameder, C. Raschner, S. Lindinger, & E. Kornexl (Eds.), *Science and Skiing II* (pp. 3-13). Hamburg: Verlag Dr. Kovač.

Ohanian, H. C. & Markert, J. T. (2007). *Physics for engineers and scientists*. New York, NY: W.W. Norton & Company, Inc.

Piziali, R. L. (1970). *The dynamics of snow skis.* Doctoral dissertation, University of California, Berkeley. (University Microfilms No. AAT 7115863)

Pourcelot, P., Audigié, F., Degueurce, C., Geiger, D., & Denoix, J. M. (2000). A method to synchronize cameras using the direct linear transformation technique. *Journal of Biomechanics, 33,* 1751-1754.

Pozzo, R., Canclini, A., Casasola, S., Ciro, D., Cotelli, C., & Baroni, G. (2005). 3-D kinematic and kinetic analysis of G-slalom at Valbadia World Cup race in 2002. *Book of Abstracts of the International Congress on Mountain and Sport: Updating study and research from laboratory to field* (pp. 48). Rovereto, Italy.

Pozzo, R., Canclini, A., Cotelli, C., & Baroni, G. (2001). 3-D kinematic analysis of slalom in elite skiers at the Bormio world cup ski finals in 2000. In J. Mester, G. King, H. Strüder, E. Tsolakidis, & A. Osterburg (Eds.), *Book of Abstracts of the 6th Annual Congress of the European College of Sport Science* (pp. 564). Cologne, Germany: Sport und Buch Strauss GmbH.

Pozzo, R., Canclini, A., Cotelli, C., & Baroni, G. (2004). 3-D kinematic and kinetic analysis of g-slalom at Val Badia world cup race in 2003. In D. Bacharach & J. Seifert (Eds.), *Abstract Book of the 3rd International Congress on Skiing and Science* (pp. 5-6). Aspen, CO.

Pozzo, R., Canclini, A., Cotelli, C., & Baroni, G. (2005). 3-D kinematics and kinetic analysis of G-Slalom in elite skiers at Val Badia World Cup race in 2002. In E. Müller, D. Bacharach, R. Klika, S. Lindinger, & H. Schwameder (Eds.), *Science and Skiing III* (pp. 125-135). Oxford: Meyer & Meyer Sport, Ltd.

Pozzo, R., Canclini, A., Cotelli, C., Martinelli, L., & Rockmann, A. (2001). 3d kinematics of the start in the downhill at the Bormio world cup in 1995. In E. Müller, H. Schwameder, C. Raschner, S. Lindinger, & E. Kornexl (Eds.), *Science and Skiing II* (pp. 95-107). Hamburg: Verlag Dr. Kovač.

References

Raschner, C., Kösters, A., Müller, E., Schwameder, H., Zallinger, G., & Niessen, W. (1999). Dynamische und kinematische Technikanalyse im Riesenslalom bei Weltklasserennläufern. *Spectrum der Sportwissenshaften, 11,* 57-64.

Raschner, C., Müller, E., & Schwameder, H. (1997). Kinematic and kinetic analysis of slalom turns as a basis for the development of specific training methods to improve strength and endurance. In E. Müller, H. Schwameder, E. Kornexl, & C. Raschner (Eds.), *Science and Skiing* (pp. 251-261). London: E & FN Spon.

Raschner, C., Schiefermüller, C., Zallinger, G., Hofer, E., Müller, E., & Brunner, F. (2001). Carving turns versus traditional parallel turns - a comparative biomechanical analysis. In E. Müller, H. Schwameder, C. Raschner, S. Lindinger, & E. Kornexl (Eds.), *Science and Skiing II* (pp. 203-217). Hamburg: Verlag Dr. Kovač.

Renshaw, A. A. & Mote, C. D. (1989). A model for the turning snow ski. *International Journal of Mechanical Sciences, 31,* 721-736.

Robertsen, D. G. E., Caldwell, G. E., Hamill, J., Kamen, G., & Whittlesey, S. N. (2004). *Research methods in biomechanics*. Champaign, IL: Human Kinetics.

Sahashi, T. & Ichino, S. (1995). Method for drawing locus of a sliding ski as observed from direction perpendicular to snow surface. *Japanese Journal of Applied Physics, 34,* 674-679.

Sahashi, T. & Ichino, S. (1998). Coefficient of friction of snow skis during turning descents. *Japanese Journal of Applied Physics, 37,* 720-727.

Savolainen, S. & Visuri, R. (1994). A review of athletic energy expenditure, using skiing as a practical example. *Journal of Applied Biomechanics, 10,* 253-269.

Schaff, P. S. & Hauser, W. (1993). 3-D video motion analysis on the slope—A practical way to analyze motion patterns in alpine skiing. In R. J. Johnson, C. D. Mote, & J. Zelcer (Eds.), *Skiing Trauma and Safety: Ninth International Symposium* (pp. 169-176). Philadelphia, PA: American Society for Testing and Materials.

Scheirman, G., Porter, J., Leigh, M., & Musick, D. (1998). An integrated method to obtain three-dimensional coordinates using panning and tilting video cameras. In H. J. Riehle & M. M. Vieten (Eds.), *Proceedings of the XVI International Symposium on Biomechanics in Sports*. Konstanz, Germany. [On-line]. Available: www.isbs.org

Schiefermüller, C., Lindinger, S., & Müller, E. (2005). The skier's centre of gravity as a reference point in movement analysis for different designated systems. In E. Müller, D. Bacharach, R. Klika, S. Lindinger, & H. Schwameder (Eds.), *Science and Skiing III* (pp. 172-185). Oxford: Meyer & Meyer Sport (UK), Ltd.

Schiestl, M. (2005). *DLT data reconstruction on Clough-Tocher interpolated G^1-surfaces for simulation in alpine skiing*. Unpublished diploma thesis in technical mathematics, Leopold-Franzens-University of Innsbruck, Innsbruck, Austria.

Schiestl, M., Kaps, P., Mössner, M., & Nachbauer, W. (2005). Snow friction and drag during the downhill race in Kitzbuhel. *Proceedings of the International Congress Mountain and sport: Updating study and research from laboratory to field* (pp. 54). Rovereto, Italy.

Schiestl, M., Kaps, P., Mössner, M., & Nachbauer, W. (2006). Calculation of friction and reaction forces during an alpine world cup downhill race. In E. F. Moritz & S. Haake (Eds.), *The engineering of sport 6, Volume 1: Developments for sports* (pp. 269-274). New York, NY: Springer Science+Business Media, LLC.

Schwameder, H., Nigg, B., v. Tscharner, V., & Stefanyshyn, D. (2001). The effect of binding position on kinetic variables in alpine skiing. In E. Müller, H. Schwameder, C. Raschner, S. Lindinger, & E. Kornexl (Eds.), *Science and Skiing II* (pp. 43-54). Hamburg: Verlag Dr. Kovač.

Scott, N. W. (2004). Measurement of joint motion and acting forces on a top athlete skiing. In M. Hubbard, R. D. Mehta, & J. M. Pallis (Eds.), *The engineering of sport 5* (Vol. 1, pp. 494-500). Sheffield: International Sports Engineering Association.

Scott, N. W., Kagawa, H., & Yoneyama, T. (2006). A unified, custom-built measuring system for a ski athlete. In E. F. Moritz & S. Haake (Eds.), *The Engineering of Sport 6, Volume 2: Developments for Disciplines* (pp. 219-224). New York, NY: Springer Sport+Business Media, LLC.

Scott, N. W., Yoneyama, T., Kagawa, H., & Osada, K. (2007). Measurment of ski snow-pressure profiles. *Sports Engineering, 10,* 145-156.

Seifriz, F. & Mester, J. (2001). Measurement and computer simulation of trajectories in alpine skiing. In E. Müller, H. Schwameder, C. Raschner, S. Lindinger, & E. Kornexl (Eds.), *Science and Skiing II* (pp. 155-164). Hamburg: Verlag Dr. Kovač.

Shapiro, R. (1978). Direct linear transformation method for three-dimensional cinematography. *Research Quarterly, 49,* 197-205.

Sjøstrand, K. (2006). Hva karaktiserer verdens beste og Norges beste slalåmløpere når det gjelder bruk av visse tekniske element?. Unpublished bachelor report, Norwegian School of Sport Sciences, Oslo, Norway.

Smith, G. (1994). An iterative segment length normalization routine for use with linked segment models. In R. J. Gregor & A. S. Litsky (Eds.), *Conference Proceedings of the 18th Annual Meeting of the American Society of Biomechanics* (pp. 35-36). Columbus, OH.

References

Spring, E., Savolainen, S., Erikkila, T., Hamalainen, T., & Pihkala, P. (1988). Drag area of a cross country skier. *International Journal of Sport Biomechanics, 4,* 103-113.

Stivers, K. A., Ariel, G. B., Vorobiev, A., Penny, M. A., Gouskov, A., & Yakunin, N. (1993). Photogrammetric transformation with panning. *Proceedings of the International Society of Biomechanics XIVth Congress,* 1288-1289. Paris, France.

Supej, M. (2003). The myth of acceleration and push-off in racing alpine skiing. Unpublished manuscript, University of Ljubljana, Slovenia.

Supej, M. (2008). Differential specific mechanical energy as a quality parameter in racing alpine skiing. *Journal of Applied Biomechanics, 24,* 121-129.

Supej, M. (2009). A step forward in 3D measurements in alpine skiing: A combination of an inertial suit and DGPS technology. In E. Müller, S. Lindinger, & T. Stöggl (Eds.), *Science and Skiing IV* (pp. 497-504). Maidenhead: Meyer & Meyer Sport (UK), Ltd.

Supej, M., Kugovnik, O., & Nemec, B. (2003). Kinematic determination of the beginning of a ski turn. *Kinesiologia Slovenica, 9,* 11-17.

Supej, M., Kugovnik, O., & Nemec, B. (2004). Modelling and simulation of two competition slalom techniques. *Kinesiology, 36,* 206-212.

Supej, M., Kugovnik, O., & Nemec, B. (2005a). Energy principle used for estimating the quality of a racing ski turn. In E. Müller, D. Bacharach, R. Klika, S. Lindinger, & H. Schwameder (Eds.), *Science and Skiing III* (pp. 228-237). Oxford: Meyer & Meyer Sport (UK), Ltd.

Supej, M., Kugovnik, O., & Nemec, B. (2005b). Advanced analysis of alpine skiing based on 3D kinematic measurements. In E. Müller, D. Bacharach, R. Klika, S. Lindinger, & H. Schwameder (Eds.), *Science and Skiing III* (pp. 216-227). Oxford: Meyer & Meyer Sport, Ltd.

Supej, M., Kugovnik, O., & Nemec, B. (2005c). Relations among performance quality (dw), ground reaction forces, acceleration, and turn radii in men wc slalom races. In D. Milanovi (Ed.), *Proceedings of the 4th International Scientific Congress on Kinesiology* (pp. 829-832). Zagreb, Croatia.

Supej, M., Nemec, B., & Kugovnik, O. (2005). Changing conditions on the slalom ski course affect competitors' performances. *Kinesiology, 37,* 151-158.

Tada, N. & Hirano, Y. (1998). Experimental determination of snow resistance forces acting on a turning snow ski. In S. Haake (Ed.), *The engineering of sport: Design and development* (pp. 423-430). Oxford: Blackwell Science.

Tada, N. & Hirano, Y. (2002). In search of the mechanics of a turning alpine ski using snow cutting force measurements. *Sports Engineering, 5,* 15-22.

Takahashi, M. & Yoneyama, T. (2001). Basic ski theory and acceleration during ski turn. In E. Müller, H. Schwameder, C. Raschner, S. Lindinger, & E. Kornexl (Eds.), *Science and Skiing II* (pp. 307-321). Hamburg: Verlag Dr. Kovač.

Takahashi, M. & Yoneyama, T. (2002). Instruction on the optimal ski turn motion. In S. Ujihaski & S. J. Haake (Eds.), *The Engineering of Sport 4* (pp. 708-715). Carlton, Australia: Blackwell Publishing.

Tatsuno, D., Yoneyama, T., Kagawa, H., Scott, N. W., & Osada, K. (2009). Measurement of ski deflection and ski-snow contacting pressure in an actual ski turn on the snow surface. In E. Müller, S. Lindinger, & T. Stöggl (Eds.), *Science and Skiing IV* (pp. 505-515). Maidenhead: Meyer & Meyer Sport (UK), Ltd.

Tesch, P. (1995). Aspects on muscle properties and use in competitive alpine skiing. *Medicine & Science in Sports & Exercise, 27,* 310-314.

Tjørhom, H. (2007). *Beskrivelse av tyngdepunktets frem / bak dynamikk i slalåm sett opp mot prestasjon ved hjelp av en 3 dimensjonal kinematisk analyse.* Unpublished master's thesis, Norwegian School of Sport Sciences, Oslo, Norway.

Van Gheluwe, B. (1978). Computerized three-dimensional cinematography for any arbitrary camera setup. In E. Asmussen & K. Jørgensen (Eds.), *Biomechanics VI-A* (pp. 343-348). Baltimore, MD: University Park Press.

van Ingen Schenau, G. J. (1982). The influence of air friction in speed skating. *Journal of Biomechanics, 15,* 449-458.

Vodičková, S., Lufinka, A., & Zůbek, T. (2005). The dynamographic and kinematographic method application for a short carving turn. In E. Müller, D. Bacharach, R. Klika, S. Lindinger, & H. Schwameder (Eds.), *Science and Skiing III* (pp. 247-256). Oxford: Meyer & Meyer Sport (UK), Ltd.

Walton, J. S. (1970). A high speed timing unit for cinematography. *Research Quarterly, 41,* 213-216.

Walton, J. S. (1981). *Close-range cine-photogrammetry: A generalized technique for quantifying gross human motion.* Doctoral dissertation, The Pennsylvania State University. (University Microfilms No. AAT 8120471)

Watanabe, K. (1981). Skiing research in Japan. *Medicine & Science in Sports & Exercise, 13,* 205-209.

References

Wimmer, A. (2001). *Kinetische und kinematische Analyse von Schwüngen im alpinen Skilauf.* Unpublished Diplomarbeit, Leopold-Franzens-Universität Innsbruck, Innsbruck, Austria.

Winter, D. A. (2005). *Biomechanics and motor control of human movement*. (3rd ed.) Hoboken, NJ: John Wiley & Sons, Inc.

Witherell, W. (1972). *How the racers ski*. New York, NY: W.W. Norton & Company, Inc.

Witherell, W. & Evrard, D. (1993). *The athletic skier*. Salt Lake City, UT: The Athletic Skier, Inc.

Wood, G. A. (1982). Data smoothing and differentiation procedures. *Exercise and Sport Science Reviews, 10*, 308-362.

Wood, G. A. & Marshall, R. N. (1986). The accuracy of DLT extrapolation in three-dimensional film analysis. *Journal of Biomechanics, 19,* 781-785.

Yamagish, T., Fujii, K., Kato, S., Tsukawaki, M., & Ozawa, T. (2003). Analysis of carving and conventional ski measured pressure distributions during carving turns. In R. J. Johnson, M. Lamont, & J. E. Shealy (Eds.), *Skiing trauma and safety: Fourteenth volume* (pp. 3-9). West Conshohocken, PA: American Society for Testing and Materials International.

Yeadon, M. R. (1989). A method for obtaining three-dimensional data on ski jumping using pan and tilt cameras. *International Journal of Sport Biomechanics, 5,* 238-247.

Yeadon, M. R. & King, M. A. (1999). A method for synchronizing digitised video data. *Journal of Biomechanics, 32,* 983-986.

Yoneyama, T., Kagawa, H., & Funahashi, N. (2002). Study on the effective turn motion using a ski robot. In S. Ujihashi & S. J. Haake (Eds.), *The Engineering of Sport 4* (pp. 463-469). Carlton, Australia: Blackwell Publishing.

Yoneyama, T., Kagawa, H., Okamoto, A., & Sawada, M. (2001). Measurement of the joint motion in the carving ski turn in comparison with normal ski turning motion. In E. Müller, H. Schwameder, C. Raschner, S. Lindinger, & E. Kornexl (Eds.), *Science and Skiing II* (pp. 218-231). Hamburg: Verlag Dr. Kovač.

Yoneyama, T., Scott, N. W., & Kagawa, H. (2006). Timing of force application and joint angles during a long turn. In E. F. Moritz & S. Haake (Eds.), *The engineering of sport 6* (Vol.1 , pp. 293-298). New York, NY: Springer Science+Business Media, LLC.

Yoneyama, T., Scott, N. W., Kagawa, H., & Osada, K. (2008). Ski deflection measurement during skiing and estimation of ski direction and edge angle. *Sports Engineering, 11,* 3-13.

Yu, B., Koh, T. J., & Hay, J. G. (1993). A panning DLT procedure for three-dimensional videography. *Journal of Biomechanics, 26,* 741-751.

Zatsiorsky, V. M. (2002). *Kinetics of human motion*. Champaign, IL: Human Kinetics.

Žvan, M. & Lešnik, B. (2007). Correlation between the length of the ski track and the velocity of top slalom skiers. *Acta Univ Palacki Olomuc Gymn, 37,* 37-44.

CORRIGENDUM

The following is a list of corrections made after the dissertation was submitted for evaluation:

- An error in the automated definition of equation numbers in Chapter 3 was corrected.
- The y-axis tick labels in Figure 6.40 on p. 260 were corrected.